STUDIES OF THE CHEMISTRY OF PHOSPHAALKYNES AND TRANSITION METAL(I) AMIDINATE AND GUANADINATE COMPLEXES

By

CHRISTIAN SCHULTEN

A thesis submitted to the School of Chemistry, Cardiff University,
for the degree of Doctor of Philosophy.
November 2008

ProQuest LLC
789 East Eisenhower Parkway
P.O. Box 1346
Ann Arbor, MI 48106-1346

Acknowledgements

I would like to thanks to Prof. Cameron Jones for giving me the opportunity to start my PhD in his laboratory as well as his guidance, enthusiasm, support and encouragement over the last three years. I also would like to thank him and Dr. Andreas Stasch for the time and effort they put into X-ray crystallography.

Special thanks go to the members of the Jones group, for general support and help. Especially, I would like to thank Dr. Richard Rose, Dr. David P. Mills and Shaun P. Green.

Thanks also go to all the technical staff at Cardiff University and Monash University for their support in all general situations, such as supplying material, NMR teaching, SQUID and fixing breakages.

Thanks also have to go to Prof. Dr. Kynast at the University of Applied Science in Münster, Germany, who encouraged me to take the opportunity to come to Cardiff in the first place.

Last but not least I would like to thank my parents, sisters and my grandmother for their support in many ways so far and hopefully in times to come.

Abstract

The work presented in this thesis is split into two chapters. The first chapter involves the studies of the chemistry of phosphaalkynes and the second chapter involves the preparation and reactivity of transition metal(I) guanidinate and amidinate complexes.

The introduction to the first chapter gives general information about the cycloaddition, co-ordination as well as oligomerisation chemistry of phosphaalkynes, and the preparation of the unhindered methyl-phosphaalkyne *via* a modified literature preparation. Part 1.3.1 shows the reaction of P≡CMe and its bulkier analogue P≡CBu^t with 2,4,6-tri-*tert*-butyl-1,3,5-triphosphabenzene and 1,3,5,7-tetraphosphabarrelene, giving differing cycloaddition and oligomerisation products. Part 1.3.2 discusses the reaction of P≡CMe with diazomethane, TMS- and 1-adamantyl-azide. Cycloaddition products were isolated and similarities with their bulkier and less bulkier phosphaalkyne analogues were highlighted and discussed. Part 1.3.3 describes the reaction of P≡CMe with $R_2E{=}ER_2$ (E = Ge or Sn, R = -$CH(SiMe_3)_2$) and $Ar_2Sn{=}SnAr_2$ (Ar = $C_6H_2Pr^i_3$-2,4,6), showing co-ordination and cycloaddition products in which a 1,3-hydrogen migration has taken place. Differences to the products from their bulkier phosphaalkyne analogues were observed and discussed. Part 1.3.4 describes the reaction of $[Cp_2Ti(NNPh_2)(py)]$ with P≡CBu^t, giving the first cycloaddition product of any transition metal hydrazide complex. Part 1.3.5 describes the cycloaddition reaction of $[W(CO)_5(THF)]$ with P≡CMe and its bulkier phosphaalkyne analogues. Differences between head to tail and head to head cycloadditions are highlighted and discussed. Part 1.3.6 shows a rare phosphaalkyne η^1-co-ordination complex formed by reacting P≡CMe with $[MH(dppe)_2]^-$ (M = Ru or Fe). The results have been compared to those from bulkier phosphaalkynes. Part 1.3.7 shows the reductive coupling reaction of a samarium(II) complex with P≡CBu^t. The resulting product was compared to similar products from reactions with alkynes and nitriles. Part 1.3.8 shows the co-ordination and cycloaddition reactions of P≡CMe with $[Pt(PCy_3)_2(\eta^2\text{-}C_2H_4)]$ and $[Pt(P\text{-}P)(\eta^2\text{-}C_2H_4)]$ (P-P = dppe or $(PEt_3)_2$). Different products have been observed and the results were compared with those from reactions with bulkier phosphaalkynes.

The introduction to the second chapter gives a general introduction to the β-diketiminate (nacnac), amidinate and guanidinate ligand systems and their main group and transition metal complexes, including those with the metal in the +1 oxidation state. Part 2.3.1 details the reduction of an iron(II) amidinate complex in a variety of solvents, under a dinitrogen or argon atmosphere. These gave iron(I) amidinate complexes. These were reacted with CO to give a iron(I) carbonyl complex. Similarities and differences with bulkier nacnac analogues have been investigated and were discussed. Part 2.3.2 shows the preparation of cobalt(II) amidinate and guanidinate halide complexes and their reduction in a variety of solvents under a dinitrogen atmosphere, giving cobalt(I) amidinate and guanidinate complexes. Those cobalt(I) complexes were reacted with CO, TMS-azide and 1-adamantyl-azide. Similarities and differences to their bulkier nacnac analogues have been investigated and were discussed. Part 2.3.3 shows the preparation of nickel(II) guanidinate halide complexes and their reduction in a variety of solvents under a dinitrogen atmosphere, giving nickel(I) guanidinate complexes. In addition, the guanidinate nickel(II) halide complexes were reacted with LiCp and the nickel(I) complexes with CO, TMS-azide and 1-adamantyl-azide. Similarities and differences to their bulkier nacnac analogues have been investigated and discussed.

A CD with CIF, INS and TEX files of the measured structures can be found at the end of this thesis

Chemical Science

A magazine providing a snapshot of the latest developments across the chemical sciences.

Unhindered phosphaalkyne Complexes

21 August 2006

The first complexes of a sterically unhindered phosphaalkyne have been studied by UK chemists.

Phosphaalkynes-molecules which contain a phosphorus-carbon triple bond are versatile starting materials for many reactions including the synthesis of organophosphorus cages, heterocycles and coordination complexes. Taking advantage of newly developed routes to the simple methyl phosphaalkyne, Cameron Jones and colleagues at Cardiff University have examined its coordination chemistry for the first time.

The chemistry of phosphaalkynes stabilised by bulky substituents has been a developing area for many years, but, despite its importance, the chemistry of the simple derivative methyl phosphaalkyne has remained unknown. According to Jones, this has been a goal for phosphorus chemists for some time and is particularly interesting because methyl phosphaalkyne is an analogue of propyne, which is an important industrial feedstock.

John Nixon, FRS, professor of chemistry at the University of Sussex, UK, and an expert in the coordination chemistry of phosphorus, is enthusiastic about the chemists' work. He explained that while the presence of bulky t-butyl groups in phosphaalkynes can provide kinetic stability, it also introduces its own steric effect on reaction pathways. 'Their initial results show that as well as exhibiting some similar behaviour to the t-butyl phosphaalkyne systems, other synthetic pathways can result using the much smaller methyl-containing derivative,' said Nixon.

One of the next challenges for chemists is the linear polymerisation of phosphaalkynes with the hope of finding useful optical or electronic properties. 'This has never been achieved because of the propensity of phosphaalkynes to form cyclic oligomers and cage complexes,' said Jones. 'With methyl phosphaalkyne, we see the potential to realise this goal.

Caroline Moore

Dalton Trans., **2006**, *31*, 3733

Inorganic Chemistry

ACS Publications

Unusual Reactivity of Methylphosphaalkyne (P≡CMe) ...

13 May 2007

Reactions of methylphosphaalkyne, PC≡Me, with a digermene, $R''_2Ge{=}GeR''_2$ ($R'' = -CH(SiMe_3)_2$), and two distannenes, $R''_2Sn{=}SnR''_2$ and $Ar'_2Sn{=}SnAr'_2$ ($Ar' = C_6H_2Pr^i_3$-2,4,6), have given moderate to high yields of the first bridged 2,3,5,6-tetraphospha-1,4-dimethylidenecyclohexanes, $[R_2E\{C(Me)(H)PC(=CH_2)P\}]_2$ (R = R″ or Ar′, E = Sn or Ge), all of which have been structurally characterized. Their mechanisms of formation are thought to involve successive [2 + 1] and [2 + 2] phosphaalkyne cycloaddition, heterocycle rearrangement, phosphaalkene/vinylphosphine tautomerization, and intermolecular hydrophosphination reactions. In one reaction, two intermediates have been spectroscopically observed and one trapped by coordination to one or two $W(CO)_5$ fragments, yielding the first diphosphagermole complexes, $\{[W(CO)_5]_{1or2}\{R''_2Ge[C(Me)PC(Me)P]\}]$, which have been structurally characterized. Differences between the reactivities of P≡CMe and P≡CBu^t are highlighted.

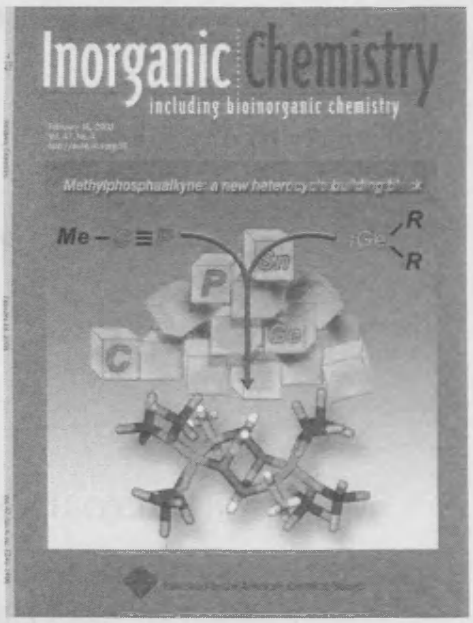

Inorg. Chem., **2008**, *47*, 1273

Abbreviations

Å	Angstrom units, 10^{-10} m
Ad	1-Adamantyl
anal.	Analysis
Ar	A general aromatic substituent
b.p.	Boiling point
br.	Broad
Bu^n	Normal butyl
Bu^t	Tertiary butyl
ca.	Approximately
cm^{-1}	Wavenumber unit for frequency (= v/c)
calc.	Calculated value
cf.	Compare with
cm	10^{-2} m
cm^3	ml
COD	1,5-Cyclooctadiene
COT	Cyclooctatetraene
Cp*	1,2,3,4,5-Pentamethylcyclopentadienyl
crypt[222]	hexaoxa-1,10-diazabicyclo[8.8.8]hexacosane
Cy	Cyclohexyl
Cp	Cyclopentyl
d	Doublet
DBU	1,8-Diazabicyclo[5.4.0]undecene-7
DCM	Dichloromethane
dd	Doublet of doublets
dec.	Decomposes
δ (Delta)	Chemical shift in ppm
Diglyme	Diethylene glycol dimethyl ether, $CH_3O(CH_2CH_2O)_2CH_3$
Dipp	2,6-diisopropylphenyl
DPPE	Bis(Diphenylphosphino)ethane-P,P'
e	Electron
E	A general non-metal

Et_2O	Diethylether
EI/CI	Electron impact / chemical ionisation
Et	Ethyl
Fc	Ferrocene ($[Fe(\eta^5\text{-}C_5H_5)_2]$)
g	Grams
η^n	Hapticity, through n atoms
HOMO	Highest occupied molecular orbital
Hz	Hertz, s^{-1}
ipso	ipso-substituent
IR	Infrared
$^nJ_{xy}$	Coupling constant between nuclei X and Y, over n bonds, in Hz
L	A general ligand
LUMO	Lowest unoccupied molecular orbital
M	A general metal or concentration in moles per litre
m.	Multiplet
M^+	Molecular ion
Me	Methyl
μ	Symbol for bridging ligands
Me	Methyl
Mes	1,3,5-Trimethylphenyl
Mes*	1,3,5-Tri-*tert*-butylphenyl
meta	meta-substituent
ml	Millilitres
MO	Molecular orbital
m.p.	Melting point
MS(APCI)	Atmospheric Presure Chemical Ionisation Mass Spectroscopy
MS(EI)	Electron Ionisation Mass Spectroscopy
MW	Molecular weight
nm	10^{-9} m
NMR	Nuclear magnetic resonance
ortho	ortho-substituent
OTf^-	Triflate anion
para	para-substituent
Ph	Phenyl

ppm	Parts per million
Pr^i	Isopropyl
Pr^n	Normal propyl
q	Quartet
R	A general non-aromatic organic substituent
RT	room temperature
s	Singlet or strong
sept	septet
Tetraglyme	Tetraethylene glycol dimethyl ether, $CH_3O(CH_2CH_2O)_4CH_3$
THF	Tetrahydrofuran
TLC	Thin layer chromatography
TMS	Trimethylsilyl
tr.	Triplet
υ	Frequency
UV	Ultra violet
X	Halide

1. Co-ordination and Cycloaddition Chemistry of Methyl- and *Tert*-butyl-Phosphaalkyne

1.1 Introduction

It was *Becker et al.* in 1981 who published the preparation of the first room temperature stable phosphaalkyne, P≡CBu^t.[1] Since then, phosphaalkynes have developed from being chemical curiosities to multifaceted synthons, that are now widely used for the preparation of organophosphorus cages, heterocyclic and acyclic compounds[2, 3] as well as phospha-organometallic, coordination and cycloaddition complexes. As there are over 700 publications on P≡CBu^t to date, this and other hindered phosphaalkynes have shown their synthetic versatility and have proven to be much more alkyne than nitrile-like in their reactivity. Although hindered phosphaalkynes have been investigated for over two decades, unhindered phosphaalkynes, *e.g.* P≡CH or P≡CMe, are still largely unexplored. To show differences and similarities between hindered and unhindered phosphaalkynes, a study of the reactivity of the unhindered phosphaalkyne, P≡CMe, with a variety of reagents were carried out. This study forms the basis of this chapter.

1.1.1 Phosphaalkyne Chemistry

The first experimental evidence for a phosphaalkyne (P≡CH) was found by *Gier* in 1961, by performing an experiment in which phosphine (PH_3) was subjected to an electronic arc struck between two graphite electrodes. By condensing the product at -196 °C, he was able to identify methylidynephosphane (P≡CH) by IR

spectroscopy. P≡CH can be stored at temperatures below -124 °C, but above this temperature it polymerises.[4] However, it can be stored under reduced pressure to up to 20 °C without polymerisation, or for a shorter period as a toluene solution below -70 °C over two days. It is worth mentioning, that the evidence for the structure of P≡CH, was obtained by reacting it with anhydrous HCl, which yielded only CH_3PCl_2. Years later, different phosphaalkynes were identified, *e.g.* P≡CMe, which was prepared in 1976,[5, 6] or $P{\equiv}CSiMe_3$ prepared in 1981.[7] Most importantly, *Becker et al.* reported in 1981 the first kinetically stabilized phosphaalkyne, $P{\equiv}CBu^t$ **(1) (Scheme 1)**.[1]

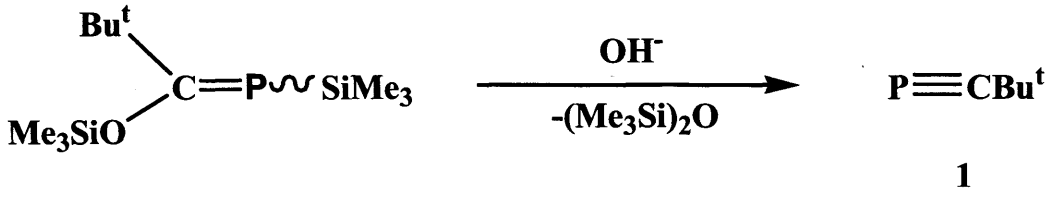

Scheme 1 Preparation of $P{\equiv}CBu^t$

$P{\equiv}CBu^t$ is a stable colourless liquid, with a boiling point of 61 °C, and is the most widely used of all phosphaalkynes. A high precision low temperature X-ray diffraction study of $P{\equiv}CBu^t$ revealed that its lone pair is located much closer to the P atom than in the phosphaalkene precursor,[8] and the P≡C bond length was found to be 1.548 Å.[9] The HOMO of this phosphaalkyne involves the π-bonding orbitals of the PC triple bond and not the P lone pair, a situation which strongly suggests that phosphaalkynes would be expected to have a chemistry closely related to that of alkynes instead of nitriles.[10, 11] Thus, the P≡C bond in phosphaalkynes is polarised in the sense $P^{\delta+}C^{\delta-}$ and it has been established that in spite of the presence of the P lone pair, protonation of $P{\equiv}CBu^t$ occurs exclusively at the carbon centre.[12]

Nixon et al. prepared the unhindered phosphaalkyne, P≡CMe (**2**) in 1976 by pyrolysis of ethyldichlorophosphine vapour at low pressure which flowed slowly through to a 900 °C hot quartz tube and was identified by a microwave spectroscopy (**Scheme 2**).[5]

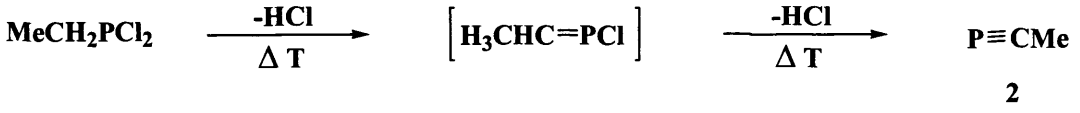

Scheme 2 Preparation of P≡CMe

Since then, a variety of different routes to prepare unhindered phosphaalkynes have been published. These preparations mostly involve VGSR (Vacuum Gas-Solid Reaction) conditions and require high temperature, high vacuum and a HCl absorbing compound *e.g.* K_2CO_3. *Guillemin at al.* published in 2001 a different way of preparing unhindered phosphaalkynes, *e.g.* P≡CR, (R = H, CH_3, Et, Bu^n), under standard conditions by chemoselective reductions of phosphonates with $AlHCl_2$, followed by HCl elimination reactions with a strong Lewis base (DBU) (**Scheme 3**).[13-16] The unhindered phosphaalkyne, P≡CMe, is a colourless liquid with a freezing point of ca. -90 °C and a boiling point of ca. 20 – 30 °C. P≡CMe is extremely pyrophoric but not moisture sensitive. It is known that pure P≡CMe is unstable at room temperature and even polymerises upon storing as a pure sample at -80 °C over days. However, as a diethylether solution, P≡CMe is stable at room temperature for days and can even be stored at -20 °C for a month before decomposition starts.

[1986]

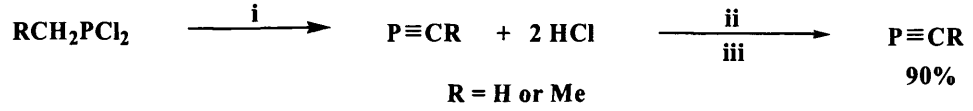

i = 10^{-3} torr, 3.5 cm i.d. x 90 cm quartz tube, 750°C
ii = horizontal half-filled column of 1,3,5-tricylohexylhexahydro-triazine
iii = cold trap at -120°C

[1991]

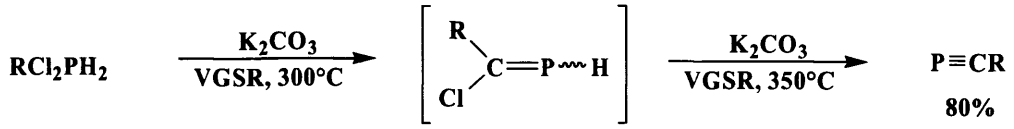

[1992]

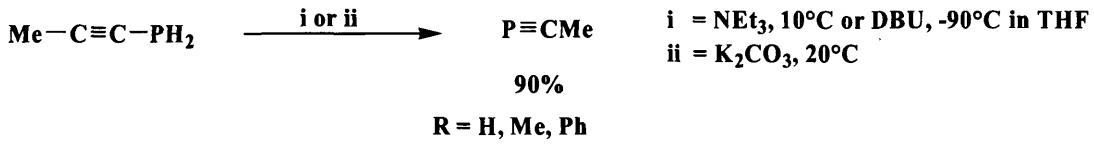

[2001]

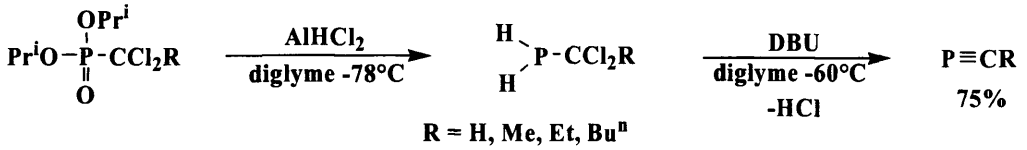

[2002]

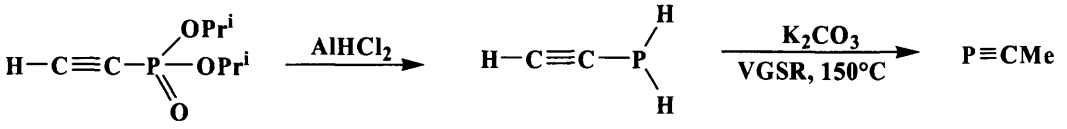

Scheme 3 A variety of ways to prepare unhindered phosphaalkynes

The theoretically optimised structure of P≡CMe shows a C−C≡P angle of 179.9° and a P≡C bond length between 1.549 to 1.557 Å.[17, 18] This is slightly longer than that of the hindered phosphaalkyne P≡CBu^t (1.548 Å).[9] The first ionisation energy, which is associated with electron excitation from the π(C≡P) bonding orbital

and not the σ non-bonding orbital, was calculated to be 9.84 eV for P≡CMe,[19, 20] and 9.61 eV for P≡CBu^t.[10] Studies have shown that the phosphaalkyne, P≡CMe, is more acidic than P≡CH, N≡CMe,[16, 18] and P≡CBu^t. The stretching vibration of the P≡C bond was found at 1559 cm $^{-1}$ for P≡CMe[15, 17, 21, 22] and 1543 cm $^{-1}$ for P≡CBu^t in their IR spectra.[1] The P≡C bond in P≡CMe is also polarised in the sense ($P^{\delta+}C^{\delta-}$)[18, 23] and calculations have shown that the stretching forces for the generalized P≡C, P=C and P–C bonds are 915 – 987, 512 – 598 and 266 – 284 Nm $^{-1}$.[21] Moreover, the phosphaalkyne, P≡CMe, has been calculated to be the global minimum of the various C_2H_3P isomers by 17 – 30 kcal/mol (**Figure 1**).[24]

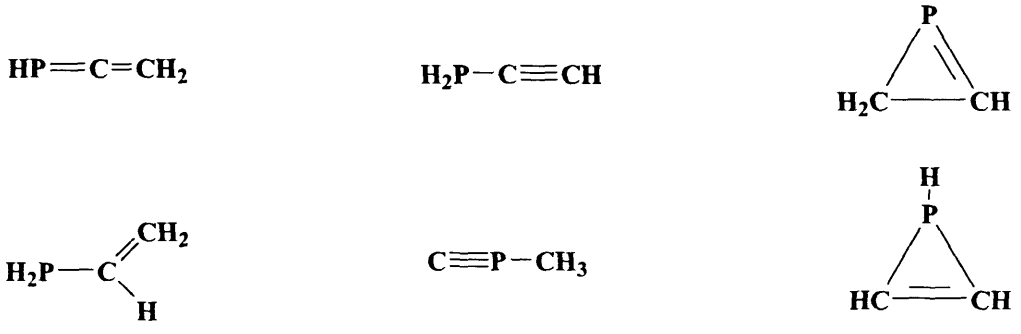

Figure 1 C_2H_3P optimised isomers

1.1.1.1 Co-ordination Chemistry

Phosphaalkynes have five possible modes of co-ordination to metal centres.[25, 26] Type **A** co-ordination occurs solely *via* the phosphorus lone pair,[27] while type **B** involves a side on co-ordination through the P-C triple bond in an η^2-fashion, which is commonly observed for alkyne co-ordination.[28] Type **C** is a combination of both **A** and **B** type co-ordination modes.

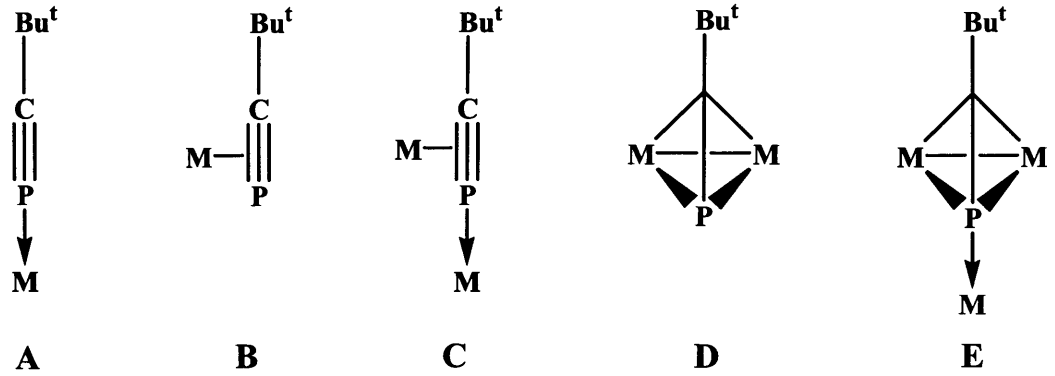

Figure 2 Co-ordination modes of phosphaalkynes

In **D** the phosphaalkyne acts as a η^2-bridge[29] and in **E** the phosphaalkyne acts simultaneously as η^2-bridge and electron pair donor (**Figure 2**).[30] The η^1-co-ordination of type **A** is the most uncommon, as the phosphaalkyne is poorly nucleophilic ($P^{\delta+}C^{\delta-}$). As a result, this mode requires bulky precursor complexes, in which an end on coordination of the linear phosphaalkyne into a sterically hindered pocket (*e.g.* that of **6**) is the only way for the phosphaalkyne to coordinate (**Figure 3**).[27] Therefore η^2-co-ordination is favoured over η^1-co-ordination, as for example, in compound **3**. Examples of type **D** and **E** coordination complexes are shown in **4** and **5** (**Figure 3**).[28]

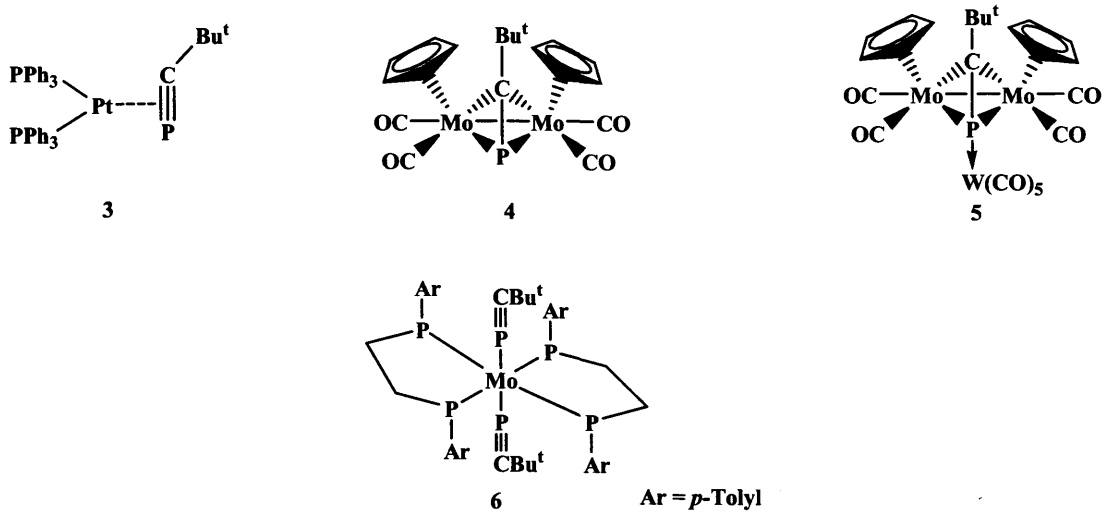

Figure 3 η^2- and η^1-co-ordination of $P{\equiv}CBu^t$ in Pt and Mo metal complexes

An interesting general feature of complexes of type **B** is their longer phosphorus-carbon distance compared to that of the free phosphaalkyne [1.548(1) Å in P≡CBu^t].[28] This phosphorus-carbon distance is an effect of the donation of π-electron density from the phosphaalkyne to the metal centre and back donation of metal d-electron density into the empty π* LUMO of the phosphaalkyne which leads to a reduction in the phosphorus-carbon bond order. This is reflected in a bending away of the *tert*-butyl group from linearity, which indicates an change in the hybridization of the phosphorus and carbon centres from sp to sp^2.[8] The lengthening of the phosphorus-carbon bond in η^2-complexes is in contrast to the phosphorus-carbon bond length of η^1-complexes which is close to that in the free phosphaalkyne and consistent with bonding through the phosphorus lone pair.[27] Type **D**[28, 29] and **E**[31, 32] complexes, *e.g.* **4** and **5**, are known, in which the phosphaalkyne can be viewed as a four or six electron donor respectively.

1.1.1.2 Cycloaddition Chemistry

Like alkynes, phosphaalkynes have the potential to readily undergo [2 + 1], [2 + 2], [3 + 2] and [4 + 2] cycloadditions with transition metal and main group fragments to give an interesting spectrum of novel heterocyclic compounds.[33, 34]

The [2 + 1] cycloadditions involving P≡CBu^t with one equivalent of the bulky heavier carbene analogous :ER$_2$ (**7a-c**) (E = Si, Ge; R = Bu^t, Mes, C$_6$H$_2${CH(SiMe$_3$)$_2$}$_3$-2,4,6, CH(SiMe$_3$)$_2$), give three-membered heterocycles, **8a-c**, containing P=C bonds which are able to undergo subsequent rearrangements. Reacting P≡CR (R = Ad or 2-methylcyclohexyl), with one equivalent of **9** forms product **11** *via* two [1 + 2] cycloaddition steps (**Scheme 4**).[35-38]

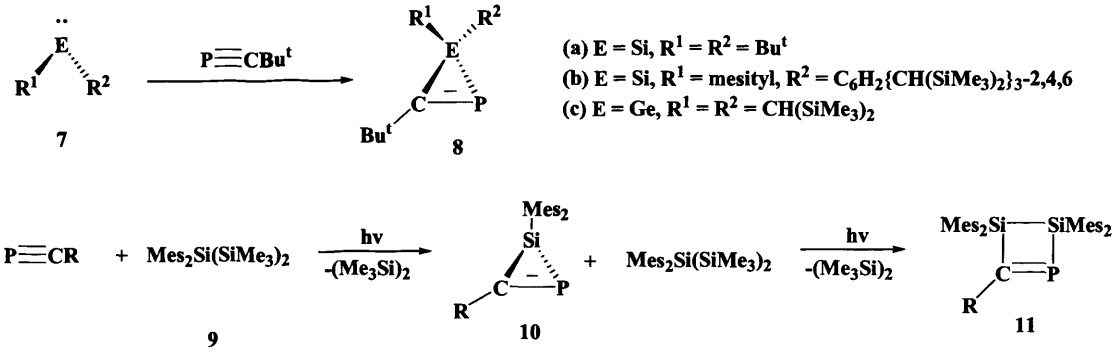

Scheme 4 [2 + 1] cycloadditions of P≡CR with group 14 precursors

[2 + 2] cycloadditions are often initiated by low coordination metal complexes. For example, one equivalent of P≡CBu^t reacts with one equivalent of [Sn{CH(SiMe$_3$)$_2$}$_2$]$_2$ (**12**) to form the four-membered heterocycle **13** (**Scheme 5**).[39]

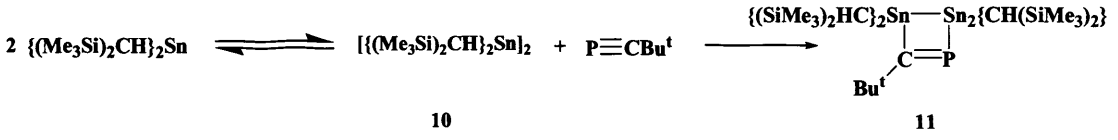

Scheme 5 [2 + 2] cycloaddition of P≡CBu^t with [Sn{CH(SiMe$_3$)$_2$}$_2$]$_2$

P≡CBu^t reacts with diazomethanes (**14a-f**) to form exclusively 3-*H*-1,2,4-diazaphosphole products (**16a-f**) *via* [3 + 2] cycloadditions in almost quantitative yields. Steric factors are typically found not to oppose the electronic factors of these reactions (**Scheme 6**). [3 + 2] cycloaddition reactions with alkylazides have also been reported.[40-43]

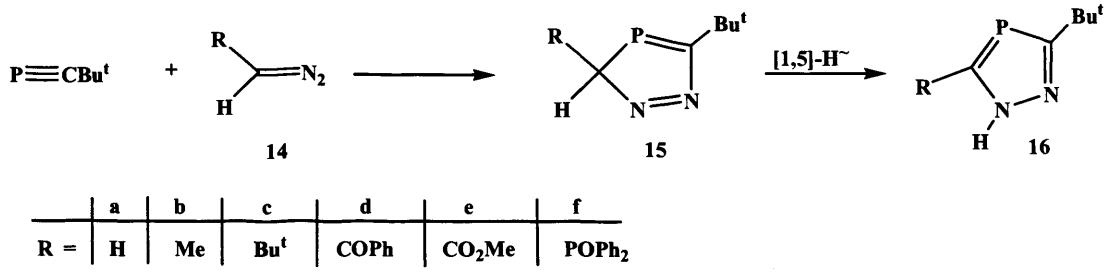

	a	b	c	d	e	f
R =	H	Me	Bu^t	COPh	CO_2Me	$POPh_2$

Scheme 6 [3 + 2] cycloadditions of P≡CBu^t with diazomethanes

An example of a [4 + 2] cycloaddition is the reaction of one equivalent of P≡CBu^t with one equivalent of 2,4,6-tri-*tert*-butyl-1,3,5-triphosphabenzene **17**[44] to form the 1,3,5,7-tetraphosphabarrelene (**18**) (**Scheme 7**).[45]

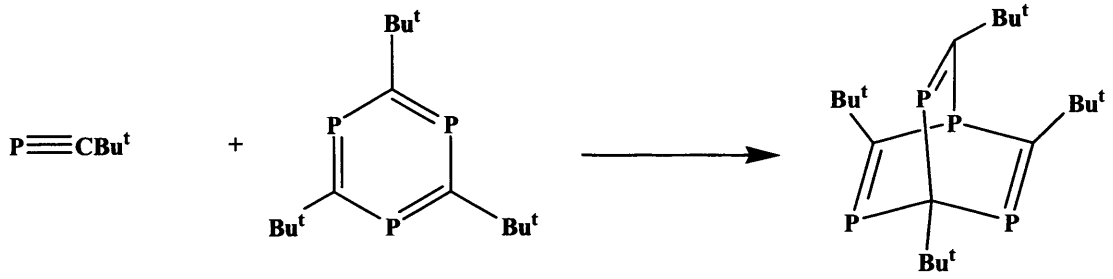

17 **18**

Scheme 7 A [4 + 2] cycloaddition of P≡CBu^t with a triphosphabenzene

1.1.1.3 Oligomerisation Chemistry

Phosphaalkynes have the ability to undergo metal mediated cyclooligomerisation reactions[25, 26] and have shown similar behaviour to that of alkynes in this respect.[34] For example, [M(η^5-C_5R_5)(η^2-C_2H_4)$_2$] (R = H, M = Co, Rh; R = Me, M = Co, Rh, Ir) (**19**) react with two equivalents of P≡CBu^t to give the 1,3-diphosphacyclobutadiene complexes (**20a-e**) *via* head to tail couplings (**Scheme 8**).[46] It is worth mentioning that theoretical studies have predicted that head to head dimerisations (to give 1,2-diphosphabicyclobutadienes) are more favourable, but most experimental studies shown only 1,3-diphosphacyclobutadiene ring formations, which is probably due to steric reasons (see also 1.3.5).[46, 47]

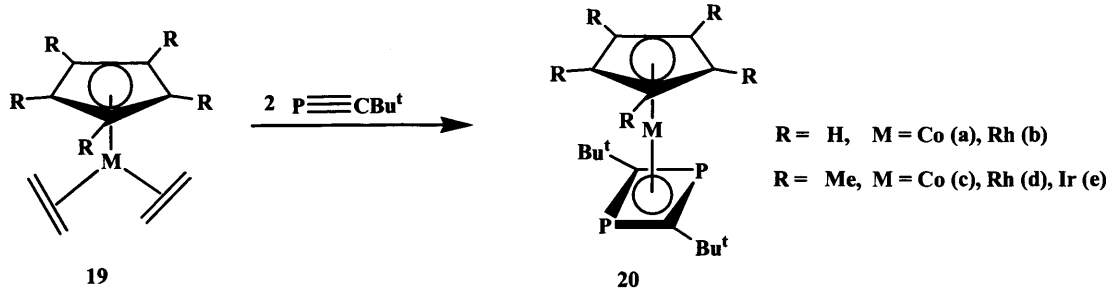

19 20

Scheme 8 Cyclodimerisations of P≡CBu^t by Co, Rh and Ir precursors

Theoretical and photoelectron studies on (**20a**) and [Fe(η^4-1,3-$P_2C_2Bu^t_2$)$(CO)_3$] have indicated that the diphosphacyclobutadiene moiety is bound more strongly than the η^4-cyclobutadiene unit of related hydrocarbon complexes.[48] It is therefore no surprise that liberation of the diphosphacyclobutadiene fragment of the complexes **20a-e** has not been achieved to date.

Three equivalents of P≡CBu^t have been reacted with [Hf(η^8-COT)(η^4-CH2=CHCH=CH_2)] (**21**) at -78 °C to give complex **22** which contains a cyclic trimer of P≡CBu^t. After treating **22** with hexachloroethane, 2,4,6-tri-*tert*-butyl-1,3,5-triphosphabenzene (**17**) was obtained in 53 % yield (**Scheme 9**).[49]

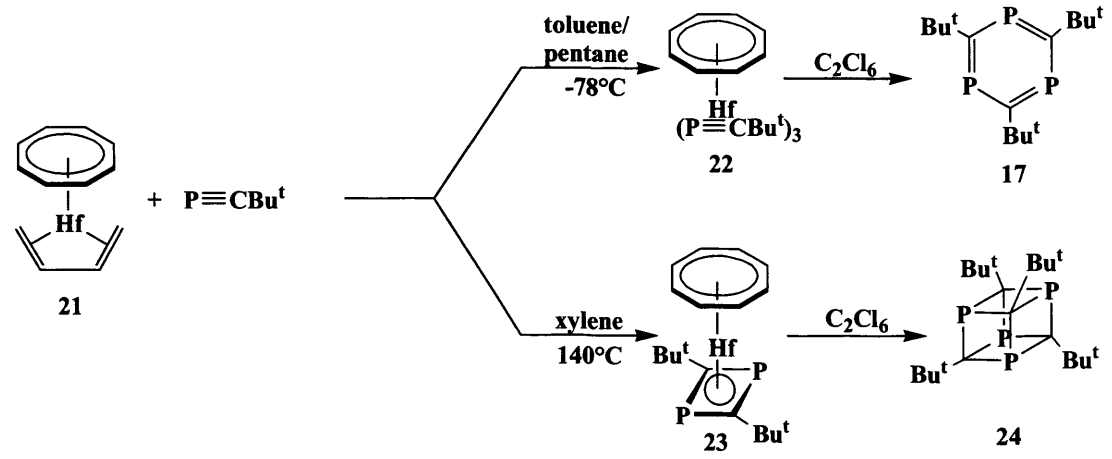

21 22 17 23 24

Scheme 9 Cyclooligomerisations of P≡CBu^t by a Hf precursor

Treatment of **21** with two equivalents of P≡CBu^t yields a complex containing a COT ligand and a head to tail coupled 1,3-diphosphacyclobutadiene fragment at the metal centre (**23**). Further treatment with hexachloroethane liberated

the 1,3-diphosphacyclobutadiene which undergoes a series of cycloadditions to give the tetraphosphacubane (**24**) in a 34 % yield (**Scheme 9**).[50] 2,4,6-tri-*tert*-butyl-1,3,5-triphosphabenzene (**17**) can also be prepared by reacting $P{\equiv}CBu^t$ with the strong Lewis acid $Bu^tN{=}VCl_3$ in toluene from -75 to 25 °C. In this reaction compound **17** was isolated in a 68% yield (**Scheme 10**).[44]

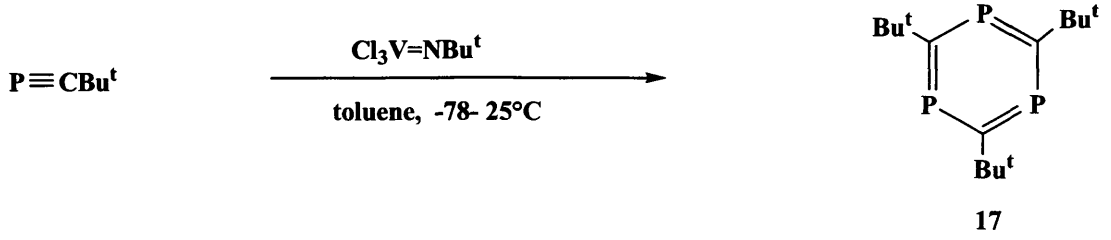

17

Scheme 10 Preparation of 2,4,6-tri-*tert*-butyl-1,3,5-triphosphabenzene by $Cl_3V{=}NBu^t$

The zirconium complex, **26**, was synthesised by the reaction of zirconocene dichloride (**25**) with $P{\equiv}CBu^t$ in the presence of Bu^nLi, in a 70 % yield. [51] When **26** is treated with hexachlorethane in benzene, **24** is formed over 5 days in a 70 % yield. Treatment of **26** with $[(PPh_3)_2NiCl_2]$ affords a further isomer of **24**, namely **27** (**Scheme 11**).[52]

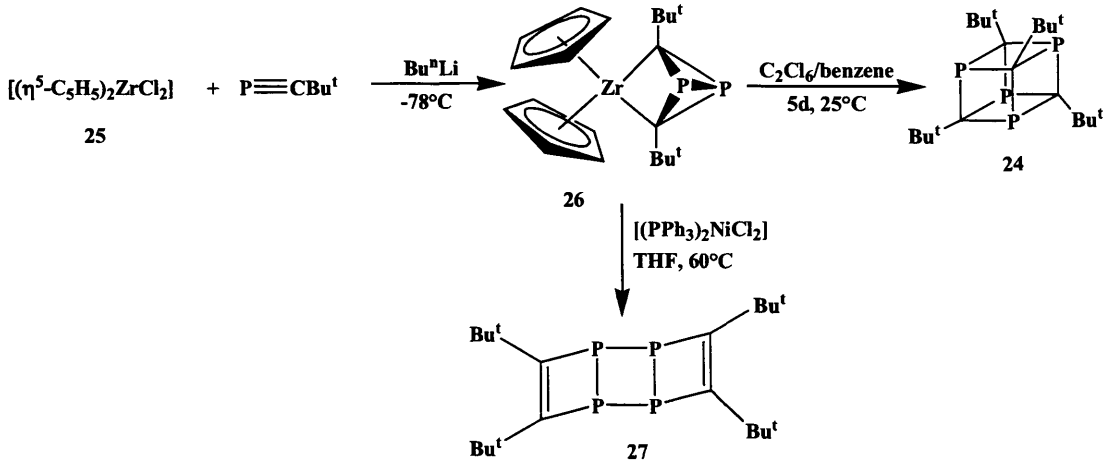

Scheme 11 $P{\equiv}CBu^t$ tetramerisations by a Zr precursor

In 1995 *Binger et al.* reported the hafnium complex **28**. Treatment of **28** with $P{\equiv}CBu^t$ yields the 1,3,5,7-tetraphosphabarrelene complex **29** in a 88 % yield.

Treatment of complex **29** with hexachloroethane gives the tetraphosphabarrelene (**18**) in a 88 % yield.[45] This compound (**18**) is air sensitive but thermally stable (**Scheme 12**).

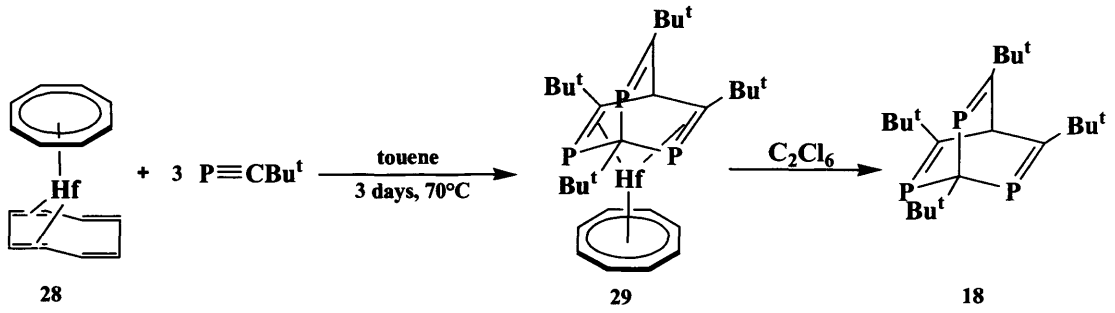

Scheme 12 Tetramerisation of P≡CBu^t by a Hf precursor

Binger et al. also reported, in 1987 and 1991, the cyclodimerisation of a phosphaalkyne with alkynes within the co-ordination sphere of transition metals[53, 54] **(Scheme 13).**

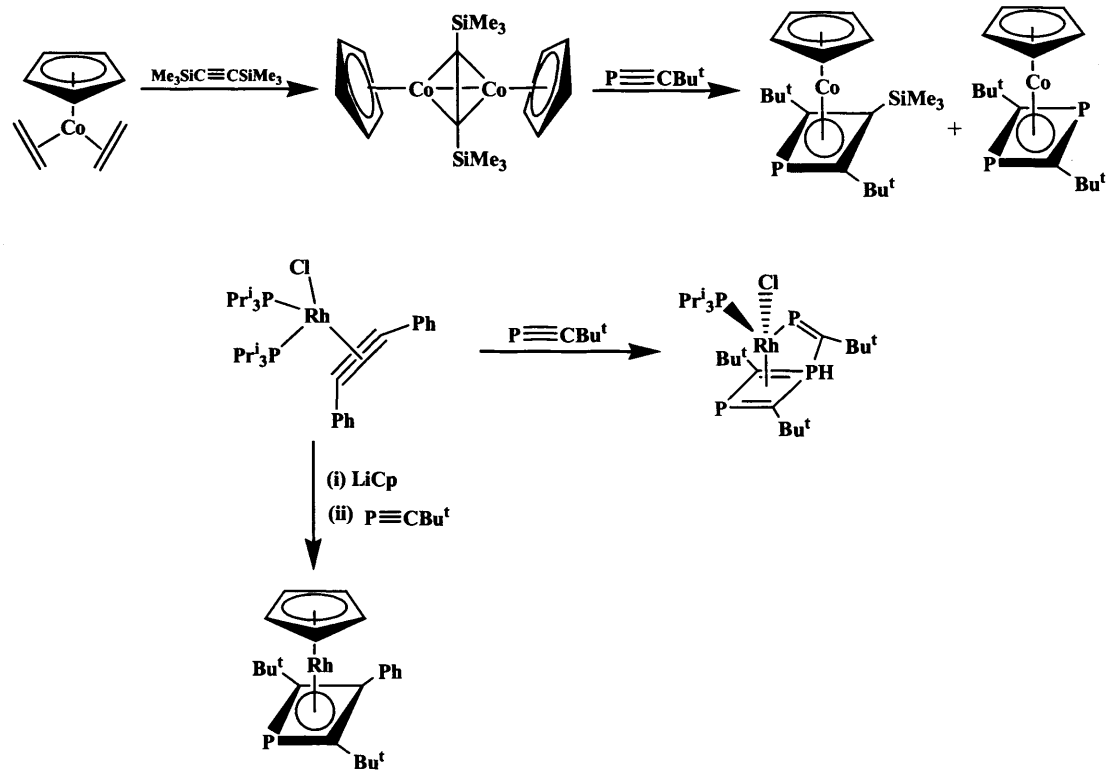

Scheme 13 Dimerisations of P≡CBu^t with alkynes bound to transition metal centres

Phosphaalkyne oligomerisations have also be observed in the absence of any metal centre. For example, heating $P{\equiv}CBu^t$ at 180 °C forms a mixture of products which include the tetraphosphacubane **24** (**Scheme 14**).[55]

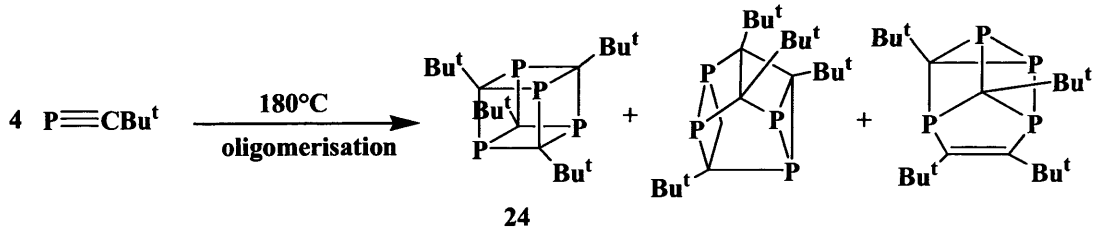

Scheme 14 Solvent free oligomerisations of $P{\equiv}CBu^t$

Oligomerisation of $P{\equiv}CBu^t$ in the presence of reactive elemental metals has also proved facile when utilising metal vapour synthesis as a technique. Here, phosphaalkyne is co-condensed at -196 °C with metal vapours. Upon warming to 25 °C a variety of novel phosphaorganometallic compounds are often formed.[56-58]

Examples of phosphaalkyne penta- and hexamers can also be found in the literature. For example a pentamer can be formed by reacting three equivalents of [Li][1,2,4-triphophacyclopentadienyl] (**30**) and two equivalents of [Li][1,3-diphosphophentacyclopentadienyl] (**31**) in DME with an excess of $FeCl_3$ or $CoBr_3$.[59] These reactions give the pentaphosphorus cage **32** in a 24% yield *via* oxidative coupling reactions. The five phosphorus atoms in product **32** are contained in two five-membered rings, three four-membered rings, and one three-membered ring.

The only known hexamer is formed on reacting **30** and **31** with $[PtCl_2(cod)]$ gave the hexaphosphorus cage, **33**, along with two pentaphosphorus cages,the known cage **32** and the new protonated cage **34** (**Scheme 15**).[60]

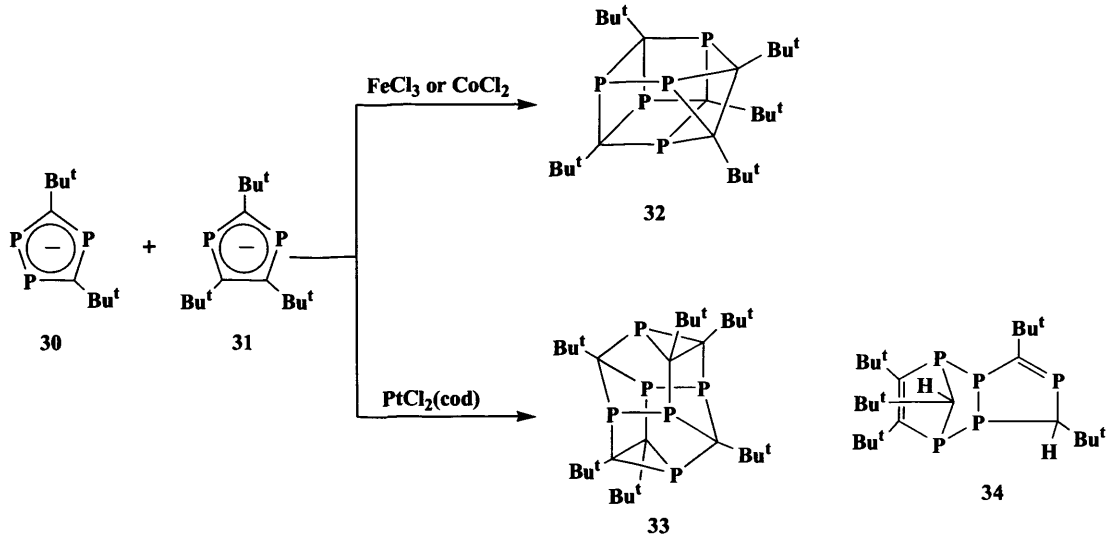

Scheme 15 Preparation of phosphaalkyne oligomers

1.1.1.4 Polymerisation Chemistry

In 2002, *Wright* and *Gates* published a report on a π-conjugated macromolecule, poly(*p*-phenylenephosphaalkene) **36**, which was prepared by a thermally induced polycondensation of the two bifunctional monomers, 2,3,5,6-tetramethylterephthaloyl dichloride and 1,4-bis-(1,1,1,3,3,3-hexamethyldisilaphosphan-2-yl)benzene.[61] The polymeric compound, **36**, may be regarded as the first phosphorus analogue of the now well known conjugated poly(*p*-phenylenevinylenes) (**35**), which have drawn attention due to the electroluminescence they often exhibit (**Figure 4**).[62, 63]

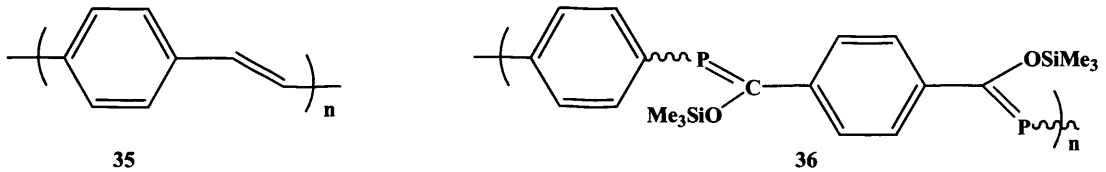

Figure 4 π-conjugated marcromolecules

Just two years later in 2004, *Smith* and *Protasiewicz* reported two further thermally stable low coordinate phosphorus polymers, **37** and **38**, (**Figure 5**).

Compound **38** is the first example of a polymer featuring multiple bonds between two heavier main group elements along a polymer backbone. This successful stabilization of diphosphene units suggests the possibility of stabilizing other, heavier, EE multiple bonds in a similar way. In this respect, an analogue of **38** having As=As units in the main chain has been prepared by the same group and is currently under investigation.[64]

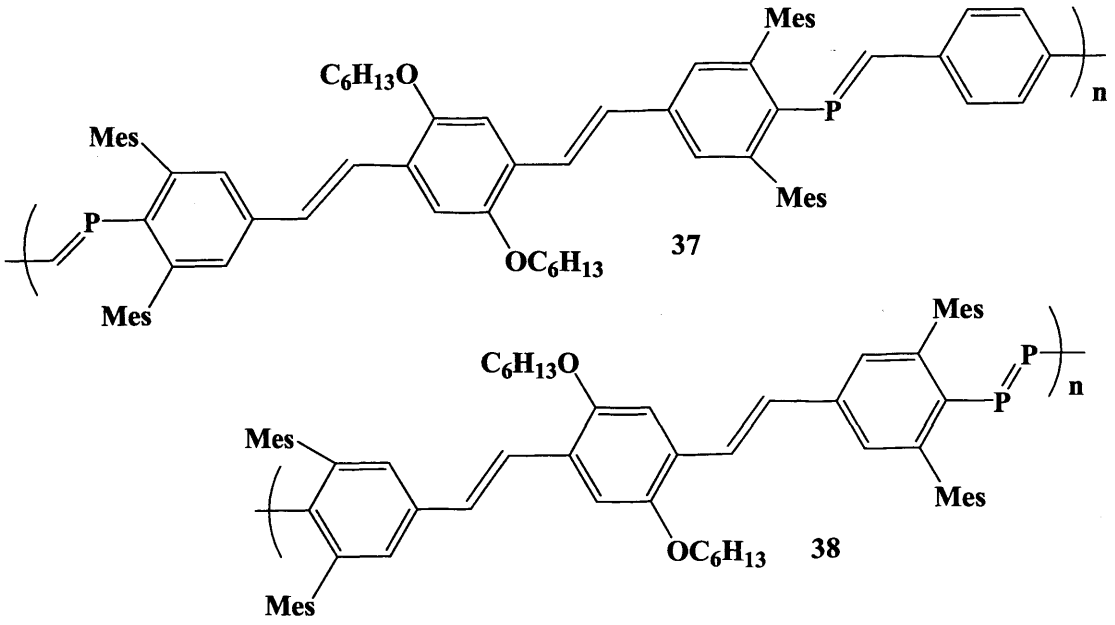

Figure 5 Low coordinate phosphorus polymers

The preparation of π-conjugated polymers incorporating phosphorus moieties opens the way for the preparation of a wide range of fundamental new materials.[65] Their preparations may involve the large variety of reactions known for phosphaalkynes *e.g.* phosphorus coupling reactions or co-ordination complex formation.[26, 33]

1.1.2 The Preparation of P≡CMe

The unhindered phosphaalkyne, P≡CMe which is used in reactions described in this thesis has been prepared *via* the following literature route and was stored after purification as a diethylether solution at -25 °C.

Compound **40** was prepared by heating tri-*iso*-propyl phosphate (**39**) at reflux with a large excess of CCl_4 over 24 h, giving **40** in 90% yield.[66] Reacting a THF solution of **40** with Bu^nLi at low temperature followed by adding dimethyl sulfate at the same temperature gave **41** in a 70% yield (**Scheme 16**).[67]

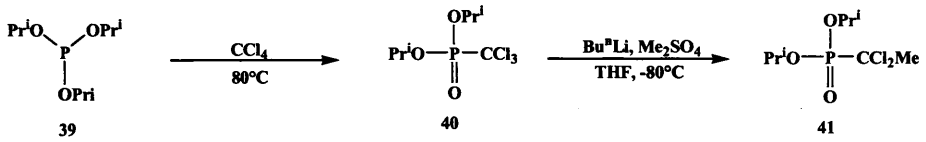

Scheme 16 Preparation of the phosphanate **40** and the phosphanate **41**

Compound **42** was prepared by reacting the phosphonate, **41**, with $AlHCl_2$ at -60 °C to give **42** in 90% yield. Treating **42** with DBU at low temperature leads to the unhindered phosphaalkyne, P≡CMe. To obtain pure samples of P≡CMe, diglyme should be used as solvent in the reduction and elimination steps. The mixture was fitted on a vacuum line equipped with two cold traps. The first one was cooled at -45 – -50 °C (acetone) to remove the solvent, while the second one cooled at -120 °C (ethanol) allowed the trapping of P≡CMe (**Scheme 17**). The low boiling compound was distilled in vacuuo (10^{-1} mbar). At the end of the distillation, this trap was disconnected from the vacuum line. Pure P≡CMe should be kept at low temperature (< -80 °C).[13]

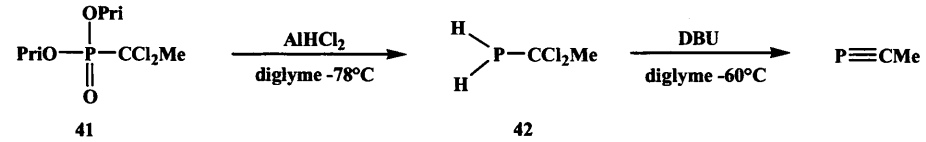

Scheme 17 Preparation of phosphine, **42**, and P≡CMe

1.2 Research Proposal

The chemistry of the hindered *tert*-butyl-phosphaalkyne (P≡CBu^t) has been investigated for over two decades. In its reactions with main group and transition metal precursors it undergoes co-ordination, cycloaddition, oligomerisation and polymerisation processes to give a variety of interesting complexes. Unhindered phosphaalkynes, *e.g.* P≡CH or P≡CMe, are still mostly unknown as reagents or reactants. This can by explained by their difficult preparation and handling, before *Guillemin et al.* reported a high yield, multi-gram synthesis for unhindered phosphaalkynes including P≡CMe in 2001.[13]

After discovering how to handle the very air and temperature sensitive phosphaalkyne, P≡CMe, *Guillemin* challenged chemists to begin the examination of the co-ordination, cycloaddition, oligomerisation and polymerisation reactions of this phosphaalkyne. With this aim in mind, an investigation to compare the chemistry of P≡CMe with its more hindered analogues and alkynes themselves were carried out. The results of this study from the basis of this chapter

1.3 Results and Discussion

1.3.1 Reactivity of Phosphaalkynes with a Triphosphabenzene and a Tetraphosphabarrelene

The previously reported thermally induced oligomerisation of P≡CBu^t ($^{31}P\{^1H\}$ NMR: δ = -67 ppm) by heating a neat sample of the phosphaalkyne to 180 °C led to a range of different oligomerisation products (**24**, **43** and **44**), including the phosphaalkyne tetramer **24** ($^{31}P\{^1H\}$ NMR: δ = 257.4 ppm) (**Scheme 18**). The mechanism of formation of compound **24** likely involves a head to tail [2 + 2] dimerisation of P≡CBu^t to yield a 1,3-diphosphacyclobutadiene, followed by a second dimerisation and an intermolecular [2 + 2] cycloaddition to form compound **24** (see 1.3.5 for mechanism).[25, 55] Investigations with the phosphaalkyne P≡CPh (**45**), have been carried out and show that it spontaneously oligomerises above 25 °C. This reaction leads to a range of unknown polyhedral oligomers (**46**) (**Scheme 18**). Although formation of linear oligomers would be unlikely if **45** oligomerises by cycloaddition mechanisms, the more modest steric requirements of the phenyl group may provide opportunities for the formation of higher molecular weight species such as ladder polymers, or even branched polymers analogous to polyphenylcarbyne.[68]

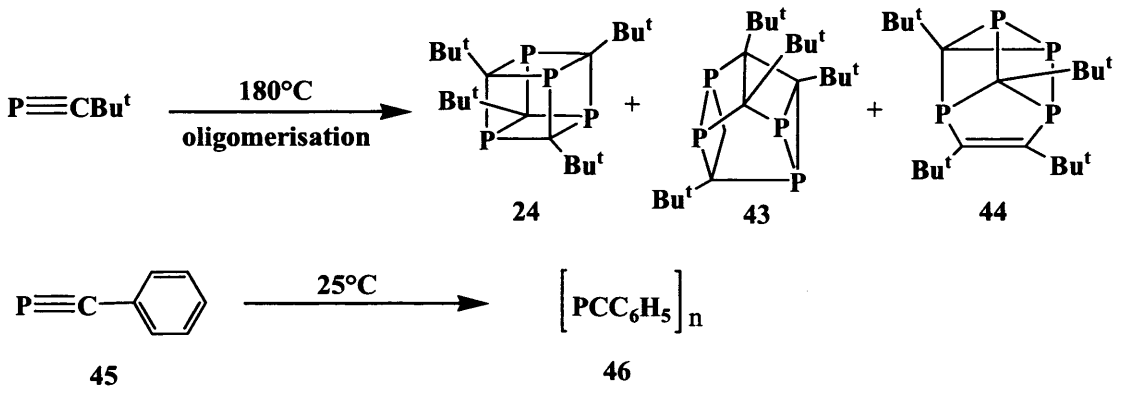

Scheme 18 Solvent free oligomerisation of phosphaalkynes

To compare the reactivity of P≡CMe with that of P≡CBu^t, a neat sample of P≡CMe was heated under reduced pressure at 50 °C and the reaction was monitored by $^{31}P\{^1H\}$ NMR spectroscopy. The $^{31}P\{^1H\}$ NMR spectrum showed many phosphorus containing products with resonances between 140 and -250 ppm. No unreacted P≡CMe was present in the mixture. Unlike the oligomerisation reaction of P≡CBu^t[25, 55] (**Scheme 18**), none of these products could be isolated or characterised. As a result, it was decided to compare the reactivity of these phosphaalkynes by their treatment with 2,4,6-tri-*tert*-butyl-1,3,5-triphosphabenzene (**17**)[44] and 1,3,5,7-tetraphosphabarrelene (**18**)[45]. These were thought good examples to understand the major differences in the reactivity between the unhindered phosphaalkyne, P≡CMe; and the hindered phosphaalkyne, P≡CBu^t.

It is well known, that 2,4,6-tri-*tert*-butyl-1,3,5-triphosphabenzene (**17**) reacts with one equivalent of P≡CBu^t *via* a [4 + 2] cycloaddition process at room temperature over 12 h to give the 1,3,5,7-tetraphosphabarrelene (**18**)[45] [$^{31}P\{^1H\}$ NMR: δ = -87 ppm (d, $^2J_{PP}$ = 35 Hz), 323 ppm (d, $^2J_{PP}$ = 12 Hz)] in almost quantitative yield.[44, 69] In a similar reaction, compound **17** [$^{31}P\{^1H\}$ NMR: δ = 133 ppm] was reacted with an excess of P≡CMe to give the mixed substituted species, **47**, in only 1 h and in a high isolated yield (66%) (**Scheme 19**). The $^{31}P\{^1H\}$ NMR spectrum of the compound exhibits two low field signals at 301 and 308 ppm corresponding to the P=C fragments, while three higher field resonances were observed at 60, 9.4 and – 100 ppm, all of which reveal J_{PP} couplings (*e.g.*, $^1J_{pp}$ = 176 Hz) in the expected ranges.[2, 3, 70]

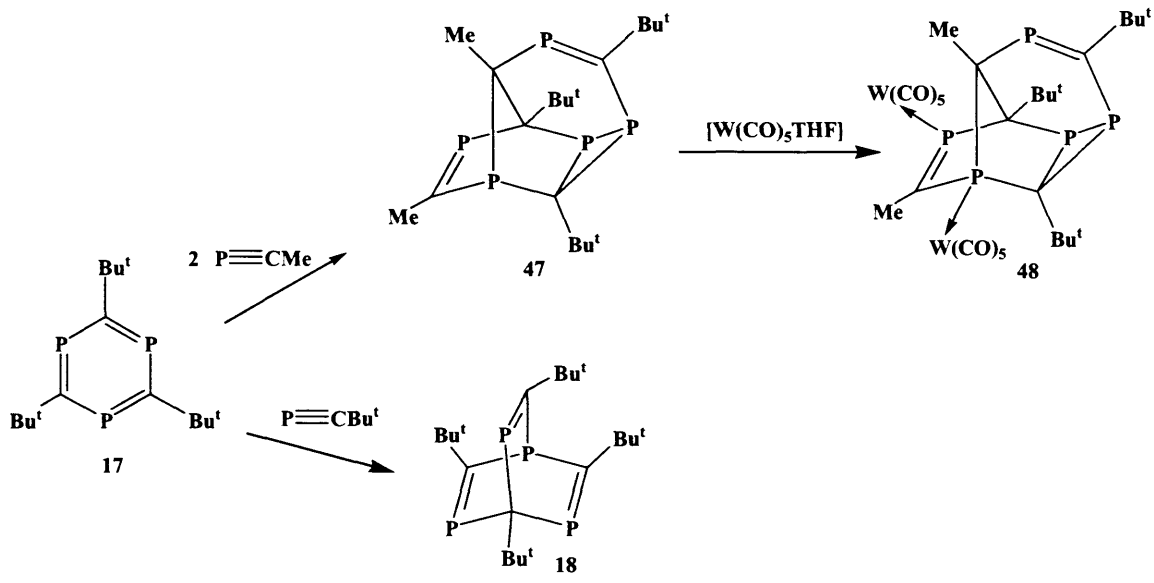

Scheme 19 Reaction of 17 with P≡CR (R = Me and Bu^t)

The rapid reaction of P≡CMe with **17** clearly illustrates that unhindered phosphaalkynes are much more reactive, and react differently, than sterically hindered phosphaalkynes. An attempt to react **17** with only one equivalent of P≡CMe was monitored by $^{31}P\{^1H\}$ NMR spectroscopy and showed the presence of **47** and the starting material, **17**, in a 50 : 50 ratio with no evidence of any intermediates. The absence of observed intermediates in this reaction eliminates the opportunity to explore its mechanism. However, it seems reasonable that the first reaction step involves a [4 + 2] cycloaddition of compound **17** with one equivalent of P≡CMe, to give a tetraphosphabarrelene analogous to **18**. It proved impossible to growe X-ray quality crystals of the cycloaddition product, **47**. To identify its core structure, it was reacted with $[W(CO)_5(THF)]$, followed by chromatographic workup (silica gel/hexane) to give compound **48** as an orange crystalline product (**Figure 6**).

The spectroscopic data for **47** and **48** are similar in that their ^1H NMR spectra each display signals due to the protons of their three chemically inequivalent *tert*-butyl groups and two methyl substituents. The $^{31}P\{^1H\}$ NMR spectrum of **48** exhibits two low field signals at 315 and 243 ppm corresponding to the P=C fragments, along

with three higher field signals at 72, 11.7 and -119 ppm, all of which reveal J_{PP} couplings ($^1J_{pp}$ = 180 Hz, $^2J_{pp}$ = 12 – 24 Hz) in the expected ranges.[2, 3, 70] In addition, two of the resonances (72 and 243 ppm) for **48** are flanked by ^{183}W satellites.

The molecular structure of **48** was determined by X-ray crystallography and its molecular structure is depicted in **Figure 6**. The structure reveals it to have a pentaphosphaisolumibullvalene cage core with two P-C double bonds [P(1)-C(1) 1.678(7) Å, P(5)-C(5) 1.673(7) Å], that are in the expected range. The P(1) and P(2) centres are both coordinated to $W(CO)_5$ fragments, seemingly because these are the least sterically hindered P-atoms.

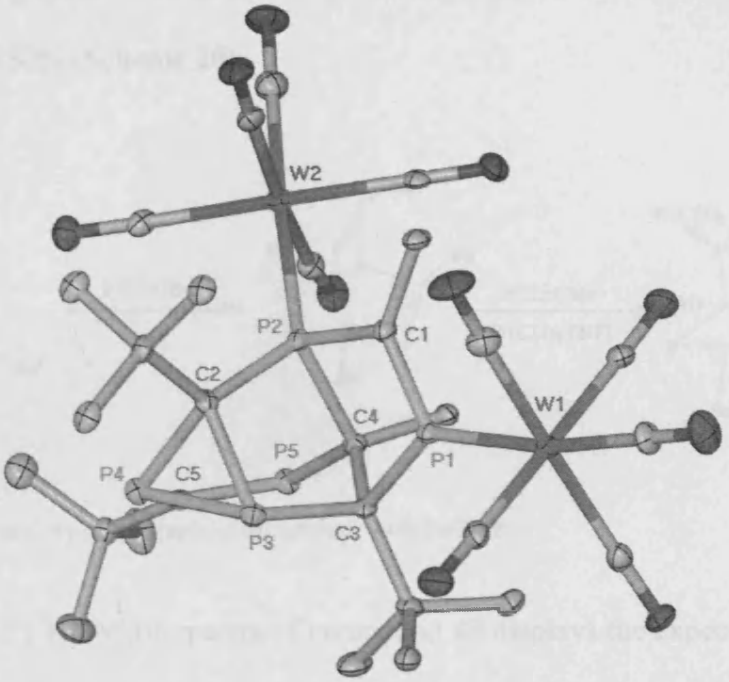

Figure 6 Molecular structure of **48** (hydrogen atoms omitted for clarity; ellipsoids shown at the 25% probability level).

Selected bond lengths (Å) and angles (°): W(1)-P(1) 2.495(2), W(2)-P(2) 2.551(2), P(1)-C(1) 1.678(7), P(1)-C(3) 1.921(7), P(2)-C(1) 1.836(7), P(2)-C(2) 1.866(7), P(2)-C(4) 1.877(7), P(3)-C(2) 1.862(7), P(3)-C(3) 1.902(7), P(3)-P(4) 2.239(3), P(4)-C(5) 1.814(7), P(4)-C(2) 1.881(7), P(5)-C(5) 1.673(7), P(5)-C(4) 1.875(8), C(3)-C(4) 1.544(10), C(1)-P(1)-C(3) 98.3(3), C(1)-P(2)-C(2) 99.9(3), C(1)-P(2)-C(4) 92.4(3), C(2)-P(2)-C(4) 97.2(3), C(2)-P(3)-C(3) 97.1(3), C(2)-P(3)-P(4) 53.7(2), C(3)-P(3)-P(4) 107.9(2), C(5)-P(4)-C(2) 109.1(3), C(5)-P(4)-P(3) 110.1(3), C(2)-P(4)-P(3) 52.9(2), C(5)-P(5)-C(4) 106.5(3).

It was also of interest to see if a similar product to **47** could be formd by reacting 1,3,5,7-tetraphosphabarrelene (**18**) with an excess of P≡CMe. However, monitoring the reaction by $^{31}P\{^{1}H\}$ NMR spectroscopy showed that a mixture of phosphorus containing products formes with numerous resonances between 360 and -239 ppm. Treating the reaction mixture with an excess of $[W(CO)_5(THF)]$, followed

by chromatographic workup (silica gel/hexane), gave **49** as the only identified product, yield 32% (**Scheme 20**).

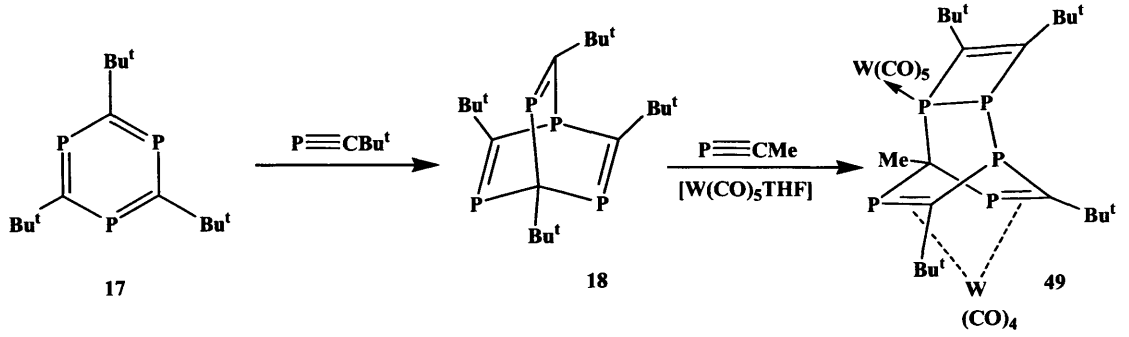

Scheme 20 Reactivity of a tetraphosphabarrelene with P≡CMe

The $^{31}P\{^1H\}$ NMR spectra of compound **49** displays the expected number of resonances, although those for the η^2-coordinated P=C fragments are at relatively high field (δ -4.9 to 53.4 ppm) and do not display observable ^{183}W satellites, presumably due to small magnitudes of the $^1J_{PW}$ couplings. The shifts of these signals are, however, similar to those seen for other η^4-coordinated $(P=C)_2$ fragments of phosphabarrelenes.[71] One other apparent anomaly in the $^{31}P\{^1H\}$ NMR spectrum of **49** is the very small $^1J_{PP}$ coupling constants ($^1J_{pp}$ = 24 and 56 Hz, $^2J_{pp}$ = 7 Hz) between the three contiguous P-centres. The magnitudes of these couplings presumably arise from the acute angles about the central P-atom which lead to a high degree of p-character in the two bonds between these three P-atoms. The mechanism of this reaction is not clear but most likely involves a series of cycloaddition and rearrangement processes.

The molecular structure of **49** was determined by X-ray crystallography, and its molecular structure is depicted in **Figure 7**. Compared to **48**, the lengths of the two P=C bonds in **49** are significantly greater, [P(2)-C(3) 1.750(6) Å, P(1)-C(18) 1.753(6) Å], because they are both η^2-coordinated to a $W(CO)_4$ fragment.

Additionally, P(3) ligates a $W(CO)_5$ unit in an η^1-fashion with a P-W distance of 2.552 Å.

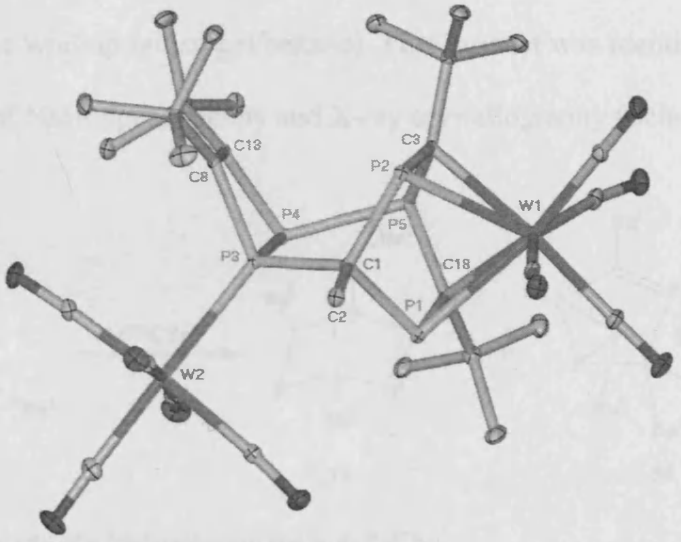

Figure 7 Molecular structure of **49** (hydrogen atoms omitted for clarity; ellipsoids shown at the 25% probability level)

Selected bond lengths (Å) and angles (°): W(1)-P(1) 2.6238(16), W(1)-P(2) 2.6518(16), W(2)-P(3) 2.5524(15), P(1)-C(18) 1.753(6), P(1)-C(1) 1.873(6), P(2)-C(3) 1.750(6), P(2)-C(1) 1.849(6), P(3)-C(1) 1.864(5), P(3)-C(8) 1.867(5), P(3)-P(4) 2.182(2), P(4)-C(13) 1.857(6), P(4)-P(5) 2.257(2), P(5)-C(3) 1.826(6), P(5)-C(18) 1.851(6), C(8)-C(13) 1.369(8), C(18)-P(1)-C(1) 107.5(3), C(3)-P(2)-C(1) 107.4(3), C(1)-P(3)-C(8) 114.0(2), C(1)-P(3)-P(4) 107.7(2), C(8)-P(3)-P(4) 79.12(19), C(13)-P(4)-P(3) 75.26(19), C(13)-P(4)-P(5) 108.14(18), P(3)-P(4)-P(5) 103.50(8), C(3)-P(5)-C(18) 95.6(3), C(3)-P(5)-P(4) 111.72(18), C(18)-P(5)-P(4) 96.82(18).

The published preparation of **18** involves the reaction of **17** with a slight excess of $P{\equiv}CBu^t$ to give a nearly quantitative yield of **18**.[44] Therefore it can be assumed that there are no significant quantities of other phosphorus containing products. However, monitoring the reaction by $^{31}P\{^1H\}$ NMR spectroscopy showed a

very small amount of a phosphorus containing by-product. In an attempt to identify the product, the reaction was repeated with an excess of P≡CBu^t at room temperature over two days, after which a new compound could be separated from **18** by chromatographic workup (silica gel/hexane). This product was identified as **50** using a combination of NMR spectroscopy and X-ray crystallography (**Scheme 21**).

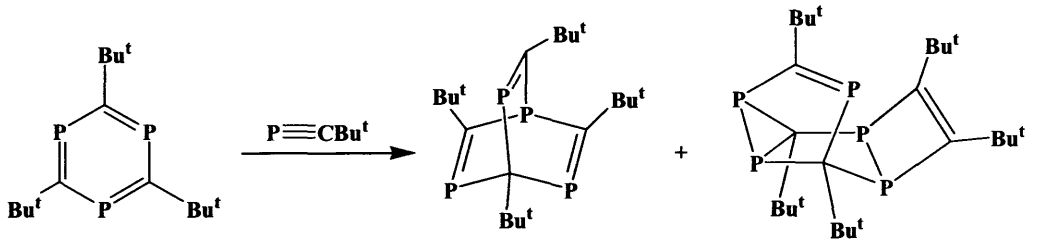

17 18 50

Scheme 21 Reactivity of a triphosphabenzene with P≡CBu^t

The ^{1}H NMR spectrum of **50** exhibits different resonances due to the presence of five inequivalent *tert*-butyl groups. Similarly, the ^{31}P{^{1}H} NMR spectrum also displays five signals, one of which is at low field (δ 387.6 ppm) and corresponds to the P=C unit in the compound. Of the two P-P bonds, one (that in the three-membered ring) has a normal $^1J_{PP}$ coupling associated with it (185 Hz), while that associated with the four-membered ring gives rise to a small coupling (60 Hz). The same reasons discussed for the small $^1J_{PP}$ couplings in **48** can be used to explain this observation. Compound **50** crystallises in the chiral space group, $P4_1$, with 2 enantiomeric molecules in the asymmetric unit. There are no significant geometric differences between the two molecules and therefore only the molecular structure of one is depicted in **Figure 8**. The compound has an "open cage" structure formed by the fusion of a three-membered, a four-membered and two five-membered rings. This leaves two unsaturated bonds, P(3)-C(11) and C(16)-C(21), the inter-atomic distances of which are consistent with bond orders of two. As no intermediates could

be observed by $^{31}P\{^{1}H\}$ NMR spectroscopy during the formation of **50**, the nature of the reaction mechanism is still unknown.[72] To confirm that compound **18** is not an intermediate of **50**, a pure sample of **18** was reacted with an excess $P{\equiv}CBu^{t}$ over 2 days. Monitoring the reaction by $^{31}P\{^{1}H\}$ NMR spectroscopy revealed that no reaction occurred.

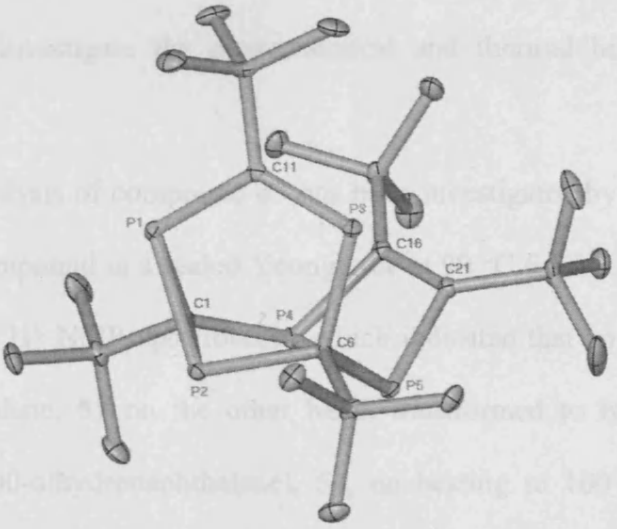

Figure 8 Molecular structure of **50** (hydrogen atoms omitted for clarity; ellipsoids shown at the 25% probability level).

Selected bond lengths (Å) and angles (°): P(1)-C(11) 1.825(3), P(1)-C(1) 1.886(3), P(1)-P(2) 2.1973(12), C(1)-P(4) 1.862(3), C(1)-P(2) 1.872(3), P(2)-C(6) 1.890(3), P(3)-C(11) 1.676(3), P(3)-C(6) 1.863(3), P(4)-C(16) 1.843(3), P(4)-P(5) 2.1986(12), P(5)-C(21) 1.872(3), P(5)-C(6) 1.915(3), C(16)-C(21) 1.361(4), C(11)-P(1)-C(1) 109.78(13), C(11)-P(1)-P(2) 98.40(11), C(1)-P(1)-P(2) 53.91(10), P(4)-C(1)-P(1) 132.57(17), P(2)-C(1)-P(1) 71.57(12), C(1)-P(2)-C(6) 99.96(13), C(1)-P(2)-P(1) 54.52(10), C(6)-P(2)-P(1) 99.05(9), C(11)-P(3)-C(6) 104.01(15), C(16)-P(4)-C(1) 119.76(14), C(16)-P(4)-P(5) 77.90(10), C(1)-P(4)-P(5) 102.51(10), C(21)-P(5)-C(6) 108.43(13), C(21)-P(5)-P(4) 75.68(10), C(6)-P(5)-P(4) 96.85(10), C(21)-C(16)-P(4) 102.1(2), C(16)-C(21)-P(5) 103.3(2).

Phosphaalkyne pentamers like compound **47** are of interest, as they are valence isoelectronic analogues of the $(CH)_{10}$ family of hydrocarbons. The $(CH)_{10}$ hydrocarbon family has 71 constitutional formulas representing isomeric forms. Many of these forms have been shown by experiment to interconvert under photochemical or thermal conditions.[72] As compound **47** represents the first example of a pentaphospha-analogue one of these isomers, isolumibullvalene, **51**, it is of interest to investigate the photochemical and thermal behaviour of these compounds.

The thermolysis of compound **47** has been investigated by heating a hexane solution of this compound in a sealed Young tube at 90 °C for 6 h. The reaction was monitored by $^{31}P\{^{1}H\}$ NMR spectroscopy which indicated that no reaction occured. The isolumibullvalene, **51** on the other hand, transformed to bicyclo[4.4.0]deca-2,4,7,9-tetraene(9,10-dihydronaphthalene), **52**, on heating to 100 °C *via* a reverse Diels-Alder reaction (**Scheme 22**).[73, 74] Compound **47** is likely not to be able to undergo this rearrangement due to the presence of bulky Bu^t groups.

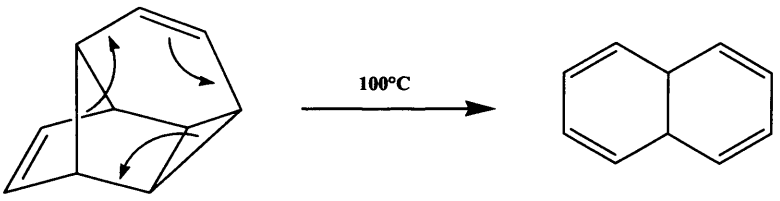

51 **52**

Scheme 22 Thermal rearrangement of isolumibullvalene

Compound **47** also exhibits different behaviour than **51** towards photolysis. A hexane solution of **47** was irradiated with UV light (λ 254 nm), and the reaction monitored by $^{31}P\{^{1}H\}$ NMR spectroscopy. This showed a complicated mixture of many phosphorus containing products after just 5 min. The large number of products made their characterisation and/or isolation very difficult. This chemistry is

significantly different to that of the isolumibullvalene **51**, which does not change upon irradiation. [73, 74]

With respect to how compound **47** could be formed, it is of interest that triphosphaisolumibullvalenes, **53**, have been prepared by two successive [4 + 2] cycloadditions of alkynes with **17**.[75] An analogous reaction might be occurring for **47**, followed by σ-rearrangement to give **47**. It is of note that, isolumibullvalene and triphosphaisolumibullvalenes are readily valence isomerised (**Scheme 23**).[74, 76]

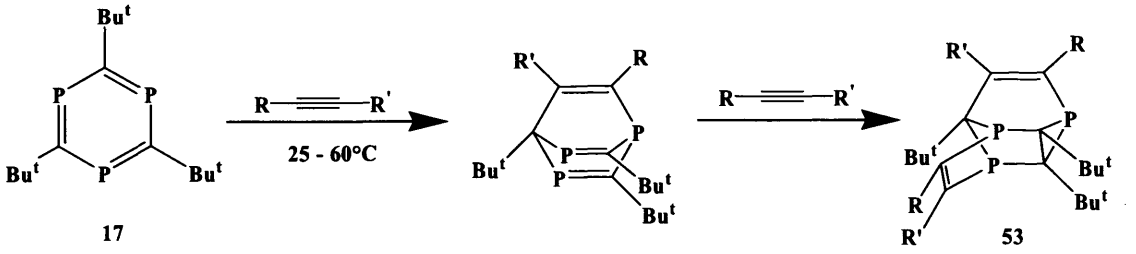

R =	Ph	H	CO_2Me	$-(CH_2)_6-$	$COMe$	Ph
R' =	H	H	H		H	D

Scheme 23 Preparation of triphosphaisolumibullvalenes, 53

1.3.2 Reaction of Phosphaalkynes with Diazomethane and Alkyl Azides

Earlier studies have shown that phosphaalkynes, *e.g.*, P≡CR (R = 1-adamantyl,[77] Pr^i,[78] neopentyl,[78] 1-methyl-1-cyclohexyl,[78] 1-methyl-1-cyclopentyl[78] or Bu^t[40]) react with different azides (**54a–h**) at 0 °C in diethylether to form 3-*R*-1,2,3,4-triazaphospholes (**55a-h**) *via* [3 + 2] cycloadditions in good yields (76 – 100%). As phosphaalkynes and azides have dipolar character, the formation of reversed dipole orientated products like 1-*R*-1,2,3,4-triazaphospholes (**56a-h**) could be understood.

However, all known reactions show only the formation of compounds **55a-h** with no evidence for the reversed dipole orientated products, *e.g.* **56**. Even if the differences of the Pauling electronegativities between phosphorus and carbon (2.1 and 2.5, respectively) are not very large, the cycloaddition is apparently electronically controlled. The fact that the reaction of P≡CBu^t with **54a-h** leads to the products **55a-h**, the product orientation cannot directly attributed to the spatial requirements of the substituents.[40]

That steric aspects are not a factor was shown by *Regitz* and *Binger et al.* who reacted **54a** with the unhindered phosphaalkyne P≡CH, in diethylether, yielding 3-methyl-1,2,3,4-triazaphosphole **57** (δ 187.8 ppm) without any sign of other products in the reaction mixture (**Scheme 24**).[43]

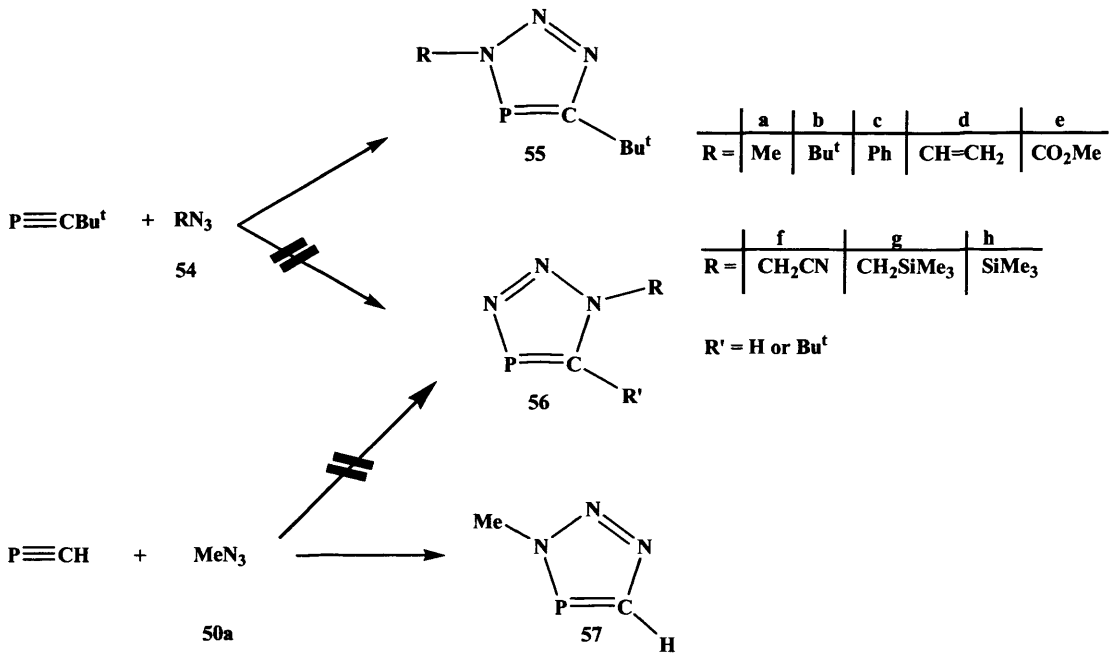

Scheme 24 Reaction of P≡CBu^t and P≡CH with alkyl azides

The reactions of diazomethane derivates **58a-f** with P≡CBu^t, and **58a** and **c** with P≡CH at room temperature in diethylether yielded the [3 + 2] cycloaddition products, 1-*H*-1,2,4-diazophosphole **60a-f** and **61a** and **c**, which are similar to the related azide products. Only the reaction yielding **60d** shows an intermediate 3-*H*-1,2,4-diazophosphole, **59d**, which could be isolated and characterised by ^{1}H NMR spectroscopy (**Scheme 25**).[41, 43]

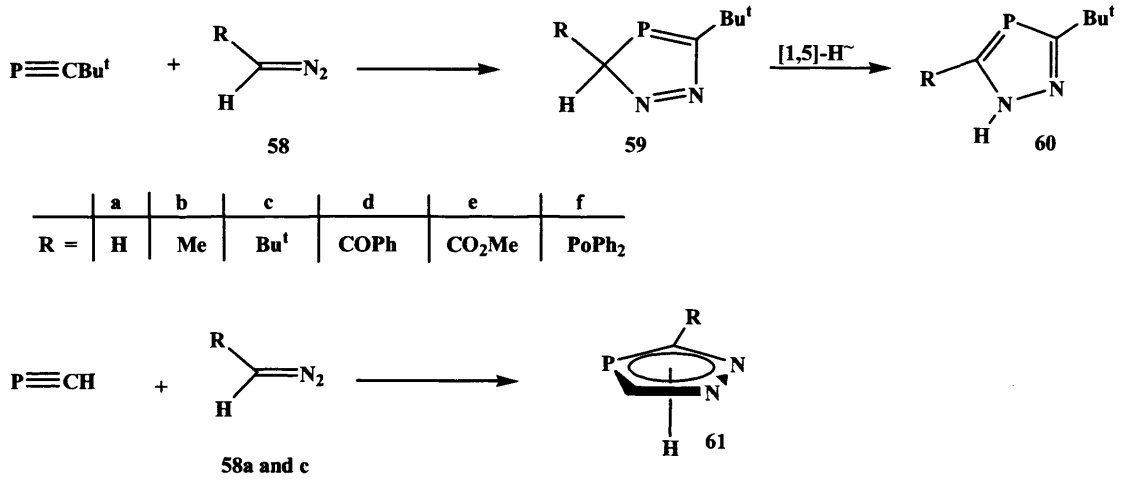

Scheme 25 Reaction of P≡CBu^t and P≡CH with diazomethane derivates

These results are in agreement with theoretical studies which have shown, that the activation energies for the formation of the reverse dipole orientated product (**TS1**) are lower than those for their dipole orientated (**TS2**) products. The activation energies are listed in **Table 1**. As a result, the acidic side of one reagent reacts with the basic side of the other reagent to form products *e.g.* **55a-h**, **57** and **60**.[79]

Reaction	E in kcal/mol	
	TS1	TS2
H_2CNN + P≡CH	5.86	6.92
H_2CNN + P≡CMe	9.47	12.37
HNNN + P≡CH	8.77	11.12
HNNN + P≡CMe	12.38	14.85

Table 1 Activation energy (kcal/mol) of products from [3 + 2] cycloadditions of phosphaalkynes with diazomethane and HN_3

In analogies with the reaction of azides and diazomethane with hindered and unhindered phosphaalkynes, it is worth mentioning, that mono-acceptor substituted acetylenes do respect the dipole orientation in their reaction with azides. Reacting one equivalent of **62** with one equivalent of phenylazide (**34c**) gives the dipole orientation product, **63**, in 75% yield. The reaction of 3-phenylpropynol (**64**) with phenylazide (**54c**) in boiling $CHCl_3$ over one day gives a 2 : 1 ratio of product **65** and **66 (Scheme 26)**.[42]

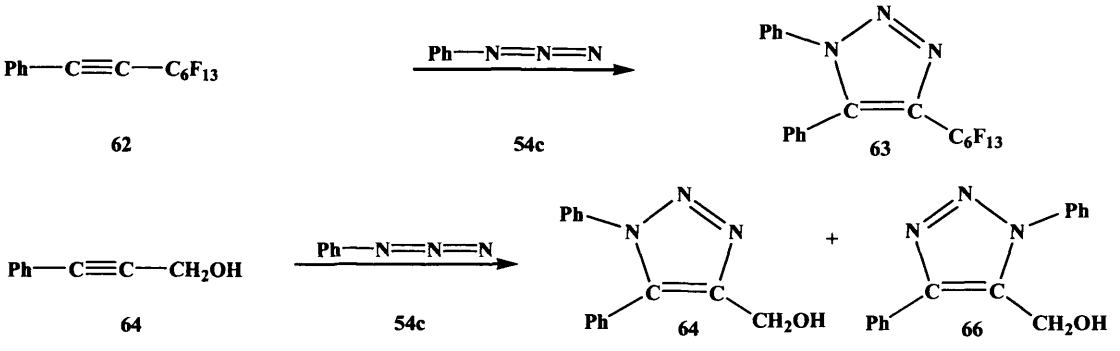

Scheme 26 Reversed dipole cycloaddition of acetylenes with phenyl azide

As steric needs are not the motivation to form dipole orientation products with hindered and unhindered phosphaalkynes in their reacions with azides, it is no surprise that similar reactions involving the unhindered phosphaalkyne, P≡CMe, yield similar products to those in **Scheme 24**.[43] Likewise, it can be observed that when excess P≡CMe was reacted with 1-adamantylazide (**67**) at room temperature in a hexane/diethylether mixture, and the reaction followed by $^{31}P\{^{1}H\}$ NMR spectroscopy, only one singlet resonance at δ 167 ppm was observed. This signal is in the same region as the P≡CBu^{t} related products, **55a-h** (δ 161 – 180 ppm) and the P≡CH related product **57** (δ 187.8 ppm). Therefore, it can be assume the formation of 3-*Ad*-1,2,3,4-triazaphosphole (**68**) *via* a [3 + 2] cycloaddition in the reaction. After all volatiles were removed *in vacuo*, the residue was redissolved in hexane and stored in a freezer yielding **68** as a crystalline product in a 90% yield (**Scheme 27**).

The reaction of an excess of P≡CMe with TMS-azide (TMS = trimethylsilyl) at room temperature in a hexane/diethylether mixture was followed by $^{31}P\{^{1}H\}$ NMR spectroscopy which showed an unexpected singlet resonance at δ 98 ppm. However, after all volatiles were removed *in vacuo*, the residue was redissolved in hexane yielding a mixture of phosphorus containing products exhibiting resonances between δ 213 and -130 ppm. No products could be characterised or isolated from this reaction.

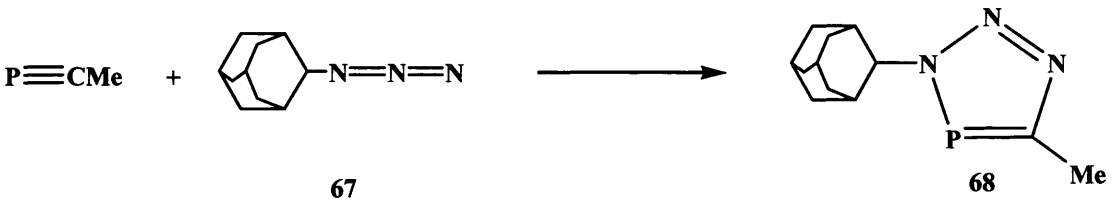

67 68

Scheme 27 Reaction of P≡CMe with 1-adamantylazide

The spectroscopic data for complex **68** are not publishable, but consistent with its structure shown in **Scheme 27**. Most informative is the $^{31}P\{^{1}H\}$ NMR spectrum which displays one low field singlet resonance at δ 167 ppm. The ^{1}H NMR spectrum displayed three signals due to the protons of the two chemically inequivalent CH_2 groups and one CH group of the adamantyl, and one signal for the methyl group.

The reaction of P≡CMe with a diazomethane (**69**) has been carried out and the results have been compared with those from similar reactions involving the unhindered phosphaalkyne, P≡CH, and the bulkier analogue, P≡CBu^{t}. An excess of P≡CMe was reacted with TMS-diazomethane (TMS = trimethylsilyl) in diethylether at room temperature. Monitoring this reaction by $^{31}P\{^{1}H\}$ NMR spectroscopy showed three resonances at δ 82.8, 83.1 and 93.6 ppm. However, after all volatiles were removed *in vacuo*, the residue was redissolved in hexane and stored at -20 °C yielding **70** (62%) as a crystalline product. The $^{31}P\{^{1}H\}$ NMR spectrum of the compound shows only one singlet resonance at δ 83.1 ppm. It is likely that the resonance at δ 93.6 ppm originates from the intermediate, **72**, while the TMS group is still attached. The signal at δ 82.8 ppm could be due to the isomer, **73**, after losing the TMS group and before the hydrogen shift. Reacting **70** in THF with $[W(CO)_5(THF)]$ at room temperature over 24 h leads to product **71**. After all volatiles were removed *in vacuo*, the residue was extracted in hexane and stored in a freezer yielding **71** (35%) ($^{31}P\{^{1}H\}$ NMR δ 74 ppm) as a crystalline solid (**Scheme 28**).

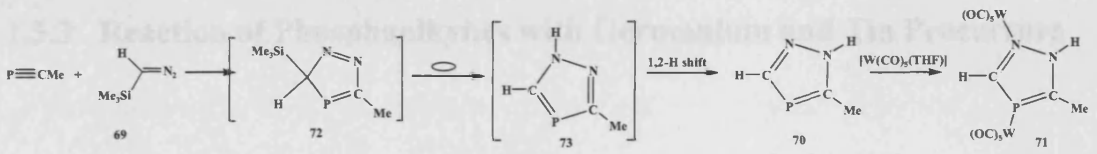

Scheme 28 Reaction of P≡CMe with TMS-diazomethane

The ^{1}H NMR spectra of **70** and **71** show the expected numbers of proton signals in the normal regions. Similarly, the $^{31}P\{^{1}H\}$ NMR spectra of both products display one signal at low field, **70** δ 83.1 ppm and **71** δ 74.8 ppm ($^{1}J_{PW}$ = 264 Hz), corresponding to the P=C unit in each compound. The molecular structure of **71** was determined by X-ray crystallography, and the molecular structure is depicted in **Figure 9**.

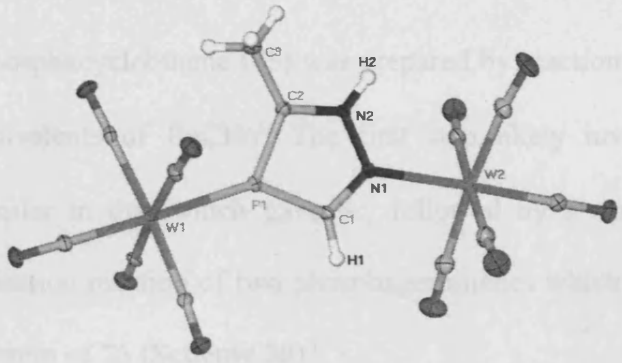

Figure 9 Molecular structure of **71** (hydrogen atoms omitted for clarity; ellipsoids shown at the 25% probability level).

Selected bond lengths (Å) and angles (°):W(1)-P(1) 2.4590(16), P(1)-C(2) 1.715(6), P(1)-C(1) 1.728(6), N(1)-C(1) 1.320(7), N(1)-N(2) 1.364(6), N(1)-W(2) 2.262(4), N(2)-C(2) 1.342(7), C(2)-C(3) 1.486(8), C(2)-P(1)-C(1) 88.9(3), C(2)-P(1)-W(1) 129.3(2), C(1)-P(1)-W(1) 141.5(2), C(1)-N(1)-N(2) 110.0(5), C(1)-N(1)-W(2) 127.5(4), N(2)-N(1)-W(2) 122.5(4), N(1)-C(1)-P(1) 114.5(5), C(2)-N(2)-N(1) 116.3(5), N(2)-C(2)-C(3) 119.9(6), N(2)-C(2)-P(1) 110.4(4), C(3)-C(2)-P(1) 129.6(5).

1.3.3 Reaction of Phosphaalkynes with Germanium and Tin Precursors

Stericaly hindered phosphaalkynes have been reacted with different Group 14 precursors to give differing co-ordination and cycloaddition products. The reactions of P≡CBu^t with precursors **7a-c** has given the three-membered heterocyclic 1 : 1 products, **8a-c**, *via* [2 + 1] cycloadditions (**Scheme 29**).[35, 36, 80]

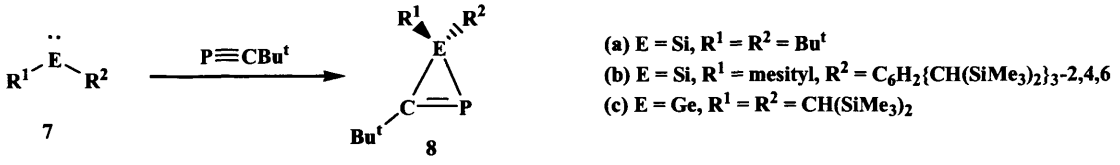

Scheme 29 Reaction of Si and Ge precursors with P≡CBu^t

Germadiphosphacyclobutene (**75**) was prepared by reaction of the germylene **74** with two equivalents of P≡CBu^t. The first step likely involves a [2 + 1] cycloaddition, similar to that which gave **8c**, followed by a ring opening and a subsequent dimerisation reaction of two phosphagermirenes which leads to the four-membered ring system of **75** (**Scheme 30**).[37]

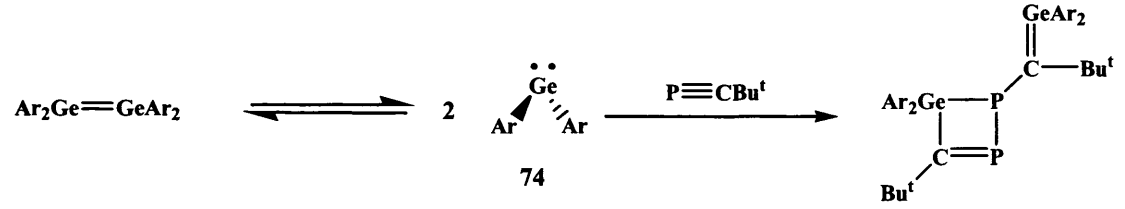

Scheme 30 Reaction of germylene with P≡CBu^t

Differing four-membered ring systems (**11** and **13**) have been formed by reacting phosphaalkynes with the distannene, **12**, and the silylene, **9**. The reaction of **12** with the phosphaalkyne, P≡CBu^t, likely involves a [2 + 2] cycloaddition to give the phosphadistannacyclobutene **13**.[39] A silicon analogue, **10**, has been reported to

from in the reaction of two equivalents of silylene, **9**, with one equivalent of P≡CR (R = adamantly or 2-methylcyclohexyl). The first step probably involves a [2 + 1] cycloaddition of one equivalent of silyene (**9**) and one equivalent of P≡CR to form **10**. The second step involves a ring opening mediated by reaction with a second silylene giving **12** (**Scheme 31**).[38]

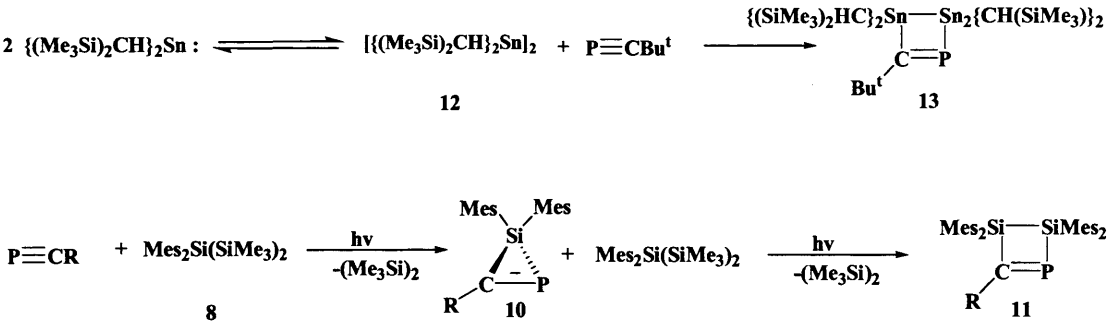

Scheme 31 Reaction of Si and Sn precursors with phosphaalkynes

P≡CMe has been reacted with similar and different Group 14 precursors, *e.g.* ER_2 (E = Si, Ge, Sn and Pb, R = $CH(SiMe_3)_2$, $C_6H_2Pr^i_3$-2,4,6) and the outcomes of these reactions compared to those from earlier studies on bulkier phosphaalkynes, P≡CR (R = Bu^t, adamantyl or 2-methylcyclohexyl).

P≡CMe was reacted with the diplumbene, $Ar_2Pb{=}PbAr'_2$ (Ar = $C_6H_2Pr^i_3$-2,4,6) and the plumbylene, $:Pb\{CH(SiMe_3)_2\}_2$, which is monomeric in the solid state. The reactions were carried out in 1 : 1, 1 : 2 and 1 : 4 stoichiometries and were followed by $^{31}P\{^1H\}$ NMR spectroscopy. Each gave an intractable mixture of phosphorus containing compounds. $[SiMes_2]_3$ is known to be a monomer in the solid state. However, irradiation of a solution of $[SiMes_2]_3$ with UV light (λ = 254 nm) provides the dimeric species $Mes_2Si{=}SiMes_2$,[81] which was reacted with P≡CMe in 1 : 1, 1 : 2 and 1 : 4 stoichiometries. Following the reactions by $^{31}P\{^1H\}$ NMR

spectroscopy showed, again, many phosphorus containing products which could not be characterised or isolated.

Cowley et al. have attempted the reaction of the monomeric :Sn{N(SiMe$_3$)$_2$}$_2$ with P≡Bu^t, but this gave no reaction.[36] Similarly the attempted reaction of P≡CMe, although it is a more reactive species, showed no reaction, as determined by $^{31}P\{^1H\}$ NMR spectroscopy.

Other precursors were needed to be found to react with P≡CMe. The ditetrelenes $R_2E{=}ER_2$ (E = Ge or Sn, R = -CH(SiMe$_3$)$_2$) (**76** and **77**) ware chosen for this task. Precursors, **76** and **77** have been reacted with P≡CMe in a 1 : 4 stoichiometry at -80 °C, followed by warming to room temperature over 4 h and stirring at this temperature for a further 18 h. Colourless crystals precipitated from these reaction mixtures which were found to be the bridged products, **79** (85% yield) (**Figure 11**) and **80** (81% yield). The distannene $Ar_2Sn{=}SnAr_2$ (Ar = $C_6H_2Pr^i_3$-2,4,6) (**78**), generated *in situ* by UV irradiation (λ = 254 nm) from the trimer [Sn(Ar$_2$)]$_3$ at -80 °C in toluene, was also reacted with P≡CMe in a 1 : 4 stoichiometry to give the related bridged product **81** in a 31% yield (**Figure 13**), (**Scheme 32**).

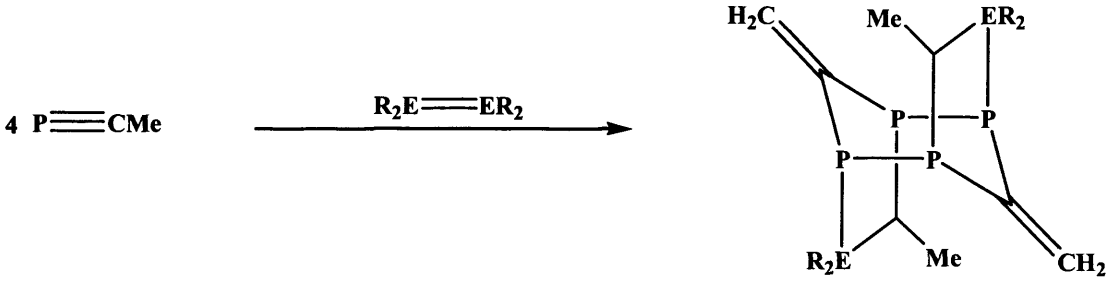

76 E = Ge, R = CH(SiMe$_3$)$_2$
77 E = Sn, R = CH(SiMe$_3$)$_2$
78 E = Sn, R = $C_6H_2Pr^i_3$-2,4,6

79 E = Ge, R = CH(SiMe$_3$)$_2$
80 E = Sn, R = CH(SiMe$_3$)$_2$
81 E = Sn, R = $C_6H_2Pr^i_3$-2,4,6

Scheme 32 Reaction of Ge and Sn precursors with P≡CMe

The low solubility of **79** to **81** leads to them precipitating from their toluene reaction solutions. It is difficult to re-dissolve these compounds in most deuterated solvents but **79** and **80** had sufficient solubility in CD_2Cl_2 or D_8-THF to obtain their ^1H and $^{31}P\{^1H\}$ NMR spectra. Similarly, these spectra can be acquired for weakly saturated C_6D_6 solutions of **81**, but meaningful $^{13}C\{^1H\}$ NMR spectra could not be obtained for any complex. Also, the NMR samples of **80** and **81** were too dilute for signals to be observed in their $^{119}Sn\{^1H\}$ NMR spectra.

The ^1H and $^{31}P\{^1H\}$ NMR spectra of **79** to **81** show that they are formed completely diastereoselectively. Four trimethylsilyl methyl singlets were observed in the ^1H NMR spectra of **79** (δ 0.19, 0.21, 0.27, 0.30 ppm) and **80** (δ 0.09, 0.19, 0.27, 0.29 ppm), while the spectra of all three complexes display two inequivalent alkenic proton signals, each split into a doublet of doublets by two $^3J_{PH}$ couplings (32 – 46 Hz) (N.B.: geminal $^2J_{HH}$ couplings for these signals were not observable). The $^{31}P\{^1H\}$ NMR spectra of **79** to **81** are similar and each consist of two doublet signals with characteristic $^1J_{PP}$ couplings. **79**: $^{31}P\{^1H\}$ NMR δ -13.7 ppm (br. d, $^1J_{PP}$ = 303.1), 31.7 ppm (br. d, $^1J_{PP}$ = 303.1 Hz), **80**: δ -63.2 ppm (br. d, $^1J_{PP}$ = 311.2 Hz, $^1J_{SnP}$ = 621.2 Hz), 16.5 ppm (br. d, $^1J_{PP}$ = 311.2 Hz), **81**: δ -76.3 ppm (d, $^1J_{PP}$ = 320 Hz, $^1J_{SnP}$ = 614 Hz), 15.8 ppm (d, $^1J_{PP}$ = 320 Hz). In addition, $^1J_{SnP}$ satellites of typical magnitudes flank the high field signals of the tin complexes, **80** (621.2 Hz) and **81** (614 Hz). Moreover, the doublets in each spectrum are broadened, presumably because of unresolved second order J_{PP} couplings. Molecular ion signals exhibiting the expected isotopic abundance patterns are present in the EI mass spectra of **79** – **81**.

The molecular structure of **79** – **81** was determined by X-ray crystallography. Complexes **79** and **80** are isomorphous so only the molecular structure of **79** is

depicted in **Figure 10**. Compound **81** has a near identical core structure to those of **79** and **80** and its molecular structure is shown in **Figure 11**.

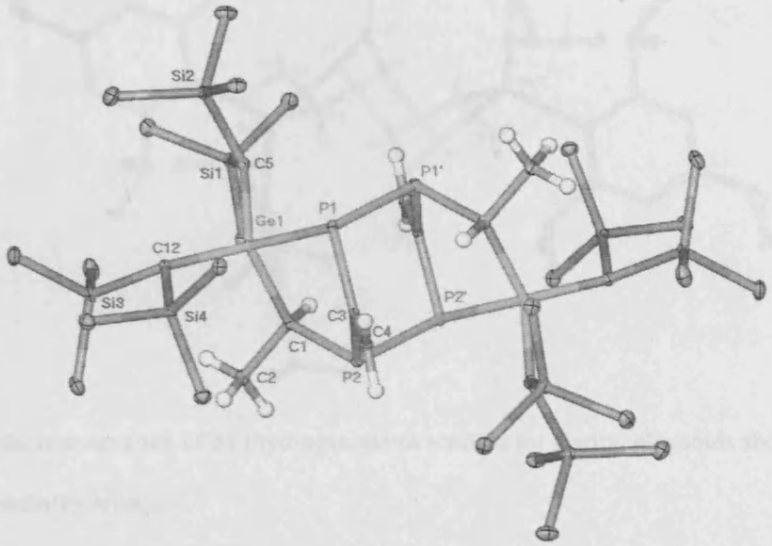

Figure 10 Molecular structure of **79** (hydrogen atoms omitted for clarity; ellipsoids shown at the 25% probability level).

Selected bond lengths (Å) and angles (°) for **79** Ge(1)-C(1) 2.020(2), Ge(1)-P(1) 2.3715(7), P(1)-C(3) 1.832(2), P(1)-P(2)' 2.2298(8), P(2)-C(3) 1.830(2), P(2)-C(1) 1.875(2), C(3)-C(4) 1.335(3), C(1)-Ge(1)-P(1) 98.30(6), C(3)-P(1)-P(2)' 100.81(7), C(3)-P(1)-Ge(1) 91.21(7), P(2)'-P(1)-Ge(1) 105.36(3), C(3)-P(2)-C(1) 101.78(9), C(3)-P(2)-P(1)' 105.21(7), C(1)-P(2)-P(1)' 97.76(7), P(2)-C(1)-Ge(1) 112.51(10), P(2)-C(3)-P(1) 121.22(11). symmetry operation: ' -x+2, -y, -z+2.

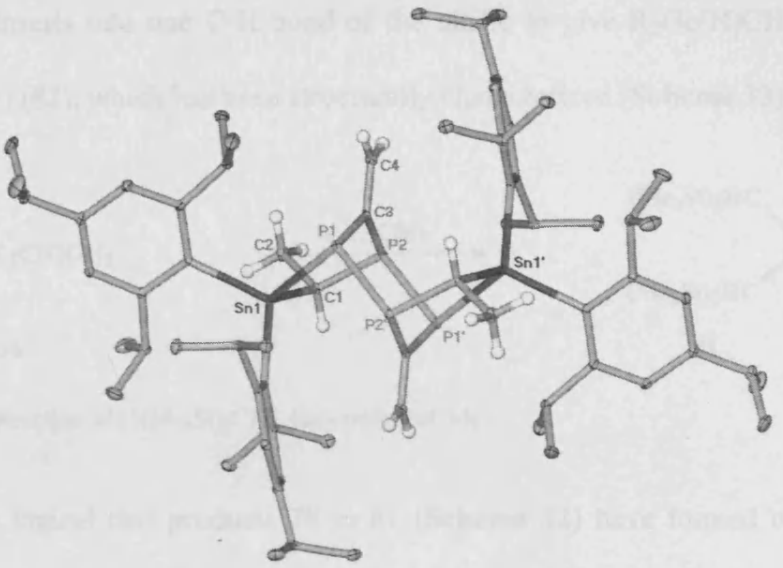

Figure 11 Molecular structure of **81** (hydrogen atoms omitted for clarity; ellipsoids shown at the 25% probability level).

Selected bond lengths (Å) and angles (°): Sn(1)-C(1) 2.202(2), Sn(1)-P(1) 2.5565(9), P(1)-C(3) 1.843(3), P(1)-P(2)' 2.2097(12), P(2)-C(3) 1.833(3), P(2)-C(1) 1.863(2), P(2)-P(1)' 2.2097(12), C(3)-C(4) 1.338(3), C(1)-Sn(1)-P(1) 94.78(7), C(3)-P(1)-P(2)' 107.75(9), C(3)-P(1)-Sn(1) 90.23(8), P(2)'-P(1)-Sn(1) 98.91(3), C(3)-P(2)-C(1) 100.00(11), C(3)-P(2)-P(1)' 106.71(8), C(1)-P(2)-P(1) 103.52(8), P(2)-C(1)-Sn(1) 112.13(12), P(2)-C(3)-P(1) 123.11(13). symmetry operation: ' -x+2, -y, -z+1.

The digermene analogue to **78**, $Ar_2Ge{=}GeAr_2$ (Ar = $C_6H_2Pr^i_3$-2,4,6), shows no reaction with P≡CMe which perhaps can be explained by the fact, that $Ar_2Ge{=}GeAr_2$ remains largely intact while $R_2E{=}ER_2$ (E = Ge, Sn; R = $CH(SiMe_3)_2$) (**76** or **77**) and $Ar_2Sn{=}SnAr_2$ (**78**) significantly dissociate into germylene or stannylene[82] fragments in solution. It is also of interest that $R_2Ge{=}GeR_2$ (R = $CH(SiMe_3)_2$) is known to react in a completely different fashion with N≡CMe, in that upon dissociation of the digermene, the germanium centre of the monomeric

germylene inserts into one C-H bond of the nitrile to give $R_2Ge(H)CH_2C{\equiv}N$ (R = $CH(SiMe_3)_2$) (**82**), which has been structurally characterized (**Scheme 33**).[83]

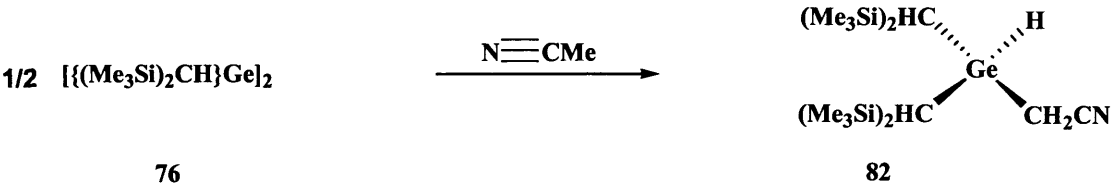

Scheme 33 Reaction of $[\{(Me_3Si)_2CH\}_2Ge]_2$ with N≡CMe

It is logical that products **79** to **81** **(Scheme 32)** have formed over several steps including a 1,3-hydrogen migration. To get an idea of the mechanism of the reaction, **76** was reacted with an excess of P≡CMe in D_8-toluene at -80 °C the reaction monitored by $^{31}P\{^1H\}$ NMR spectroscopy. An immediate reaction could be observed at -80 °C giving rise to a singlet resonance at δ 436.6 ppm. This resonance completely disappears after 5 min giving rise to two signals at δ 319.8 and 305.5 ppm; $^2J_{PP}$ = 29.8 Hz, with the simultaneous consumption of the P≡CMe reactant (δ -60.49 ppm). It can be assumed that the low field singlet resonance at δ 436.6 ppm (**83**) is due to an analogous [2 + 1] cycloaddition product of **8a**, which gives a singlet resonance at δ 315 ppm[36]. Compound **83** likely further reacts rapidly with excess P≡CMe to give a diphosphagermole, **84**, (*cf.* the 2,4-diphosphatellurole, $TeP_2C_2Bu^t_2$: δ 299, 302 ppm; $^2J_{PP}$ = 50.8 Hz).[84] Even if there is no direct evidence for the formation of **84** from **83**, it is likely that there is a [2 + 2] cycloaddition of **47** with another P≡CMe involved to give intermediate **86**, which rapidly rearranges to **84** *via* a 1,3-hydrogen migration and likely stays in equilibrium with **85**. The intermediates, **84** and **85**, stay present in solution at -80 °C until warming to room temperature whereupon two molecules of **85** react *via* hydrophosphination of the P=C bond of each other to give **79**. Product **79** has low solubility and precipitates from the

reaction mixture over a period of ca. 12 h (**Scheme 34**). The reaction to form products **80** and **81** have also been monitored by $^{31}P\{^{1}H\}$ NMR spectroscopy, and no short lived intermediates could not be observed.

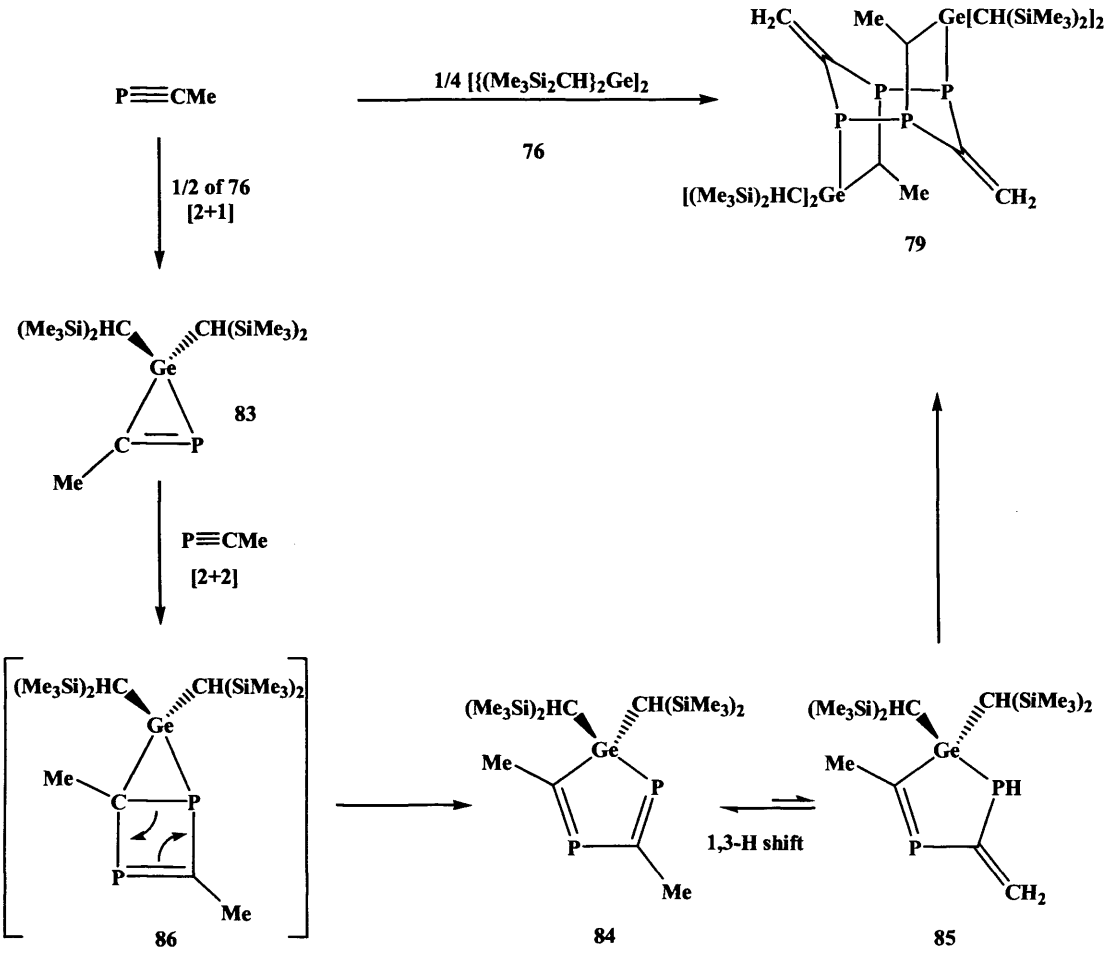

Scheme 34 Mechanism of formation of **79**

As **83** and **84** are long lived enough to be observed by $^{31}P\{^{1}H\}$ NMR spectroscopy, attempts were made to isolate these intermediates. Reacting P≡CMe with an excess of **76**, gave the phosphagermirene intermediate, **83**, which is stable in solution below -50 °C but decomposed into unidentified products upon warming to room temperature. A more promising intermediate to isolate is the longer lived **84**. Precursor **76** was reacted with an excess of P≡CMe at room temperature in THF to generate intermediate **83**, followed by adding [$(W(CO)_5)$(THF)] after 5 min and

stirring for 20 h. After chromatographic workup (silica gel/hexane), two low yield products **87** (13%) and **88** (15%) were obtained as crystalline solids (**Scheme 35**). The isolation of these compounds gives strong support to the proposed structure of **86**. Both compounds are indefinitely stable in solution as they are presumably prohibited from further intermolecular reactions to give tungsten carbonyl complexes of **79** or related species.

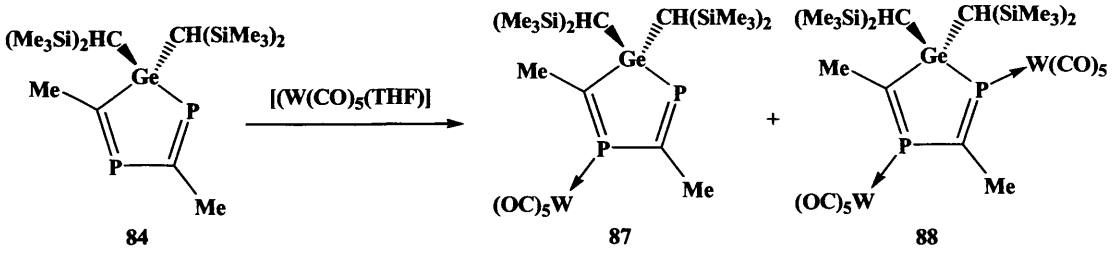

84 87 88

Scheme 35 Reaction of **84** with $[W(CO)_5(THF)]$

The spectroscopic data for the tungsten carbonyl complexes, **87** and **88**, are consistent with their structures. Most informative are their $^{31}P\{^1H\}$ NMR spectra which each display two low field doublet signals related by mutual $^2J_{PP}$ couplings **87**: δ 247 ppm (d, $^2J_{PP}$ = 53.8 Hz, $^1J_{WP}$ = 257 Hz), 342 ppm (d, $^2J_{PP}$ =83.8 Hz) **88**: δ 251 ppm (d, $^2J_{PP}$ = 66 Hz, $^1J_{WP}$ = 245 Hz), 287 ppm (d, $^2J_{PP}$ = 66 Hz, $^1J_{WP}$ = 256 Hz). Both resonances in the spectrum of **88** possess $^1J_{WP}$ satellites while only the higher field signal in the spectrum of **87** does. It is of note that the phosphaalkenic resonances for **87** and **88** are in the normal low field range.[2, 3, 70]

The molecular structures of **87** and **88** were determined by X-ray crystallography. As the heterocycle geometries of **87** and **88** are not significantly different, only the molecular structure of **87** is depicted in **Figure 12**.

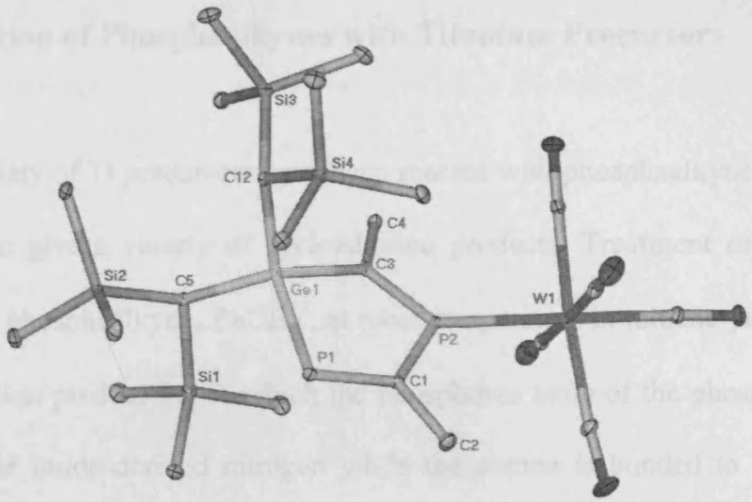

Figure 12 Molecular structure of 87 (hydrogen atoms omitted for clarity; ellipsoids shown at the 25% probability level).

Selected bond lengths (Å) and angles (°): W(1)-P(2) 2.4848(12), Ge(1)-C(3) 1.975(3), Ge(1)-P(1) 2.3403(9), P(1)-C(1) 1.691(3), P(2)-C(3) 1.674(2), P(2)-C(1) 1.813(2), C(1)-P(1)-Ge(1) 96.10(8), C(3)-P(2)-C(1) 106.85(12), C(3)-P(2)-W(1) 128.08(9), C(1)-P(2)-W(1) 124.85(9), P(1)-C(1)-P(2) 124.09(14), P(2)-C(3)-Ge(1) 114.25(12).

1.3.4 Reaction of Phosphaalkynes with Titanium Precursors

A variety of Ti precursors have been reacted with phosphaalkynes, alkynes or acetonitrile to give a variety of cycloaddition products. Treatment of **89** with an excess of the phosphaalkyne, P≡CBu^t, at room temperature in toluene yields the [2 + 2] cycloaddition product **90**, in which the phosphorus atom of the phosphaalkyne is bonded to the imido-derived nitrogen while the carbon is bonded to the titanium centre (**Scheme 36**). The $^{31}P\{^1H\}$ NMR spectrum of **90** shows a low field signal at δ 209.4 ppm.[85]

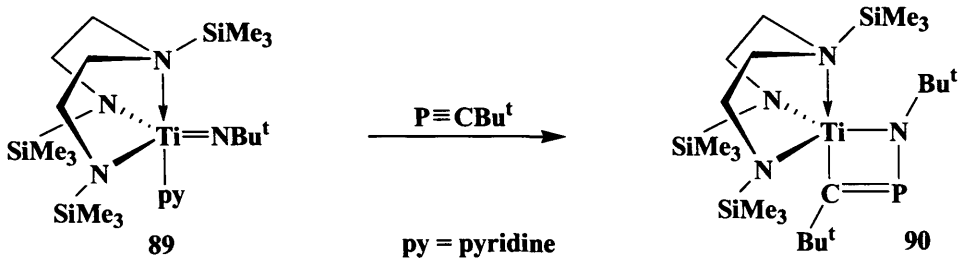

Scheme 36 Reaction of P≡CBu^t with a Ti=NBu^t precursor

The reaction of **91a** with alkynes MeC≡CR (R = Me or Ph) led [2+2] cycloaddition reactions and the titanazetidine products, **93a-b**, which were also formed by reacting **91a** with Me(H)C=C=CH$_2$ or Ph(H)C=C=CH$_2$. It was proposed that addition of a methyl C-H bond across the Ti=NR linkage occurs, followed by a proton shift and the formation of a σ-bonded allene ligand. [2+2] cycloadditions then give the titanazetidine products, **93a-b**. It is worth mentioning that similar precursors, **91b-c**, react with aryl acetylenes (HC≡CR, R= Ph or tolyl) to form the [2 + 2] cycloaddition complexes, **92**.

The reaction of **91** with N≡CMe generates the binuclear derivative **94**. The titanium centrers in **94** form part of a ladder-type motif composed of three four-

membered metallacyclic rings. In **94**, the carbon atom of the N≡CMe moiety is bonded to the imido-derived nitrogen, which is in contrast to **90** in which the N-P co-ordination is formed (**Scheme 37**).[86-88]

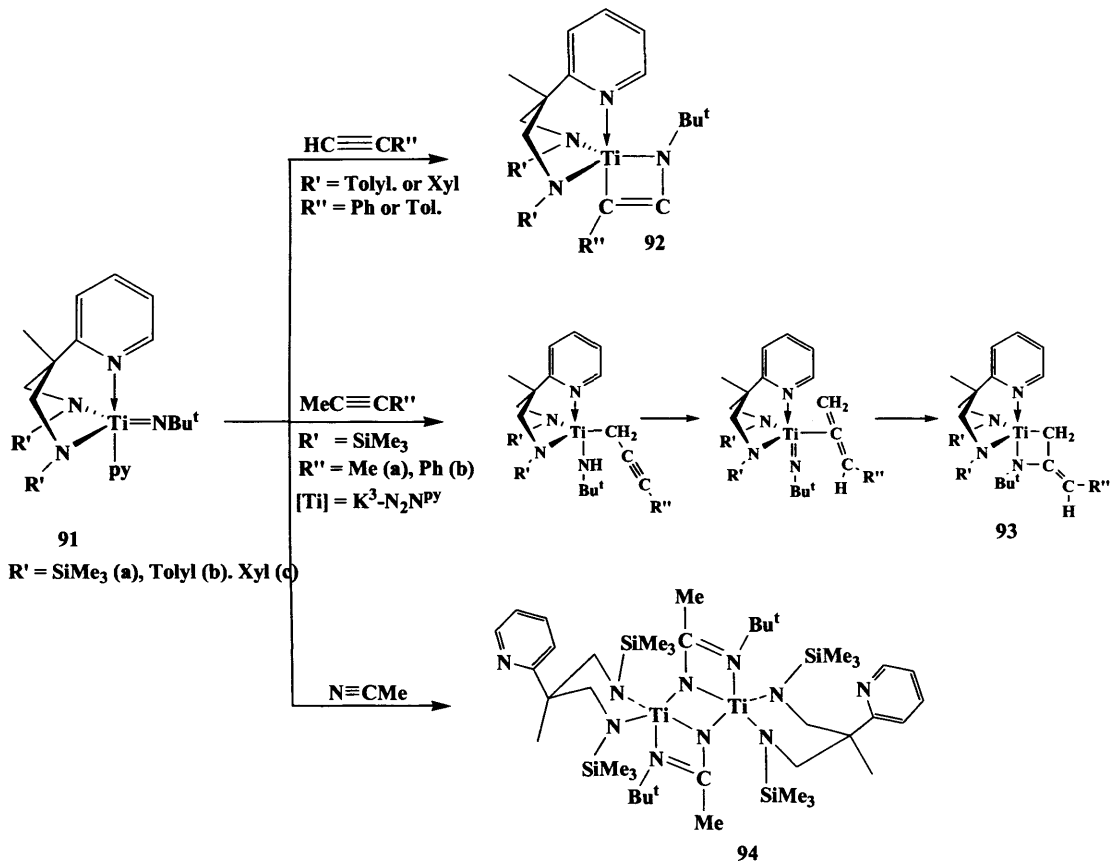

Scheme 37 Reaction of P≡CBu^t, alkynes or N≡CMe with Ti=NBu^t precursors

The reaction of two equivalents of P≡CBu^t with **95a** at 55 °C in toluene gives **97** in which the phosphorus atom is bonded to the imido derived nitrogen substituent. It is likely that the formation of **97** is *via* two stepwise [2 + 2] cycloadditions. The first step involves one equivalent of P≡CBu^t which reacts with **95a** to form the intermediate **96**, before reacting with a second equivalent of P≡CBu^t to form the final product, **97**. The $^{31}P\{^1H\}$ NMR spectrum of **97** shows two resonances for its two inequivalent phosphorus atoms at δ 296.5 and -139.5 ppm, $^2J_{PP}$ 40.5 Hz. It is of interest that the products of this type of reaction depend on the imido ligand substituents, as illustrated in the reactions of **95b** (R ≠ Bu^t) with P≡CBu^t, which give

the metal free 1,2,4-azadiphosphole rings **98b-d** (**Scheme 38**) The $^{31}P\{^{1}H\}$ NMR spectra of **98b** and **98d** show two resonances for their inequivalent phosphorus atoms in the unsaturated region (**98b**: δ 262.5, 153.5 ppm, $^{2}J_{PP}$ = 29.2 Hz, **98d**: δ 247.3, 148.1 ppm, $^{2}J_{PP}$ = 34.9 Hz).[85, 86, 89]

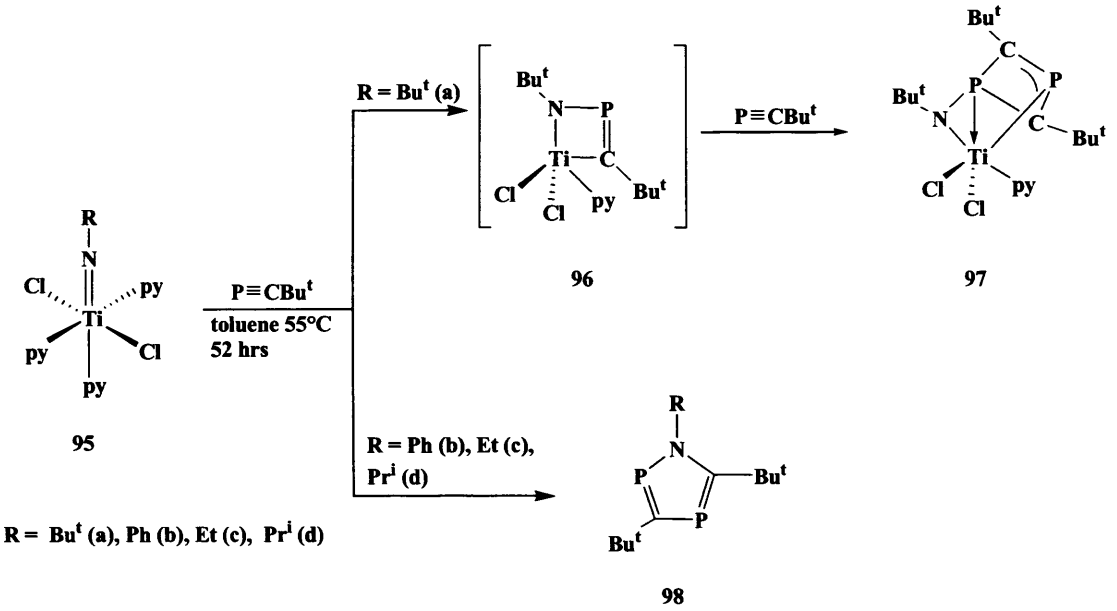

Scheme 38 Reaction of P≡CBu^{t} with [Ti(NR)Cl$_2$(py)$_3$]

The reactions of **99a-b** with two equivalents of P≡CBu^{t} in toluene at room temperature gives the products **100a-b** in 71% and 75% yields respectively ($^{31}P\{^{1}H\}$ NMR spectrum of **100a**: δ 215.4, -190.8 ppm, $^{2}J_{P\text{-}P}$ = 38.7 Hz and **100b**: δ 216.9, -192.9 $^{2}J_{P\text{-}P}$ = 39.6 Hz). In contrast, reacting an excess of P≡CBu^{t} with precursor **101** the non metal containing 1,2,4-azadiphophole ring systems, **102** which one analogous yields to **98b-c** (**Scheme 39**). The $^{31}P\{^{1}H\}$ NMR spectrum of **102** shows two resonances for inequivalent phosphorus atoms in the unsaturated region (δ 260.0 ppm and 154.6 ppm, $^{2}J_{P\text{-}P}$ = 29.2 Hz).[90]

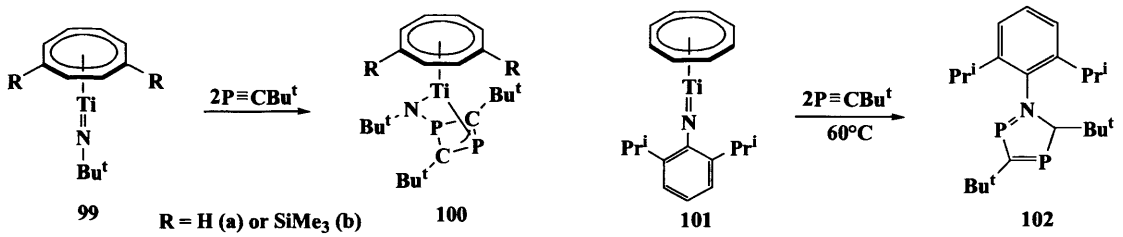

Scheme 39 Reaction of P≡CBu^t with titanium imide precursors

We reacted the precursors **95**, **99** and **101** with the unhindered phosphaalkyne, P≡CMe, in attempt to investigate differences and or similarities with the P≡CBu^t reactions. Following these reactions by $^{31}P\{^1H\}$ NMR spectroscopy showed no resonances except those of the phosphaalkyne, P≡CMe (δ –60.49 ppm). No products could be isolated.

Mountford et al. reported in 2007 the preparation of the terminal hydrazide [Ti(N_2N^{py})($NNPh_2$)(py)] (**103**) which was reacted with alkynes and N≡CMe (**Scheme 40**).[91] Reaction of **103** with PhC≡CMe in C_6D_6 gave an equilibrium mixture containing the cycloaddition product [Ti(N_2N^{py}){N(NPh_2)C(Me)CPh}] (**107**) and starting material **103**. Removal of the volatiles and redissolving the residue in C_6D_6 showed the compound to be pure as judged by NMR spectroscopy.[87, 88] Addition of an excess of pyridine to pure **107** reformed **103** and free PhC≡CMe, confirming the reversibility of the cycloaddition process. Although a cycloaddition species is the kinetic product for the reaction of **103** and PhC≡CMe, over time (3 days at RT) or upon briefly heating (15 mins at 100 °C) new products were formed from which the N_α-N_β *insertion* product [Ti(N_2N^{py}){NC(Ph)C(Me)NPh_2}(py)] **108** was obtained (**Scheme 40**). Reaction of **103** with the sterically less demanding alkyne, PhC≡CH, gave quantitative conversion to the cycloaddition product [Ti(N_2N^{py}){N(NPh_2)C(H)CPh}] (**106**) in *ca.* 60% yield. Addition of pyridine to pure **106** reformed **103** along with

PhC≡CH.[87] Reaction of **103** with N≡CMe gave the [2+2] cycloaddition dimer $[Ti_2(N_2N^{py})_2\{\mu\text{-}N(NPh_2)C(Me)N\}_2]$ **(104)** **(Scheme 40)**.

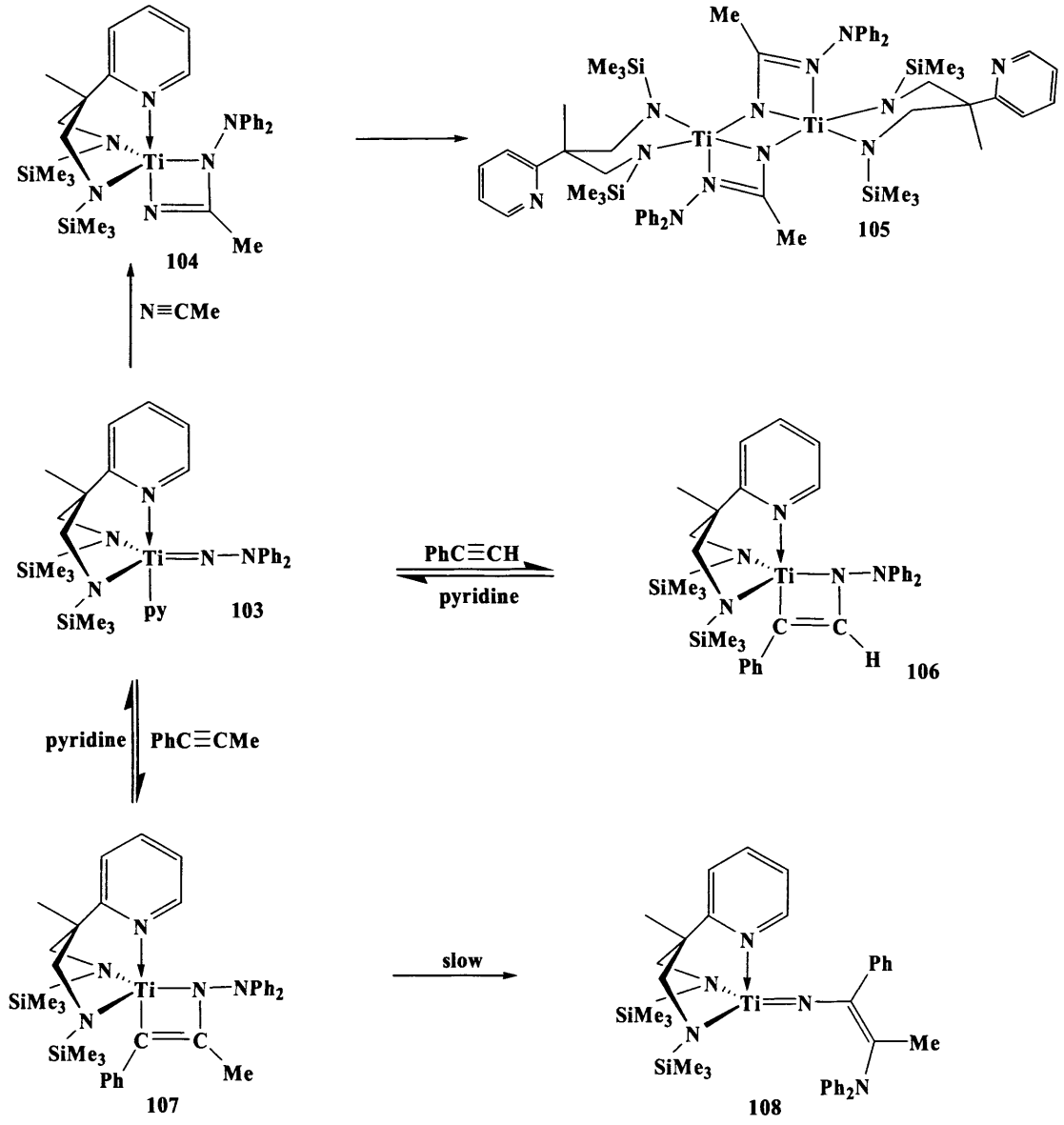

Scheme 40 Reactions of **103** with alkynes and N≡CMe

The successful use of a heteroalkyne in stabilizing **105** encouraged us to explore reactions of **103** with phosphaalkynes which have known similarities with alkynes.[3] The reaction of $[Ti(N_2N^{py})\{N(NPh_2)C(Me)CPh\}]$ with the phosphaalkyne, $P{\equiv}CBu^t$, was followed by $^{31}P\{^1H\}$ NMR spectroscopy which revealed that no reaction occurred. After all volatiles were removed *in vacuo*, a

^{1}H NMR spectrum was obtained in benzene-d_6. This revealed only starting material was present.

Mindful of previous reports of the reactions of imidozirconocenes "$Cp_2Zr(NR)$" (R = Bu^t or aryl) (**109a-b**) with $P{\equiv}CBu^t$ (**Scheme 41**)[85] A reaction of the of the very recently reported $[Cp_2Ti(NNPh_2)(py)]$ (**111**)[91], with $P{\equiv}CBu^t$ were carried out. Brown crystals of $[Cp_2Ti\{N(NPh_2)PCBu^t\}]$ (**112**) (**Scheme 41**) were isolated in 70% yield after 30 h at room temperature.

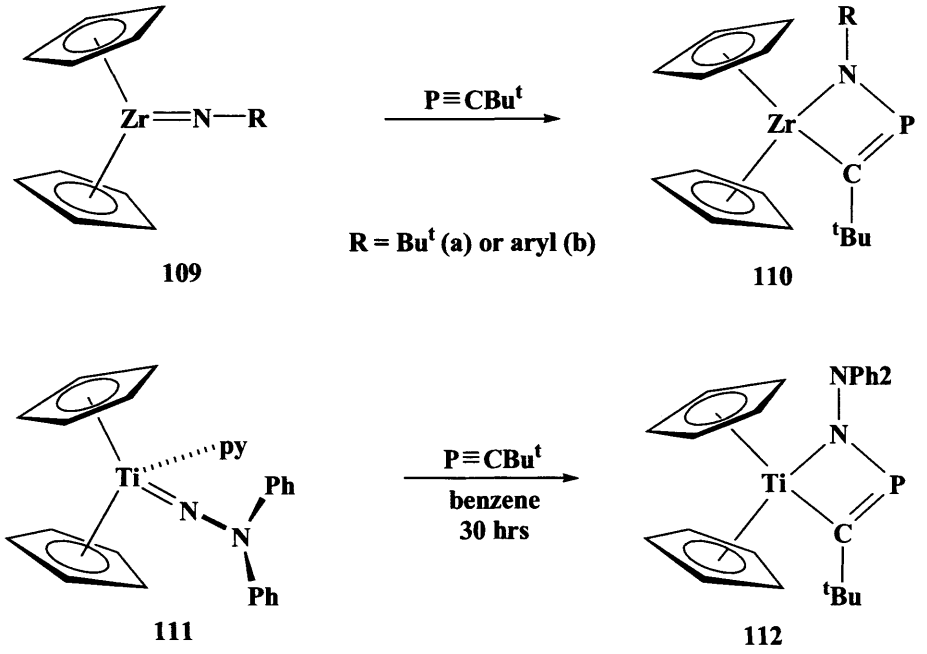

Scheme 41 Reaction of $P{\equiv}CBu^t$ with $[Cp_2Zr(NR)]$ and $[Cp_2Ti(NNPh_2)(py)]$

The ^{1}H and $^{31}P\{^1H\}$ NMR spectra of **112** show all the expected signals. The protons of the *tert*-butyl group resonate at δ 1.48 ppm and the Cp protons at 5.45 ppm in the ^{1}H NMR spectra. The $^{31}P\{^1H\}$ NMR spectra of **112** shows one singlet resonance at δ -28.9 ppm. This resonance is rather upfield compared to **110**, (*ca.* 60 to 80 ppm)[85] or **90**, (209.4 ppm).[85, 92]

The molecular structure of **112** is shown in **Figure 13**, confirming it as a monomeric [2+2] cycloaddition product. Compound **112** is the first example of a

product from the reaction of an $M{=}NNR_2$ species with a phosphaalkyne. The N(1)-P(1) and C(1)-P(1) distances (1.7329 and 1.677 Å) within the metallacyclic core of **112** are comparable to those in imido-based [(L)M{N(R)PCR}] units, e.g. **110** (1.729 and 1.692 Å).

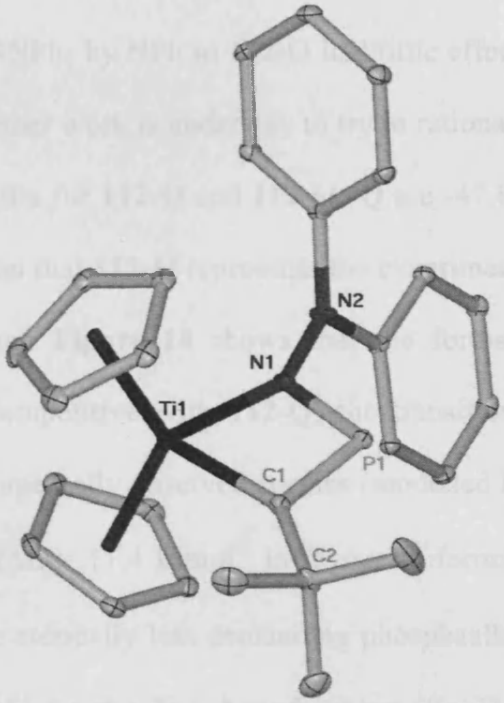

Figure 13 Molecular structure of **112** (hydrogen atoms omitted for clarity; ellipsoids shown at the 25% probability level).

Selected bond lengths (Å) and angles (°): Ti(1)-N(1) 1.9772(17), Ti(1)-C(1) 2.115(2), N(1)-P(1) 1.7329(18), C(1)-P(1) 1.677(2), N(1)-N(2) 1.400(2), N(1)-P(1)-C(1) 98.93(9), N(1)-Ti(1)-C(1) 78.51(7).

The orientation of the [2+2] cycloaddition process found in the formation of **112** appears to be favoured on steric grounds and is analogous to those previously reported for imido-derived examples, [(L)M{N(R)PCR}] *e.g.* **110**. However, the orientation of the less sterically demanding NCMe fragment in **104** and **105** is the opposite to that in **112** (Ti-heteroatom formation in **104** *vs.* Ti-C formation in **112**). Calculations were carried out by Eric Clot on the alternative regioisomers

of **112** (**112-Q** and **112-alt-Q**) using DFT (B3PW91) (**Figure 15**). According to the DFT-studies, **112-alt-Q** is *more* stable (but only marginally, by *ca.* 6 $kJmol^{-1}$) than the experimentally observed one in terms of electronic energies. As mentioned, the observed and calculated ^{31}P shifts for **112** are more upfield than expected. At first sight this could be attributed to the $NNPh_2$ fragment in **112**. However, replacing $NNPh_2$ by NPh in **112-Q** had little effect on the ^{31}P chemical shift (-53.1 ppm). Further work is underway to try to rationalise these differences. The calculated ^{31}P shifts for **112-Q** and **112-alt-Q** are -47.8 and +319 ppm. This supports the suggestion that **112-Q** represents the experimental solution and solid state species. Although **Figure 14** shows that the formation of **112-alt-Q** is thermodynamically competitive with **112-Q**, the transition state (TS) energies predict that the experimentally observed species (modelled by **112-Q**) is certainly kinetically favoured (ΔE = 11.4 $kJmol^{-1}$ in favour of forming **112-Q** [27]). Further calculations using the sterically less demanding phosphaalkyne P≡CMe gave $\Delta_r E$ values of -97.7 $kJmol^{-1}$ for the Ti-C bound isomer $[Cp_2Ti\{N(NPh_2)PCMe\}]$ but -134.1 $kJmol^{-1}$ for the Ti-P bound alternative $[Cp_2Ti\{N(NPh_2)C(Me)P\}]$. This confirms that the Ti-P/N-C orientated [2+2] cycloaddition process is the electronically preferred one.

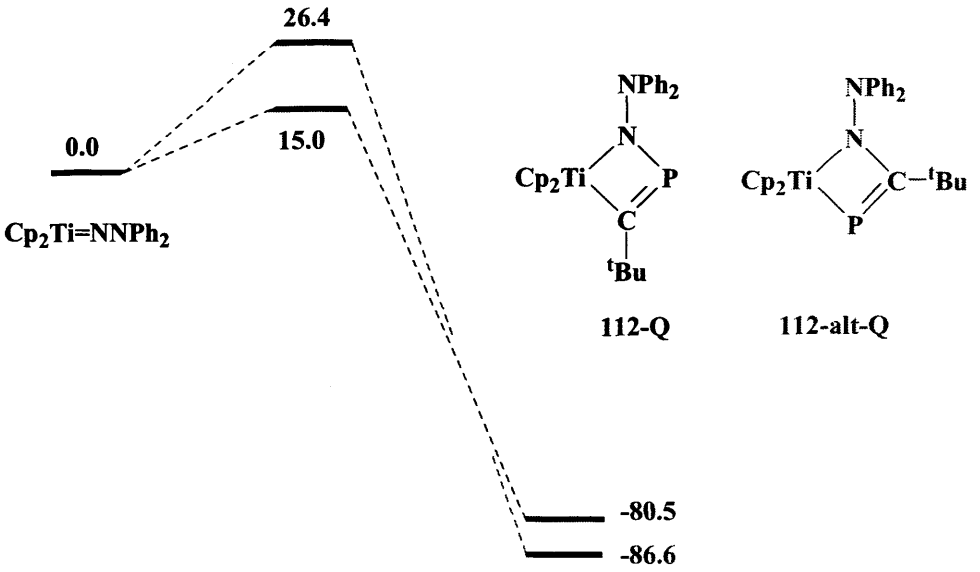

Figure 14 Schematic representation of the two TS and product electronic energies (B3PW91, kJ mol^{-1}) for the reaction of base-free $Cp_2Ti(NNPh_2)$ with $P{\equiv}CBu^t$

Carrying out the reactions of **109** and **111** with excess P≡CMe led to no new resonances in their $^{31}P\{^1H\}$ NMR spetra, and only that for the free phosphaalkyne, P≡CMe, was observerd. However, the ^1H NMR spectra from the reactions of **109** and **111** with excess P≡CMe changed, and no signals for their starting materials (**109** or **111**) could be seen. Attemps to crystallise any products failed.

1.3.5 Reaction of Phosphaalkynes with a Tungsten Precursor

As mentioned in 1.2.1 two equivalents of P≡CBu^t undergo a thermal [2 + 2] cycloaddition to yield the head to tail 1,3-diphosphacyclobutadiene (**113**) as an intermediate. This is followed by a dimerisation and an intramolecular [2 + 2] cycloaddition to form the phosphaalkyne tetramer cube (**114**) (**Scheme 42**).[25, 26, 55, 56]

Theoretical studies on such dimerisations have suggested that head to tail 1,3-diphosphacyclobutadiene complexes are more favoured for bulky groups, P≡CR (R = Bu^t, Mes), while head to head 1,2-diphosphacyclobutadiene complexes are significantly more thermodynamically favourable for small groups, P≡CR (R = H, Me). The reason here is that the energy difference between model 1,2- or 1,3-hetrocyclic complexes for P≡CMe compounds is 48 kJ/mol. However, for P≡CBu^t, there is little energy difference between the resultant 1,2- or 1,3-hetrocyclic complexes (3kJ/mol), a consequence of the steric influence of the bulky *tert*-butyl groups.[93]

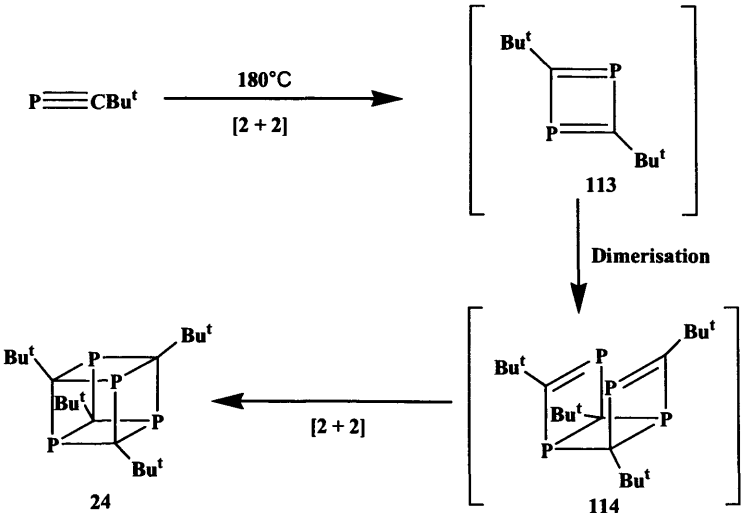

Scheme 42 Solvent free oligomerisation of *tert*-butyl-phosphaalkyne

Bulky phosphaalkynes are well known to dimerise in the co-ordination sphere of low valent transition metal fragments to give η^4-diphosphacyclobutadiene complexes.[2, 3, 70] Almost invariably, this occurs in a head to tail fashion to give the 1,3-isomer of the heterocycle. This is indeed the case in the reactions of P≡CR, R = Bu^t or Mes, with $[W(CO)_5(THF)]$ which have yielded a variety of 1,3-diphosphacyclobutadiene complexes including **115** and **116** (**Scheme 43**).[94]

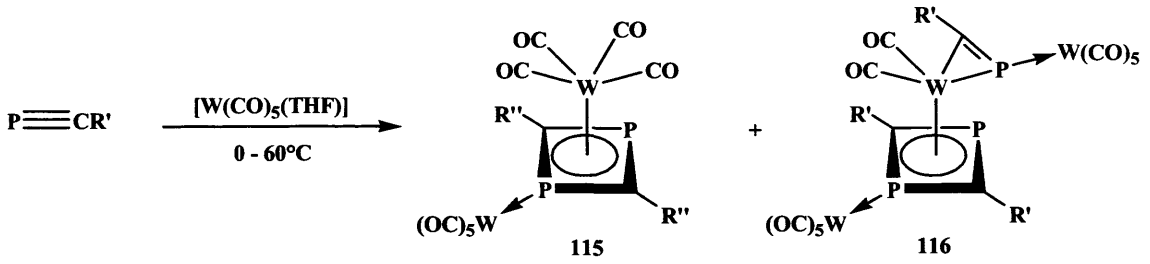

R' = Bu^t and Mes
R'' = Mes

Scheme 43 Dimerisation of phosphaalkynes with $[W(CO)_5(THF)]$

In an attempt to confirm the differences seen in the theoretical studies on hindered phosphaalkyne dimerisation, P≡CR (R = Bu^t, Mes) versus that of unhindered phosphaalkynes, P≡CR (R = H, Me), P≡CMe was reacted with $[W(CO)_5(THF)]$ at low temperature. In contrast to the related reaction with P≡CBu^t, both head to head and head to tail coupled complexes, **117** and **118**, were observed in the reaction mixture in a *ca.* 80 : 20 ratio (**Scheme 44**).

The complexes were subsequently purified by column chromatography (silica gel/hexane) and recrystallisation. In accord with the afore mentioned theoretical study, the preferential formation of **117** does suggest that metal mediated head to head couplings of unhindered phosphaalkynes are favoured over head to tail couplings.

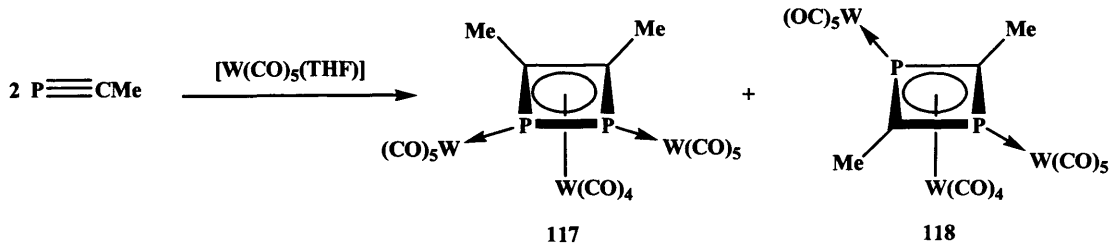

117 118

Scheme 44 Dimerisation of P≡CMe with [W(CO)$_5$(THF)]

Most informative of the characteristic data for **117** and **118** are their $^{31}P\{^1H\}$ NMR spectra which exhibit singlets with ^{183}W satellites having characteristic one bond J_{PW} couplings (**117**: δ -74.8 ppm, $^1J_{WP}$ = 148.2 Hz; **118** : δ -4.0 ppm, $^1J_{WP}$ = 251.2 Hz). Crystal structure analyses of both complexes were carried out and the molecular structure of **117** is depicted in **Figure 15** and that of **118** in **Figure 16**. The intra-ring distances in both are suggestive of significant delocalisation, as has been previously observed in many 1,3-diphosphacyclobutadiene complexes,[2, 3, 70] and the only structurally characterised complexes containing a 1,2-isomer of this heterocycle type, *viz.* [Ti(COT)(η^4-1,2-$P_2C_2Bu^t_2$)], COT = cyclooctatetraarene,[95] and [Fe(CO)$_3${η^4-1,2-P_2[W(CO)$_5$]$_2C_2Bu^t_2$}][96] (N.B. the latter complex was not formed *via* a phosphaalkyne dimerisation).

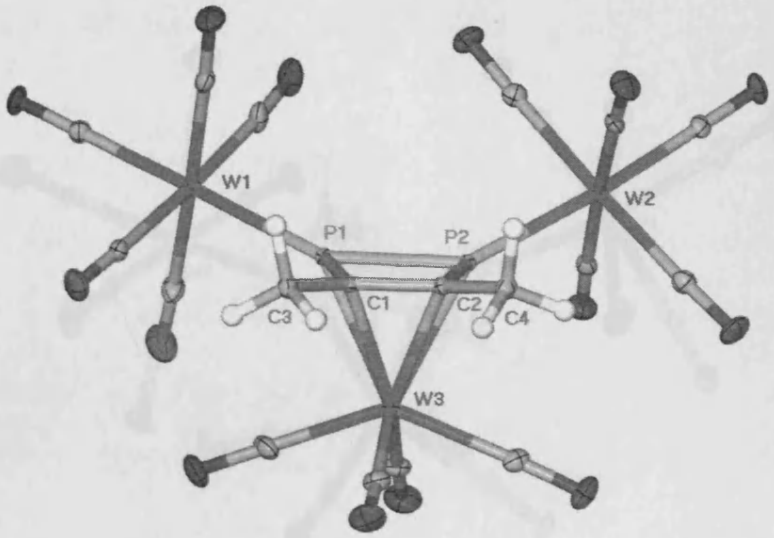

Figure 15 Molecular structure of **117** (hydrogen atoms omitted for clarity; ellipsoids shown at the 25% probability level).

Selected bond lengths (Å) and angles (°): W(1)-P(1) 2.4772(15), P(1)-C(1) 1.799(6), P(1)-P(2) 2.161(2), P(1)-W(3) 2.5314(15), C(1)-C(3) 1.527(8), C(1)-W(3) 2.353(5), W(2)-P(2) 2.4721(14), P(2)-C(2) 1.818(6), P(2)-W(3) 2.5099(14), C(2)-C(4) 1.501(7), C(2)-W(3) 2.366(5), C(1)-P(1)-P(2) 78.04(18), C(2)-C(1)-C(3) 127.2(5), C(2)-C(1)-P(1) 102.7(4), C(3)-C(1)-P(1) 129.3(4), C(2)-P(2)-P(1) 77.91(18), C(1)-C(2)-P(2) 101.4(4).

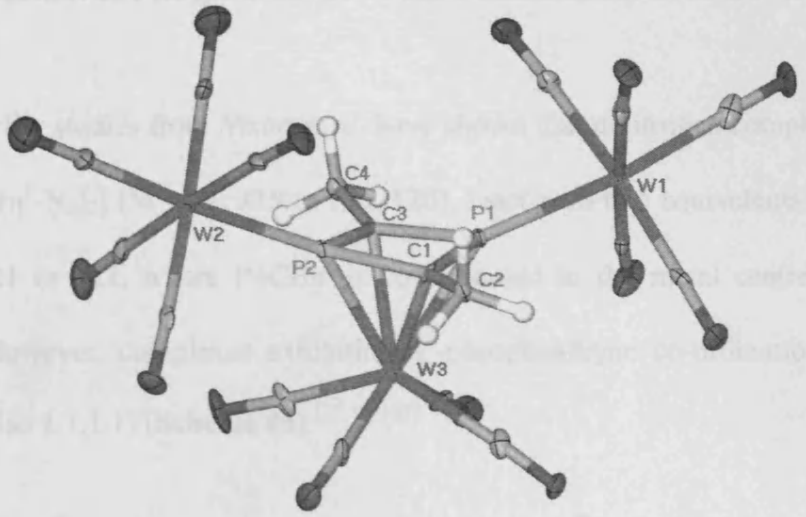

Figure 16 Molecular structure of **118** (hydrogen atoms omitted for clarity; ellipsoids shown at the 25% probability level).

Selected bond lengths (Å) and angles (°): W(1)-P1 2.440(5), P(1)-C(3) 1.765(16), P(1)-C(1) 1.797(17), P(1)-W(3) 2.494(5), C(1)-P(2) 1.806(16), W(2)-P(2) 2.440(4), P(2)-C(3) 1.755(17), P(2)-W(3) 2.492(4), C(3)-P(1)-C(1) 84.2(8), C(3)-P(1)-W(1) 135.3(6) C(1)-P(1)-W(1) 136.1(6), C(2)-C(1)-P(1) 131.8(13), C(2)-C(1)-P(2) 132.2(13), P(1)-C(1)-P(2) 93.8(7), C(3)-P(2)-C(1) 84.3(7), C(3)-P(2)-W(2) 135.0(6), C(1)-P(2)-W(2) 135.7(5), P(2)-C(3)-P(1) 96.8(8).

1.3.6 Reaction of Phosphaalkynes with a Ruthenium Precursor

Earlier studies from *Nixon et al.* have shown that dinitrogen complexes trans-$[M(dppe)_2(\eta^1\text{-}N_2)_2]$ (M = W, **119** or Mo, **120**), react with two equivalents of $P{\equiv}CBu^t$ to give **121** or **122**, where $P{\equiv}CBu^t$ is co-ordinated to the metal centre in an η^1-fashion. However, complexes exhibiting η^1-phosphaalkyne co-ordination are very rare (see also 1.1.1.1) (**Scheme 45**).[27, 97-101]

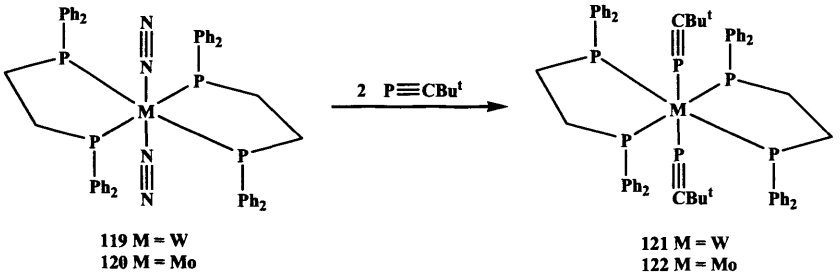

Scheme 45 Reaction of $[M(dppe)_2(\eta^1\text{-}N_2)_2]$ with $P{\equiv}CBu^t$

Considering the above, efforts have been made to prepare the first example of a complex displaying η^1-co-ordination of an unhindered phosphaalkyne, by reacting **119** with an excess of P≡CMe. Surprisingly, no reaction could be observed when monitoring the reaction by $^{31}P\{^1H\}$ NMR spectroscopy. It is likely that the less electron donating methyl group, compared to the *tert*-butyl-group, makes P≡CMe a weaker Lewis base than $P{\equiv}CBu^t$. As a result, other bulky unsaturated metal fragments needed to be found, which had the potential to co-ordinate P≡CMe without the need to displace other ligands. The cationic complexes, $[MH(dppe)_2]^+$ (M = Ru[97] or Fe [102]), were chosen as bulky phosphaalkynes (P≡CR, R = Bu^t, $SiPh_3$, CPh_3) are known to co-ordinate to them in an η^1-fashion (**123**, **125**, **126**). It is worth mentioning, that *Grützmacher et al.* have prepared the first example of a phosphorus

"cyaphide" complex (**124**) by reacting $[RuH(dppe)_2(P{\equiv}CSiPh_3)]^+$ (**123**), with NaOPh (**Scheme 46**).[98]

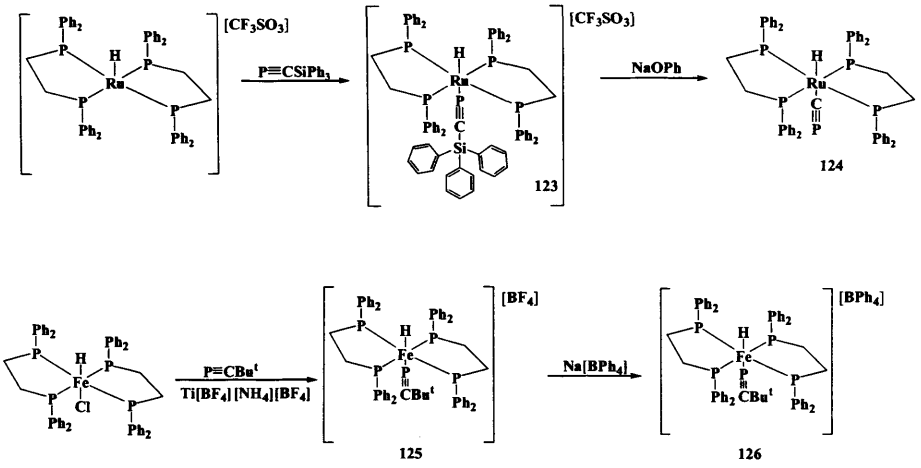

Scheme 46 η^1-co-ordination of phosphaalkynes

For purpose of comparison, P≡CMe was reacted with $[RuH(dppe)_2][CF_3SO_3]$ in dichloromethane at room temperature to give an analogue of **123**, *e.g.* **127**, in 75% yield after crystallising from a dichloromethane/hexane mixture (**Scheme 47**). P≡CMe was also reacted with $[FeH(dppe)_2][BPh_4]$. The reaction was monitored by $^{31}P\{^1H\}$ NMR spectroscopy and this showed a mixture of phosphorus containing compounds which probably includes $[FeH(dppe)_2(P{\equiv}CMe)][BPh_4]$. However, this compound could not be isolated upon work up.

The $^{31}P\{^1H\}$ NMR spectrum of compound **127** is similar to that of **123**. It displays a doublet signal for the dppe ligands (δ 61.5 ppm, $^2J_{PP}$ = 30 Hz) and a quintet for the phosphaalkyne at a chemical shift (δ -38.7 ppm) significantly downfield from that of the free phosphaalkyne (δ -60.5 ppm).[13] The hydride signal in the ^1H NMR spectrum of the compound appears as a doublet of quintets (δ -9.60 ppm, $^2J_{PH}$ = 127 and 17 Hz). Similar spectral patterns have been observed for the complexes, $[RuH(dppe)_2(P{\equiv}CR)][CF_3SO_3]$ (R = $SiPh_3$[98] or CPh_3[97]).

The molecular structure of **127** was determined by X-ray crystallography, and its cationic component is depicted in **Figure 17.** Its P-C triple bond length (1.535 Å) is close to those in the few structurally characterized free phosphaalkynes (e.g. 1.538 Å in $P{\equiv}CCPh_3$[97] and 1.532 Å (mean) in the diphosphaalkyne, $P{\equiv}CC(C_6H_4)_3CC{\equiv}P$),[103] but significantly shorter than the P-C bonds in η^2-complexes of methyl-phosphaalkyne (e.g. 1.617 Å in $[Pt(PCy_3)_2(\eta^2\text{-}P{\equiv}CMe)]$. Although the phosphaalkyne in **127** is close to linear, its coordination to the distorted octahedral ruthenium centre deviates significantly from linear (Ru-P-C 153.7(2)°) because of interactions with the surrounding phenyl groups.

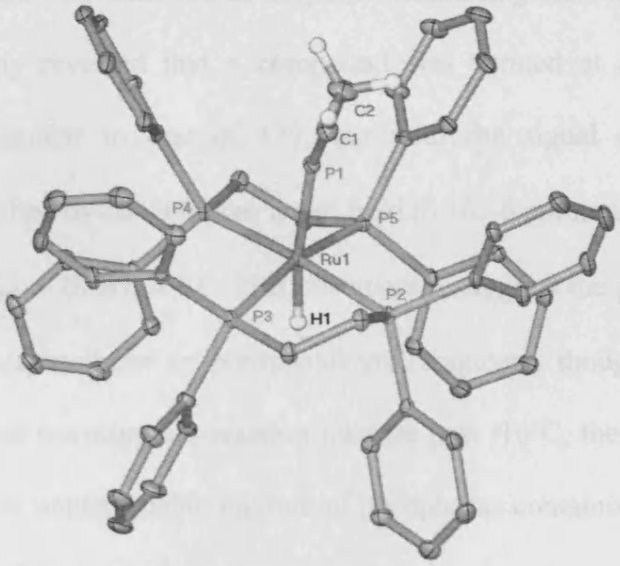

Figure 17 Molecular structure of **127** (hydrogen atoms omitted for clarity; ellipsoids shown at the 25% probability level).

Selected bond lengths (Å) and angles (°): Ru(1)-P(1) 2.3148(13), Ru(1)-P(5) 2.3453(11), Ru(1)-P(2) 2.3592(11), Ru(1)-P(4) 2.3682(11), Ru(1)-P(3) 2.3786(11), P(1)-C(1) 1.535(6), C(1)-C(2) 1.474(8), C(1)-P(1)-Ru(1) 153.7(2), C(2)-C(1)-P(1) 174.7(5), P(2)-Ru(1)-P(3) 80.82(3), P(5)-Ru(1)-P(4) 82.94(4).

As mentioned before, treatment of the related complex $[RuH(dppe)_2(P{\equiv}CSiPh_3)]^+$ (**123**) with NaOPh has been reported to give the first terminal "cyaphide" complex, $[RuH(dppe)_2(C{\equiv}P)]$ (**124**).[98] A prior theoretical study on P≡CMe concluded that its methyl protons are quite acidic compared to those of N≡CMe and that it should be more easily deprotonated. [16] As a result, it seemed that compound **127** could prove useful as a platform to test the further reactivity of P≡CMe towards electrophiles and nucleophiles. Accordingly, treatment of **127** with a variety of bases (e.g. NaOH, $KOBu^t$, NaOPh and $LiNPr^i_2$) but all reactions led to intractable mixtures of products. Attention then turned to the reaction of the electrophilic reagent MeI with **127** in CH_2Cl_2. Monitoring this reaction by $^{31}P\{^1H\}$ NMR spectroscopy revealed that a compound was formed at *ca.* -50°C with a spectral pattern similar to that of **127**, but with the signal derived from the phosphaalkyne shifted by *ca.* 200 ppm down field (δ 165.6 ppm, quint., $^2J_{PP}$ = 28 Hz, δ 65.2 ppm, d, $^2J_{PP}$ = 28 Hz, 4 P). This observation suggests the product contains a P-coordinated phosphaalkene or phosphaalkenyl fragment, though its structure is unknown.[104] Upon warming the reaction mixture past -10°C, the product appeared to decompose to an unidentifiable mixture of phosphorus containing products which prohibited its isolation and further characterization.

Previous studies have shown that bulky η^1-P-coordinated phosphaalkynes can be transformed to, for example, phosphaalkenes,[99] phosphines[99]and phosphorus heterocycles[97] upon treatment with proton sources. In a similar vein, the reaction of **127** with a excess of a diethylether solution of HBF_4 ledes to a moderate yield of the difluorophosphine complex, **128** (**Scheme 47**), after recrystallisation from a hexane/dichloromethane solution. In this reaction, the HBF_4 is presumably acting as a source of HF which doubly reduces the coordinated phosphaalkyne. The HBF_4 is

also the source of the counter anion in **128**. It is noteworthy that P≡CBu^t (within the complex *trans*-[FeH(dppe)$_2$(η^1-P≡CBu^t)]$^+$) has been similarly reduced to $F_2PCH_2Bu^t$ by treatment with HBF_4.[99] In that reaction, the stepwise nature of the reduction was confirmed by the isolation of an intermediate containing a P-coordinated fluorophosphaalkene, FP=CHBu^t. No similar intermediate (*viz.* *trans*-[RuH(dppe)$_2${η^1-P(F)=C(H)Me}]$^+$) was observed in the current reaction, which is perhaps in line with the previously demonstrated greater reactivity of P≡CMe over P≡CBu^t. Indeed, treating **127** with one equivalent of HBF_4 led only to a mixture of **128** and unreacted **127**.

The spectroscopic data for **128** are compatible with its solid state structure. In its $^{31}P\{^1H\}$ NMR spectrum the fluorophosphine signal appears as a triplet of quintets at low field (δ 244.4 ppm) displaying characteristic $^1J_{PF}$ and $^2J_{PP}$ couplings (1094 and 30 Hz respectively). The low field position of this signal is not surprising in light of the electron withdrawing nature of the fluorine substituents and it can be compared to a chemical shift of δ 279.5 ppm for the corresponding signal in the spectrum of *trans*-[FeH(dppe)$_2${η^1-P(F)$_2$C(H)$_2$Bu^t}]$^+$.[100] The structure of the cationic component of **128** (**Figure 18**) reveals its ruthenium centre to have a similar octahedral geometry to that of **127**, while the geometry of the PF_2Et ligand is unremarkable. Saying this, there has been no previous crystallographic elucidation of this phosphine.

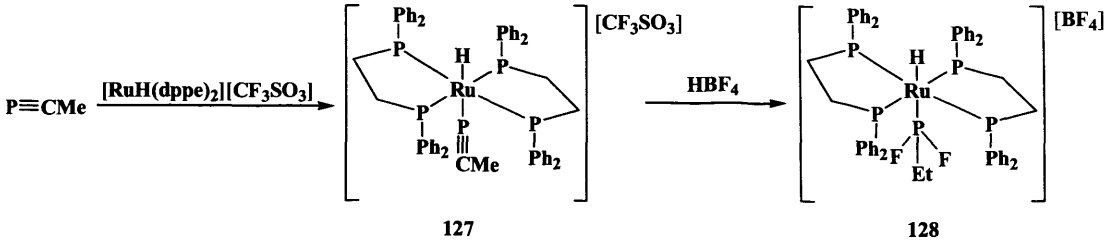

Scheme 47 Reaction of P≡CMe with [RuH(dppe)$_2$][CF_3SO_3]

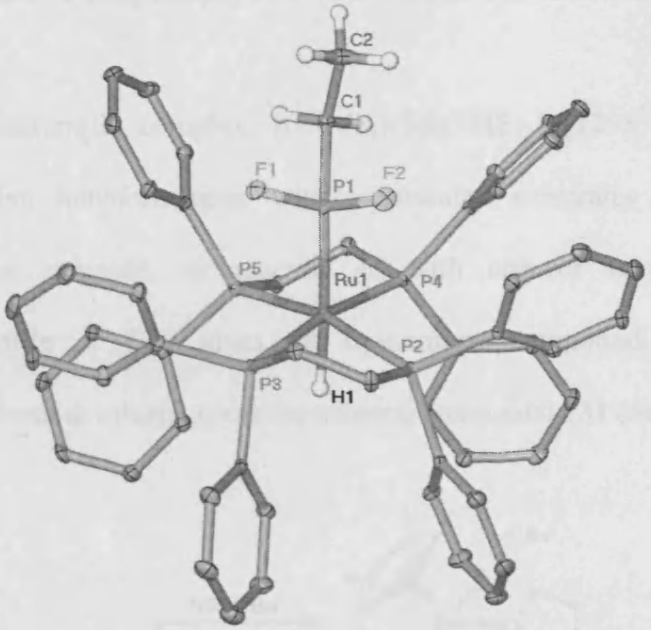

Figure 18 Molecular structure of 128 (hydrogen atoms omitted for clarity; ellipsoids shown at the 25% probability level).

Selected bond lengths (Å) and angles (°): Ru(1)-P(1) 2.2941(13), Ru(1)-P(5) 2.3394(12), Ru(1)-P(3) 2.3607(13), Ru(1)-P(4) 2.3684(13), Ru(1)-P(2) 2.3783(13), P(1)-F(2) 1.583(3), P(1)-F(1) 1.610(3), P(1)-C(1) 1.811(4), C(1)-C(2) 1.518(7), F(2)-P(1)-F(1) 98.66(15), F(2)-P(1)-C(1) 103.21(19), F(1)-P(1)-C(1) 96.86(18), P(3)-Ru(1)-P(2) 78.79(4), P(5)-Ru(1)-P(4) 84.40(4), C(2)-C(1)-P(1) 115.6(3).

1.3.7 Reaction of Phosphaalkynes with a Samarium Precursor

The samarium(II) complex, $[(C_5Me_5)_2Sm(THF)_2]$ (**129**),[105] is known to undergo reductive transformations with unsaturated substrates in a variety of ways.[106-109] For example, its reaction of with one or two equivalents of trimethylacetonitrile in THF gives the monomeric compound, **130**. However, changing the solvent to toluene gives the trimeric compound **131** (**Scheme 48**).[108]

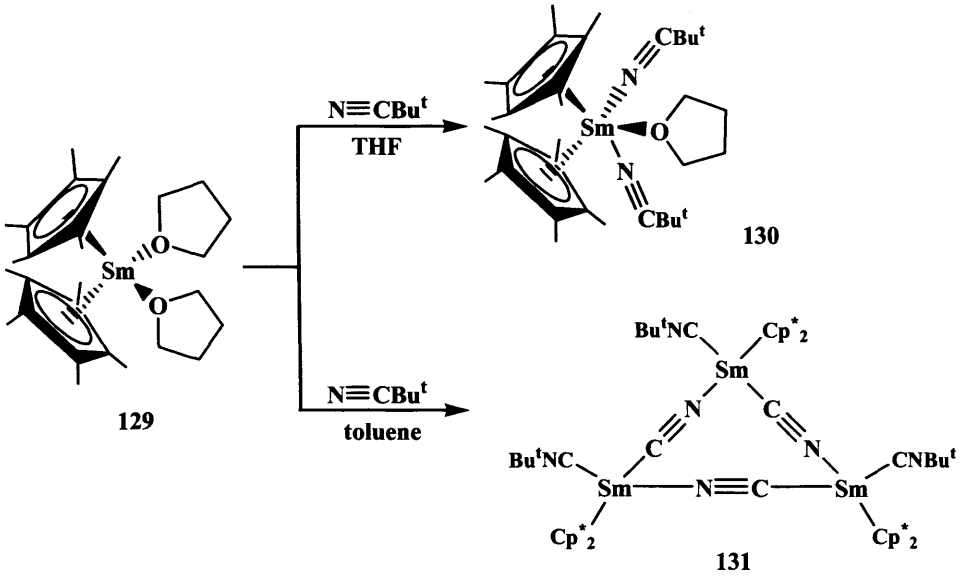

Scheme 48 Reaction of a $[(Cp^*)_2Sm(THF)_2]$ (**129**) with a nitrile

Examples of reactions of samarium(II) complexes with alkynes can also be found in the literature. The reactions of the samarium(II) complex, **129**, with alkynes, **132a-e**, in toluene, give the monomeric samarium(III) complexes, **133a-e**. These complexes have been formed *via* reductive C-H cleavage of the alkynes at the samarium centre, to form the THF-solvent alkynides **133a-e**. However, the THF free samarium(II) complex, **134**,[110, 111] shows different behaviour in its reaction with alkynes, **132e-f**. These give the dimeric samarium(III) complexes **135e-f**, formed *via* reductive C-H cleavage and coupling of the alkynes (**Scheme 49**).[109]

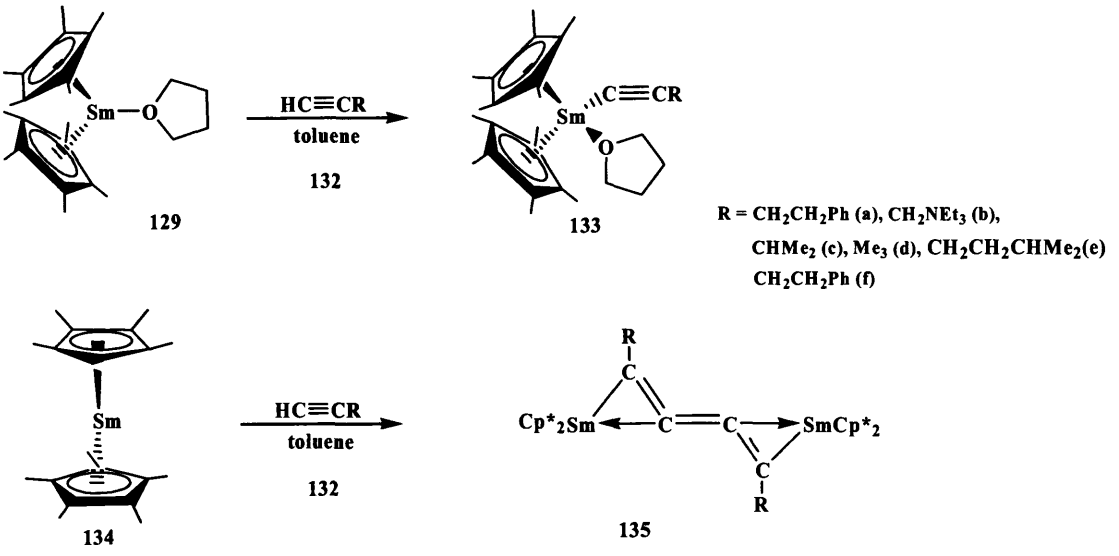

Scheme 49 Reaction of $[(Cp^*)_2Sm(THF)_2]$ **129** and $[Sm(Cp^*)_2]$ **134** with alkynes

The samarium(II) complex, $[(C_5Me_5)_2Sm(THF)_2]$ (**129**) was also reacted with two equivalents of the phosphaalkyne, P≡CBu^t, in toluene, giving the dimeric complex, **136**, *via* reductive coupling.[112]

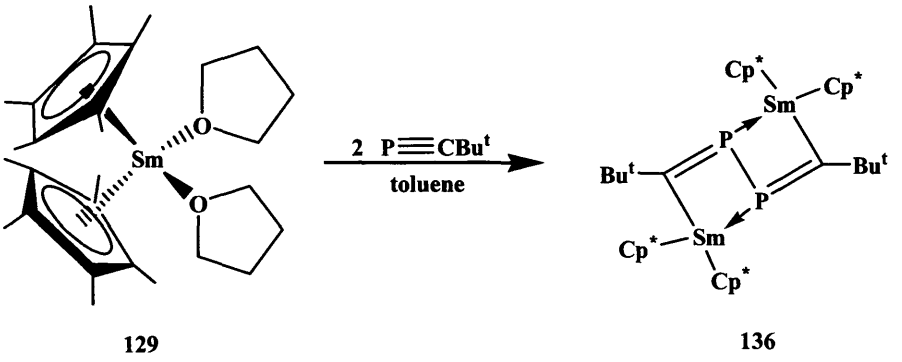

Scheme 50 Reaction of $[(Cp^*_2)Sm(THF)_2]$ (**129**) with P≡CBu^t

In this curent study a samarium(II) complex, **137**,[113] were reacted with phosphaalkynes, P≡CMe and P≡CBu^t. The reaction of **137** with an excess of P≡CMe in toluene at -90 °C was followed by $^{31}P\{^1H\}$ NMR spectroscopy. This showed an intractable mixture of phosphorus containing compounds, from which no product could be isolated. However, the reaction of **137** with an excess of P≡CBu^t followed by $^{31}P\{^1H\}$ NMR spectroscopy, showed no new resonances, most likely due to paramagnetic nature of the products. After all volatiles were removed *in vacuo*, the

residue was extracted with hexane and stored at -25 °C to give the dimeric product **138** (**Scheme 51**). As phosphaalkynes have been shown to be more alkyne than nitrile like in there reaction, it is no surprise seeing similarities between the alkyne product **135e-f**, and the two phosphaalkyne products, **136** and **138**.

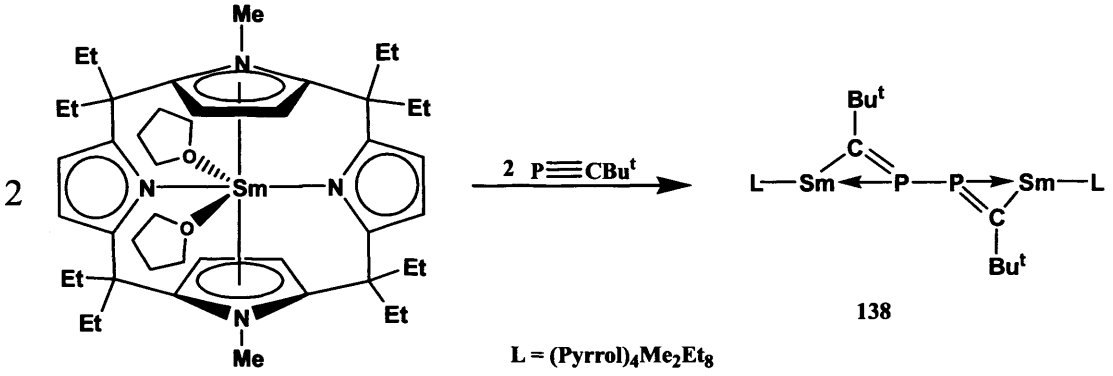

137 138

Scheme 51 Reaction of a samarium(II) precursor with P≡CBu^t

The molecular structure of **138** was determined by X-ray crystallography, revealing to contain two coupled phosphaalkyne molecules bridging between two samarium fragments (**Figure 19**). The C=P bond lengths are 1.660 Å (P(1)-C(1)) and 1.673 Å (P(2)-C(6)) which are slightly shorter than those found in **136** (1.694 and 1.698) and consistend with C=P double bounds.

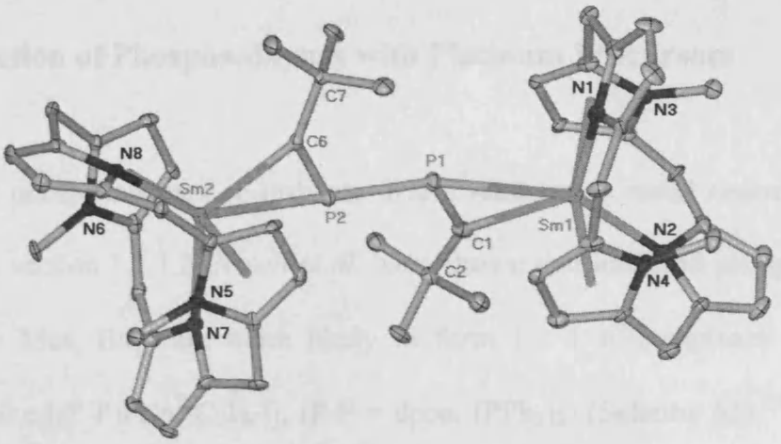

Figure 19 Molecular structure of 138 (hydrogen atoms omitted for clarity; ellipsoids shown at the 25% probability level)

Selected bond lengths (Å) and angles (°): Sm(1)-C(1) 2.524(12), Sm(2)-C(6) 2.520(11), P(1)-C(1) 1.660(12), P(1)-P(2) 2.267(5), P(2)-C(6) 1.673(11), C(1)-C(2) 1.539(15), C(6)-C(7) 1.521(14), C(1)-P(1)-P(2) 116.3(5), C(1)-P(1)-Sm(1) 59.2(4), P(2)-P(1)-Sm(1) 165.32(17), C(6)-P(2)-P(1) 114.8(4), C(6)-P(2)-Sm(2) 56.9(4), P(1)-P(2)-Sm(2) 165.41(16), C(2)-C(1)-P(1) 132.0(10), C(2)-C(1)-Sm(1) 141.3(8), P(1)-C(1)-Sm(1) 86.5(5), C(7)-C(6)-P(2) 132.8(9), C(7)-C(6)-Sm(2) 137.8(7), P(2)-C(6)-Sm(2) 89.3(5).

1.3.8 Reaction of Phosphaalkynes with Platinum Precursors

That phosphaalkynes co-ordinate in a η^2-fashion to metal centres has been discussed in section 1.1.1.2. *Nixon et al.* have shown that hindered phosphaalkynes, P≡CR (R = Mes, Bu^t), are more likely to form 1 : 1 η^2-complexes with Pt(0) precursors like [(P-P)Pt(η^2-C_2H_4)], (P-P = dppe, $(PPh_3)_2$) (**Scheme 52**),[28, 114] while unhindered phosphaalkynes, P≡CR (R = H, Me), could react differently as their smaller substituents give space for further co-ordination and/or cycloaddition processes.

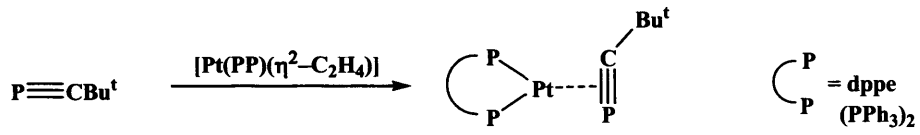

Scheme 52 Reactivity of [Pt(PP)(η^2-C_2H_4)] (PP = dppe, $(PPh_3)_2$) with P≡CBu^t

The reaction of [Pt$(PCy_3)_2$(η^2-C_2H_4)] (**139**) with an excess of P≡CMe at room temperature was followed by $^{31}P\{^1H\}$ NMR spectroscopy over 24 h and this showed a resonance form at δ 86.6 ppm, similar to that seen for [Pt(PP)(η^2-P≡CMes)] (PP = PPh_3) = 89.4 ppm. Thus, it can be assumed that an η^2-co-ordination to the metal centre has occurred. After all volatiles were removed from the reaction mixture *in vacuo*, the residue was redissolved in toluene and the extract stored in a freezer yielding **140 (Figure 20)** as a crystalline product (**Scheme 53**).

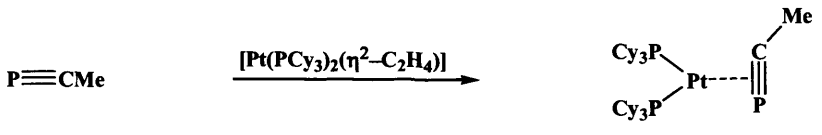

139 **140**

Scheme 53 Reaction of [Pt$(PCy_3)_2$(η^2-C_2H_4)] (**139**) with P≡CMe

The $^{31}P\{^{1}H\}$ NMR spectroscopic data for **140** are similar to those for related complexes, e.g. $[Pt(dppe)(\eta^2\text{-}P{\equiv}CBu^t)]$,[115] and in particular, the phosphaalkyne resonance displays a very small $^{1}J_{PtP}$ coupling constant (143.6 Hz).

The molecular structure of **140** was determined by X-ray crystallography displaying disorder of the coordinated phosphaalkyne over two sites. Although successfully modelled, this disorder affects the reliability of comment on the phosphaalkyne co-ordination geometry to some extent. The structure of **140** is comparable with that of, for example, $[Pt(PPh_3)_2(\eta^2\text{-}P{\equiv}CBu^t)]$,[10] as both exhibit phosphaalkyne P-C distances (1.623 Å (mean) and 1.672(17) Å respectively) longer than that in free $P{\equiv}CBu^t$ (1.548(1) Å).[8]

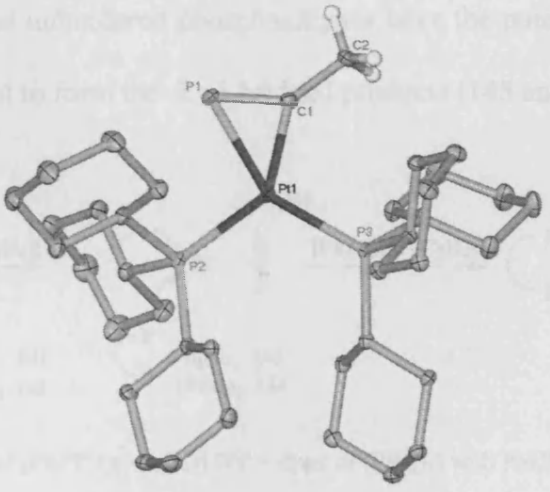

Figure 20 Molecular structure of **140** (hydrogen atoms omitted for clarity; ellipsoids shown at the 25% probability level)

Selected bond lengths (Å) and angles (°): Pt(1)-C(1) 2.034(8), Pt(1)-P(3) 2.3035(11), Pt(1)-P(2) 2.3072(10), Pt(1)-P(1) 2.354(3), P(1)-C(1) 1.623(9), C(1)-C(2) 1.505(11), C(1)-Pt(1)-P(3) 106.7(3), C(1)-Pt(1)-P(2) 140.0(3), P(3)-Pt(1)-P(2) 113.32(3), C(1)-Pt(1)-P(1) 42.6(3), P(3)-Pt(1)-P(1) 149.35(8), P(2)-Pt(1)-P(1) 97.33(8), C(1)-P(1)-Pt(1) 58.1(3), C(2)-C(1)-P(1) 140.9(6), C(2)-C(1)-Pt(1) 139.8(6), P(1)-C(1)-Pt(1) 79.2(4).

Further investigations have been carried out with less bulky Pt(0) precursors including [Pt(P-P)(η^2-C_2H_4)] (P-P = dppe or $(PEt_3)_2$), **141** or **142**. Treatment of precursors **141** and **142** with an excess of P≡CMe was followed by $^{31}P\{^1H\}$ NMR spectroscopy and this showed resonances appear at δ 102.4 ppm (**143**) and δ 90.4 ppm (**144**). Once again it can be assumed that there is a η^2-P≡CMe co-ordination to the metal centre which leads to the 1 : 1 product. However, after volatiles were removed *in vacuo* and the residues redissolved, the $^{31}P\{^1H\}$ NMR spectra had substantially changed. The η^2-P≡CMe observed resonances had shifted up-field by *ca.* 200 ppm (**145**: δ -101.2, **146**: δ -115.5 ppm) suggesting the presence of saturated P-centres in the final product (**Scheme 54**). The change to less bulkier Pt(0) reaction precursors, shows that unhindered phosphaalkynes have the potential to react with a second Pt(0) fragment to form the 2 : 1 bridged products (**145** and **146**).

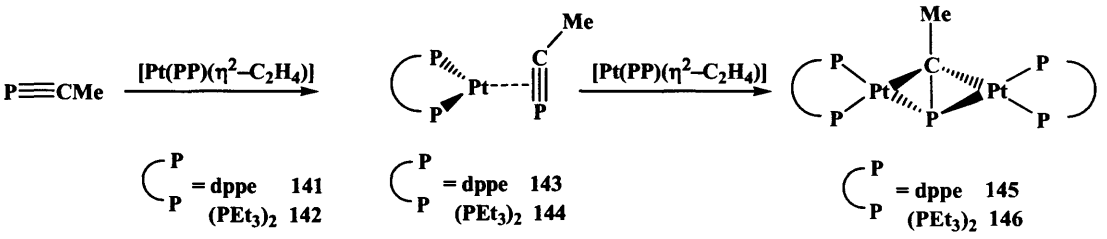

Scheme 54 Reactivity of [Pt(PP)(η^2-C_2H_4)] (PP = dppe or $(PEt_3)_2$) with P≡CMe

The molecular crystal structures of these compounds, **145** and **146**, determined by X-ray crystallography reveal each to contain a phosphaalkyne molecule bridging two platinum fragments. The mechanism of formation of **145** and **146** probably involves **143** and **144** being in equilibrium with the free phosphaalkyne, thus allowing attack of **143** and **144** by a second "Pt^0(P-P)" fragment upon removal of volatiles, including P≡CMe, from the reaction mixtures. Similar secondary reactions do not occur for complexes of bulkier phosphaalkyne-

platinum(0) complexes, e.g. [Pt(dppe)(η^2-P≡CBu^t)],[115] presumably because attack at the P-C multiple bond is not facile for steric reasons.

The $^{31}P\{^1H\}$ NMR spectroscopic data for **143** and **144** are similar to those for related complexes, e.g. [Pt(dppe)(η^2-P≡CBu^t)],[115] and in particular, their phosphaalkyne resonances display very small $^1J_{PtP}$ coupling constants (**143** 178.0, **144** 167.5 Hz). Interestingly, these couplings for the bridged complexes, **145** and **146**, are too small to be observable. The high field position of the phosphaalkyne resonances (**145** δ -101.2 ppm, **146** δ -115.5 ppm) in these complexes can, however, be compared to those in other phosphaalkyne bridged complexes, e.g. [{CpMo(CO)$_2$}$_2$(μ-P≡CBu^t)], δ -110 ppm.[116]

The molecular structure of **154** and **146** was determined by X-ray crystallography displayed disorder of the coordinated phosphaalkyne over two sites. Although successfully modelled, this disorder affects the reliability of comment on the phosphaalkyne co-ordination geometry to some extent. The P-C distances of **145** (1.744 Å mean), (**Figure 21**) and **146** (1.728 Å mean) are longer those of **140** (1.623 Å mean) and the free P≡CBu^t (1.548(1) Å).[8] Also of note are the Pt_2PC fragments of **145** and **146**, which are non-planar and exhibit angles between their three-membered rings of 96.4° and 96.8°, respectively.

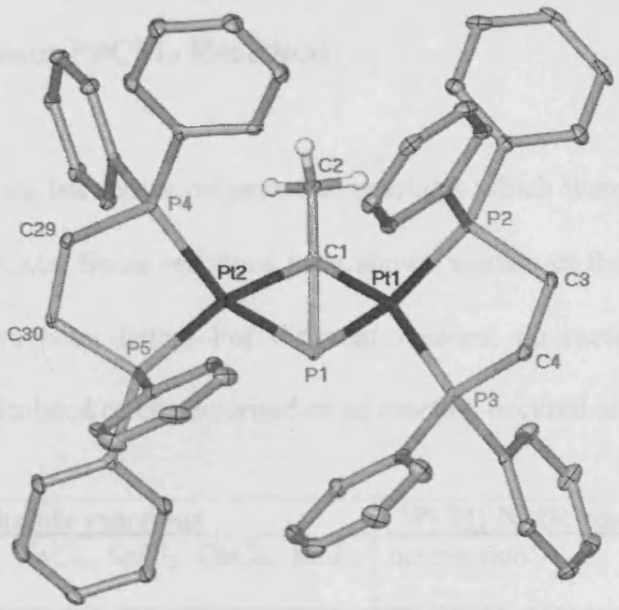

Figure 21 Molecular structure of **145** (25% thermal ellipsoids, non-methyl hydrogens omitted for sake of clarity)

Selected bond lengths (Å) and angles (°) relating to one of the two components of the disordered PCMe ligand: Pt(1)-C(1) 2.075(13), Pt(1)-P(2) 2.2568(12), Pt(1)-P(3) 2.2618(12), P(1)-C(1) 1.734(12), P(1)-Pt(2) 2.347(2), C(1)-C(2) 1.537(10), C(1)-Pt(2) 2.059(11), Pt(2)-P(4) 2.2498(10), Pt(2)-P(5) 2.2611(10), C(1)-Pt(1)-P(1) 45.4(3), P(2)-Pt(1)-P(3) 86.75(4), C(1)-Pt(2)-P(1) 45.8(3), P(4)-Pt(2)-P(5) 86.43(4), C(1)-P(1)-Pt(2) 58.3(4), C(1)-P(1)-Pt(1) 58.4(5), Pt(2)-P(1)-Pt(1) 80.34(7), P(1)-C(1)-Pt(2) 75.9(4), P(1)-C(1)-Pt(1) 76.3(5), Pt(2)-C(1)-Pt(1) 94.7(4).

1.3.9 Miscellaneous P≡CMe Reactions

The following list shows reagents and reactants which were reacted with the phosphaalkyne P≡CMe. Some reactions have shown signals in their $^{31}P\{^{1}H\}$ NMR spectra which have been listed. For different reasons, no raction, or tracteblle products could be isolated or characterised or no reaction occured at all.

Metal and metal halide reactions	**$^{31}P\{^{1}H\}$ NMR resonances**
$GeCl_2$, CuI, $GaCl_3$, $TaCl_5$, $SnCl_2$, $GeCl_4$, SmI_2, InI, InBr, GaI	no reaction
Na,	δ d 324 ppm
K, Mg	decomposition / polymerisation
Metal carbonyls	
$Co(CO)_8$	decomposition
$Fe(CO)_9$	δ s 150, s 98, s 84, s 1 ppm
Ru precursors	
$RuHCl(PPh_3)_2(CO)$	δ s 463, s 458, m 35, m 26, s -4 ppm
$RuCl_2(PPh_3)_3$	δ m 63, m 60, m 49, m 41, m -1 ppm
$RuH_2(dppe)_2$	no reaction
$(RuCp^*H_2)_2$	no reaction
$[RuCp^*(CH_3CN_3)]^{3+}$	no reaction
Rh precursors	
$[RhCl(PPh_3)_3]_2$	δ s 24, s -4 ppm
$RhCl(CS)(PPh_3)_2$	decomposition
$[RhCl(COE)_2]_2$	decomposition
Amidinates (Bu^t)C(NDip$_2$) (Dip = $C_6H_3Pr^i_2$-2,6) (Piso) and Guanadinate (R_2N)C(NDip$_2$) (R = Pr^i (Priso) or Cy (Giso))	
(Giso)GeCl	no reaction
$[(Giso)Ge]^+$ $[GeCl_4]^-$	no reaction
(Giso)Ga	no reaction
(Giso)SnCl	no reaction
$\{(Gsio)NiBr\}_2$	decomposition
$\{(Priso)NiBr\}_2$	decomposition
$\{(Priso)Ni\}_2$(μ-toluene)	decomposition
$\{(Priso]Ni\}_2$	decomposition
$\{(Piso)FeN\}_2$	decomposition
$(Priso)Co)_2$	decomposition

$\{(Giso)As\}_2$	decomposition
$(Giso)AlH_2$	decomposition
Lewis Acids and Bases	
n-Buli	δ s 178, s -10, m. -14, s -28, s -31 ppm
$LiN(Pr^i)_2$	δ s 296, s 274, s 263, s 212, s 177 ppm
NaOPh	no reaction
HBF_4	no reaction
Others	
$Pd(PPh_3)_4$	δ s 29, s 4 ppm
MgCyCl	δ m -28 ppm
MgPhBr	δ m 7, ppm
PI_3	δ m 136, s 98, s 89, s 57 ppm
PCl_3	δ s 264, s 219 ppm
$\{Ir(COD)Cl_2\}_2$	decomposition
$ZnEt_2$	decomposition
$Ni(COD)_2$	decomposition
$Pt(COD)Cl_2$	decomposition
Cp_2ZrCl_2	no reaction
P_4	no reaction

1.4 Conclusion

Phosphaalkynes are interesting compounds as they undergo co-ordination, cycloaddition, oligomerisation and polymerisation reactions with main group and transition metal precursors in which their behaviour is more like alkynes than nitriles.[10]

Special focus in this part of this thesis was on the mostly unexplored methyl-phosphaalkyne. After investigating the preparation and handling of the unhindered phosphaalkyne, P≡CMe, (which was revealed to be more challenging than that of the hindered phsophaalkyne P≡CBu^t) it was shown to have interesting reactivity towards main group and transition metal complexes. The results of this study have revealed significant differences as well as similarities to the reactivity of bulkier phosphaalkyne analogues. This can mainly be explained on steric grounds. This is just the beginning of the investigation of unhindered phosphaalkynes and there is much more potential which is waiting to be discovered. Further study of methyl-phosphaalkyne chemistry will be maintained in the Jones group, using these results as the basis for future work.

1.5 Experimental

General considerations. All manipulations were carried out using standard Schlenk and glove box techniques under an atmosphere of high purity argon or N_2. Hexane, THF and toluene were distilled over potassium whilst diethylether was distilled over Na/K then freeze/thaw degassed prior to use. ^1H and $^{31}P\{^1H\}$ NMR spectra were recorded on either a Bruker DXP400 or a Jeol Eclipse 300 spectrometer and were referenced to the residual ^1H resonances of the solvent used or external 85% H_3PO_4 respectively. Mass spectra were obtained from the EPSRC National Mass Spectrometry Service at Swansea University. IR spectra were recorded using a Nicolet 510 FT-IR spectrometer as Nujol mulls between NaCl plates. Melting points were determined in sealed glass capillaries under argon or N_2, and are uncorrected. 1,3,5-$P_3C_3Bu^t_3$ (**17**)[44, 69], 1,3,5,7-$P_4C_4Bu^t_4$ (**18**)[117], $[Ge\{CH(SiMe_3)_2\}_2]_2$ (**76**)[118], $[Sn\{CH(SiMe_3)_2\}_2]_2$ (**77**)[118], $[Sn(Ar)_2]_3$ (Ar = $C_6H_2Pr^i_3$-2,4,6) (**78**)[119], $[Pt(Cy_3P)_2(\eta^2\text{-}C_2H_4)]$), (**139**)[121], $[Pt(dppe)(\eta^2\text{-}C_2H_4)]$ (**141**)[120], *cis*-$[Pt(PEt_3)_2(\eta^2\text{-}C_2H_4)]$ (**142**)[122], $[Ru(H)_2(dppe)_2]$[123], $[RuH(dppe)_2][OTF]$[124], $[RuH(dppe)_2][BF4]$[123], $[FeH(dppe)_2][BPh4]$[102] were synthesised by literature procedures. $P{\equiv}CBu^t$ was synthesised by the $[Li\{N(SiMe_3)_2\}]$ catalysed elimination of hexamethyldisiloxane from $(Me_3Si)P{=}C(Bu^t)(OSiMe_3)$[125]. $P{\equiv}CMe$[13, 66, 67] was prepared by modified literature procedures, while all other chemicals were obtained from commercial sources and used as supplied.

$CCl_3P(O)(OPr^i)_2$ (40)

Triisopropyl phosphite (14.2 g, 68.04 mmol) was heated at refluxed overnight with CCl_4 (95.5 g, 0.62 mol). All volatiles were removed *in vacuo* and the residue distilled, b.p. 62 – 64 °C 0.07 mmHg, yielding phosphonate **40** as a colourless liquid.

(17.2 g, 90%); ^1H NMR (400 MHz, $CDCl_3$, 298 K): δ 1.28 (v. trip, $^3J_{HH}$ = 6.3 Hz, $^4J_{PH}$ = 7.7 Hz, 12H, Pr^i), 4.90 (sept, $^3J_{HH}$ = 6.3 Hz, 2H, Pr^i-H); $^{31}P\{^1H\}$ NMR (121.6 MHz, $CDCl_3$, 298 K): δ 4.28 (s); $^{13}C\{^1H\}$ NMR (62.9 MHz, $CDCl_3$, 303 K): δ 23.42 (s, $CH(CH_3)_2$), 24.23 (s, $CH(CH_3)_2$), 40.0 (s, CCl_3), 87.60 (s, $C(CH_3)$), 90.75 (s, $C(CH_3)$).

$MeCCl_2(O)(OPr^i)_2$ (41)

$LiBu^n$ (18 ml of a 1.6 M solution in hexane, 28.8 mmol) was added dropwise over 20 min to a solution of phosphonate **40** (7.86 g, 27.94 mmol) in THF (80 cm^3) at -85 °C and stirred at this temperature for 5 min. MeI (4.1 g, 28.8 mmol) was added dropwise over 15 min to the reaction mixture at -85 °C and the mixture was stirred for 1 h before warming to room temperature. Organic workup with half saturated $NaHCO_3$ solution, and distillation of the organic phase (b.p. 52 – 54 °C, 0.07 mmHg) gave phosphanate **41** as a colourless liquid.

(5.8 g, 80%); ^1H NMR (400 MHz, $CDCl_3$, 298 K): δ 1.3 (v. trip, $^3J_{HH}$ = 2.7 Hz, $^4J_{PH}$ = 3.5 Hz, 12H, Pr^i), 2.3 (d, $^3J_{PH}$ = 12 Hz), 4.82 (sept, $^3J_{HH}$ = 6.4 Hz, 2H, Pr^i-H); $^{31}P\{^1H\}$ NMR (121.6 MHz, $CDCl_3$, 298 K): δ 11.65 (s);

$MeCCl_2PH_2$ (42)

$AlCl_3$ (5.6g, 42 mmol) was slowly added over 5 min to a suspension of $LiAlH_4$ (0.53 g, 14 mmol) in diglyme (40 cm^3) at -70 °C. The mixture was allowed to warm up to -

10 °C and the suspension cooled to -80 °C. Phosphanate **41** (2.62 g, 9.96 mmol) in diglyme (10 cm^3) was added dropwise over 10 min, maintaining the temperature below -60 °C. The suspension was allowed to warm up to -30 °C and degassed water (5ml) was added dropwise over 10 min. The suspension was heated to 0 °C and filtered through celite into a Schlenk flask containing 20g $MgSO_4$. This was stored for 12 h at -25 °C. The suspension was filtered and the solution, containing phosphine **42**, was used in the next step to make P≡CMe (**2**).

(1.0 g, 80%); ^1H NMR (400 MHz, $CDCl_3$, 298 K): δ 2.4 (d, $^3J_{PH}$ = 7 Hz, 3H, CH_3), 4.0 (s, 2H, PH_2); $^{31}P\{^1H\}$ NMR (121.6 MHz, $CDCl_3$, 298 K): δ -45.7 (s).

P≡CMe (2)

DBU (2.8 g, 18.33 mmol) was added dropwise over 10 min to phosphine **42** (1.0 g, 6.64 mmol) in diglyme (50 cm^3) maintaining the temperature under -60 °C. The suspension was allowed to warm to -10 °C and purified by trap to trap distillation, in which the first trap was cooled to -45 to 50 °C and the second trap cooled to -120 °C. **2**, which freezes at ca. -90 °C, was collected in the -120 °C trap and was later condensed into a Youngs Schlenk, then dissolved in diethylether to give a ca. 0.25 M solution.

(300 mg, 68%); ^1H NMR (400 MHz, C_6D_6, 298 K): δ 1.50 (d, $^3J_{PH}$ = 15 Hz, 3H, CH_3); $^{31}P\{^1H\}$ NMR (121.6 MHz, $CDCl_3$, 298 K): δ -60.49 (s); $^{13}C\{^1H\}$ NMR (75 MHz, C_6D_6, 303 K): δ 14.5 (d, $^2J_{PC}$ = 20 Hz, *C*H_3), 171.20 (d, $^1J_{PC}$ = 49 Hz, *C*P).

$P_5C_5Me_2Bu^t_3$ (47)

P≡CMe (6.8 cm^3 of a 0.25 M solution in diethylether, 1.71 mmol) was added to a solution of 1,3,5-$P_3C_3Bu^t_3$ (170 mg, 0.57 mmol) in hexane (15 cm^3) at room temperature. After 1h, all volatiles were removed *in vacuo* yielding a yellow solid.

This was extracted with hexane (2 x 5 cm^3), filtered, concentrated to 3 cm^3 and stored at -30 °C yielding **47** as yellow crystals.

(155 mg, 66%); M.p.: 206 – 208 °C; ^{1}H NMR (400 MHz, C_6D_6, 298 K): δ 1.18 (s, 9H, Bu^t), 1.23 (s, 9H, Bu^t), 1.56 (s, 9H, Bu^t), 1.73 (v. tr, $^3J_{PH} = {}^3J_{PH}$ = 19 Hz, 3H, CH_3-C(1)), 2.73 (ddd, $^3J_{PH}$ = 30 Hz, $^3J_{PH}$ = 14 Hz, $^4J_{PH}$ = 7 Hz, 3H, Me on C(4)); $^{31}P\{^1H\}$ NMR (121.6 MHz, C_6D_6, 298 K): δ -100.1 (br. d, $^1J_{PP}$ = 176 Hz, P(3)), 9.4 (br. d, $^1J_{PP}$ = 176 Hz, P(4)), 60.0 (br, P(2)), 301.9 (br., P(1)), 308.8 (br, P(5)); IR ν/cm^{-1} (Nujol): 1377m, 1260m, 1105m, 1022m, 802m, 723m; MS (EI/70eV), *m/z* (%): 416 [M^+, 25], 58 [Bu^tH^+, 100]; EI Acc. Mass.: on M^+: calc. for $C_{19}H_{33}P_5$: 416.1265, found 416.1269.

[{W(CO)$_5$}$_2$(μ-η^1: η ^{1}-P$_5$C$_5$Me$_2$Bu$^t_3$)] (48)

Compound [$P_5C_5Me_2Bu^t_3$] (**47**) (150 mg, 0.36 mmol) was dissolved in THF (3 cm^3) and [$W(CO)_5$(THF)] (0.75 mmol) in THF (50 cm^3) was added to the solution at room temperature. After stirring for 17 h, volatiles were removed *in vacuo* and the residue purefied by chromatography (silica gel/hexane). An orange band was collected and concentrated to *ca.* 2 cm^3. Storage of this at -30°C overnight yielded **48** as an orange crystalline solid.

(273 mg, 45%); M.p.: 148 – 152 °C; ^{1}H NMR (400 MHz, C_6D_6, 298 K): δ 1.12 (s, 9H, Bu^t), 1.15 (s, 9H, Bu^t), 1.56 (s, 9H, Bu^t), 1.80 (v. tr., $^3J_{PH} = {}^3J_{PH}$ = 19 Hz, 3H, Me on C(1)), 2.63. (ddd, $^3J_{PH}$ = 30 Hz, $^3J_{PH}$ = 15 Hz, $^4J_{PH}$ = 8 Hz, 3H, Me on C(4)); $^{31}P\{^1H\}$ NMR (121.6 MHz, C_6D_6, 298 K): δ -119.6 (dd, $^1J_{P3P4}$ = 180 Hz, $^2J_{P3P1}$ = 24 Hz, P(3)), 11.7 (d of v. tr, $^1J_{P4P3}$ = 180 Hz, $^2J_{P4P2} = {}^2J_{P4P5}$ = 12 Hz, P(4)), 72.0 (br. v. tr, $^2J_{P2P4} = {}^2J_{P2P5}$ = 12 Hz, $^1J_{PW}$ = 255 Hz, P(2)), 243.1 (d, $^2J_{P1P3}$ = 24 Hz, $^1J_{PW}$ = 225 Hz, P(1)), 315.8 (br. unres. m, P(5)); IR ν/cm^{-1} (Nujol): 2069m, 1952br.s, 1938s (CO str.); MS (EI/70eV), *m/z* (%): 1064 [M^+, 18], 741 [M^+ - $W(CO)_5$, 36], 418 [M^+ -

$2W(CO)_5$, 100]; EI Acc. Mass.: on M^+: calc. for $C_{29}H_{33}O_{10}P_5W_2$: 1063.9775, found 1063.9778.

[{W(CO)$_5$}{W(CO)$_4$}(μ-η^1: η ^{4}-P$_5$C$_5$MeBu$^t_4$)] (49)

P≡CMe (0.9 cm^3 of a 0.25 M solution in diethylether, 0.22 mmol) was added to a solution of 1,3,5,7-$P_4C_4Bu^t_4$ (84 mg, 0.20 mmol) in hexane (5 cm^3) at room temperature. After stirring for 1.5 h, volatiles were removed *in vacuo* and the residue dissolved in THF (5 cm^3). [$W(CO)_5$(THF)] (0.50 mmol) in THF (50 cm^3) was then added to the solution at room temperature. After stirring overnight, volatiles were removed *in vacuo* and the residue purefied by chromatography (silica gel/hexane). The orange band was collected and concentrated to *ca.* 2 cm^3. Storage of this at -30°C overnight yields **49** as an orange crystalline solid.

(69 mg, 32%); M.p.: 184 – 187 °C; ^{1}H NMR (400 MHz, C_6D_6, 298 K): δ 1.01 (s, 9H Bu^t), 1.04 (s, 9H Bu^t), 1.10 (s, 9H Bu^t), 1.25 (s, 9H Bu^t), 2.02 (v. quint, $^3J_{HP} = {}^3J_{HP} = {}^3J_{HP}$ = 18 Hz, 3H, Me); $^{31}P\{^1H\}$ NMR (121.6 MHz, C_6D_6, 298 K): δ -5.5 (dd, $^1J_{P5P4}$ = 56 Hz, $^2J_{P5P2}$ = 7 Hz, P(5)), - 4.9 (v. tr, $^2J_{P2P5} = {}^2J_{P2P3}$ = 7 Hz, P(2)), 0.5 (dd, $^1J_{P4P5}$ = 56 Hz , $^1J_{P4P3}$ = 24 Hz, P(4)), 30.2 (dd, $^1J_{P3P4}$ = 24 Hz, $^2J_{P3P2}$ = 7 Hz, $^1J_{PW}$ = 196 Hz, P(3)), 53.4 (br., P(1)); IR ν/cm^{-1} (Nujol): 2068s, 2050s, 1983s, 1942s, 1918s (CO str.); MS (EI/70eV), *m/z* (%): 1078 [M^+, 25], 782 [M^+-$W(CO)_4$, 18], 548 [M^+-$W_2(CO)_9$, 13]; EI Acc. Mass.: on M^+: calc. for $C_{31}H_{39}O_9P_5W_2$: 1078.0295, found 1078.0302, parameters, R(observed) = R1 = 0.0382, wR2 = 0.0802, R1 = 0.0567, wR2 = 0.0872, largest difference peak and hole: 1.707 and -1.269 e.$Å^{-3}$.

P$_5$C$_5$Bu$^t_5$ (50)

P≡CBu^t (249 mg, 2.47 mmol) was added to a solution of 1,3,5-$P_3C_3Bu^t_3$ (250 mg, 0.83 mmol) in hexane (30 cm^3) at room temperature. After stirring for 48 h, the

solution was concentrated to 2 cm^3 and purefied by chromatography (silica gel/hexane). The first yellow band was collected and found to contain the tetraphosphabarrelene, **18**. The second yellow band was collected, concentrated to 3 cm^3 and stored at -30°C overnight to yield **50** as a yellow crystalline solid.

(82 mg, 21%); M.p.: 112 – 114 °C; ^1H NMR (400 MHz, C_6D_6, 298 K): δ 1.22 (s, 9H, Bu^t), 1.28 (s, 9H, Bu^t), 1.64 (s, 9H, Bu^t), 1.73 (s, 9H, Bu^t), 1.78 (s, 9H, Bu^t); $^{31}P\{^1H\}$ NMR (121.6 MHz, C_6D_6, 298 K): δ -33.1 (ddd, $^1J_{P1P2}$ = 185 Hz, $^2J_{P1P4}$ = 12 Hz, $^2J_{P1P3}$ = 24 Hz, P(1)), 19.0 (dd, $^1J_{P4P5}$ = 60 Hz, $^2J_{P4P1}$ = 12 Hz, P(4)), 23.5 (d of v. tr, $^1J_{P2P1}$ = 185 Hz, $^2J_{P2P3}$ = $^2J_{P2P5}$ = 12 Hz, P(2)), 73.6 (dd, $^1J_{P5P4}$ = 60 Hz, $^2J_{P5P2}$ = 12 Hz, P(5)), 387.6 (dd, $^2J_{P3P1}$ = 24 Hz, $^2J_{P3P2}$ = 12 Hz, P(3)); IR ν/cm^{-1} (Nujol): 1362m, 1260m, 1193m, 1103m, 1042m, 1020m, 862m, 810; EI Acc. Mass.: on M^+: calc. for $C_{25}H_{45}P_5$: 500.2204, found 500.2204, parameters, R(observed) = 0.2438, wR2 = 0.4166, largest difference peak and hole: 1.226 and -0.570 $e.Å^{-3}$.

MeCPN$_3$-Ad (68)

P≡CMe (4.3 cm^3 of a 0.52 M solution in diethylether, 2.24 mmol) was added to a solution of 1-azidoadamantane (100 mg, 0.56 mmol) in hexane (30 cm^3) at -90 °C. The solution was warmed to room temperature over 3 h and stirred at this temperature for 24 h. All volatiles were removed *in vacuo* and the residue extracted in hexane (30 cm^3). Concentration to 8 cm^3 and storing at -30 °C, overnight, yielded **68** as a crystalline solid.

(100 mg, 90%); M.p.: 80 – 82 °C; ^1H NMR (300 MHz, C_6D_6, 303 K): 1.41 (t, $^3J_{HH}$ = 3 Hz, 6 H, Ad-CH_2), 2.13 (d, $^3J_{HH}$ = 3 Hz, 6 H, Ad-CH_2), 1,83 (br. s, 3 H, Ad-H), 2.50 (d, $^3J_{PH}$ = 11 Hz, 3 H, CH_3); $^{31}P\{^1H\}$ NMR (121.6 MHz, C_6D_6, 298 K): 167.4 (s, P=CMe); $^{13}C\{^1H\}$ NMR (74.4 MHz, C_6D_6, 303 K): 14.34 (d, $^2J_{PC}$ = 25 Hz, P=CCH_3), 30.00 (s, Ad.-CH_2), 36.00 (s, Ad-CH), 45.41 (d, $^3J_{PC}$ = 7 Hz, Ad.-CH_2),

61.71 (d, $^3J_{PC}$ = 5 Hz, Ad.-*C*NP), 177.57 (d, $^1J_{PC}$ = 47 Hz, P=*C*CH_3); IR ν/cm^{-1} (Nujol): 1346 m, 1301 m, 1259 m, 1179 m, 1101 m, 1025 m, 817 m, 694 m, 580 m; acc. MS/EI m/z (%): 235 [M^+, 57], 135 [M^+-$PCMeN_3$, 100]; MS (EI) calc. for: $C_{12}H_{18}N_3P$: 235.1233, found: 235.1231.

PCMeNHNCH (70) and

[{W(CO)$_5$}PCMeNH{NW(CO)$_5$)}(CH)] (71)

MeC≡P (2.5 cm^3 of a 0.53 M solution in diethylether, 0.437 mmol) was added to a solution of trimethylsilyl diazomethane (50 mg, 0.239 mmol) in diethylether (10 cm^3) at room temperature. After stirring over 24 h all volatiles were removed *in vacuo* and the residue extraced in hexane (3 cm^3). Storing at -30 °C, overnight, yielded **70** as a yellow crystalline solid.

(70 mg, 93%); M.P.: 67 °C; ^{1}H NMR (400 MHz, C_6D_6, 298 K): δ2.16 (br.s, 3H, CH_3), 8.16 (br.m, 1H, CH), 12.48 (br.m, 1H, NH); ^{31}P{^{1}H} NMR (121.6 MHz, C_6D_6, 298 K): δ 83.1 (s, P=CMe); ^{13}C{^{1}H} NMR (100.6 MHz, C_6D_6, 298 K): 15.1 (br. s, P=C*C*H$_3$), 160.9 (br. s, P=*C*CH$_3$), 172.8 (br. s, CH); IR ν/cm^{-1} (Nujol): 3320 (br., NH str.); EI Acc. Mass.: on M+H$^+$: calc. for $C_3H_5N_2P$: 100.0185, found 100.0185

[W(CO)$_5$(THF)] (237 mg, 0.60 mmol) in THF (100 cm^3) was added to a solution of **70** (30 mg, 0.3 mmol) in THF (5 cm^3) at room temperature. After stirring for 24 h all volatiles were removed *in vacuo*. The residue was extracted with hexane (2 x 10 cm^3), concentrated to 5 cm^3 and stored at -30 °C, overnight, to give **71** as a yellow crystalline solid.

(60 mg, 22%); M.p.: 100 – 103 °C; ^{1}H NMR (400 MHz, C_6D_6, 298 K): δ 2.06 (d, $^3J_{PH}$ = 14.0 Hz, 3H, CH_3), 7.88 (d, $^2J_{PH}$ = 43 Hz), 9.19 (br, 1H, NH); ^{31}P{^{1}H} NMR (121.6 MHz, C_6D_6, 298 K): δ; 74.8 (s, $^1J_{WP}$ = 264 Hz, PCMe); ^{13}C{^{1}H} NMR (100.6

MHz, C_6D_6, 298 K): 12.3 (br. s, P=C*C*H$_3$), 164.4 (s, P=*C*CH$_3$), 190.9 (s, CH); IR ν/cm^{-1} (Nujol): 3320 (NH str.), 2084, 2075, 1980, 1955 (br CO str.); EI Acc. Mass.: on M+H$^+$: calc. for $C_{13}H_5N_2O_{10}P_1W_2$: 743.8640, found 743.86440m, 862m, 810; EI Acc. Mass.: on M$^+$: calc. for $C_{25}H_{45}P_5$: 500.2204, found 500.2204, parameters, R(observed) = R1 0.0537, wR2 = 0.0650, largest difference peak and hole: 0.910 and -1.037 e.Å^{-3}.

[R$_2$Ge{C(Me)(H)PC(=CH$_2$)P}]$_2$ (R = CH(SiMe$_3$)$_2$) (79)

P≡CMe (1.2 cm^3 of a 0.52 M solution in diethylether, 0.62 mmol) was added to a solution of [Ge{CH(SiMe$_3$)$_2$}$_2$]$_2$ (100 mg, 0.13 mmol) in toluene (20 cm^3) at -80°C. The resultant solution was warmed to room temperature and stirred for 48 h during which time **79** deposited as a colorless crystalline solid. The solid was isolated by filtration and dried under a stream of argon.

(Yield 110 mg, 85%); M.p.: 197 – 199 °C. ^{1}H NMR (400 MHz, CD_2Cl_2, 298 K): δ 0.14 (s, 2H, C*H*SiMe$_3$), 0.15 (s, 2H, C*H*SiMe$_3$), 0.19 (s, 18H, SiMe$_3$), 0.21 (s, 18H SiMe$_3$), 0.27 (s, 18H, SiMe$_3$), 0.30 (s, 18H, SiMe$_3$), 1.59 (dd, $^3J_{HH}$ = 7.8 Hz, $^3J_{PH}$ = 23.4 Hz, 6H, CH$_3$), 2.99 (br. m, 2H, CH), 6.25 (dd, 2H, $^3J_{PH}$ = 46 and 10 Hz, =C*H*H), 6.52 (dd, 2H, $^3J_{PH}$ = 33 and 16 Hz, =C*H*H); ^{31}P{^{1}H} NMR (121.6 MHz, D_8-THF, 298 K): δ -13.7 (br. d, $^1J_{PP}$ = 303.1 Hz, PGe), 31.7 (br. d, $^1J_{PP}$ = 303.1 Hz, P*P*CCH$_2$); IR ν/cm^{-1} (Nujol): 1570w, 1377m, 1307m, 1250s, 1169m, 1087m, 1056m, 1025m; (MS/EI) m/z (%): 1014 [M$^+$, 55], 855 [M$^+$-CH(SiMe$_3$)$_2$, 25], 624 [M$^+$ - Ge{CH(SiMe$_3$)$_2$}$_2$, 56], parameters, R(observed) = 0.0336, wR2 = 0.0690, largest difference peak and hole: 0.305 and -0.334 e.Å^{-3}.

[R$_2$Sn{C(Me)(H)PC(=CH$_2$)P}]$_2$ (R = CH(SiMe$_3$)$_2$) (80)

P≡CMe (3.3 cm^3 of a 0.25 M solution in diethylether, 0.82 mmol) was added to a solution of $[Sn\{CH(SiMe_3)_2\}_2]_2$ (120 mg, 0.14 mmol) in toluene (20 cm^3) at -80°C. The resultant solution was warmed to room temperature and stirred for 48 h during which time **80** deposited as a coluorless crystalline solid. The solid was isolated by filtration and dried under a stream of argon.

(Yield 122 mg, 81%); M.p.: 240 – 245 °C. ^1H NMR (400 MHz, CD_2Cl_2, 298 K): δ 0.00 (s, 2H, C*H*$SiMe_3$), 0.02 (s, 2H, C*H*$SiMe_3$), 0.08 (s, 18H, $SiMe_3$), 0.19 (s, 18H, $SiMe_3$), 0.27 (s, 18H, $SiMe_3$), 0.29 (s, 18H, $SiMe_3$), 1.53 (dd, $^3J_{HH}$ = 8.0 Hz, $^3J_{PH}$ = 15.5 Hz, 6H, CH_3), 2.76 (br. m, 2H, CH), 6.18 (dd, 2H, $^3J_{PH}$ = 43 and 11 Hz, =C*H*H), 6.65 (dd, 2H, $^3J_{PH}$ = 32 and 19 Hz, =C*H*H); $^{31}P\{^1H\}$ NMR (121.6 MHz, CD_2Cl_2, 298 K): δ -63.2 (br. d, $^1J_{PP}$ = 311.2 Hz, $^1J_{SnP}$ = 621.2 Hz, PSn), 16.5 (br. d, $^1J_{PP}$ = 311.2 Hz, P*P*CCH_2); IR ν/cm^{-1} (Nujol): 1564w, 1376m, 1246m, 1026m, 996m, 982m; (MS/EI) m/z (%): 1107 [M^+, 6], 948 [M^+ -$CH(SiMe_3)_2$, 28], 670 [M^+ - $Sn\{CH(SiMe_3)\}_2$, 12], parameters, R(observed) = 0.0872, wR2 = 0.0879, largest difference peak and hole: 0.652 and -0.447 e.$Å^{-3}$.

$[Ar_2Sn\{C(Me)(H)PC(=CH_2)P\}]_2$ (Ar = $C_6H_2Pr^i_3$-2,4,6) (81)

P≡CMe (1.0 cm^3 of a 0.51 M solution in diethylether, 0.51 mmol) was added to a toluene solution (50 cm^3) of $[Sn(Ar)_2]_2$ (120 mg, 0.13mmol) at -80°C (which had been generated *in situ* by UV irradiation (δ = 254 nm) of $[Sn(Ar)_2]_3$ at -80°C). The resultant solution was warmed to room temperature and stirred for 48 h, during which time **81** deposited as a colourless crystalline solid. The solid was isolated by filtration and dried under vacuum.

(Yield 50 mg, 31%); M.p.: 210 – 215 °C (dec.). ^1H NMR (400 MHz, C_6D_6, 298 K): δ 0.83 (2 x overlapping br., 24H, $CH(CH_3)_2$), 1.30 (br. overlapping m, 48H, $CH(CH_3)_2$), 1.60 (br. m, 6H, CH_3), 2.72, 2.93 (2 x br., 2 x 4H, $CH(CH_3)_2$), 2.92 (br.

m, 2H, PC*H*(CH_3)), 3.25, 3.46 (2 x br., 2 x 2H, C*H*(CH_3)$_2$), 5.80 (dd, 2H, $^3J_{PH}$ = 35 and 18 Hz, =C*H*H), 6.19 (dd, 2H, $^3J_{PH}$ = 46 and 12 Hz, =C*H*H), 7.03 (br., 8H, ArH); $^{31}P\{^1H\}$ NMR (121.6 MHz, C_6D_6, 298 K): δ -76.3 (d, $^1J_{PP}$ = 320 Hz, $^1J_{SnP}$ = 614 Hz, PSn), 15.8 (d, $^1J_{PP}$ = 320 Hz, PP); IR ν/cm^{-1} (Nujol): 1594w, 1377m, 1260m, 1154m, 1096m, 1018m; (MS/EI) m/z (%): 1283 [M$^+$, 7], 1079 [M$^+$-Ar', 10], 758 [M$^+$-Sn(Ar')$_2$, 20], parameters, R(observed) = 0.0361, wR2 = 0.0723, largest difference peak and hole: 0.708 and -0.422 e.Å^{-3}.

[{W(CO)$_5$}{R$_2$Ge[C(Me)PC(Me)P]}] (R = CH(SiMe$_3$)$_2$) (87) and

[{W(CO)$_5$}$_2${R$_2$Ge[C(Me)PC(Me)P]}] (R = CH(SiMe$_3$)$_2$) (88)

P≡CMe (1.2 cm^3 of a 0.52 M solution in diethylether, 0.62 mmol) was added to a solution of [Ge{CH(SiMe$_3$)$_2$}$_2$]$_2$ (100 mg, 0.13 mmol) in toluene (20 cm^3) at room temperature. After 5 min. [W(CO)$_5$(THF)] (198 mg, 0.501 mmol) in THF (50 cm^3) was added to the solution. After stirring for 24 h volatiles were removed *in vacuo* and the residue extracted with hexane (5 cm^3) and purefied by chromatography (silica gel/hexane). A yellow and red bands were collected, both bands were concentrated *in vacuo* yielding yellow **87** and red **88** as crystalline solids.

87: (38 mg, 13%); M.p.: 83 – 85 °C; ^{1}H NMR (400 MHz, C_6D_6, 298 K): δ 0.05 (br s, 2H, C*H*SiMe$_3$), 0.22 (br, 18H, SiMe$_3$), 0.25 (br, 18H, SiMe$_3$), 2.56 (d, $^3J_{PH}$ = 31 Hz, 3H, GeC(C*H*$_3$)P), 2.71 (v. tr, $^3J_{PH}$ = $^3J_{PH}$ = 20Hz, 3H, P$_2$C(C*H*$_3$)); $^{31}P\{^1H\}$ NMR (121.6 MHz, C_6D_6, 298 K): δ 247.5 (d, $^2J_{PP}$ = 53.8 Hz, $^1J_{PW}$ = 257 Hz, PCMe), 342.0 (d, $^2J_{PP}$ = 53.8 Hz, GePCMe); IR ν/cm^{-1} (Nujol): 2072s, 1977s, 1948s (CO str.); (MS/EI) m/z (%): 831 (M$^+$, 16), 803 (M$^+$-CO, 12), 392 (R"$_2$GeH$^+$, 46); EI Acc. Mass.: on M$^+$: calc. for $C_{23}H_{44}O_5{}^{70}Ge_1P_2Si_4{}^{182}W_1$: 826.0460, found 826.0462, parameters, R(observed) = 0.0257, wR2 = 0.0513, largest difference peak and hole: 0.572 and -1.282 e.Å^{-3}.

88: (32 mg, 15%); M.p.: 55 – 58 °C; ^{1}H NMR (400 MHz, C_6D_6, 298 K): δ 0.05 (br, 2H, C*H*SiMe$_3$), 0.28 (br, 18H, SiMe$_3$), 0.33 (br, 18H, SiMe$_3$), 2.40 (dd, $^{3}J_{PH}$ = 35 Hz, $^{4}J_{PH}$ = 8 Hz, 3H, GeC(C*H*$_3$)P), 2.68 (dd, $^{3}J_{PH}$ = 29 Hz, $^{3}J_{PH}$ = 20 Hz, P$_2$C(C*H*$_3$)); ^{31}P{^{1}H} NMR (121.6 MHz, C_6D_6, 298 K): δ 251.0 (d, $^{2}J_{PP}$ = 66 Hz, $^{1}J_{PW}$ = 245 Hz, CPCMe), 287.5 (d, $^{2}J_{PP}$ = 66 Hz, $^{1}J_{PW}$ = 256 Hz, GePCMe); IR ν/cm^{-1} (Nujol): 2068s, 1982sh, 1966s, 1955s (CO str.); (MS/EI) m/z (%): 1155 [M$^+$, 2], 392 [R"$_2$GeH$^+$, 86%], parameters, R(observed) = 0.0264, wR2 = 0.0538, largest difference peak and hole: 0.784 and -1.406 e.Å^{-3}.

[Cp$_2$TiN(NPh$_2$)PC(Bu^t)] (112)

P≡CBu^t (102 mg, 1.02 mmol) was added to a solution of [Cp$_2$Ti(Py)(NNPh$_2$)] (150 mg, 0.34 mmol) in toluene (20 cm^3) at 20°C over 5 mins. After stirring for 3 h the solution was concentrated to 5 cm^3 and stored at -30°C for 30 h to yield brown crystals of **112**.

(110 mg, 70%); M.P.: 149 – 150 °C. ^{1}H NMR (300 MHz, C_6D_6, 303 K): δ 1.48 (d, $^{4}J_{PH}$ =1.2 Hz, 9 H, Bu^t), 5.45 (s, 10 H, Cp), 6.83-7.10 (m, 10H, Ar-H); ^{31}P{^{1}H} NMR (121.4 MHz, C_6D_6, 303 K): δ -28.9; ^{13}C{^{1}H} NMR (74.4 MHz, C_6D_6, 303 K): 36.6 (d, $^{3}J_{PC}$ =12 Hz, C(*C*H$_3$)$_3$), 45.6 (d, $^{2}J_{PC}$ =14 Hz, *C*(CH$_3$)$_3$), 110.4 (Cp), 121.4 (*o*-C$_6$H$_5$), 122.6 (*p*-C$_6$H$_5$), 129.6 (*m*-C$_6$H$_5$) 148.8 (*ipso*-C$_6$H$_5$); IR ν/cm^{-1} (Nujol): 1586 m, 1489 m, 1352 m, 1321 m, 1296 m, 1237 m,1074 m, 843 m; acc. MS/EI m/z (%): 461 [M$^+$, 4], 403 [M$^+$-Bu, 12], 178 [Cp$_2$Ti$^+$, 100]; MS (EI) calc. for $C_{27}H_{29}N_2P_1Ti_1$: 460.1542, found: 60.152; anal. calc. for $C_{27}H_{29}N_2P_1Ti_1$: C 70.44, H 6.35, N 6.08. Found: C 70.59, H 6.46, N 6.18, parameters, R(observed) = 0.0586, wR2 = 0.1063, largest difference peak and hole: 0.341 and -0.524 e.Å^{-3}.

[(PCMe)$_2${W(CO)$_5$}$_2${W(CO)$_4$}] (117 head to head product) and (118 head to tail product)

P≡CMe (1.0 cm^3 of a 0.25 M solution in diethylether, 0.25 mmol) was added to a solution of [W(CO)$_5$(THF)] (100 mg, 0.25 mmol) in THF (50 cm^3) at room temperature. After stirring for 24 h volatiles were removed *in vacuo* and the residue was extracted with hexane (20 cm^3). This was concentrated *in vacuo* yielding **117** and **118**, in a ca. 80 : 20 ratio, as brown crystalline solids after storing at -30 °C overnight.

117: (mg, 23%); M.p.: 98 – 100 °C; ^{1}H NMR (400 MHz, C_6D_6, 298K): δ 1.32 (v. tr, $^3J_{PH}$ = 6.0 Hz, 6H, PCMe); ^{31}P{^{1}H} NMR (121.6 MHz, C_6D_6, 298K): δ -74.8 (s, $^1J_{WP}$ = 148.2 Hz, PCMe); IR (Nujol) ν/cm^{-1}: 2075(m), 2060(m), 1980(s), 1961(s.), 1927 (sh), 1914 (sh); (MS/EI) m/z (on a crystalline mixture of isomers **6.5** and **6.6**): 1059 [M$^+$, 64%], 1003 [M$^+$-2CO, 13%], 919 [M$^+$-5CO, 14%], 835 [M$^+$-8CO, 62%], 664 [M$^+$-14CO, 100%]; acc. MS (EI) calc. for $C_{18}H_6O_{14}P_2W_3$: 1059.7755, found 1059.7757; **7**: (11%), parameters, R(observed) = 0.0343, wR2 = 0.0518, largest difference peak and hole: 1.285 and -0.728 e.Å^{-3}.

118: M.p.: 100 – 103 °C; ^{1}H NMR (400 MHz, C_6D_6, 298K): δ 1.20 (tr, $^3J_{PH}$ = 16.0 Hz, 6H, PCMe); ^{31}P{^{1}H} NMR (121.6 MHz, C_6D_6, 298K): δ -4.0 (s, $^1J_{WP}$ = 252.2 Hz, PCMe); IR (Nujol) ν/cm^{-1}: 2075(m), 2059(m), 1976(sh), 1963(br.s.), 1929 (br.s.), 1914 (sh), parameters, R(observed) = 0.0859, wR2 = 0.1469, largest difference peak and hole: 1.552 and -1.850 e.Å^{-3}.

[RuH(dppe)$_2$(η^1-P≡CMe)][CF$_3$SO$_3$] (127)

P≡CMe (0.56 cm^3 of a 0.34 M solution in diethylether, 0.190 mmol) was added to a solution of [RuH(dppe)$_2$][CF$_3$SO$_3$] (100 mg, 0.101 mmol) in dichloromethane (10 cm^3) at room temperature to give a yellow solution. After 3 h volatiles were removed

in vacuo and the residue dissolved in dichloromethane (1 cm^3). Layering this with hexane (10 cm^3), at room temperature, yielded **127** as yellow crystals overnight. (90 mg, 75%); M.p.: 188 - 190 °C; ^1H NMR (500 MHz, C_6D_6, 298 K): δ – 9.6 (d of quin, 1 H, $^2J_{P(dppe)H}$ = 17 Hz, $^2J_{P(PCMe)H}$ = 127 Hz, Ru*H*), 2.02 (d, 3 H, $^3J_{PH}$ = 14Hz, CH_3) 2.10 (br, 4 H, CH_2), 2.52 (br, 4 H, CH_2), 7.01 – 7.32 (m, 40 H, Ar-*H*); $^{31}P\{^1H\}$ NMR (121.6 MHz, C_6D_6, 298 K): δ -38.7 (quin, $^2J_{PP}$, = 30 Hz, *P*CMe), 61.5 (d, $^2J_{PP}$, = 30 Hz, dppe); $^{19}F\{^1H\}$ NMR (281.3 MHz, C_6D_6, 298 K): δ –78.5 (s, CF_3SO_3); IR ν/cm^{-1} (Nujol): 1560w (P≡C), 1458m, 1376m, 1309m, 1272m, 1187m, 1053m, 998m; (MS/EI) m/z (%): 958 [$RuH(dppe)_2(PCMe)^+$, 3], 899 [$RuH(dppe)_2^+$, 32%], 398 [$dppe^+$, 100].

[RuH(dppe)$_2$(η^1-PF$_2$Et)][BF$_4$] (128)

HBF_4 (0.18 cm^3 of a 54 % solution in diethylether, 0.135 mmol) was added to a solution of **127** (50 mg, 0.045 mmol) in dichloromethane (5 cm^3) at room temperature. After 12 h volatiles were removed *in vacuo* and the residue dissolved in dichloromethane (1 cm^3). Layering this with hexane (10 cm^3), at room temperature overnight , yielded **128** as yellow crystals overnight.

(20 mg, 40%); M.P.: 176-182°C; ^{1}H NMR (500 MHz, CD_2Cl_2, 298 K): δ –7.9 (d of quin, $^2J_{PH}$ = 115 Hz and 21 Hz, 1 H, Ru*H*), 2.06 – 2.50 (m, 8 H, PCH_2 and 3H, CH_3), 2.80 (m, 2 H, PCH_2), 7.11 – 7.33 (m, 40 H, Ar-*H*); ^{31}P{^{1}H} NMR (121.6 MHz, CD_2Cl_2, 298 K): δ 62.5 (d, $^2J_{PP}$, = 30 Hz, dppe), 244.4 (tr. of quin, $^2J_{PP}$, = 30 Hz, $^1J_{PF}$, = 1094 Hz, *P*F$_2$); ^{19}F{^{1}H} NMR (281.3 MHz, CD_2Cl_2, 298 K): δ –153.2 (4 F, B*F*$_4$), -56.2 (d, 2 F, $^1J_{PF}$ = 1094 Hz); IR ν/cm^{-1} (Nujol): 1376m, 1261m, 1225m, 1029m, 890m; (MS/EI) m/z (%): 1000 [RuH(dppe)$_2$(PF$_2$Et)$^+$, 83%], 899 [RuH(dppe)$_2^+$, 100%].

[{Sm[(pyrole)$_4$(CEt$_2$)$_4$Me$_2$]}(μ-P$_2$C$_2$Bu$^t_2$)] (pyrol = NC_4H_2) **(138)**

P≡CBu^t (46 mg, 0.46 mmol) was added to a solution of the samarium(II) complex (**136**) (80 mg, 0.093 mmol) in toluene (10 cm^3) at room temperature. After 10 min volatiles were removed *in vacuo* and the residue extracted in hexane (10 cm^3). The extract was concentrated *in vacuo* to 2 cm^3 and stored overnight at -30 °C, yielding **138** as a green crystalline solid.

(30 mg, 33%); Dec.: 190 °C

Parameters, R(observed) = 0.2149, wR2 = 0.1881, largest difference peak and hole: 1.184 and -0.810 e.Å^{-3}.

No other analysis results could be obtained.

[(PCy$_3$)$_2$Pt(MeCP)] (140)

P≡CMe (0.4 cm^3 of a 0.34 M solution in diethylether, 0.132 mmol) was added to a solution of [Pt(PCy$_3$)$_2$(η^2-CH$_2$CH$_2$)] (50 mg, 0.066 mmol) in toluene (20 cm^3) at room temperature. After 24 h volatiles were removed *in vacuo* and the residue extracted in toluene (10 cm^3). The extract was concentrated to 3 cm^3 and stored at -30 °C yielding **140** as crystalline solid.

(24 mg, 47%); M.P.: 133 – 135 °C (dec.); ^{1}H NMR (400 MHz, C$_6$D$_6$, 298K): δ 1.21 – 2.62 (m, 66H, CyH), 3.61 (m, 3H, PCCH$_3$); ^{31}P{^{1}H} NMR (121.6 MHz, C$_6$D$_6$, 298K): δ 32.7 (v. tr., $^2J_{PP}$ = 24.0 Hz, $^1J_{PtP}$ = 3195 Hz, PCy$_3$), 44.4 (v. tr., $^2J_{PP}$ = 24.0 Hz, $^1J_{PtP}$ = 3195 Hz, PCy$_3$), 86.6 (v. tr., $^2J_{PP}$ = 24.0 Hz, $^1J_{PtP}$ = 143.6 Hz, PCMe); m/z (EI): 752 [Pt(PCy$_3$)$_2^+$, 5%], 280 [PCy$_3^+$, 100%], parameters, R(observed) = 0.0331, wR2 = 0.0665, largest difference peak and hole: 0.740 and -0.556 e.Å^{-3}.

[{Pt(dppe)}$_2$(MeCP)] (145)

P≡CMe (1.9 cm^3 of a 0.34 M solution in diethylether, 0.653 mmol) was added to a solution of [Pt(dppe)(η^2-CH$_2$CH$_2$)] (100 mg, 0.161 mmol) in toluene (10 cm^3) at room temperature. After 24 h volatiles were removed *in vacuo* and the residue extracted in toluene (10 cm^3). Concentration to 3 cm^3 and storage at -30 °C over night, yielded **145** as crystalline solid.

(34 mg, 34%); M.P.: 156 – 160 °C; ^{1}H NMR (400 MHz, C$_6$D$_6$, 298K): δ 1.85 (m, 8H, PCH$_2$), 4.12 (m, 3H, CCH$_3$), 6.67 – 8.15 (m, 40H, ArH); ^{31}P{^{1}H} NMR (121.6 MHz, C$_6$D$_6$, 298K): δ -101.2 (unresolv. m., PCMe), 36.4 (unresolv. m., $^1J_{PtP}$ = 3512 Hz, dppe), 45.8 (unresolv. m., $^1J_{PtP}$ = 3123 Hz, dppe); (MS/EI) m/z: 1244 [M+, 5%], 651 [(dppe)Pt(PCMe)$^+$, 16%], 593 [(dppe)Pt$^+$, 12%], 398 [dppe$^+$, 100%]; acc. MS

(EI) calc. for $C_{54}H_{51}P_5Pt_2$: 1244.1969, found 1244.1977, parameters, R(observed) = 0.0375, wR2 = 0.0526, largest difference peak and hole: 0.689 and -0.802 e.Å^{-3}.

[{Pt(PEt$_3$)$_2$}$_2$MeCP] (146)

P≡CMe (2.2 cm^3 of a 0.34 M solution in diethylether, 0.758 mmol) was added to a solution of [Pt(PEt$_3$)$_2$(η^2-CH$_2$CH$_2$)] (80 mg, 0.256 mmol) in THF (20 cm^3) at room temperature. After 24 h volatiles were removed *in vacuo* and the residue extracted in toluene (10 cm^3). Concentration to 3 cm^3 and storage at -30 °C over night yielded **146** as crystalline solid.

(45 mg, 57%); M.P.: 187 – 190 °C; ^{1}H NMR (400 MHz, C_6D_6, 298K): δ 1.15 (m, 36H, PCH$_3$), 1.92 (m, 24H, PCH$_2$), 3.92 (m, 3H, PCCH$_3$); ^{31}P{^{1}H} NMR (121.6 MHz, C_6D_6, 298K): δ -115.5 (unresolv. m., PCMe), 6.6 (unresolv. m., $^1J_{PtP}$ = 3147 Hz, dppe), 7.7 (unresolv. m., $^1J_{PtP}$ = 3596 Hz); (MS/EI) m/z: 920 [M$^+$, 11%], 802 [M$^+$-PEt$_3$, 13%], 684 [M$^+$-2PEt$_3$, 20%], 489 [M$^+$-Pt(PEt$_3$)$_2$, 18%], 431 [Pt(PEt$_3$)$_2^+$, 100%]; acc. MS (EI) calc. for $C_{26}H_{63}P_5Pt_2$: 920.2908, found 920.2917, parameters, R(observed) = 0.0575, wR2 = 0.1147, largest difference peak and hole: 1.533 and -2.424 e.Å^{-3}.

1.6 References

[1] G. Becker, G. Gresser, W. Uhl, *Z. Naturforsch. B.* **1981**, 16.

[2] F. Mathey, *Angew. Chem. Int. Ed.* **2003**, *42*, 1578.

[3] K. B. Dillon, F. Mathey, J. F. Nixon, *in Phosphorus: The Carbon Copy*, Wiley, Chichester, **1998**.

[4] T. E. Gier, *J. Am. Chem. Soc.* **1961**, *83*, 1769.

[5] M. J. Hopkinson, H. W. Kroto., J. F. Nixon, N. P. C. Simmons, *Chem. Phys. Lett.* **1976**, *42*, 460.

[6] N. P. C. Westwood, H. W. Kroto, J. F. Nixon, N. P. C. Simmons, *J. Chem. Soc., Dalton Trans.* **1979**, 1405.

[7] R. Appel, A. Westerhaus, *Tetrahedron Lett.* **1981**, *22*, 2159.

[8] M. Y. Antipin, A. N. Chernega, K. A. Lysenko, Y. T. Struchkov, J. F. Nixon, *J. Chem. Soc., Chem. Commun.* **1995**, 505.

[9] H. Oberhammer, G. Berker., G. Gresser, *J. Mol. Spectrosc.* **1981**, *75*, 283.

[10] J. C. T. R. Burckett-St. Laurent, M. A. King, H. W. Kroto, J. F. Nixon, R. J. Suffolk, *J. Chem. Soc., Dalton Trans.* **1983**, 755.

[11] B. Solouk, H. Bock, R. Appel, A. Westerhaus, G. Becker, G. Uhl, *Chem. Ber.* **1982**, 3747.

[12] K. K. Laali, B. Geissler, M. Regitz, J. J. Houser, *J. Org. Chem.* **1995**, *60*, 6362.

[13] J. C. Guillemin, T. Janati, J. M. Denis, *J. Org. Chem.* **2001**, *66*, 7864.

[14] B. Pellerin, J.-M. Denis, J. Perrocheau, R. Carrie, *Tetrahedron Lett.* **1986**, *27*, 5723.

[15] J. C. Guillemin, T. Janati, P. Guenot, P. Savignac, J. M. Denis, *Angew. Chem.* **1991**, *103*, 191.

[16] O. Mó, M. Yáñez, J.-C. Guillemin, E. H.Riague, J.-F. Gal, P.-C. Maria, C. D. Poliart, *Chem. Eur. J.* **2002**, *8*, 4919.

[17] M. B. Steven, *J. Comput. Chem.* **1989**, *10*, 392.

[18] J. Keerthi, *Int. J. Quantum Chem.* **1992**, *44*, 327.

[19] L. T. Nguyen, F. D. P. v. Luong, D. Minh, T. Nguyen, P. Geerlings, *J. Phys. Org. Chem.* **2003**, *16*, 615.

[20] J. C. T. R. Burckett-St. Laurent, T. A. Cooper, H. W. Kroto, J. F. Nixon, Ohashi, K. Ohno, *J. Mol. Spectrosc.* **1982**, 215

[21] E. Kurita, Y. Tomonaga, S. Matsumoto, K. Ohno, H. Matsuura, *J. Mol. Spectrosc.* **2003**, *639*, 53.

[22] K. Ohno, H. Matsuura, *Bull. Chem. Soc. Jpn* **1987**, 2265

[23] M. F. Lucas, M. C. Michelini, N. Russo, E. Sicilia, *J. Chem. Theory Comput.* **2008**, *4*, 397.

[24] D. J. Berger, P. P. Gaspar, *Organometallics* **1994**, 640.

[25] J. F. Nixon, *Chem. Rev.* **1988**, *88*, 1327.

[26] J. F. Nixon, *Chem. Soc. Rev.* **1995**, 319.

[27] P. B. Hitchcock, M. J. Maah, J. F. Nixon, J. A. Zora, G. J. Leigh, M. A. Bakar, *Angew. Chem. Int. Ed.* **1987**, *26*, 474.

[28] J. C. T. R. Burckett-St. Laurent, P. B. Hitchcock, H. W. Kroto, J. F. Nixon, *J. Chem. Soc., Chem. Commun.* **1981**, 1141.

[29] G. Becker, W. A. Herrmann, W. Kalcher, G. W. Kriechbaum, C. Pahl, C. T. Wagner, M. L. Ziegler, *Angew. Chem. Int. Ed.* **1983**, *22*, 413.

[30] J. C. T. R. Burckett-St. Laurent, P. B. Hitchcock, H. W. Kroto, M. F. Meidine, J. F. Nixon, *J. Organomet. Chem.* **1982**, *238*, C82.

[31] A. J. Ashe, *J. Am. Chem. Soc.* **1971**, *93*, 3293.

[32] P. J. Davidson, M. F. Lappert, *J. Chem. Soc., Chem. Commun.* **1973**, 317.

[33] M. Regitz, *Chem. Rev.* **1990**, *90*, 191.

[34] N. E. Schore, *Chem. Rev.* **1988**, *88*, 1081.

[35] A. Schäfer, M. Weidenbruch, W. Saak, S. Pohl, *Angew. Chem. Int. Ed.* **1987**, *26*, 776.

[36] A. H. Cowley, S. W. Hall, C. M. Nunn, J. M. Power, *J. Chem. Soc., Chem. Commun.* **1988**, 753.

[37] F. Meiners, W. Saak, M. Weidenbruch, *Chem. Commun.* **2001**, 215.

[38] M. Weidenbruch, S. Olthoff, K. Peters, G. v. Schnering, *Chem. Commun.* **1997**, 1433.

[39] A. H. Cowley, S. W. Hall, C. M. Nunn, J. M. Power, *Angew. Chem. Int. Ed.* **1988**, *27*, 838.

[40] W. Rösch, T. Facklam, M. Regitz, *Tetrahedron* **1987**, *43*, 3247.

[41] W. Rösch, M. Regitz, *Angew. Chem.* **1984**, *96*, 898.

[42] W. Lwowski, *in 1,3-dipolar Cycloaddition Chemistry (A. Padwa, ed.) 1st Edn., Vol1*, Wiley, New York **1984**.

[43] E. P. O. Fuchs, M. Hermesdorf, W. Schnurr, W. Rösch, H. Heydt, M. Regitz, P. Binger, *J. Organomet. Chem.* **1988**, *338*, 329.

[44] F. Tabellion, A. Nachbauer, S. Leininger, C. Peters, F. Preuss, M. Regitz, *Angew. Chem. Int. Ed.* **1998**, *37*, 1233.

[45] P. Binger, G. Glaser, B. Gabor, R. Mynott, *Angew. Chem. Int. Ed.* **1995**, *34*, 81.

[46] P.B. Hitchcock, M. J. Maah, J. F. Nixon, *J. Chem. Soc., Chem. Commun.* **1986**, 737.

[47] M. T. Nguyen, L. Landuyt, L. G. Vanquickenborne, *J. Org. Chem.* **1993**, *58*, 2817.

[48] A. H. Cowley, S. W. Hall, *Polyhedron* **1989**, *8*, 849.

[49] R. Bartsch, J. F. Nixon, *J. Organomet. Chem.* **1991**, *415*, C15.

[50] P. Binger, J. Stannek, B. Gabor, R. Mynott, J. Bruckmann, C. Krüger, S. Leininger, *Angew. Chem. Int. Ed.* **1995**, *34*, 2227.

[51] T. Wettling, B. Geissler, R. Schneider, S. Barth, P. Binger, M. Regitz, *Angew. Chem. Int. Ed.* **1992**, *31*, 758.

[52] B. Geissler, S. Barth, U. Bergsträsser, M. Slany, J. Durkin, P. B. Hitchcock, M.Hofmann, P. Binger, J. F. Nixon, P. v. R. Schleyer, M. Regitz, *Angew. Chem. Int. Ed.* **1995**, *34*, 484.

[53] P. Binger, R. Milczarek, R. Mynott, M. Regitz, *J. Organomet. Chem.* **1987**, *323*, C35.

[54] P. Binger, J. Haas, A. T. Herrmann, F. Langhauser, C. Krüger, *Angew. Chem. Int. Ed.* **1991**, *30*, 310.

[55] T. Wettling, J. Schneider, O. Wagner, C. G. Kreiter, M. Regitz, *Angew. Chem. Int. Ed.* **1989**, *28*, 1013.

[56] J. F. Nixon, *Coord. Chem. Rev.* **1995**, *145*, 201.

[57] F. G. N. Cloke, P. B. Hitchcock, J. F. Nixon, D. M. Vickers, *Comptes Rendus Chimie* **2004**, *7*, 931.

[58] F. G. N. Cloke, K. R. Flower, P. B. Hitchcock, J. F. Nixon, *J. Chem. Soc., Chem. Commun.* **1995**, 1659.

[59] R. Bartsch, P. B. Hitchcock, J. F. Nixon, *J. Organomet. Chem.* **1989**, *375*, C31.

[60] V. Caliman, P. B. Hitchcock, J. F. Nixon, M. Hofmann, P. v. R. Schleyer, *Angew. Chem. Int. Ed.* **1994**, *33*, 2202.

[61] V. A. Wright, D. P. Gates, *Angew. Chem. Int. Ed.* **2002**, *41*, 2389.

[62] A. Kraft, A. C. Grimsdale, A. B. Holmes, *Angew. Chem. Int. Ed.* **1998**, *37*, 402.

[63] J. H. Burroughes, D. D. C. Bradley, A. R. Brown, R. N. Marks, K. Mackay, R. H. Friend, P. L. Burns, A. B. Holmes, *Nature* **1990**, *347*, 539.

[64] R. C. Smith, J. D. Protasiewicz, *J. Am. Chem. Soc.* **2004**, *126*, 2268.

[65] M. Hissler, P. W. Dyer, R. Réau, *Coord. Chem. Rev.* **2003**, *244*, 1.

[66] G. M. Kosolapoff, *J. Am. Chem. Soc.* **1947**, *69*, 1002.

[67] D. Seyferth, R. S. Marmor, *J. Organomet. Chem.* **1973**, *59*, 237.

[68] D. A. Loy, G. M. Jamison, M. D. McClain, T. M. Alam, *J. Polym. Sci., Part A: Polym. Chem.* **1999**, *37*, 129.

[69] H. Heydt, *Top. Curr. Chem.* **2003**, 215.

[70] F. Mathey, *Phosphorus-Carbon Heterocyclic Chemistry: The Rise of a New Domain*, Pergamon, Amsterdam, **2001**.

[71] C. Peters, H. Disteldorf, E. Fuchs, S. Werner, S.Stutzmann, J. Bruckmann, C. Krüger, P. Binger, H. Heydt, M. Regitz, *Eur. J. Org. Chem.* **2001**, *2001*, 3425.

[72] A. T. Balaban, M. Banciu, *J. Chem. Educ.* **1984**, 767.

[73] M. Jones, S. D. Reich, L. T. Scott, *J. Am. Chem. Soc.* **1970**, *92*, 3118.

[74] M. Jones, *J. Am. Chem. Soc.* **1967**, *89*, 4236.

[75] C. Peters, S. Stutzmann, H. Disteldorf, S. Werner, U. Bergsträßer, C. Krüger, P. Binger, M. Regitz, *Synthesis* **2000**, 529.

[76] H. Disteldorf, J. Renner, H. Heydt, P. Binger, M. Regitz, *Eur. J. Org. Chem.* **2003**, *2003*, 4292.

[77] T. Allspach, M. Regitz, G. Becker, E. Becker, *Synthesis* **1986**, 31.

[78] W. Rösch, U. Vogelbacher, T. Allspach, M. Regitz, *J. Organomet. Chem.* **1986**, *306*, 39.

[79] A. K. Chandra, A. Michalak, M. T. Nguyen, R. F. Nalewajski, *J. Phys. Chem. A* **1998**, *102*, 10182.

[80] N. Tokitoh, H. Suzuki, N. Takeda, T. Kajiwara, T. Sasamori, R. Okazaki, *Silicon Chem.* **2002**, 313.

[81] R. Okazaki, R. West, *Adv. Organomet. Chem.* **1996**, 231.

[82] H. Schafer, W. Saak, M. Weidenbruch, *Organometallics* **1999**, *18*, 3159.

[83] K. A. Miller, T. W. Watson, J. E. Bender, M. M. B. Holl, J. W. Kampf, *J. Am. Chem. Soc.* **2001**, *123*, 982.

[84] M. D. Francis, C. Jones, C. P. Morley, *Tetrahedron Lett.* **1999**, *40*, 3815.

[85] F. Geoffrey, N. Cloke, P. B. Hitchcock, J. F. Nixon, D. J. Wilson, P. Mountford, *Chem. Commun.* **1999**, 661

[86] N. Hazari, P. Mountford, *Acc. Chem. Res.* **2005**, *38*, 839.

[87] B. D. Ward, A. Maisse-Francois, P. Mountford, L. H. Gade, *Chem. Commun.* **2004**, 704.

[88] N. Vujkovic, B. D. Ward, A. Maisse-Francois, H. Wadepohl, P. Mountford, L. H. Gade, *Organometallics* **2007**, *26*, 5522.

[89] F. Geoffrey, N. Cloke, B. Hitchcock, J. F. Nixon, D. James, F. Tabellion, U. Fischbeck, F. Preuss, M. Regitz, L. Nyulazi, *Chem. Commun.* **1999**, 2363.

[90] F. G. N. Cloke, J. C. Green, N. Hazari, P. B. Hitchcock, P. Mountford, J. F. Nixon, D. J. Wilson, *Organometallics* **2006**, *25*, 3688.

[91] J. D. Selby, C. D. Manley, M. Feliz, A. D. Schwarz, E. Clot, P. Mountford, *Chem. Commun.* **2007**, 4937.

[92] M. Boca, P. Baran, R. Boca, H. Fuess, G. Kickelbick, W. Linert, F. Renz, I. Svoboda, *Inorg. Chem.* **2000**, *39*, 3205.

[93] S. Creve, M. T. Nguyen, L. G. Vanquickenborne, *Eur. J. Inorg. Chem.* **1999**, *1999*, 1281.

[94] P. Kramkowski, M. Scheer, *Eur. J. Inorg. Chem.* **2000**, *2000*, 1869.

[95] P. Binger, G. Glaser, S. Albus, C. Krüger, *Chem. Ber.* **1995**, 1261.

[96] F. W. Heinemann, S. Kummer, U. Seiss-Brandl, U. Zenneck, *Organometallics* **1999**, *18*, 2021.

[97] J. G. Cordaro, D. Stein, H. Grutzmacher, *J. Am. Chem. Soc.* **2006**, *128*, 14962.

[98] J. G. Cordaro, D. Stein, H. Rüegger, H. Grützmacher, *Angew. Chem. Int. Ed.* **2006**, 6159.

[99] M. F. Meidine, M. A. N. D. A. Lemos, A. J. L. Pombiero, J. F. Nixon, P. B. Hitchcock, *J. Chem. Soc., Dalton Trans.* **1998**, 3319.

[100] T. Groer, G. Baum, M. Scheer, *Organometallics* **1998**, *17*, 5916.

[101] R. B. Bedford, A. F. Hill, J. D. E. T. Wilton-Ely, M. D. Francis, C. Jones, *Inorg. Chem.* **1997**, *36*, 5142.

[102] P. Giannoccaro, A. Sacco, S. D. Ittel, M. A. Cushing, *Inorg. Synth.* **1977**, 69.

[103] M. Brym, C. Jones, *J. Chem. Soc., Dalton Trans.* **2003**, 3665.

[104] L. Weber, *Coord. Chem. Rev.* **2005**, *249*, 741.

[105] W. J. Evans, J. W. Grate, H. W. Choi, I. Bloom, W. E. Hunter, J. L. Atwood, *J. Am. Chem. Soc.* **1985**, *107*, 941.

[106] W. J. Evans, *J. Alloys Compd.* **1993**, *192*, 205.

[107] W. J. Evans, *J. Organomet. Chem.* **2002**, *652*, 61.

[108] W. J. Evans, E. Montalvo, S. E. Foster, K. A. Harada, J. W. Ziller, *Organometallics* **2007**, *26*, 2904.

[109] J. E. William, A. K. Roy, W. Z. Joseph, *Organometallics* **1993**, 2618.

[110] J. E. William, A. H. Laura, P. H. Timothy, *Organometallics* **1986**, *5*, 1285.

[111] W. J. Evans, L. A. Hughes, T. P. Hanusa, *J. Am. Chem. Soc.* **1984**, 4270.

[112] A. Recknagel, D. Stalke, H. W. Roesky, F. T. Edelmann, *Angew. Chem. Int. Ed.* **1989**, *28*, 445.

[113] J. Wang, A. K. J. Dick, M. G. Gardiner, B. F. Yates, E. J. Peacock, B. W. Skelton, A. H. White, *Eur. J. Inorg. Chem.* **2004**, *2004*, 1992.

[114] D. Himmel, M. Seitz, M. Scheer, *Z. anorg. allg. Chem.* **2004**, *630*, 1220.

[115] S. I. Al-Resayes, P. B. Hitchcock, M. F. Meidine, J. F. Nixon, *J. Chem. Soc., Chem. Commun.* **1984**, 1080.

[116] M. F. Meidine, C. J. Meir, S. Morton, J. F. Nixon, *J. Organomet. Chem.* **1985**, *297*, 255.

[117] P. Binger, S. Stutzmann, J. Bruckmann, C. Krüger, J. Grobe, D. L. Van, T. Pohlmeyer, *Eur. J. Inorg. Chem.* **1998**, *1998*, 2071.

[118] T. Fjeldberg, A. Haaland, B. E. R. Schilling, M. F. Lappert, A. J. J. Thorne, *J. Chem. Soc., Dalton Trans.* **1986**, 1551.

[119] M. Weidenbruch, A. Schäfer, H. Kilian, S. Pohl, W. Saak, H. Marsmann, *Chem. Ber.* **1992**, *125*, 563.

[120] T. Yoshida, S. Otsuka, *Inorg. Synth.* **1990**, *28*, 120.

[121] J. D. Feldman, G. P. Mitchell, J.-O. Nolte, T. D. Tilley, *Can. J. Chem.* **2003**, *81*, 1127.

[122] R. A. Head, *Inorg. Synth.* **1990**, 132.

[123] S. P. Nolan, T. R. Belderrain, R. H. Grubbs, *Organometallics* **1997**, *16*, 5569.

[124] J. G. Cordaro, D. Stein, H. Rüegger, H. Grützmacher, *Angew. Chem. Int. Ed.* **2006**, *45*, 6159.

[125] M. D. Francis, *PhD Thesis, University of Wales, Swansea* **1998**.

2. Preparation and Reactivity of Transition Metal(I) Guanidinate and Amidinate Complexes

2.1 Introduction

Organometallic transition metal chemistry escalated after the discovery of ferrocene (Fc), $[Fe(\eta^5\text{-}C_5H_5)_2]$, in 1951.[1] The unusual stability of this transition metal complex fascinated many researchers.[2] Since then, the field has been dominated by complexes which follow the 18-electron rule. According to molecular orbital theory, maximum stability for a generic ML_n organometallic complex with n ligands results, when all the valence shell orbitals are doubly occupied, giving rise to a closed-shell 18-electron configuration. Since the ligand field splitting, or HOMO-LUMO gap, is large, for complexes with carbon-based π-acidic ligands (e.g. CO, Cp, olefins etc.), such complexes readily adopt a diamagnetic (spin-paired) configuration. However, paramagnetism can also arise in 18-electron complexes, if the ligand field splitting is small. An example is the monomeric, paramagnetic, 18-electron, spin-equilibrium molecule Cp*Ni(acac) (acac = acetylacetonate), which is diamagnetic below 150K but becomes paramagnetic with increasing temperature.[3]

There are a growing number of organometallic systems, in particular for the first row transition metals, that are stable with less than 18-electrons.[4] The general concept that low valent metal compounds may be more reactive and therefore potentially more important as catalytic intermediates has added interest to the study of these systems.[5, 6]As a result, a field completely dominated by the idea that only diamagnetic even-electron (16 or 18) species could be involved in catalytic processes, has been increasingly enlightened by the potential of paramagnetic

systems.[7, 8] The presence of unpaired electrons also allows completely different reactivity to be observed (e.g. one-electron redox processes) compared with the more familiar diamagnetic systems.[2]

To stabilize transition metal centres with low co-ordination numbers, the employment of sterically demanding ligands is important.[9] For instance, the bulky β-diketiminato ligand systems (e.g. nacnac$^-$, i.e. [{ArNC(R)}$_2$CH]$^-$ Ar = 2,6-diisopropylphenyl, R = Me (^{Me}nacnac$^-$) (**1**) or Bu^t (^{Bu}nacnac$^-$) (**2**)) have shown their potential in this respect, by stabilising Group 5 – 12 first row transition metal(I) complexes. Over the past few years, these have displayed interesting chemistry, due to their high reactivity.

For comparison, the investigation of the potential of the related, sterically demanding amidinate [ArNC(Bu^t)NAr]$^-$ (Ar = 2,6-diisopropylphenyl) Piso$^-$ (**3**) and guanidinate ligand systems [ArNC(NR$_2$)NAr]$^-$ (R = cyclohexyl (Giso$^-$, **4**) or Pr^i (Priso$^-$, **5**)), for the stabilisation of group 8 – 10 first row transition metal(I) complexes. Amidinates and guanidinates have great potential in this field, due to their effective tenability through the systematic variation of their substituents.[10] If acquirable, these potentially reactive metallacycles could lend themselves to an array of synthetic applications, including uses as reagents for small molecule activations, reductive couplings, metal imide formations etc.[9, 11-18] This work forms the basis of this chapter.

2.1.1 β-Diketiminato Ligand Systems

β-diketiminato ligand systems, *e.g.* **III**, have been known since the late 1960s.[11-13] These ligands have great tuning potential, as their substituents can vary from hydrogen, to alkyl, aryl or silyl and can also be incorporated into six-membered (**IV**) or five-membered (**V**) heterocyclic ring systems. β-diketiminato ligands and other isoelectronic systems (*e.g.* β-diketonato **I** ($acac^-$) and β-enaminoketonato **II**) are shown in **Figure 1.** [14]

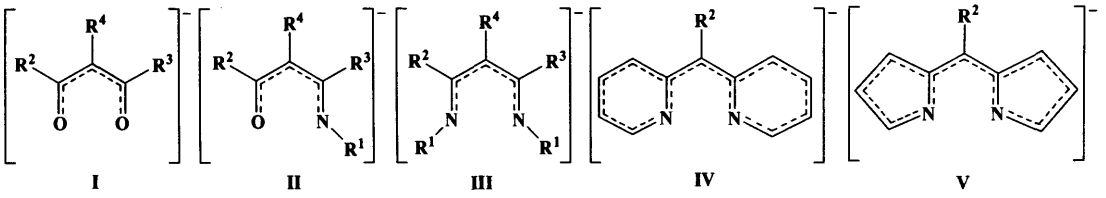

Figure 1 Ligand systems **I** – **V**

There are a variety of methods to prepare β-diketiminato ligand systems. One route, published by *McGeachin* in 1968, is the condensation reaction of a primary amine with a β-diketone, to form the β-diketiminato conjugate acid ligand **VI** (**Scheme 1**), in which the substituents in this ligand system can vary from hydrogen to alkyl, aryl or silyl.[11]

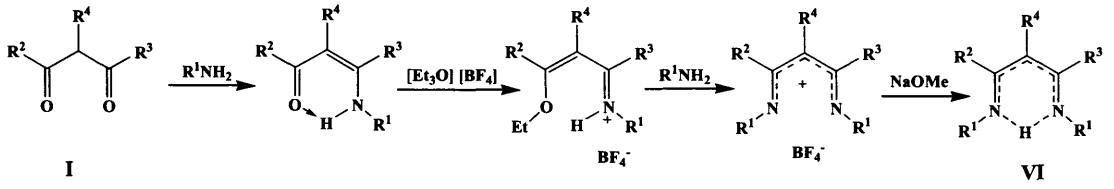

Scheme 1 McGeachin's route to prepare β-diketiminato ligands **VI**

In 1997, *Feldmann et al.* published the preparation of the most common β-diketimine [^{Me}nacnacH] (**1H**), by reacting 2,4-pentanedione (**6**) with $ArNH_2$ (Ar = 2,6-diisopropylphenyl) in ethanol (**Scheme 2**).[22, 23]

The deprotonated ^{Me}nacnac ligand (**1**) and the ^{Bu}nacnac ligand (**2**), are important β-diketiminato ligand systems that have received significant attention over the past five years for stabilising metals in the +1 oxidation state.

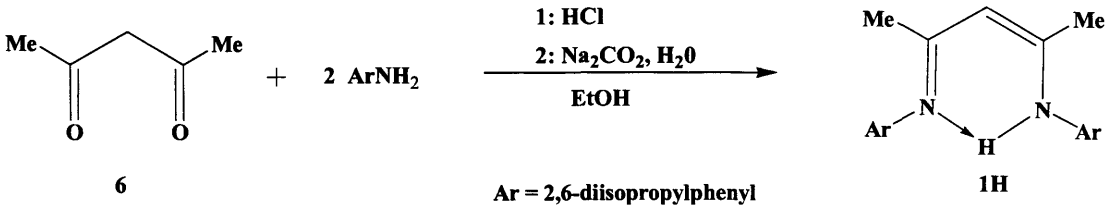

Scheme 2 Feldmann's route to prepare ^{Me}nacnacH (**1H**)

β-diketiminato metal complexes can be prepared, either by reacting α-hydrogen-free nitriles,[15] or isonitriles[16-18] with a metal alkyl. The mechanism in these reactions involves a C–C coupling process and two 1,3 migrations of the trimethylsilyl group from the carbon to the nitrogen atom, to form the β-diketiminato metal complexes, *e.g.* **VII (Scheme 3)**. Other routes can be found in the literature.[19-28]

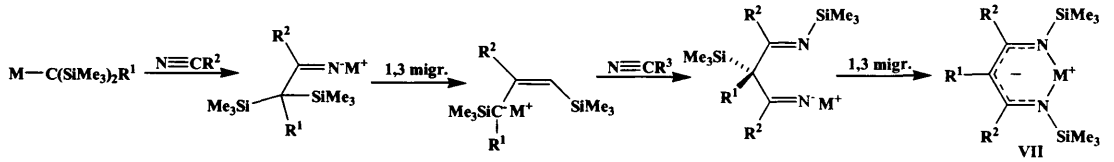

Scheme 3 The nitrile route to β-diketiminato metal complexes **VII**

2.1.1.1 Metal Co-ordination Chemistry of β-Diketiminato Ligands

A variety of co-ordination modes can be found for β-diketiminato metal complexes which are displayed in **Figure 2**. Examples of each co-ordination mode will be discussed.

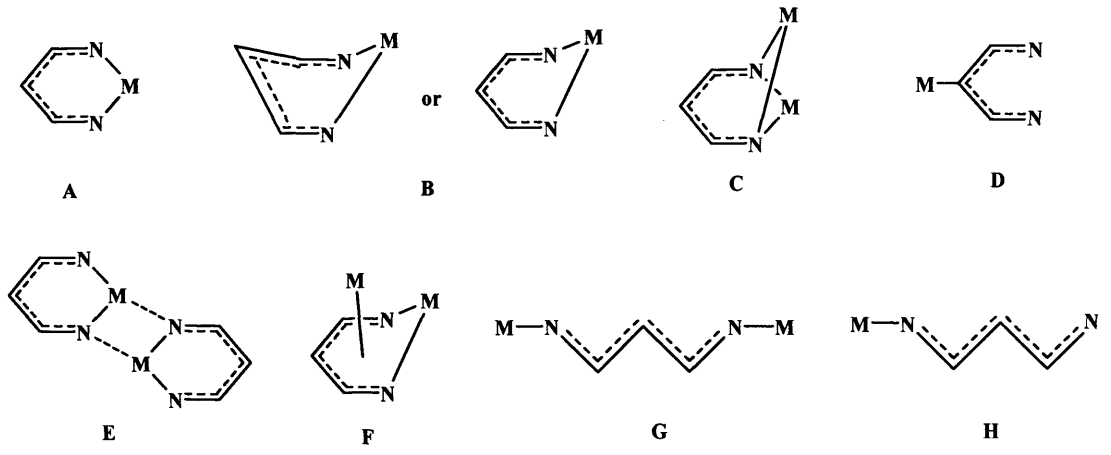

Figure 2 General co-ordination modes of β-diketiminato ligands

β-diketiminato metal complexes, having a tetrahedral or distorted tetrahedral co-ordination environment, generally accept the co-ordination mode **A**. Mode **A** displays a planar ring system in which the ligand behaves in a N,N'-chelating fashion. An example of this complex type is **8**, prepared by reacting **7** with $CoSO_4$ in H_2O. Complex **9** also shows the co-ordination mode **A** but with a trigonal planar environment (**Scheme 4**).[29-32] For complexes of metals having low-lying empty d-orbitals of appropriate symmetry, there is the possibility of the β-diketiminato ligand involving not only σ- but also π-bonding and it can act as a 4- or 6-electron donor. There are many other examples of type **A** co-ordination which can be found in the literature.[24, 37, 38, 41]

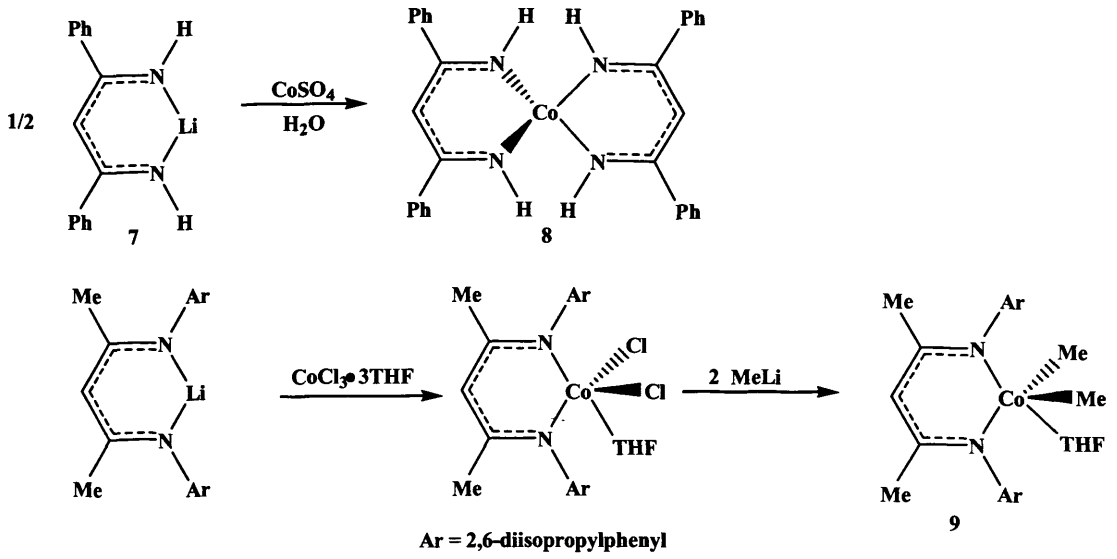

Scheme 4 β-diketiminato metal complexes displaying co-ordination mode A

In contrast to co-ordination mode **A**, co-ordination type **B** displays a heterocycle in the boat form, in which the metal is out of plane. The extreme of this co-ordination mode can be viewed as the ligand acting in an η^5 mode, but only if the metal has unfilled accepting d-orbitals. Examples of co-ordination mode **B** can be found in complexes **10**[33] and **11**.[29, 34] The co-ordination type **B** generally results from steric crowding around the metal centre, which forces the metal to bend away from the ligand (**Scheme 5**). Other examples have also been reported.[34-37]

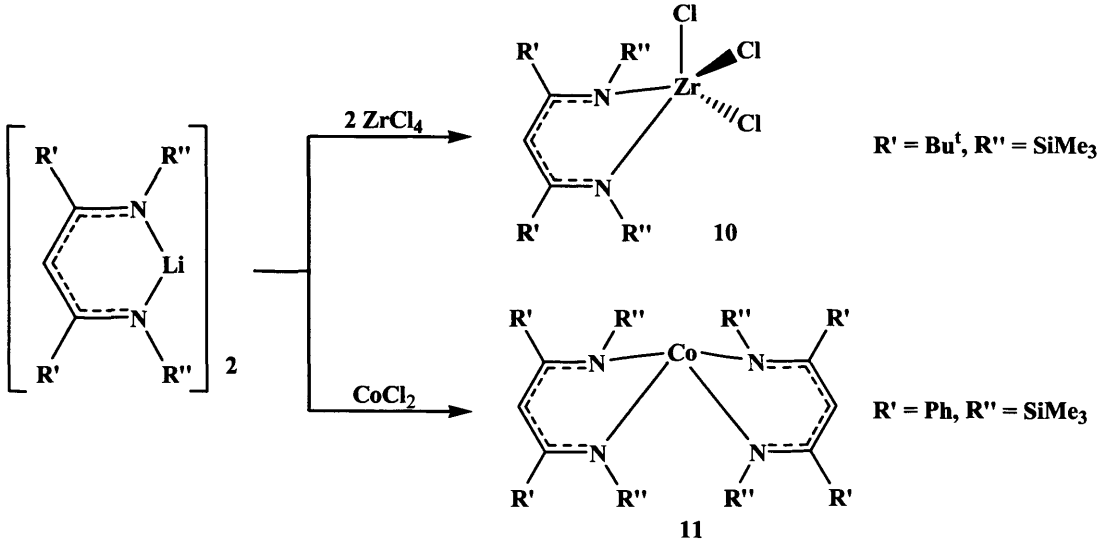

Scheme 5 β-diketiminato metal complexes in co-ordination mode B

Type C co-ordination involves chelating as well as bridging, in which both nitrogen atoms are four co-ordinated. Only a few examples of complexes with this co-ordination mode are known in the literature. Complex **12** is one of them and is displayed in **Scheme 6.**

The co-ordination type **D** is very rare and only one example (**13**) is known in the literature to date (**Scheme 6**). In this mode, one nitrogen atom and one carbon is co-ordinated to the metal.[38, 39]

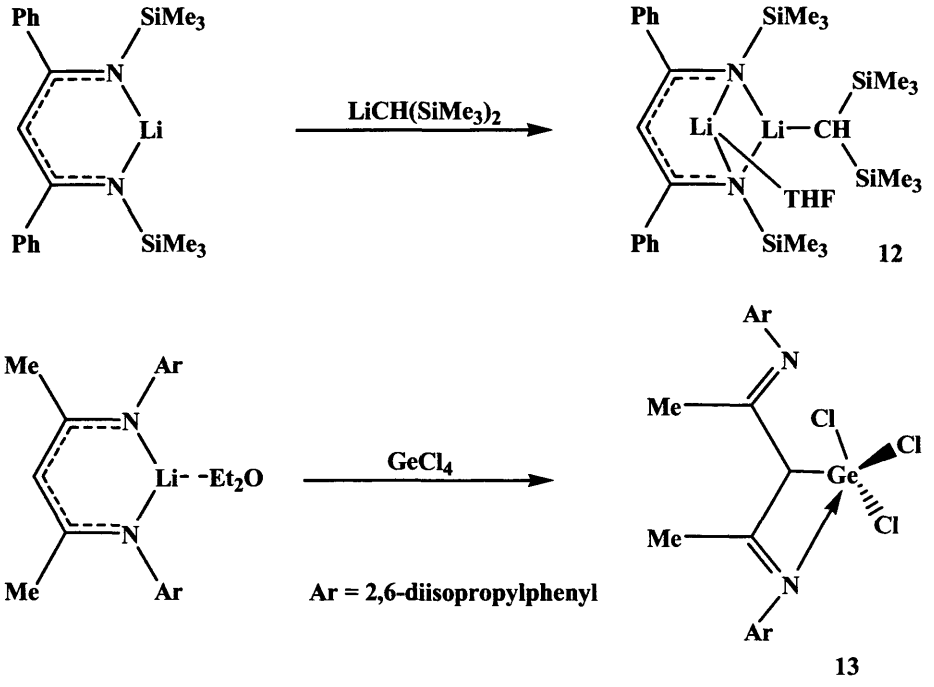

Scheme 6 β-diketiminato metal complexes showing co-ordination modes C and D

Examples of the co-ordination mode type E can also be found in the literature. Two examples of this co-ordination type can be seen in complexes **14** and **15 (Scheme 7).**[15, 38] This co-ordination mode exhibits chelating as well as bridged N,-centres.

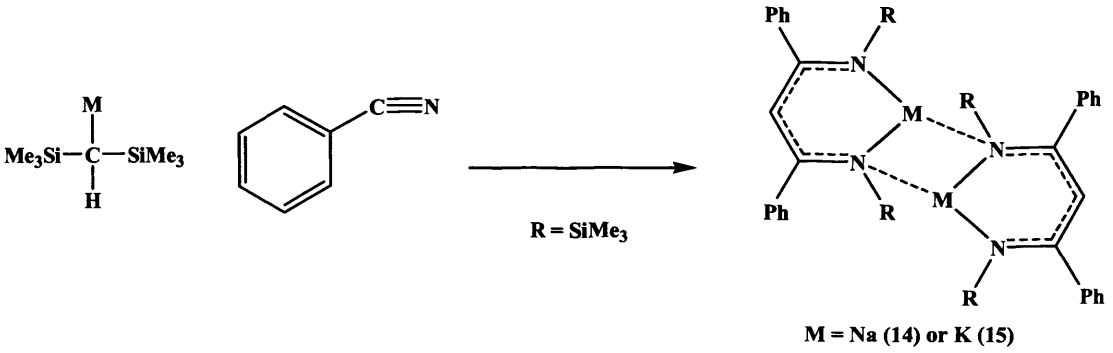

Scheme 7 β-diketiminato metal complexes showing co-ordination mode **E**

The barium complex, **16**, shown in **Scheme 8** is rather unusual and its structure displays three of the co-ordination types in the one molecular unit (**B**, **F** and **G**).[40]

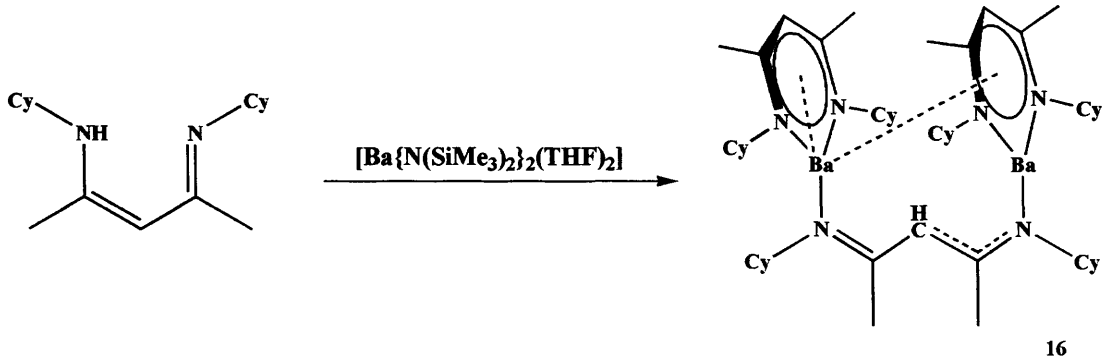

Scheme 8 A β-diketiminato barium complex exhibiting co-ordination mode **B**, **F** and **G**

Complex **17** displays the co-ordination type **H** and is shown in **Scheme 9**. The co-ordination type **H** is in principle a monomeric ligand system, which is N,C chelating (**Scheme 9**).[25]

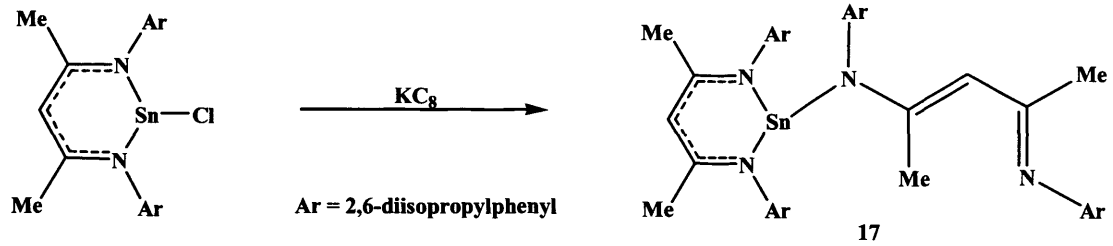

Scheme 9 A β-diketiminato metal complex showing co-ordination mode **H**

2.1.1.2 Low Oxidation State d-block β-Diketiminato Complexes

Over the past five years, sterically hindered examples of β-diketiminates (e.g. **1** or **2**) have been utilised for the preparation of a variety of stable group 5 - 12 first row transition metal(I) complexes. These low oxidation state complexes are generally synthesized by the reduction of β-diketiminate metal halide precursors with s-block metals. The study of transition metal(I) complexes is an area of inorganic and organometallic chemistry that has enjoyed a resurgence in recent years.[41]

Examples of first row low oxidation state β-diketiminate transition metal complexes and their reactions can be found as follows.

The reduction of $[V^{III}(^{Me}nacnac)Cl_2]$ (**18**),[42] with four equivalents of KC_8 in toluene under a dinitrogen atmosphere, gives the toluene capped vanadium(I) complex $[\{V^{I}(^{Me}nacnac)\}_2(\eta^3:\eta^3\text{-}C_7H_8)]$ (**19**) (**Scheme 10**).[9] The effective magnetic moment of ca. 4.6 μ_B at 9–300 K is in agreement with an $S = 2$ spin-only system, and **19** is therefore best thought of as a V(I)–V(I) complex, in which each V(I) centre possesses two unpaired electrons.[9] It is worth mentioning, that $[V^{III}\{Me_3SiN(CH_2CH_2NSiMe_3)\}(\mu\text{-}Cl)]_2$ reacts with KC_8 in toluene under a dinitrogen atmosphere to give the nitrogen bridged complex $[V^{V}\{Me_3SiN(CH_2CH_2NSiMe_3)\}(\mu\text{-}N)]_2$.[43]

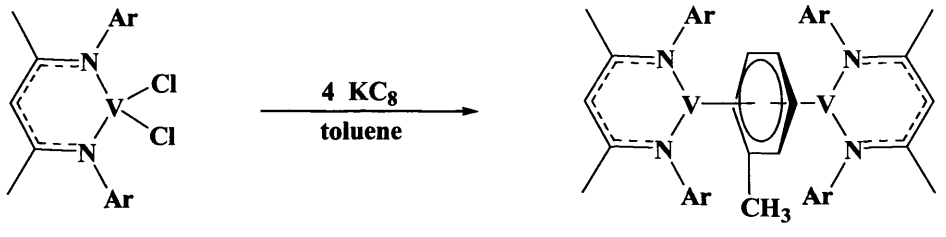

18 **19**

Scheme 10 Preparation of the divanadium(I) complex **19**

Reactions of the divanadium(I) complex **19** can also be found in the literature. Nitrous oxide, N_2O, which can either be split by low-valent and low-co-ordinate metal complexes to form dinitrogen and metal oxides,[44-47] or metal nitride and nitrosyl complexes,[44] was reacted with **19** in diethylether to give the bridged vanadium(IV) oxide complex **20**. The magnetic moment of 2.71 μ_B at 293 K, is consistent with an S = 1 spin-only system (**Scheme 11**).[9]

The reaction of complex **19** with two equivalents of azobenzene in diethylether leads to the vanadium(V) bis(imido) complex [$V^V(^{Me}$nacnac)$(NPh)_2$] (**21**) (**Scheme 11**).[9]

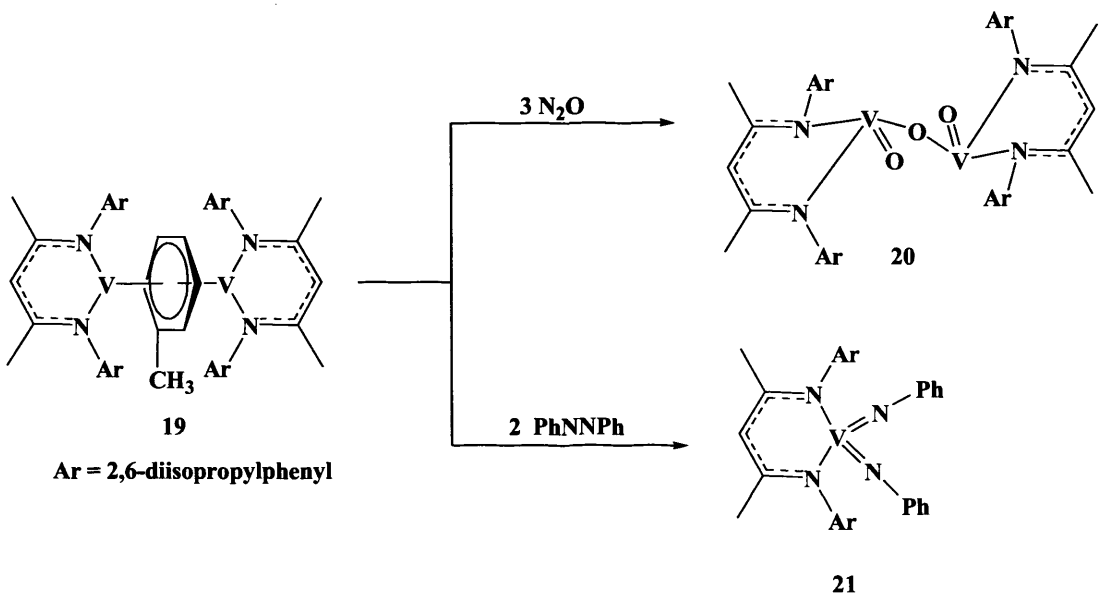

Scheme 11 Reactions of the divanadium(I) complex **19** with N_2O and PhNNPh

A magnesium reduction of [$Cr^{II}(^{Me}$nacnac)$(\mu$-Cl)$]_2$ (**22**)[45] in THF in the presence of a small amount of benzene gives the benzene bridged chromium(I) complex [{$Cr^I(^{Me}$nacnac)$\}_2(\eta^3:\eta^3$-C_6H_6)] (**23**) (**Scheme 12**). The magnetic moment of 7.4 μ_B per dimer at 293 K is close to the spin-only moment for a strongly coupled system with six unpaired electrons ($S = 3$, $\mu_{eff} = 6.93\ \mu_B$).[46]

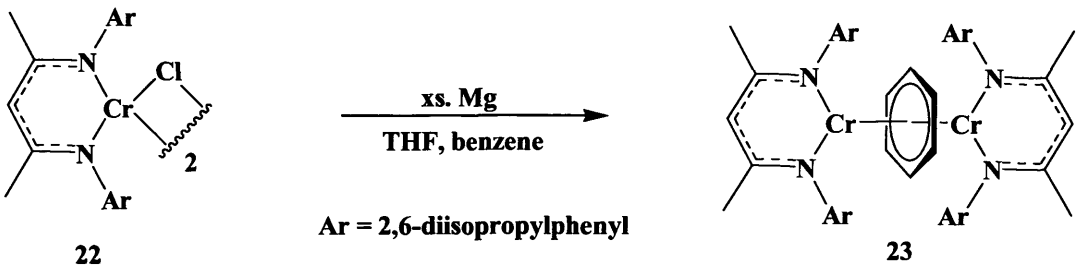

Scheme 12 Preparation of the benzene capped dichromium(I) complex **23**

The reaction of $[\{Cr^{I}(^{Me}nacnac)\}_2(\eta^3:\eta^3\text{-}C_6H_6)]$ (**23**) with an excess of dry oxygen in diethylether at room-temperature, gives the mononuclear dioxo chromium(V) complex $[Cr^{V}(^{Me}nacnac)(O)_2]$ (**24**) (**Scheme 13**).[47]

Complex **23** was also reacted with four equivalents of N_3Mes (Mes = 2,4,6-$Me_3C_6H_2$) in diethylether, which leads to the tetrahedral chromium(V) complex $[Cr^{V}(^{Me}nacnac)(NMes)_2]$ (**25**). The magnetic moment of 2.02 μ_B at 293 K is consistent with an $S = ½$ spin-only system (**Scheme 13**).[47]

The treatment of **23** with one equivalent of azobenzene in THF leads to the chromium(III) phenylimido-bridged dimer $[Cr^{III}(^{Me}nacnac)(\mu\text{-}NPh)]_2$ (**26**) with a magnetic moment of 3.87 μ_B at 293 K which implies, that **26** exhibits antiferromagnetic behaviour (**Scheme 13**).[47]

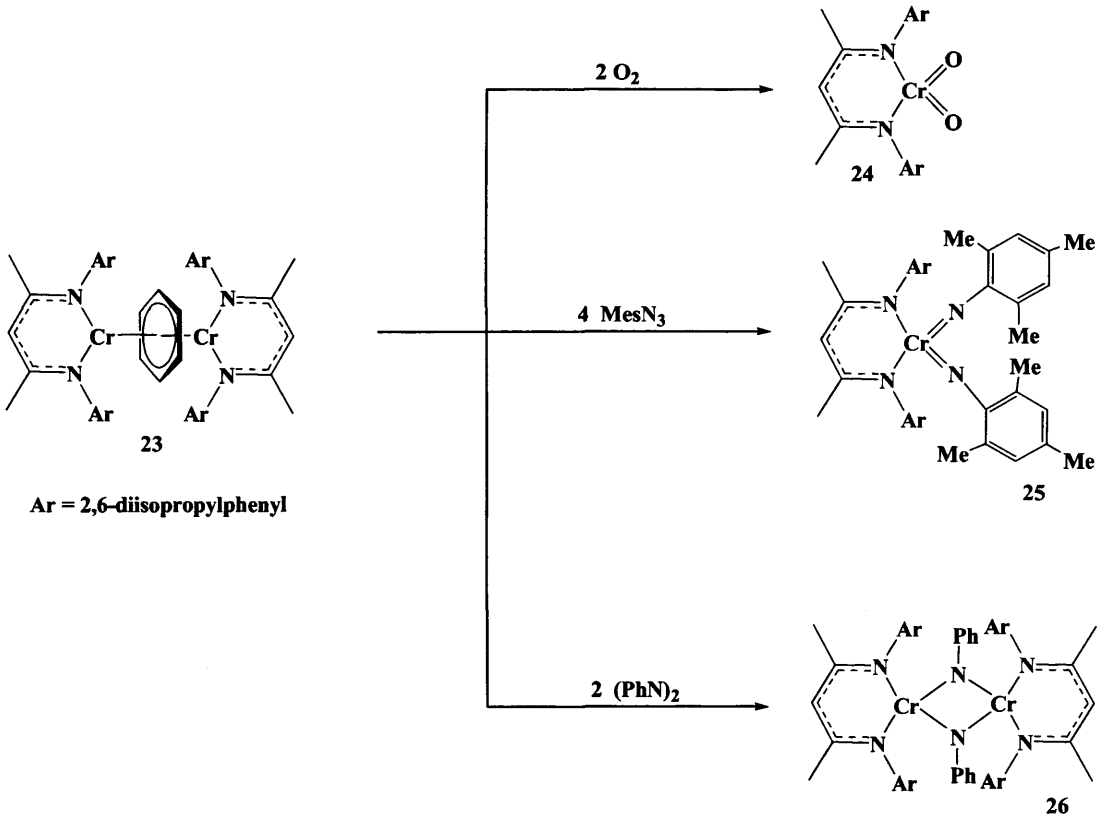

Scheme 13 Reactions of the benzene capped dichromium(I) complex **23** with O_2, $MesN_3$ and $(PhN)_2$

The reduction of the complex $[Mn^{II}(^{Me}nacnac)(\mu\text{-}I)]_2$ (**27**)[48] with a Na/K alloy in toluene at room temperature gives the dimeric manganese(I) complex $[Mn^{I}(^{Me}nacnac)]_2$ (**28**) (**Scheme 14**). DFT calculations have indicated a strong s-s interaction of the two Mn(I) ions with the open shell configuration ($3d^54s^1$). Its magnetic moment of 3.98 μ_B at 290 K suggests that the magnetic behaviour of **28** could be correctly described as the coupling between two $S_1 = S_2 = {}^5/_2$ spin centres.[49]

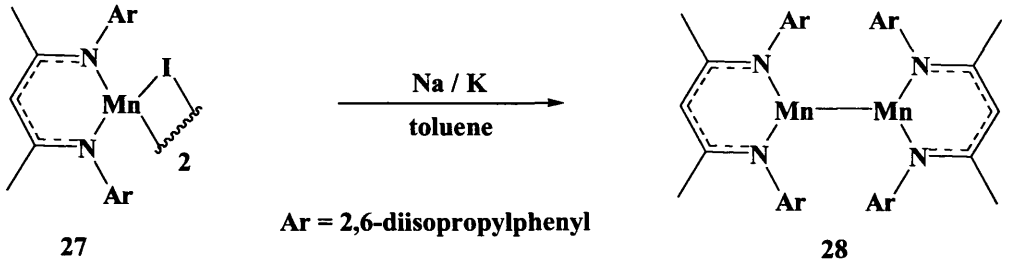

Scheme 14 Preparation of the dimanganese(I) complex **28**

The reaction of **28** with an excess of $KMnO_4$ in toluene at room temperature gives the dimeric manganese(III) oxide $[Mn^{III}(^{Me}nacnac)(\mu\text{-}O)]_2$ (**29**) (**Scheme 15**). Alternatively, the same product could be found by reacting **28** with predried dioxygen.[49]

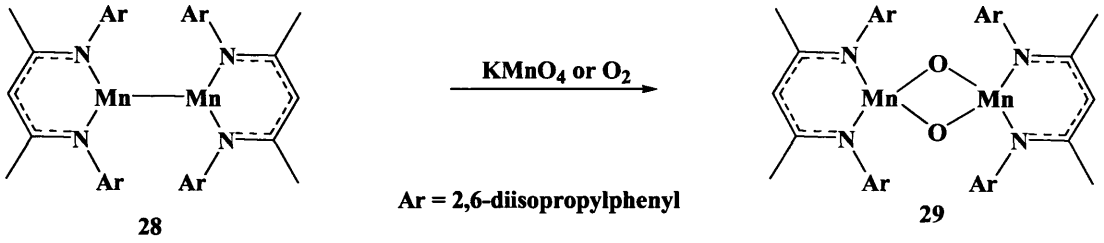

Scheme 15 Oxidation of the dimanganese(I) complex **28**

The reduction of $[Fe^{II}(^{Me}nacnac)_2(\mu\text{-}Cl)]_2$ (**30a**) or $[Fe^{II}(^{Bu}nacnac)(\mu\text{-}Cl)]$ (**30b**), with KC_8 in toluene, (**30a**),[50] or Et_2O, (**30b**),[51] under a dinitrogen atmosphere, gives the dimeric dinitrogen bridged iron(I) complexes $[Fe(^{Me}nacnac)_2(\mu\text{-}N)]_2$ (**31a**) or $[Fe(^{Bu}nacnac)(\mu\text{-}N)]_2$ (**31b**) (**Scheme 16**). The magnetic moments of these complexes are 7.9 μ_B for **31a** and 8.4 μ_B for **31b** per dimer. The N-N bond lengths in **31a** are 1.18 Å, and in **31b**, 1.192 Å, which indicates a substantial N-N bond weakening relative to free dinitrogen (1.098 Å).[52]

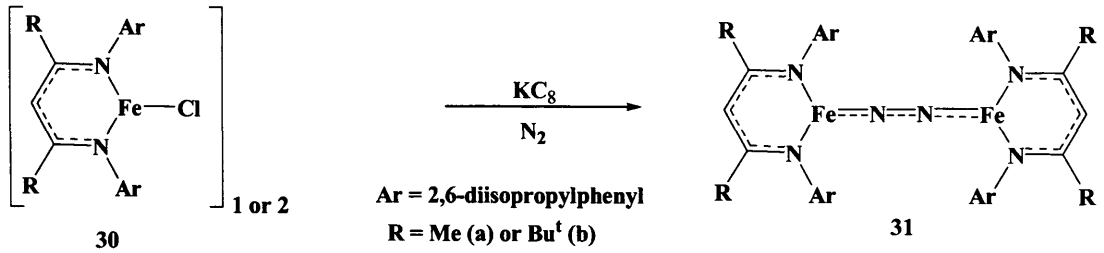

Scheme 16 Preparation of the dinitrogen bridged iron(I) complexes **31**

The dinitrogen bridged iron complexes **31a-b** were reacted with a variety of ligands and these reactions are displayed in **Scheme 17**. The reaction of **31a** with excess CO in diethylether affords the complex $[Fe^{I}(^{Me}nacnac)(CO)_3]$ (**32a**). The

magnetic moment of 2.0 μ_B indicates that **32a** has a low-spin (S = 1/2) electronic configuration at the iron centre.[52]

The reactions of the dinitrogen bridged iron(I) complexes **31a-b** with ligands **33a-j** gives the [Fe(^{Me}nacnac)(Ligand)] complexes **34a-j**. These reactions and some of the magnetic moments can be found in **Scheme 17**.[52, 53]

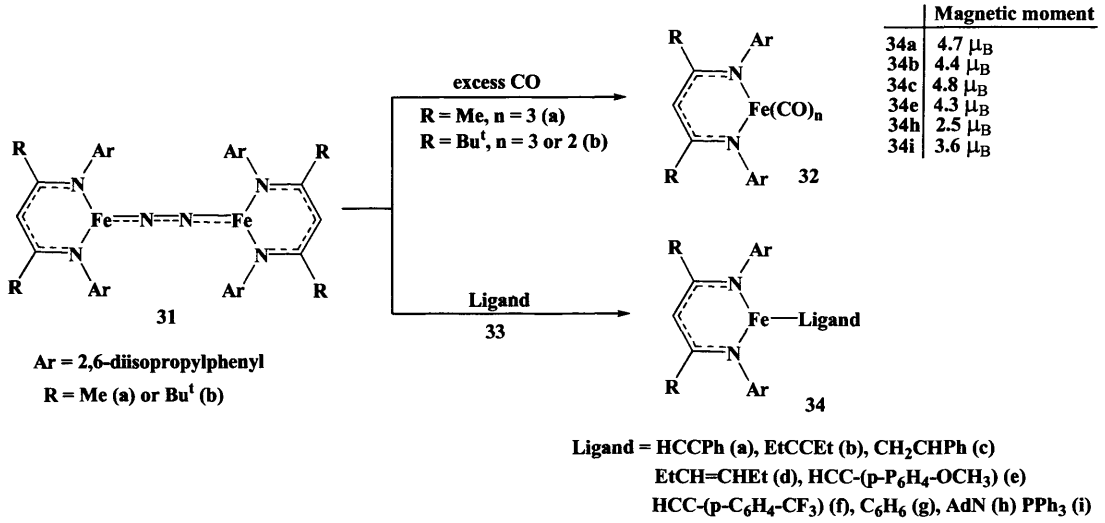

	Magnetic moment
34a	4.7 μ_B
34b	4.4 μ_B
34c	4.8 μ_B
34e	4.3 μ_B
34h	2.5 μ_B
34i	3.6 μ_B

Scheme 17 Reaction of dinitrogen bridge iron(I) complexes **31** with CO and ligands **33a-j**

The cobalt(II) complex **35** was reduced with Mg powder in toluene to give the toluene capped complex [Co^I{(Ar'NCMe)$_2$CH}(η^6-C$_7$H$_8$)] (**36**) (Ar' = 2,6-dimethylphenyl) (**Scheme 18**). The magnetic moment of 2.7 μ_B at 293 K in toluene-d_8 indicates that **36** is a d^8 high spin complex.[54]

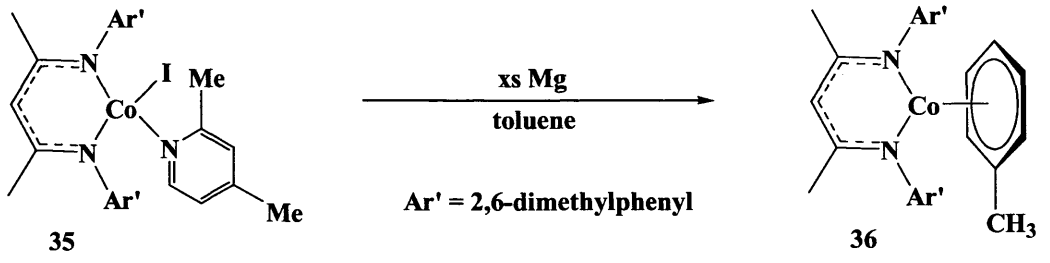

Scheme 18 Preparation of the η^6-toluene capped cobalt(I) complex **36**

Complex **36** has been reacted with a variety of ligands (*e.g.* O_2, N_3Ar'' (Ar'' = 3,5-Me$_2$C$_6$H$_3$), N_3Ad (Ad = 1-adamantyl) and O=NAr'' (Ar'' = 3,5-Me$_2$C$_6$H$_3$))

and the products of the reaction are displayed in **Scheme 19**. The addition of an excess of dry oxygen to **36** in diethylether at room temperature yields the dimeric complex $[Co^{III}\{(Ar'NCMe)_2CH\}(\mu\text{-}O)]_2$ (**37**). Complex **37** follows Curie-Weiss behavior from 50 to 200 K for which an average $\mu_{eff} = 3.5\ \mu_B$ (**Scheme 19**).[54]

The reaction of **36** with N_3Ar'' (Ar'" = 3,5-$Me_2C_6H_3$) in diethylether gives the Co(III)-imido bridged dimer $[Co^{III}\{(Ar'NCMe)_2CH\}\mu\text{-}NAr")]_2$ (**38**). Its solution magnetic moment was found to be 8.8 μ_B at room temperature (benzene-d_6) and is consistent with two non-interacting, high-spin d^6 centres. The solid-state magnetic susceptibility data revealed antiferromagnetic coupling with a Neel temperature of 25 K (**Scheme 19**).[54]

The reaction of **36** with the more sterically demanding azide N_3Ad (Ad = 1-adamantyl), compared to N_3Ar" (Ar" = 3,5-$Me_2C_6H_3$), leads to the formation of the three co-ordinate terminal imide complex, $[Co^{III}\{(Ar'NCMe)_2CH\}(NAd)]$ (**39**). DFT calculations gave support for the presence of a low-spin d^6 cobalt(III) centre in **39**, which is stabilized by a $1\sigma,2\pi$-donation from the imido ligand. This leads to considerable multiple bond character in this 16-electron, three co-ordinate complex (**Scheme 19**).[54]

Complex **36** has also been reacted with O=NAr'' (Ar'' = 3,5-$Me_2C_6H_3$) in diethylether which gives complex $[\{Co^{III}(Ar'NCMe)_2CH\}_2(\mu\text{-}O{:}\mu\text{-}NAr'')]$ (**40**). This 4-electron reduction of a nitrosobenzene stands in contrast to the reaction of the related $[Co(Cp)(C_2H_4)_2]$ with O=NPh which leads to complex $[Co(Cp)(\eta^2{:}\eta^1\text{-}PhNO)]_2$.[55] The Curie-Weiss behavior of **40** over 50-300 K exhibits an average μ_{eff} of 4.4 μ_B and the solution magnetic moment at of 4.9 μ_B at 293 K in benzene-d_6 indicate an $S = 2$ spin only system (**Scheme 19**).[54]

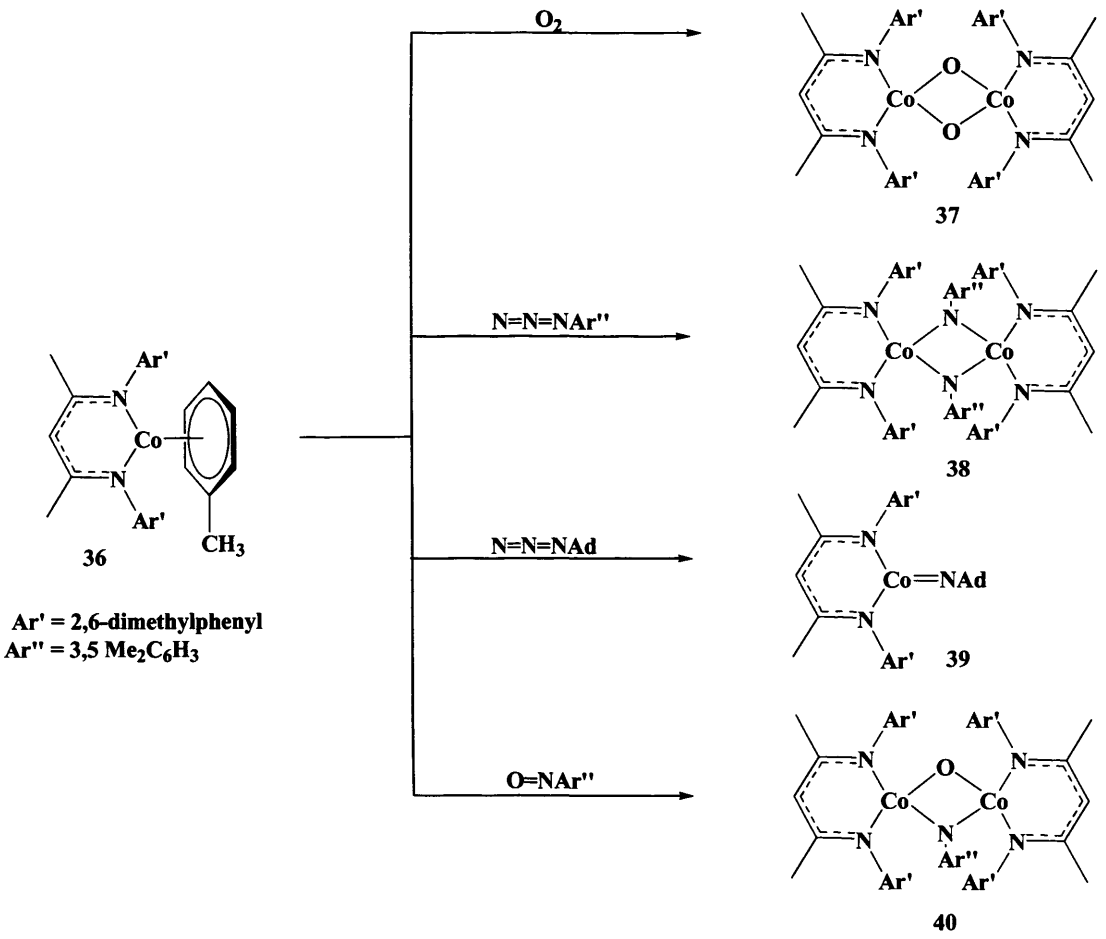

Scheme 19 Reactions of a η^6-toluene capped cobalt(I) complex, **36**, with O_2, azides and O=NAr''

The reduction of complex $[Ni^{II}(^{Me}nacnac)Br_2Li(THF)_2]$ (**41**) with K/Na alloy at 25 °C in toluene gives the diamagnetic toluene bridged nickel dimer, $[\{Ni^{II}(^{Me}nacnac)\}_2(\eta^3{:}\eta^3\text{-}C_7H_8)]$ (**42**). It has been proposed that complex **42** is a nickel(II) dimer, bridged by a reduced C_7H_8 fragment, and the complex behaves as a convenient nickel(I) synthon. Alternatively, **42** can also by prepared by the reduction of **41** with MeMgBr in toluene (**Scheme 20**).[41]

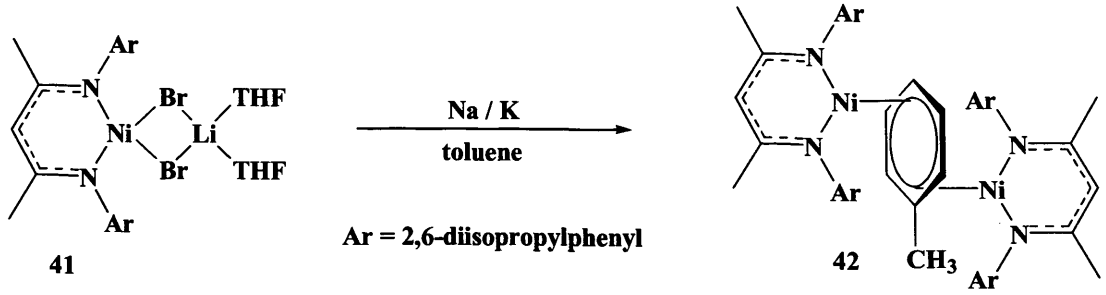

Scheme 20 Preparation of the η^3-toluene bridged nickel(II) dimeric complex **42**

Compound **42** has been reacted with a variety of different ligands (**43a-i**), which gave the products [{Ni(^{Me}nacnac)}$_2$(Ligand)] **44a-f** (**Scheme 21**).[41, 56] There are also other examples which can be found in the literature.[57]

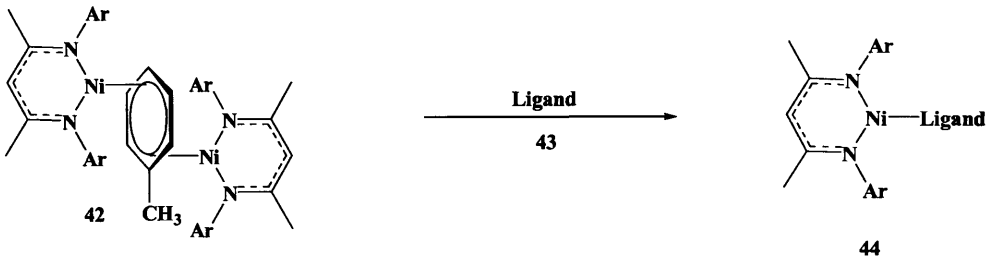

Ar = 2,6-diisopropylphenyl

Ligand = PhCCPh (a), $Me_3SiCCSiMe_3$ (b), NCPh (c) Ph_2CCH_2 (d) Ph_2CO (e), PCy_3 (f), $CH_2(PPh_2)_2$ (g)

Scheme 21 Reaction of **42** with ligands **43a-f**

The reaction of complex **42** with reactants **45a-b** gives different types of complexes compared to the products in **Scheme 22**.[41] A reductive CC coupling reaction of **42** with $C_5H_5CMe_2$ (**45a**) in toluene gives the complex [{Ni^{II}(^{Me}nacnac)}$_2$(η^5:η^5-$C_5H_4CMe_2$)$_2$] (**46**) in which two capped ligand fragments (**45a**) are bridged between two [Ni^{II}(^{Me}nacnac)] units. Another bridged complex, [Ni^{II}(^{Me}nacnac)(μ-PPh)]$_2$ (**47**), was formed by reacting **42** with P_5Ph_5 (**45b**), giving the bimetallic product containing two [Ni^{II}(^{Me}nacnac)] units, which are bridged by a $(PPh)_2$ fragment (**Scheme 22**).[41, 57]

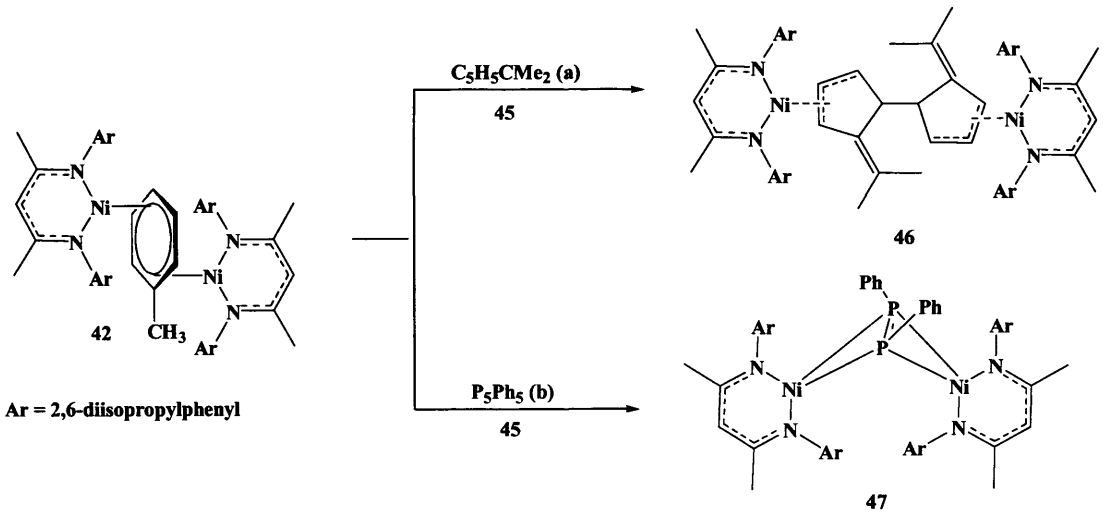

Scheme 22 Reaction of **42** with **45a-b**

Examples of copper(I) β-diketiminato complexes can also be found in the literature. The monomeric toluene capped copper(I) complex **49** was prepared by reacting the thallium precursor **48a** with CuBr in toluene.[58] The reaction of **48b** with $CuBr{\cdot}SMe_2$ in the presence of either ethylene or styrene (**50a-b**) in benzene or toluene provides the thermally stable copper(I) complexes **51a-b** (**Scheme 23**).[59]

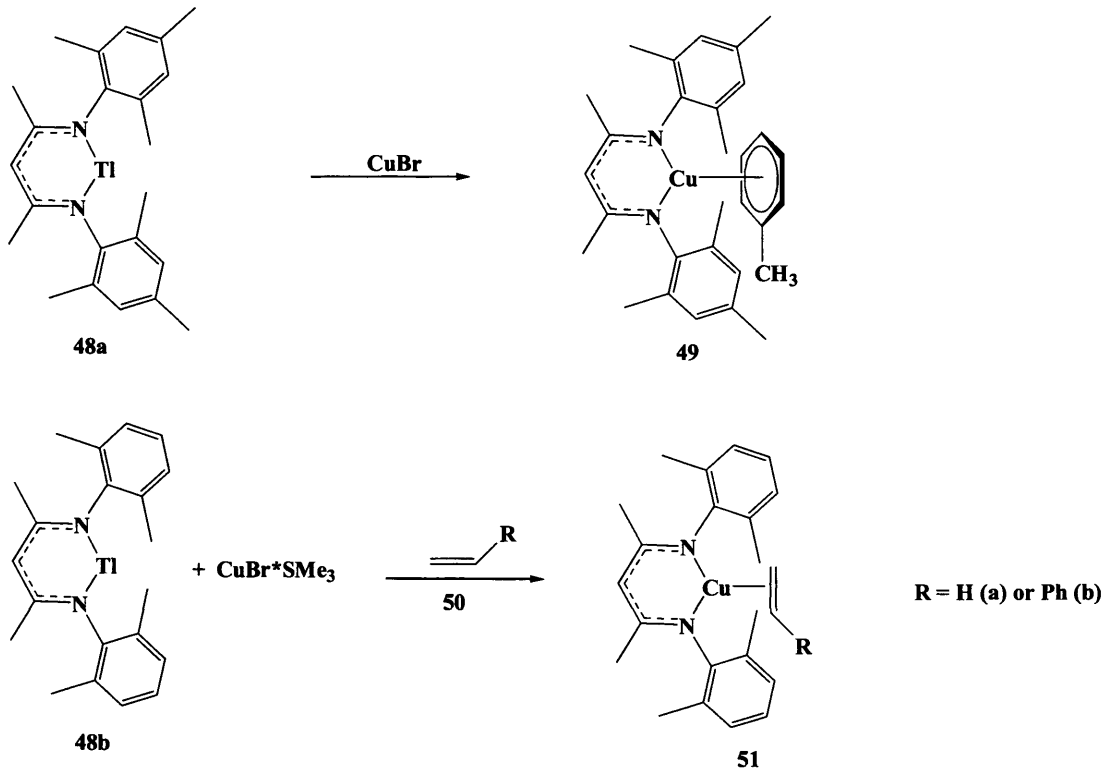

Scheme 23 Preparation of copper(I) complexes **49** and **51**

The complexes **49** and **51a** were reacted with N_2CPh_2, giving the monomeric complex **52** and the dimeric complex **53**. As the ligand in complex **49** is more sterically hindered than **51a**, the differences in the observed products likely result from steric bulk of the ligands (**Scheme 24**).[58]

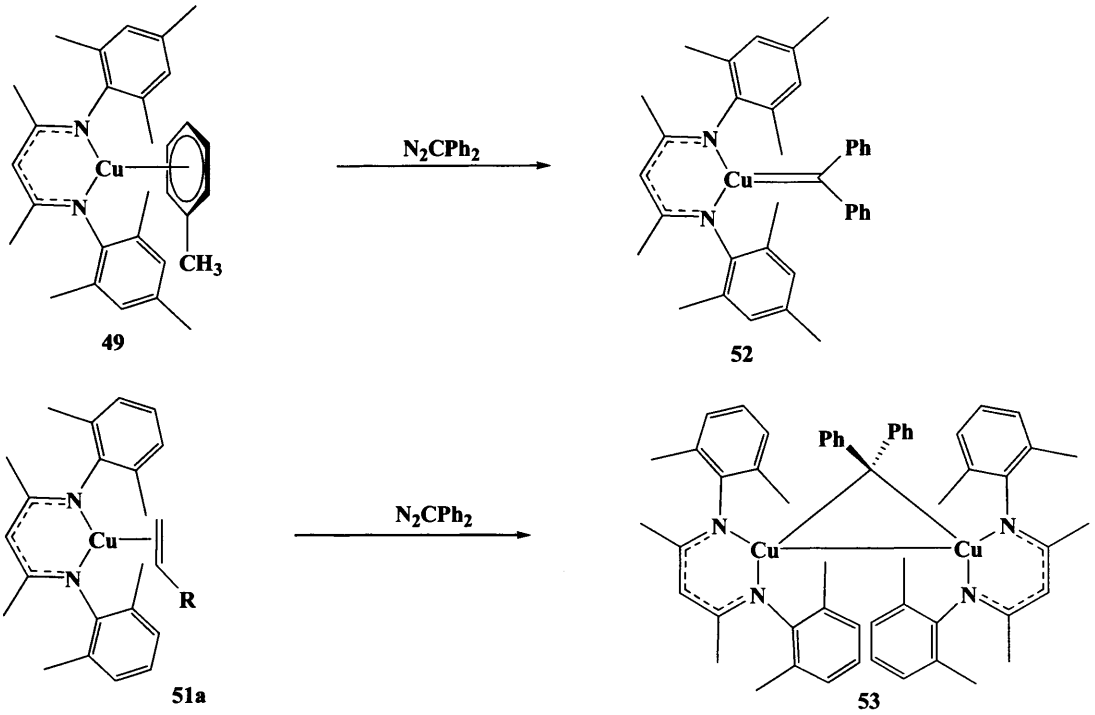

Scheme 24 Reactions of complexes 49 and 51a with N_2CPh_2

The reduction of $[Zn^{II}(^{Me}nacnac)I_2Li(Et_2O)_2]$ (**54**),[60] with potassium/sodium alloy in toluene gives the dizinc complex $[Zn^{I}(^{Me}nacnac)]_2$ (**55**) (**Scheme 25**).[61] No reactions with this complex (**55**) can be found in the literature to date.

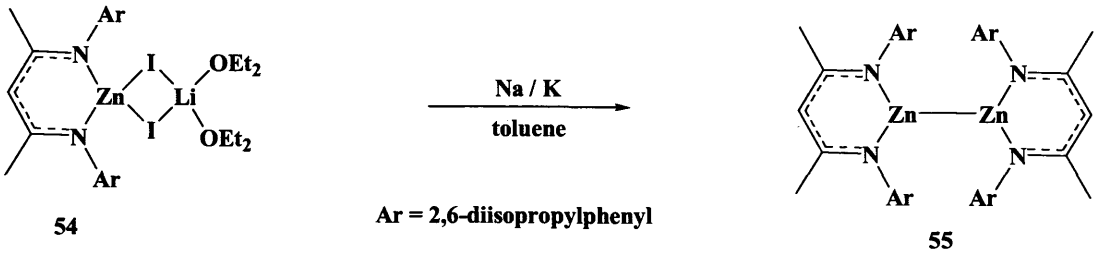

Scheme 25 Preparation of the dizinc(I) complex 55

2.1.2 Amidinate and Guanidinate Ligand Systems

The amidinate ligand system, *e.g.* **VIII**, is the nitrogen analogue of the carboxylate anion and has been widely explored in main group and transition metal co-ordination chemistry. This type of ligand is of great interest due to the large degree of variability that is substituents can bear, in terms of steric and electronic properties (**Figure 3**).[10]

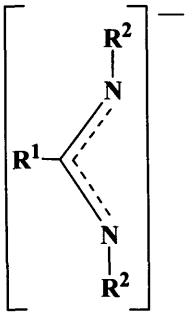

VIII

R^1 = H, alkyl, aryl, etc.

R^2 = H, alkyl, cycloalkyl, aryl, trimethylsilyl, etc.

Figure 3 The amidinate ligand system

The first amidinate ligand was published by *Sanger* in 1973. He prepared the N,N'-bis(trimethylsilyl)benzamidinate **56a** *via* a two step synthesis (**Scheme 26**).[62] *Oakley et al.* improved this preparation in 1987 and published the preparation of products with a variety of differing substituents on the carbon backbone (**56b-j**) (**Scheme 26**).[63]

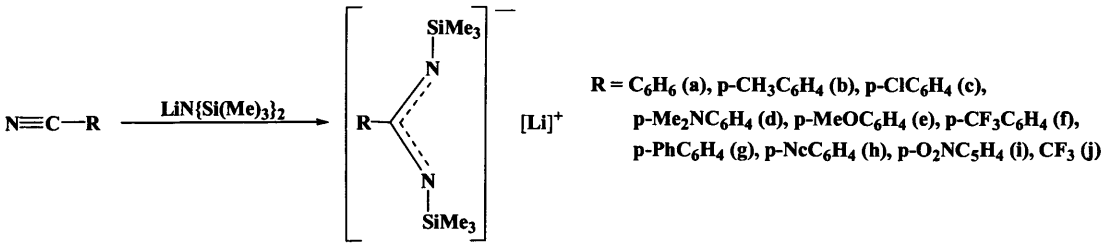

56

Scheme 26 The first amidinates

Closely related to the amidinate ligand system are the guanidinates, *e.g.* **IX**. The differences between these ligands is the substituents on the carbon backbone, which are changed to an amino group in guanidinates **IX** (**Figure 4**). Changing the fuktional group, effects the orientation of the nitrogen lone pairs of the amidinate fragment, and can therefore change its co-ordination chemistry. Further explanation of this point can be found at the beginning of section 2.1.2.1.

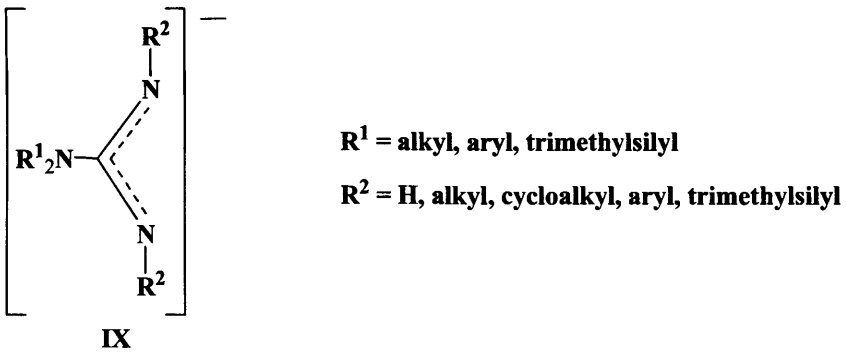

IX

Figure 4 The guanidinate ligand system

Beside the amidinate and guanidinate anions, **VIII** and **IX**, there are several isoelectronic chelating ligand systems which have been reported in the literature. These include diiminosulfinate anions, **X**,[64-66] the diiminophosphinate anions, **XI**,[67-71] and the dianionic boraamidinate anion, **XII**[72-74] (**Figure 5**).

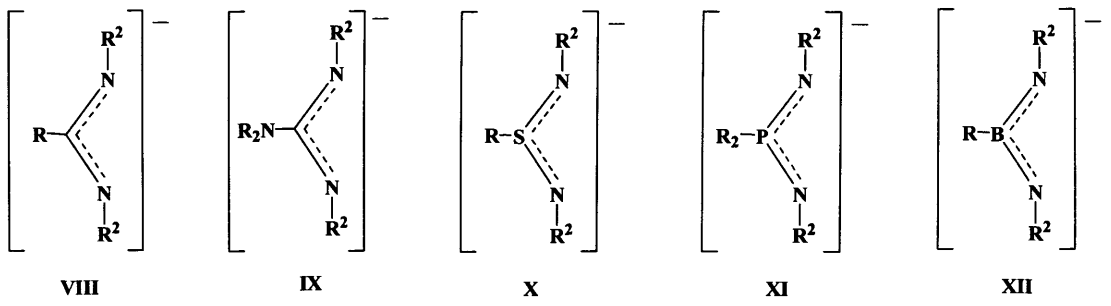

Figure 5 Isoelectronic chelating ligand systems

Of relevance to this study are the bulky amidinate $[(ArN)_2C(Bu^t)]^-$, (Ar = 2,6-diisopropylphenyl) (Piso$^-$) (**3**)[75] and the guanidinates $[(ArN)_2C(NR_2)]$ (R = cyclohexyl: Giso$^-$ (**4**)[76] or Pr^i; Priso$^-$ (**5**) which have been prepared *via* following route.

The amidine **3H** was prepared by reacting the carbodiimide (**57**) in diethylether with LiBu^t at 0 °C. An aqueous work-up gives the amidine PisoH (**3H**) in moderate yield. The guanidine systems **4H** or **5H** were prepared by reacting Li[NR_2] (R = cyclohexyl or Pr^i) with the carbodiimide (**57**) at 0 °C in THF. An aqueous work-up yields GisoH (**4H**) and PrisoH (**5H**) in moderate yields (**Scheme 27**).[77, 78]

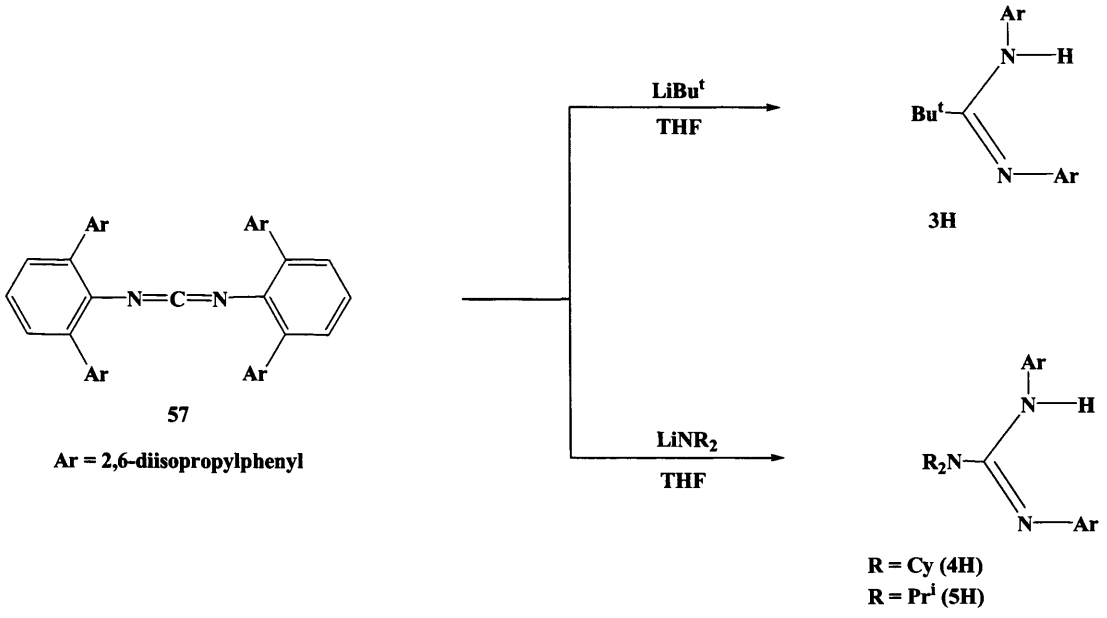

Scheme 27 Preparation of PisoH (**3H**), GisoH (**4H**), and PrisoH (**5H**)

2.1.2.1 Metal Co-ordination Chemistry of Bulky Amidinate and Guanidinate Ligands

The general bonding modes for amidinates and guanidinates are displayed in **Figure 6**. The most common co-ordination mode for amidinates and guanidinates are the chelating type **I**, and the bridged co-ordination type **J**, which can be found in transition metal and main group complexes. The rarest co-ordination mode is displayed in **K**. This type can be found with amidinate and guanidinate ligands with very bulky substituents (**Figure 6**).[10]

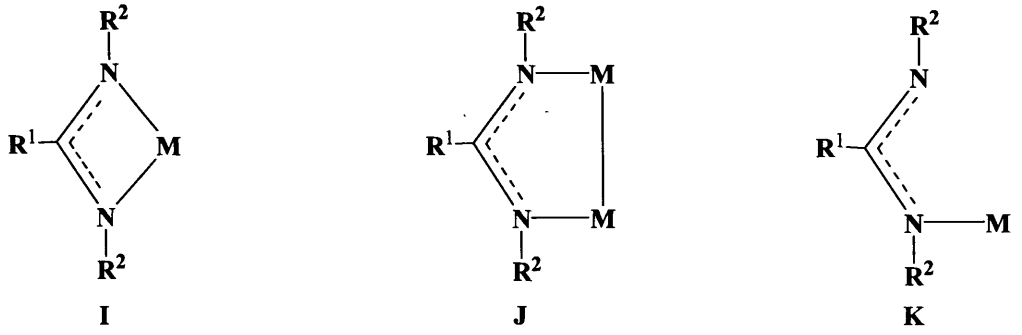

Figure 6 Bonding modes of amidinate and guanidinate ligand systems

Whether amidinates or guanidinates co-ordinate in a chelating (**I**) or a bridged (**J**) mode depends on their substituents.[79] The formation of chelating complexes **I** is favoured by large substituents on the carbon backbone, as they compress the lone pairs of the nitrogen centres. Small substituents often support the bridged co-ordination mode, **K**, which leads to a parallel orientation of the N^- lone pairs. The steric protection of the N-M-N fragment can be achieved by steric substituents on the nitrogen atoms and in this respect, the 2,6-diisopropylphenyl group has been very useful.[80-83] Examples of each of the co-ordination modes will be shown and discussed.

The paramagnetic iron(II) amidinate complexes $[Fe(RN)_2CBu^t]_2$ (R = cyclohexyl or Pr^i) (**59a-b**), were prepared by reacting $[Li\{(RN)_2CBu^t\}]$ (**58a-b**) with $FeCl_2$. The co-ordination geometry around the iron(II) centre is distorted tetrahedral in each case (**Scheme 28**).[84]

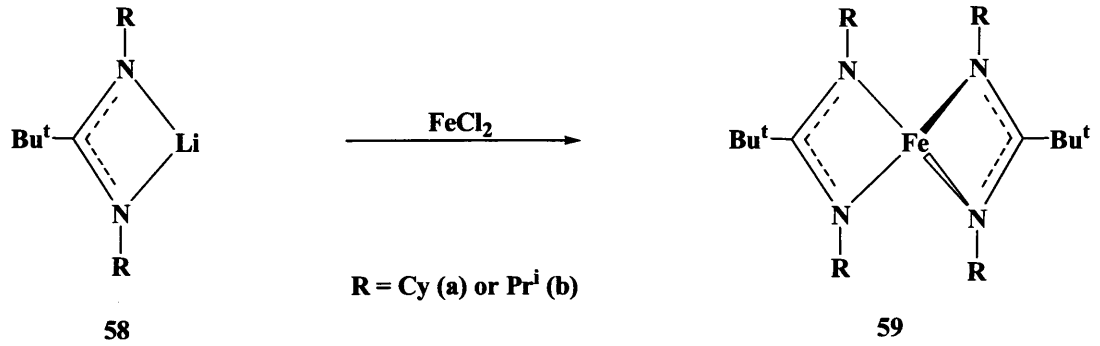

Scheme 28 Preparation of the iron(II) complexes **59a-b**

The iron(II) complexes **59a-b** were reacted with CO to give the diamagnetic Fe(II) dicarbonyls $[Fe^{II}\{(RN)_2CBu^t\}_2(CO)_2]$ (R = cyclohexyl or Pr^i) (**60a-b**) (**Scheme 29**). Compound **60b** has a heavily distorted octahedral geometry with the carbonyls in cis-positions.[84]

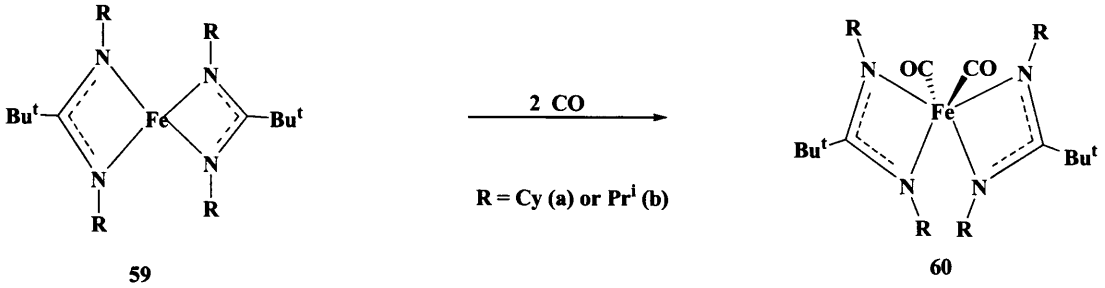

Scheme 29 Reactions of **59a-b** with CO

The reaction of half an equivalent of $FeCl_3$ with a solution of $[Li\{(Pr^iN)_2C(HNPr^i)\}]$ (**61b**) gives the bis(guanidinate) iron(III) chloride complex $[Fe^{III}\{(Pr^iN)_2C(HNPr^i)\}_2(Cl)]$ (**62**) (**Scheme 30**). [85]

A similar reaction of one and a half equivalents of $FeBr_2$ with $[Li\{(CyN)_2C(HNCy)\}]$ (**61a**) gives the complex $[Fe^{II}\{\mu$-

$(CyN)_2C(HNCy)\}\{(CyN)_2C(HNCy)\}]_2$ (**63**) (**Scheme 30**). The magnetic moment for **63** (7.28 μ_B) is consistent with two antiferromagnetically coupled high-spin Fe(II) centres. [85]

The reaction of $[Li\{(CyN)_2C(HNCy)\}]$ (**61a**), with one equivalent of $FeBr_2$, gives complex **64** (**Scheme 30**). Complex **64** is a dinuclear Fe(II) complex where the two metal centres are held in proximity by two bridging monoanionic guanidinate ligands. A terminal bromide completes the pseudotetrahedral co-ordination environment of each iron centre. The magnetic moment of 8.63 μ_B obtained for **64** suggests two independent high-spin Fe(II) centres in this complex.[85]

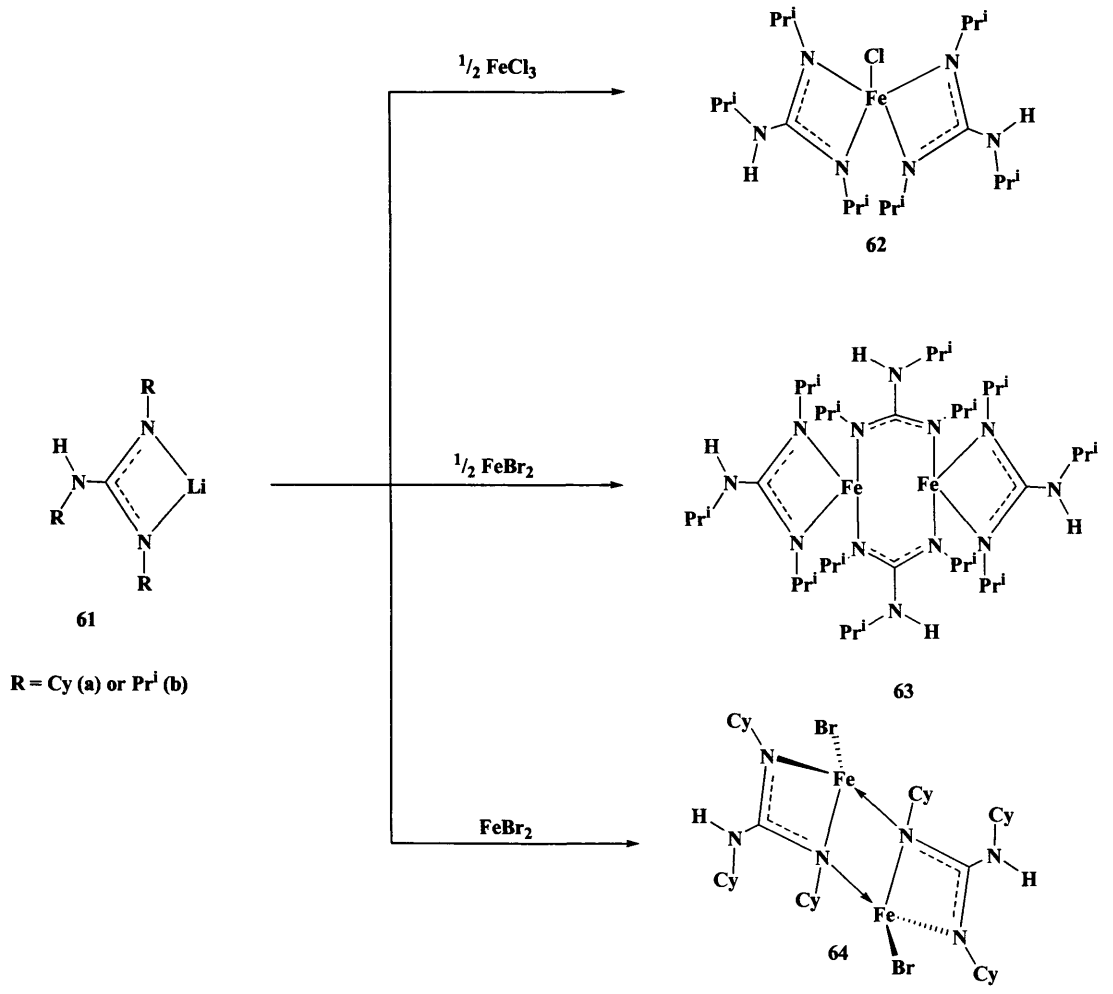

Scheme 30 Reactions of **61a-b** with $FeCl_3$ and $FeBr_2$

A reaction of $CoBr_2$ with two equivalents of the amidinate $[Li\{(CyN)_2C(Fc)\}(Et_2O)]$ (**65**) (Fc = ferrocenyl) in THF gave the trimetallic complex $[Co^{II}\{(NCy)_2(Fc)\}_2]$ (**66**) (**Scheme 31**).[86, 87] Other cobalt(II) amidinate complexes, *e.g.* **68a-e**, were prepared by reacting the lithium salt of the amidinates (**67a-e**) with $CoCl_2$ (**Scheme 31**). Analogous manganese and iron complexes (*cf.* **68a**) and a nickel complex (*cf.* **68e**) have also been reported. [88-90]

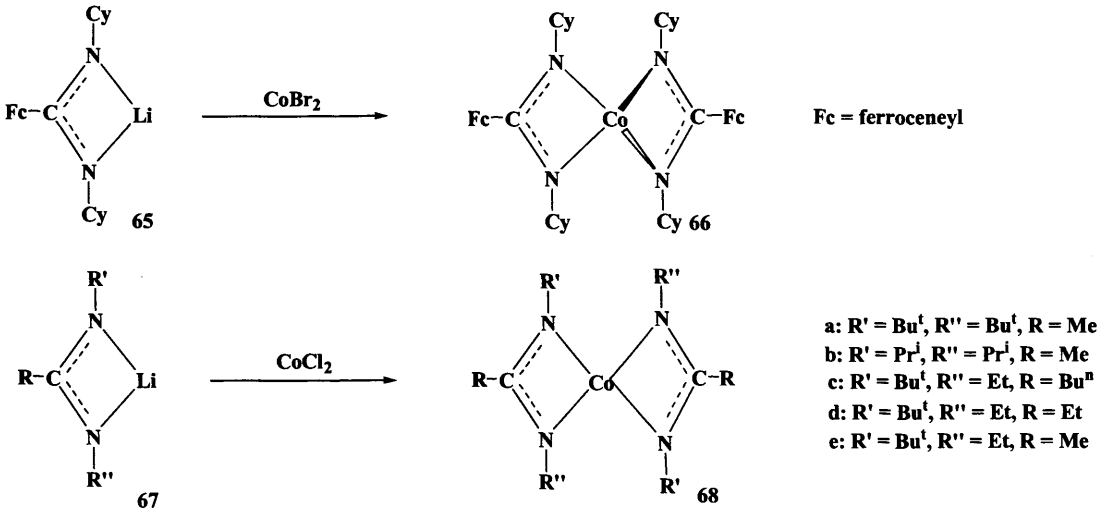

Scheme 31 Preparation of the cobalt(II) complexes **66** and **68**

The bis(benzamidinate) complex $[Ni^{II}\{CPh(NSiMe_3)_2\}_2]$ (**70**) has been prepared by reacting $NiBr_2(DME)$ with $[Li\{CPh(NSiMe_3)_2\}(THF)_2\}]$ (**69**) in diethyl ether (**Scheme 32**).[91]

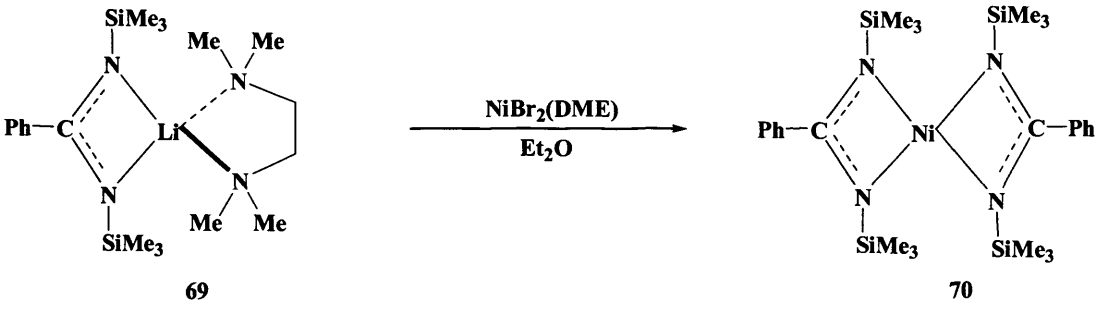

Scheme 32 Preparation of the nickel(II) complex **70**

Two equivalents of the bulky lithium amidinate **71** were found to react readily with $NiCl_2$ in THF at -78 °C to yield the bis-amidinate metal complex **72**. In this complex both halide ligands were substituted by amidinate ligands (**Scheme 33**).[92] It is worth mentioning that the analogous Cr, Mn, Fe, and Co complexes of **72** have also been prepared.[92]

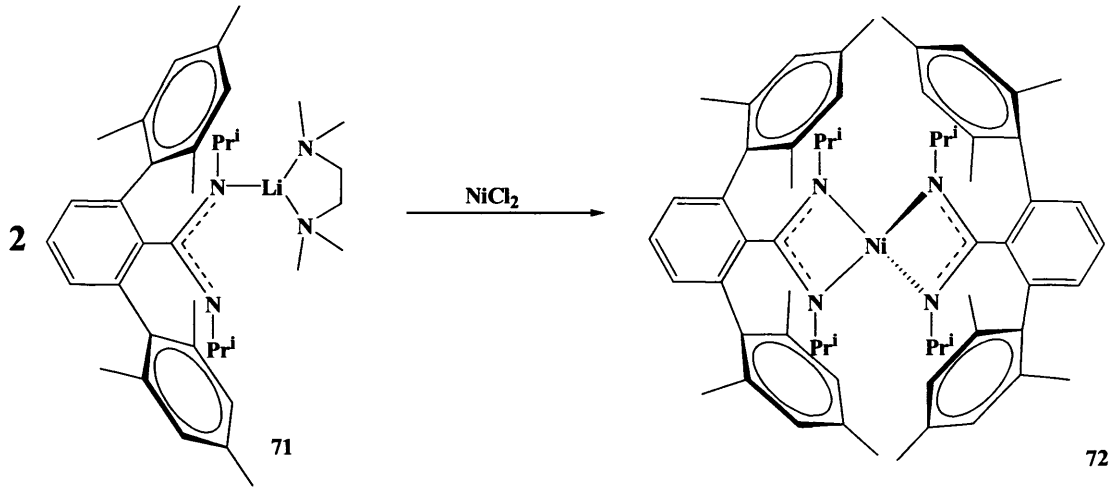

Scheme 33 Preparation of the nickel(II) complex **72**

2.1.2.2 Unusual Low Oxidation State Amidinate and Guanidinate Complexes

Examples of low oxidation state amidinate and guanidinate complexes involving the bulky Piso$^-$, Priso$^-$ or Giso$^-$ ligands can be found in the literature. To date, most of these incorporated main group elements. Examples of these types of complexes are displayed in **Figure 7**.[93-97]

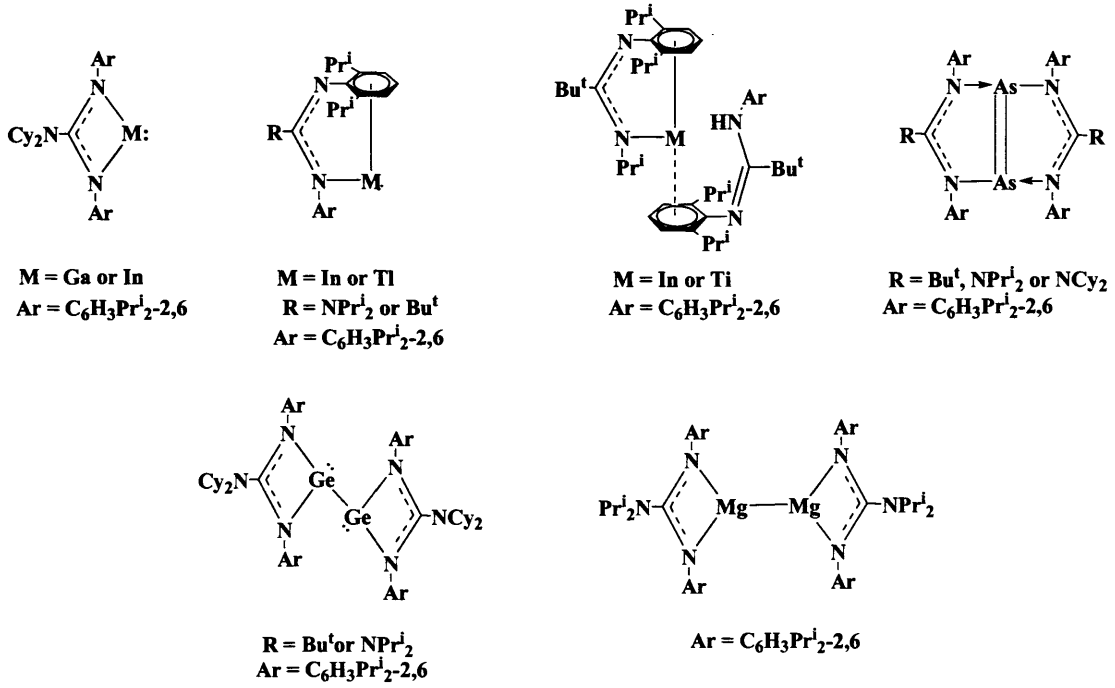

Figure 7 Examples of low oxidation state main group metal guanidinate and amidinate complexes

Examples of bulky guanidinate or amidinate transition metal(I) complexes are very rare, and only chromium,[98] rhodium,[99] copper,[100-102] gold[103-107] and nickel[91] complexes are known in the literature to date. As copper(I) and gold(I) complexes are not unusual, only the chromium(I), rhodium(I) and nickel(I) examples are shown as follows.

Reacently, *Tsai et al.* published the chromium(I) amidinate complex **75**,[98] which was prepared *via* two reductive steps. The first step involves the reduction of

the dichromium complex, **73**,[108] with one and a half equivalents of KC_8 in THF, giving the mixed-valence dichromium complex, **74**, with a Cr-Cr bond order of 4.5. Complex **74** is paramagnetic, with an solid-state magnetic moment of about 2.21 μ_B, and accordingly has one unpaired electron.[98]

Further reducion of **74** in THF with one equivalent KC_8 in the presence of 4,7,13,16,21,24-hexaoxa-1,10-diazabicyclo[8.8.8]hexacosane (crypt[222]), gives the one-electron reduced chromium(I) species **75**, with a Cr-Cr bond order of 5.0 **(Scheme 34)**.[98]

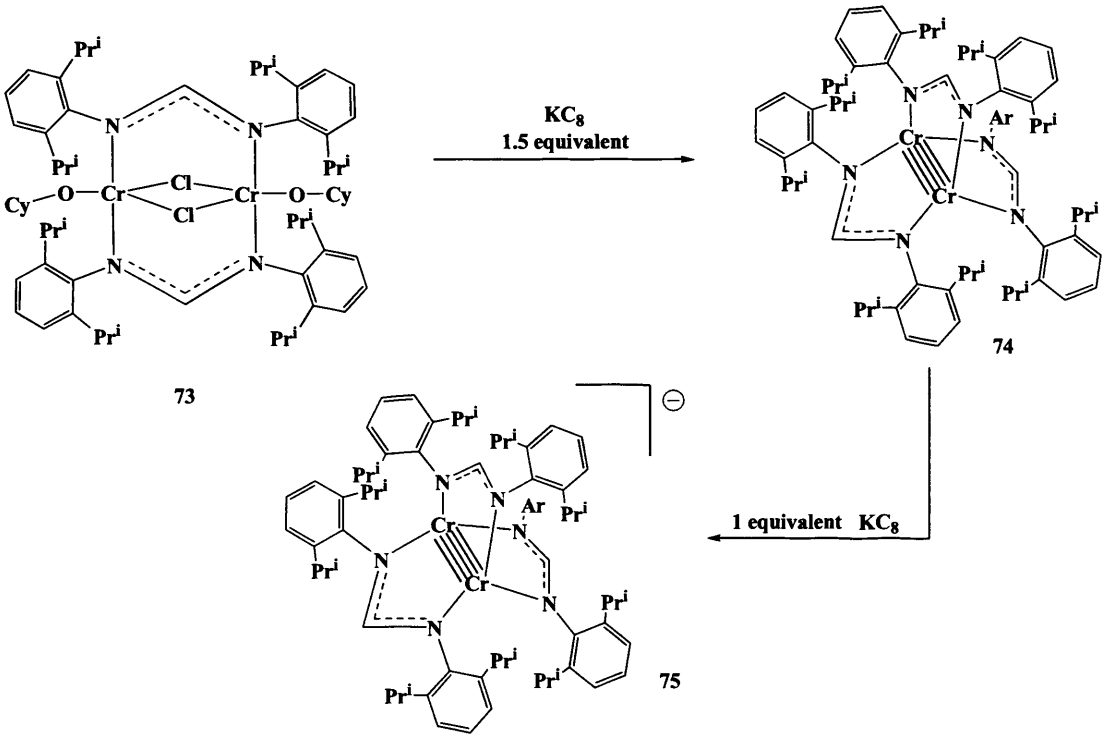

Scheme 34 Preparation of the Cr(I) amidinate complex **75**

The reaction of $[Rh_2(\eta^4\text{-}COD)_2Cl_2]$ with two equivalents of [K(Piso)] (**3K**), [K(Priso)] (**5K**) or [K(Giso)] (**4K**) in toluene or THF leads to the η^5-cyclohexadienyl amidinate and guanidinate complexes, **76a-c (Scheme 35).** Thermal isomerisation of these complexes was achieved by heating toluene solutions at 80 °C for 5 h, yielding the 16-electron N,N-chelated rhodium(I) isomers **77a-c (Scheme**

35).[99] Another rhodium(I) complex *e.g.* $[Rh^{I}\{\kappa^{2}\text{-}N,N'\text{-}(PhN)_2CPh\}(COD)]$,[109] has also been published in the literature.

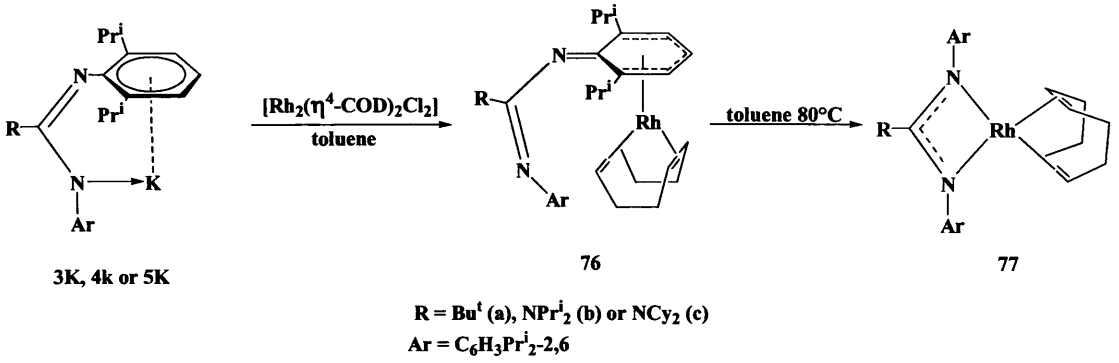

Scheme 35 Preparation of the rhodium(I) amidinate and guanidinate complexes **76a-c** and **77a-c**

The reduction of two equivalents of the nickel(II) complex **78** with MeLi·LiBr in diethylether at -79 °C gives the nickel(I) complex $[Ni^{I}\{CPh(NSiMe)_2\}]_2$ (**79**) (**Scheme 36**). Complex **79** is very temperature sensitive due to the small groups on the nitrogen of the amidinate ligand, and therefore decomposes at room temperature in solution by disproportionation to metallic nickel(0) and the nickel(II) complex $[Ni^{II}\{CPh(NSiMe)_2\}_2]$ (**80**).[91]

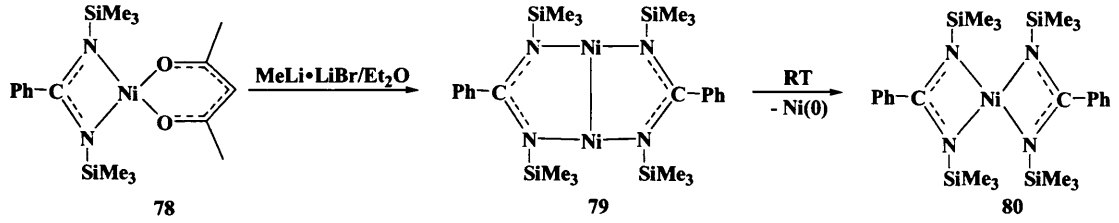

Scheme 36 Preparation of the nickel(I) complex **79**

2.2 Research Proposal

Stable group 5-12 first row β-diketiminate transition metal(I) complexes (e.g. incorporating ^{Me}nacnac$^-$ (**1**) and (^{Bu}nacnac$^-$) (**2**)) have been investigated for several years, and their high reactivity is lending them to an increasing array of synthetic applications which include small molecule activations, reductive couplings, metal imide formations etc.[9, 41, 46, 49, 52, 54, 58, 61]

Amidinate and guanidinate transition metal(I) complex are very rare and only a few examples of first row transition metal(I) complexes, *e.g.* those of chromium,[98] copper[100-102] and nickel[91] are known in the literature to date. Inspired by the comparable abilities of amidinates and guanidinates to stabilize first row transition metal in the +1 oxidation state, an investigation ware carried out of similar and differing bulky amidinate and guanidinates as ligands in complexes with the first row transition metals iron, cobalt, and nickel. As seen before, these ligand systems should have comparable abilities to those of the β-diketiminato ligands to stabilize transition metals in the +1 oxidation. The formed complexes should be highly reactive and have much synthetic potential. With this aim in mind, an investigation were carried out to compare the chemistry of first row transition metal β-diketiminato complexes with that of bulky amidinate and guanidinate complexes.

2.3 Results and Discussion

2.3.1 Preparation and Reactivity of an Iron(I) Amidinate Complex

Of most relevance to this study is the work of *Holland et al.* who have shown that β-diketiminate iron(I) fragments can activate dinitrogen to give the iron(I) complexes $[Fe^{I}(^{L}nacnac)(\mu\text{-}N)]_2$ (L = Me (**31a**) or Bu^t (**31b**)), with partially reduced N-N bonds (**31a**: N-N distance 1.18 Å mean; **31b**: N-N distance 1.182 Å) that are significantly elongated with respect to that in gaseous dinitrogen (1.0976 Å) (**Scheme 37**).[50, 52]

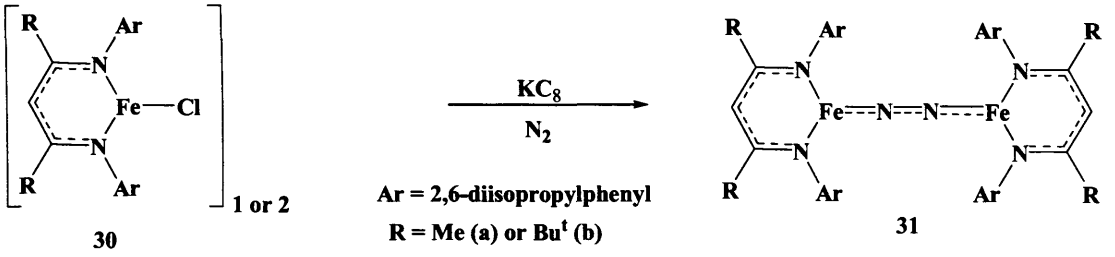

Scheme 37 Preparation of 31a-b

Other structurally characterized dinuclear, β-diketiminate free Fe(I) complexes bearing bridging dinitrogen ligands, *viz.* $[\{Fe^{I}[PhB(CH_2PPr^{i}_2)_3]\}_2]$ (**81**)[110, 111] and $[\{Fe^{I}[N(SiMe_3NBu^{t})(C_2H_4PPr^{i}_2)_2]\}_2(\mu\text{-}N_2)]$ (**82**),[112] which are 4-co-ordinate and display intermediate degrees of dinitrogen reduction, are displayed in **Scheme 38**.

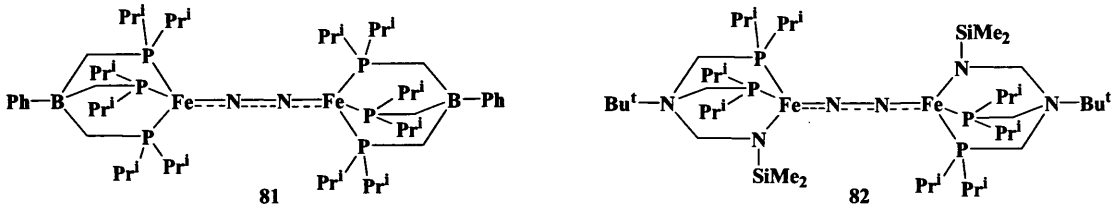

Scheme 38 Fe(I) dinitrogen bridged complexes

The iron(I) β-diketiminato complexes, **31a-b**, have been reacted with a variety of ligands (see **Scheme 17** in 2.1.1.2). These include the reactions of **31a-b** with CO or benzene. The reactions with an excess CO in diethyl ether at room temperature under a dinitrogen atmosphere, yield the monomeric species $[Fe^{I}(^{L}nacnac)(CO)_3]$ (**32a-b**) *via* displacement of the dinitrogen ligand (**Scheme 39**).

The reaction of **31a** with two equivalents of benzene gives the monomeric benzene capped complex $[Fe^{I}(^{Me}nacnac)(\eta^6\text{-}C_6H_6)]$ (**34g**) in which the benzene co-ordinates to the iron centres after displacing the dinitrogen ligand (**Scheme 39**).[52, 53]

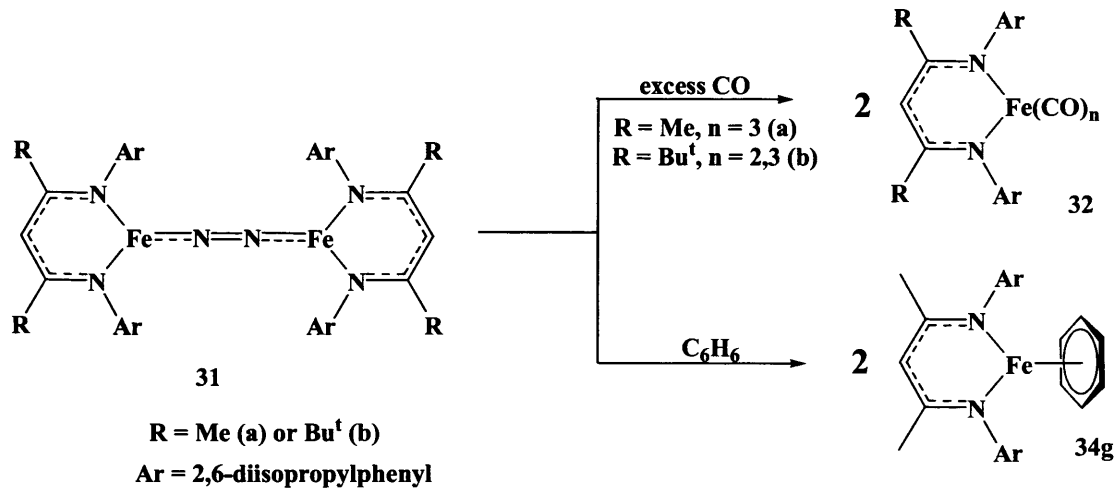

Scheme 39 Reaction of **31a-b** with CO and C_6H_6

An attempt was made by us, using the bulky amidinate ligand Piso$^-$ (**3**)[75] to prepare analogues of these iron(I) β-diketiminate complexes. To this end, the precursor complex $[Fe^{II}(\kappa^2\text{-N,N'-Piso})Br]_2$ (**83**) was readily prepared in good yield by

treating $FeBr_2$ with one equivalent of K[Piso] (**3K**) in THF at low temperature yielding 77% of complex **83** after recrystallising form hexane (**Scheme 40**).

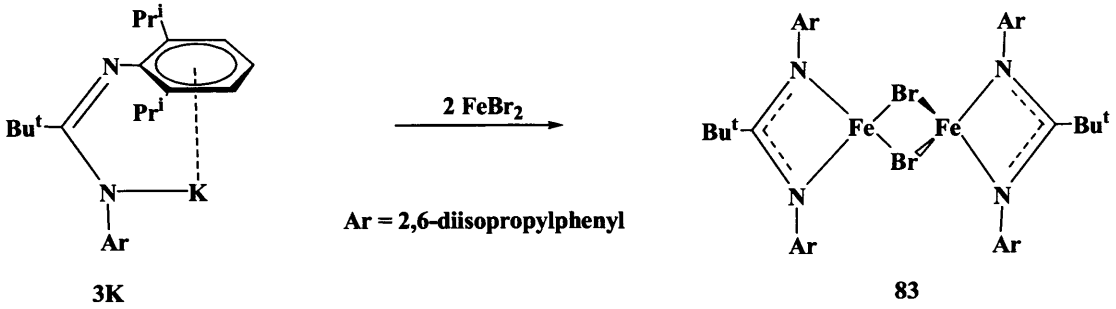

3K **83**

Scheme 40 Preparation of the amidinato iron(II) halide complex **83**

This differs from the closely related, but less hindered, heteroleptic iron(II) amidinate complex, $[Fe^{II}\{(ArN)_2CPh\}Cl_2Li(THF)_3]$ (**84**),[113] which readily redistributes in toluene at room temperature to give the homoleptic complex $[Fe^{II}\{(ArN)_2CPh\}_2]$ (**85**) (**Scheme 41**).

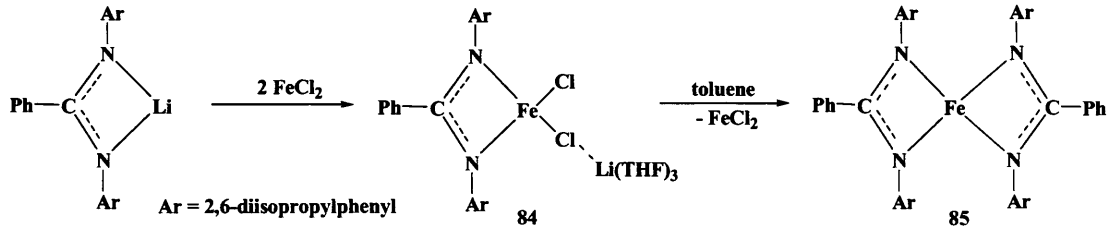

Scheme 41 Preparation of the amidinato iron(II) halide complex **84** and the homoleptic complex **85**

An X-ray crystallographic analysis of **83** revealed it to be a bromide bridged dimer with iron centres co-ordinated by delocalized $Piso^-$ ligands (**Figure 8**). The metal centres have differing geometries that both lie between square planar and tetrahedral. It is of note that the complex is thermally stable in the solid state and in solutions of non-co-ordinating solvents.

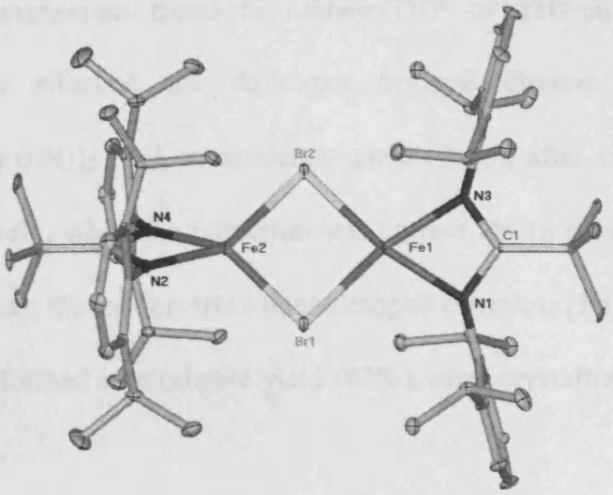

Figure 8 Molecular structure of **83** (25% thermal ellipsoids; hydrogen atoms omitted).

Selected bond lengths (Å) and angles (°): Br(1)-Fe(2) 2.4742(11), Br(1)-Fe(1) 2.4809(11), Fe(1)-N(1) 2.031(5), Fe(1)-Br(2) 2.4809(11), Fe(2)-N(2) 2.025(5), N(1)-C(1) 1.344(7), N(2)-C(18) 1.341(7), Fe(2)-Br(1)-Fe(1) 87.25(4), N(3)-Fe(1)-N(1) 65.5(3), N(3)-Fe(1)-Br(1) 158.89(15), N(1)-Fe(1)-Br(1) 103.25(14), Br(1)-Fe(1)-Br(2) 92.59(5), N(4)-Fe(2)-N(2) 65.4(3), N(2)-Fe(2)-Br(2) 148.36(15), N(2)-Fe(2)-Br(1) 107.95(15), Br(2)-Fe(2)-Br(1) 92.91(5), N(1)-C(1)-N(3) 109.7(7), N(4)-C(18)-N(2) 109.3(7).

Little useful information could be obtained from the ^{1}H NMR spectra of the paramagnetic complex, **83**. Its solution magnetic moment (5.4 μ_B) in benzene-d_6 is consistent with the magnetic moment (5.5 μ_B) proposed for the monomeric complex [Fe^{II}(^{Bu}nacnac)(μ-Cl)] (**30b**), and supports the assumption of an high spin iron(II) complex with a S = 2 ground state.[114] The magnetic moment of the dimeric complex [Fe^{II}(^{Me}nacnac)$_2$(μ-Cl)]$_2$ (**30a**) has not been determined due to its insolubility in non coordinating solvents.[114]

The solution state thermal stability of **86** allowed investigation of its

reduction with magnesium metal in toluene/THF or THF under a dinitrogen atmosphere. This afforded the dnitrogen bridged dimeric iron(I) complex, $[Fe^{I}(N,arene\text{-}Piso)(\mu\text{-}N)]_2$ **(86)**, in moderate yield (71%), after crystallization from hexane. Alternatively, when the reduction was carried out in toluene/THF under an atmosphere of argon, the monomeric toluene capped complex, $[Fe^{I}(\kappa^2\text{-}N,N'\text{-}Piso)(\eta^6\text{-}C_7H_8)]$ **(87)**, was formed in moderate yield (67%), after crystallization from hexane **(Scheme 42)**.

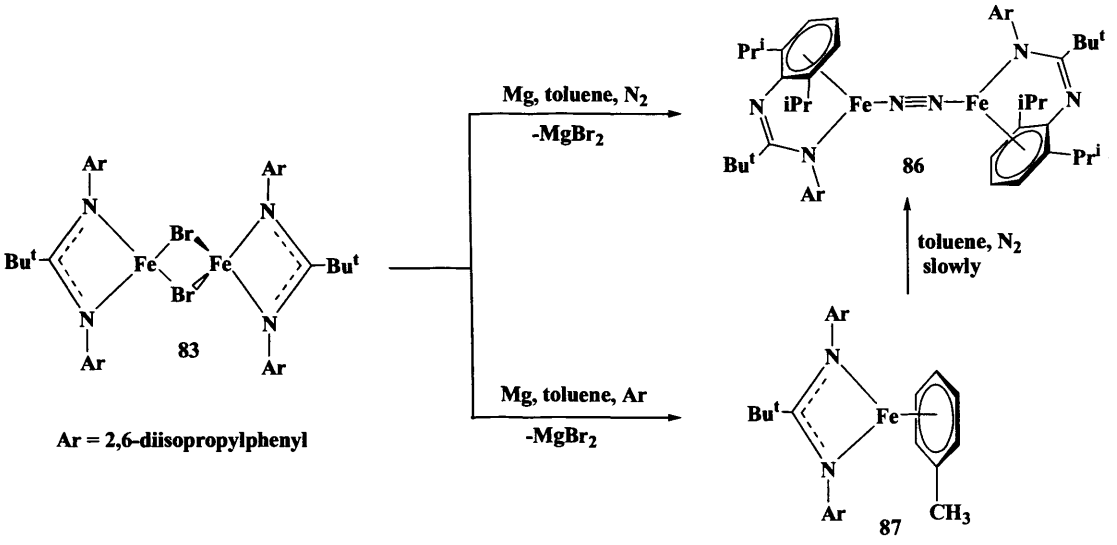

Scheme 42 Reduction of **83** with Mg under dinitrogen or a argon atmospheres

Although the similarities between $[\{Fe^{I}(^{Me}nacnac)\}_2(\eta^6\text{-}C_6H_6)]$ **(34g)** and $[Fe^{I}(\kappa^2\text{-}N,N'\text{-}Piso)(\eta^6\text{-}C_7H_8)]$ **(87)** are obvious, it is interesting to note that **34g** is formed by the irreversible displacement of neutral dinitrogen from $[Fe^{I}(^{Me}nacnac)_2(\mu\text{-}N)]_2$ **(31a)** upon its treatment with benzene.[52] This occurs despite the significant Fe-N multiple bond character implied by marked reduction of the bridging dinitrogen ligand of **31a**. Conversely, treatment of toluene solutions of **87** with dinitrogen slowly led to the displacement of its toluene ligand and the formation of $[Fe^{I}(N,arene\text{-}Piso)(\mu\text{-}N)]_2$ **(86)**, despite the fact that the degree of dinitrogen reduction (and concomitant Fe-N multiple bond character) is much less pronounced

than for the β-diketiminate analogues (*vide infra*). This displacement is irreversible, as evidenced by the fact that **86** can be recrystallized intact from toluene under an argon atmosphere. The differences in the reactivity of **31a** and **86** towards arene solvents most likely result from the ability of the Piso$^-$ ligand (**3**) to vary its co-ordination mode between N,N'- and N,arene-chelating. In the case of **86**, this presumably leads to its Fe(I) centres being more electronically satisfied than those of **31a**.

The molecular structure of $[Fe^{I}(N,arene\text{-}Piso)(\mu\text{-}N)]_2$ (**86**) and $[Fe^{I}(\kappa^2\text{-}N,N'\text{-}Piso)(\eta^6\text{-}C_7H_8)]$ (**87**) was determined by X-ray crystallography and are displayed in **Figure 9** and **Figure 10**. The structure of **87** is closely related to that of $[\{Fe^{I}(^{Me}nacnac)\}_2(\eta^6\text{-}C_6H_6)]$ (**34g**) in that its delocalized amidinate ligand co-ordinates an iron(I) centre in an N,N'-chelating fashion. The distance from the iron centre to the centroid of the η^6-co-ordinated toluene ligand in **87** (1.564 Å) is markedly shorter than the equivalent distance in **34g** (1.63 Å).[4, 81] A reasonable explanation for this observation derives from the smaller cone angle of the Piso$^-$ ligand (*vs.* nacnac$^-$) which leads to a lesser steric interaction with the η^6-arene ligand. In addition, toluene might be expected to be a better donor towards Fe(I) than the less electron rich benzene ligand in **34g**.

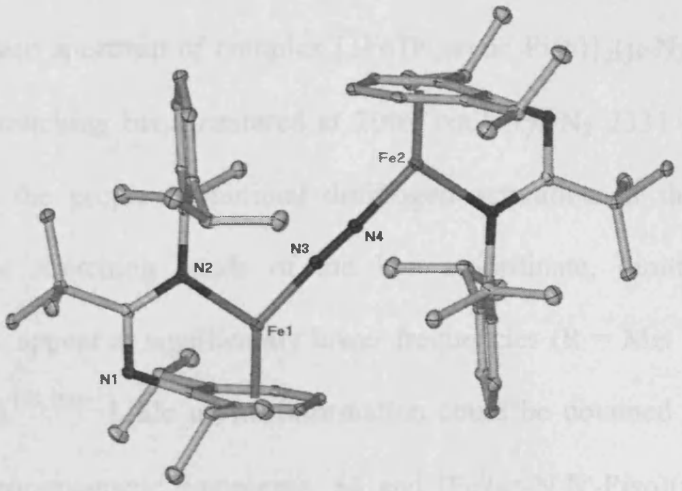

Figure 9 Molecular structure of **86** (25% thermal ellipsoids; hydrogen atoms omitted).

Selected bond lengths (Å) and angles (°): Fe(1)-N(3) 1.834(3), Fe(1)-N(2) 1.945(3), N(3)-N(4) 1.124(6), N(1)-C(1) 1.307(5), N(2)-C(1) 1.373(5), N(1)-C(6) 1.407(5), Fe(1)-centroid 1.560(3), N(3)-Fe(1)-N(2) 100.30(14), N(4)-N(3)-Fe(1) 176.9(4), C(1)-N(2)-Fe(1) 114.4(2), N(1)-C(1)-N(2) 120.0(3), C(1)-N(1)-C(6) 111.4(3).

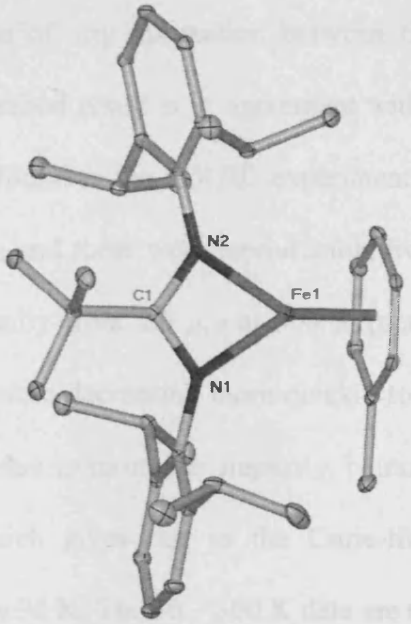

Figure 10 Molecular structure of **87** (25% thermal ellipsoids; hydrogen atoms omitted).

Selected bond lengths (Å) and angles (°): Fe(1)-N(2) 1.969(2), Fe(1)-N(1) 1.9724(18), N(1)-C(1) 1.339(3), N(2)-C(1) 1.344(3), Fe(1)-centroid 1.564(3), N(2)-Fe(1)-N(1) 66.57(8), N(1)-C(1)-N(2) 107.4(2).

The Raman spectrum of complex [{Fe^{I}(N,arene-Piso)}$_2$(μ-N_2)] (**86**) exhibits a strong N-N stretching band centered at 2005 cm^{-1} (*cf.* N_2 2331 cm^{-1}), which is consistent with the proposed minimal dinitrogen activation in that complex. In comparison, the stretching bands of the low co-ordinate, dinitrogen activated complexes, **31a**, appear at significantly lower frequencies (R = Me: 1810 cm^{-1}; R = Bu^t: 1778 cm^{-1}).[50, 52] Little useful information could be obtained from the NMR spectra of the paramagnetic complexes, **86** and [Fe^{I}(κ^2-N,N'-Piso)(η^6-C_7H_8)] (**87**), though the solution magnetic moment (Evan's method) of each complex was determined. The value measured for **87** (2.3 μ_B) is similar to that for **34g** (2.5 μ_B),[50] and both are indicative of low spin Fe(I) systems (S = 1/2 ground state).

The Evans method measurements for the iron(I) complex **86** in benzene-d_6 (2.6 μ_B per dimer) suggests the compound possesses two low-spin (S = 1/2) iron(I) centres, though the nature of any interaction between these centres is yet to be determined. The Evans method result is in agreement with the variable temperature solid state magnetic data found in the SQUID experiment. In **Figure 11** the μ_{eff} vs. temperature data are given and these were reproducible from sample to sample. The μ_{eff} values decrease gradually from 2.5 μ_{eff} at 300 K (per dimer) to ~0.9 μ_{eff}, then plateaus down to 10 K, before decreasing more quickly to reach 0.6 μ_{eff} at 2 K. The behaviour below 30 K is due to monomer impurity, common in dinuclear magnetic susceptibility studies, which gives rise to the Curie-like increase in the molar susceptibility values below 30 K. The 30 – 300 K data are typical of what is expected for weak/medium antiferromagnetic coupling with a maximum in χ_m at ~80 K. The data fitted very well, by Dr Boujemaa Moubaraki, to a Heisenberg model $-2J\mathbf{S}_1.\mathbf{S}_2$ using $S_1 = S_2 = ½$ for a Fe(I) low-spin d^7 (**Figure 11**).

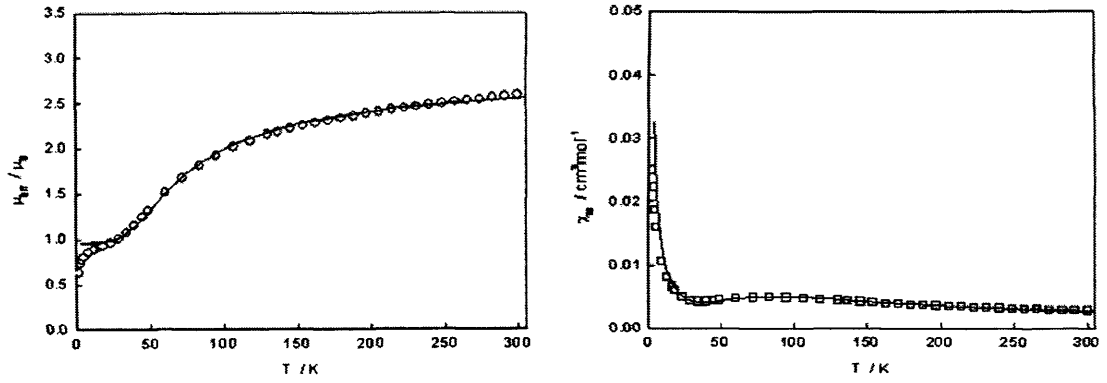

Figure 11 μ_{eff} v. T and χ_m v. T plot of [{Fe^I(N,arene-Piso)}$_2$(μ-N$_2$)] (**86**)

In contrast, the low co-ordinate iron complexes, **31a-b**, have much higher solution magnetic moments (R = Me: 7.9 μ_B; R = Bu^t: 8.4 μ_B[4, 77]). These have been assigned as arising from the ferromagnetic coupling of two high-spin Fe(I) centres (each S = 3/2) leading to an S = 3 ground state.[50] An alternative assignment also proposes an S = 3 ground state, but resulting from strong anti-ferromagnetic coupling of two high-spin Fe(II) centres ($S_A = S_B = 2$; $S_{AB} = 4$) with a bridging triplet N_2^{2-} (S_C = 1) ligand.[115]

There are significant differences between the structures of [{Fe^I(N,arene-Piso)}$_2$(μ-N$_2$)] (**86**) and [Fe^I(κ^2-N,N'-Piso)(η^6-C$_7$H$_8$)] (**87**). Most notably, the Piso$^-$ ligands in the latter act as localized imino-amides which chelate the iron(I) centres in an N,arene-fashion. A similar co-ordination mode has been seen for this ligand in its monomeric indium(I) and thallium(I) complexes (**Figure 12**).[96]

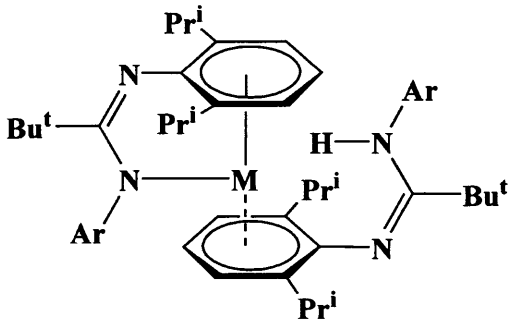

R = In or Tl

Ar = 2,6-diisopropylphenyl

Figure 12 Indium(I) and thallium(I) complexes of the Piso$^-$ ligand

Despite the differences in the structures, the Fe-η^6-arene centroid **87** and Fe-N(amido) distances are similar in both complexes. The co-ordinative flexibility of Piso$^-$ leads to the iron centres of **86** having a higher co-ordination number (C.N. = 5) than they would if the ligand were acting in an N,N'-chelating mode. In contrast, β-diketiminates almost invariably act as N,N'-chelating ligands,[9, 41, 46, 49, 52, 54, 58, 61] which in the case of **31a**, results in 3-co-ordinate iron centre. It has been proposed that there is an inverse correlation between the metal co-ordination number and degree of dinitrogen ligand reduction (i.e. Fe→N(π*) back-bonding) in Fe(N_2) complexes.[52] In line with this proposal is the significant dinitrogen reduction observed for 3-co-ordinate **31a** (R = Me: N-N distance 1.18 Å mean; R = Bu^t: N-N distance 1.182(5) Å)[50, 52] and the apparently minimal reduction of the dinitrogen ligand of 5-co-ordinate **86** (N-N distance 1.124(6) Å). These values can be compared to [Fe{PhB($CH_2PPr^i_2$)$_3$}(μ-N)]$_2$ **(81)** and [Fe{N($SiMe_3NtBu$)($C_2H_4PiPr_2$)$_2$}(μ-N)]$_2$ **(82)** which are 4-co-ordinate and display intermediate degrees of dinitrogen reduction (N-N distances of 1.138(6) Å and 1.166(3) Å respectively).

There are parallels between the reactivities of **31a** and **86**, in that their treatment with excess CO leads to the structurally similar square pyramidal

complexes **32a**,[52] and $[Fe^{I}(\kappa^{2}\text{-N,N'-Priso})(CO)_3]$ (**88**) respectively, *via* displacement of the dinitrogen ligand. In addition, the toluene ligand of **87** is readily displaced by CO to give **88** (**Scheme 43**).

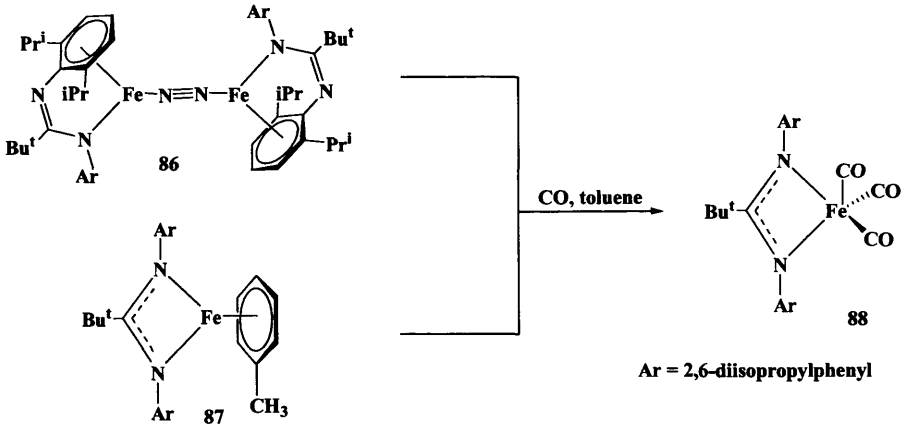

Scheme 43 Reaction of **86** and **87** with CO

Similarities can be found between complexes **31a** and **87** as both are co-ordinated to three CO ligands. However, the reaction of $[Fe^{I}(^{Bu}nacnac)_2(\mu\text{-N})]_2$ (**31b**) with excess CO gives a mixture of the tricarbonyl and the dicarbonyl complexes in which the dicarbonyl complex differs by the loss of the axial CO ligand. The dicarbonyl complex could not be separated to date and therefore no specific data have been determined for it.

The molecular structure of **88** was determined by X-ray crystallography and the molecular structure is depicted **Figure 13**. Compound **88** is closely related to that of $[Fe^{I}(^{Me}nacnac)(CO)_3]$ (**32a**) as both have been prepared from the nitrogen bridged precursors (**31a** and **87**) respectively. The geometry around the iron centre is square pyramidal, where one of the carbonyl groups is in the axial position of the square pyramid. The bond length of the axial Fe-C bond (**32a**: 1.871 **88**: 1.842 Å) is slightly longer than the other two Fe-C bonds (**32a**: 1.795, **88**: 1.785 and 1.797Å) as would

be expected. The IR spectrum of **88** (2050, 1965 cm^{-1}) and **32a** (2042, 1971, 1960 cm^{-1}) in Nujol shown both bands in the expected carbonyl stretching region. In contrast to **32a**, complex **88** shows only two bands in which one (1965 cm^{-1}) is very broad, which is likely due to the overlapping of two bands

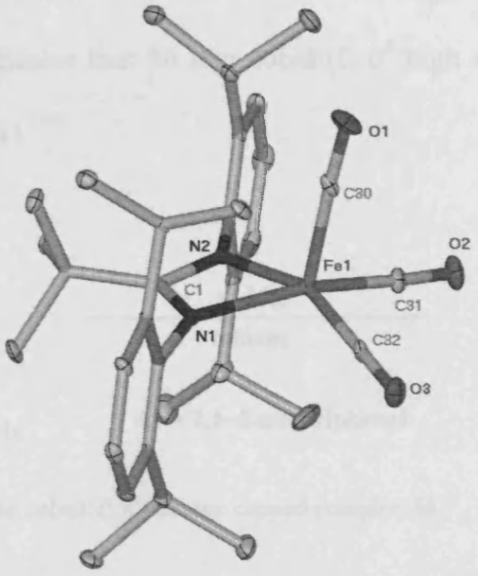

Figure 13 Molecular structure of **88** (25% thermal ellipsoids; hydrogen atoms omitted).

Selected bond lengths (Å) and angles (°): Fe(1)-C(32) 1.785(5), Fe(1)-C(31) 1.797(5), Fe(1)-C(30) 1.842(5), Fe(1)-N(2) 1.975(4), Fe(1)-N(1) 1.976(4), N(1)-C(1) 1.327(6), C(1)-N(2) 1.321(5), C(32)-Fe(1)-C(31) 93.5(2), C(32)-Fe(1)-C(30) 95.9(2), C(31)-Fe(1)-C(30) 93.3(2), C(32)-Fe(1)-N(2) 157.74(18), C(31)-Fe(1)-N(2) 97.95(18), C(30)-Fe(1)-N(2) 102.42(19), C(32)-Fe(1)-N(1) 97.38(18), C(31)-Fe(1)-N(1) 156.93(18), C(30)-Fe(1)-N(1) 105.66(19), N(2)-Fe(1)-N(1) 65.63(14), N(2)-C(1)-N(1) 107.9(4).

Little useful information could be obtained from the NMR spectra of this paramagnetic complex. The magnetic moment for complex **87** (2.4 μ_B) is relatively high compared to complex **32a**[52] (2.0 μ_B). However, both complexes should be seen as d^7 low-spin complexes with an S = 1/2 ground state.

2.3.2 Preparation and Reactivity of Cobalt(I) Amidinate and Guanidinate Complexes

Warren et al. published in 2004 the preparation of $[Co^{I}\{(ArNCMe)_2CH\}(\eta^6\text{-}C_7H_8)]$ (**36**) as discussed in 2.1.1.2 (**Scheme 44**). The magnetic moment of 2.7 μ_B at 293 K in toluene-d_8 indicates that **36** is a cobalt(I) d^8 high spin complex with two unpaired electrons (S = 1).[54]

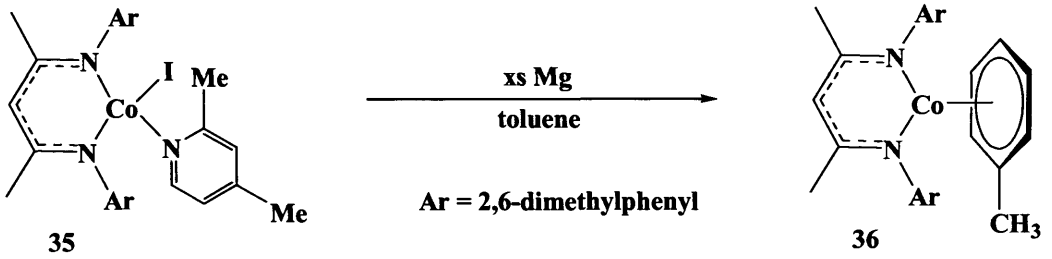

Scheme 44 Preparation of the cobalt(I) η^6-toluene capped complex **36**

It is of note that the bulky amidinate, Piso$^-$ and guanidinate, Giso$^-$ (**4**), Priso$^-$ (**5**), ligand systems should have comparable abilities to stabilize cobalt in the +1 oxidation state. As amidinate and guanidinate cobalt(I) complexes are unknown in the literature to date and the Piso$^-$ ligand (**3**) was successful in stabilising iron in the +1 oxidation state (see 2.3.1), An investigation into the ability of these ligand systems to stabilise cobalt in the +1 oxidation state was investigated.

Amidinato and guanidinato cobalt(II) halides are promising precursors for the target cobalt(I) complexes. The reaction of $CoBr_2$ with one equivalent of the amidinate K[Piso] (**3K**) or the guanidinates K[Giso] (**4K**) and K[Priso] (**5K**) in THF at low temperature, yielded the paramagnetic cobalt(II) complexes $[Co^{II}(\kappa^2\text{-N,N'-Ligand})Br]_2$ (Ligand = Piso$^-$ (**89**), Giso$^-$ (**90**) and Priso$^-$ (**91**)) in moderate yields (48 – 58%) (**Scheme 45**).

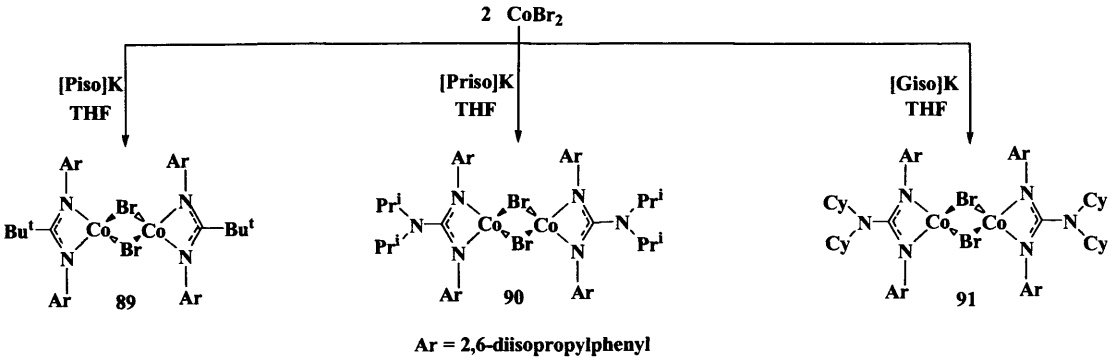

Scheme 45 Preparation of complexes [{Co(κ^2-N,N'-Ligand)Br}$_2$] **89 – 91**

The complexes **89 – 91** were assumed to be paramagnetic, with two cobalt(II) d^7 high spin centres and six unpaired electrons (S = 3). The magnetic moment found for the dimeic complex **90** (3.4 μ_B), however, is quite low compared to the monomeric cobalt(II) complex **35** (3.6 μ_B). Therefore complex **90** could be considered as containing two low spin d^7 cobalt(II) centers (S = 1 per dimer) with spin-orbit coupling leading to the higher expected μ_{eff} value. Alternatively it could posses two high spin d^7 cobalt(II) centres (S = 3 per dimer) that are antiferromagnetically coupled. Further magnetic magnetically experiments (SQUID) will resolve this issue.

The solution state thermal stability of **89 – 91** allowed us to investigate their reduction with potassium or magnesium metal in toluene, toluene/THF or cyclohexane under a dinitrogen atmosphere. The reduction of complexes **89 – 91** with magnesium or potassium in toluene leads to the paramagnetic cobalt(I) η^6-toluene capped complexes [$Co^I(\kappa^2$-N,N'-Ligand)(η^6-C_7H_8)] (Ligand = Piso$^-$ (**92**), Priso$^-$ (**93**), Giso$^-$ (**94**)) after crystallisation from hexane in 70 – 85% yields (**Scheme 46**).

Alternatively, the reduction of **89** and **91** with potassium in cyclohexane gives the bridged solvent free complexes [$Co^I(\kappa^2$-N,N'-Ligand)]$_2$ (Ligand = Piso$^-$

(**95**), Giso$^-$ (**96**)) after crystallisation from cyclohexane in 52 – 57% yields (**Scheme 46**).

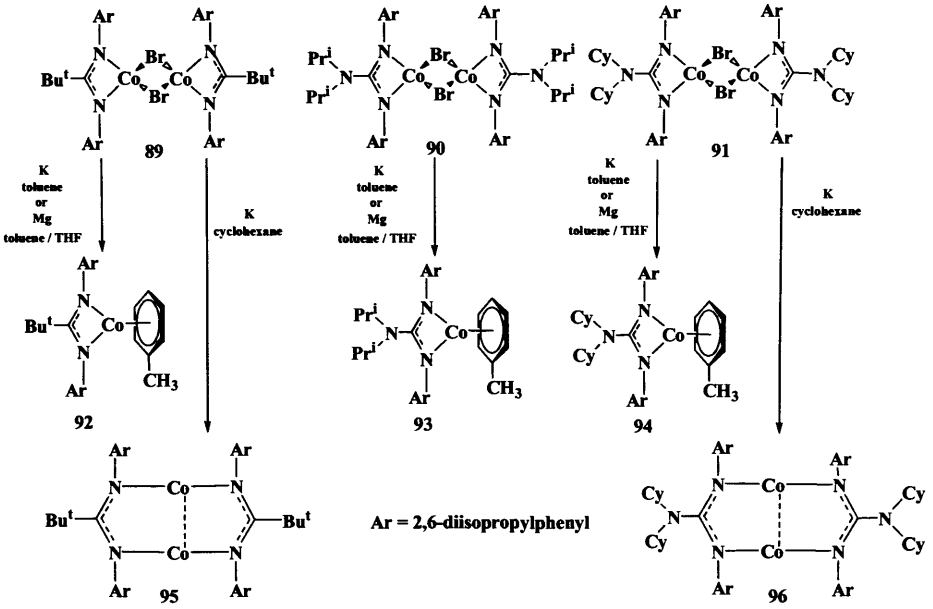

Scheme 46 Preparation of the cobalt(I) amidinate and guanidinate complexes **92** – **96**

Complexes **92** – **94** are the analogues of complex $[Co^{I}\{(ArNCMe)_2CH\}(\eta^6\text{-}C_7H_8)]$ (**36**) as all complexes show a η^6-co-ordinated toluene ligand and a trigonal planar cobalt centre.

The bridged co-ordination mode found in the dimeric complexes $[Co(\kappa^2\text{-}N,N'\text{-Ligand})]_2$ (**95** and **96**) has not been observed for transition metal β-diketiminato complexes. This can likely be explained by the Ar groups (Ar = 2,6-diisopropylphenyl) in β-diketiminato complexes enforcing N,N'-chelation of the metal centre in those cases.

It is of note that the reduction of complex $[Fe^{II}(\kappa^2\text{-}N,N'\text{-Piso})(\mu\text{-Br})]_2$ (**83**) under a dinitrogen atmosphere gives the nitrogen bridged complex $[Fe^{I}(N,\text{arene-Piso})(\mu\text{-}N)]_2$ (**86**) (see 2.3.1). However, no evidence for any dinitrogen bridged complexes could be found by the reduction of the cobalt(II) complexes **89** – **91** under a dinitrogen atmosphere.

The molecular structure of **92** – **94** was determined by X-ray crystallography and as there are no significant geometric differences between them, only the structure of complex **93** is shown in **Figure 14**. The trigonal planar cobalt centre is co-ordinated to a delocalised Priso$^-$ ligand and is η^6-co-ordinated to a toluene ligand. The distances from the cobalt centre to the centroid of the η^6-co-ordinated toluene ligand of **92** (1.695 Å), **93** (1.662 Å) and **94** (1.668 Å) are markedly shorter compared to the distance in the analogous complex $[Co^I\{(ArNCMe)_2CH\}(\eta^6\text{-}C_7H_8)]$ (**36**) (1.747 Å). A reasonable explanation for this observation derives from the smaller cone angle of the amidinate and guanidinate ligands (*vs.* nacnac$^-$) which leads to less steric interaction with the η^6-arene ligand.

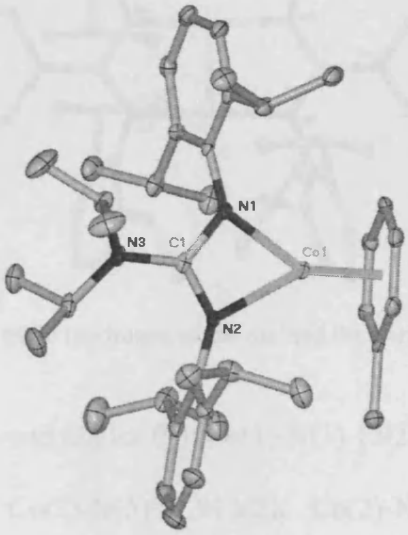

Figure 14 Molecular structure of **93** (hydrogen atoms omitted for clarity; ellipsoids shown at the 25% probability level).

Selected bond lengths (Å) and angles (°): Co(1)-N(1) 2.058(4), Co(1)-N(2) 2.102(5), Co(1)-centroid 1.659(4), N(1)-C(8) 1.351(7), N(2)-C(8) 1.336(7), N(3)-C(36) 1.477(8), N(3)-C(8) 1.406(7), N(1)-Co(1)-N(2) 64.40(18), C(8)-N(1)-Co(1) 92.9(3), C(8)-N(2)-Co(1) 91.4(3), N(2)-C(8)-N(1) 111.2(5), N(2)-C(8)-N(3) 126.0(5), N(1)-C(8)-N(3) 122.8(5), N(3)-C(33)-C(35) 115.3(5).

The molecular structure of **95** – **96** was determined by X-ray crystallography and as there are no significant geometric differences between them, only the structure of complex **96** is shown in **Figure 15**. The cobalt centres are trigonal planar with bond angles of N-Co-Co 91.33° and N-Co-N 175.49°. The Co-N bonds (1.923, 1.913 Å) are significantly shorter then those in the chelated complexes **92** (2.057, 2.089 Å), **93** (2.058, 2.102 Å) and **94** (2.086, 2.046 Å). The Co-Co distance in **96** (2.135 Å) is the shortest yet reported.

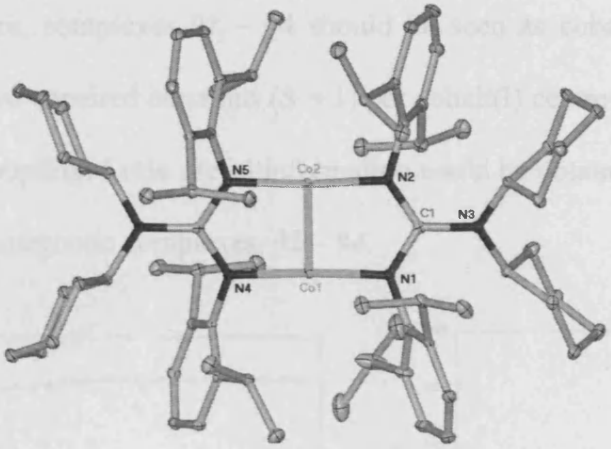

Figure 15 Molecular structure of **96** (hydrogen atoms omitted for clarity; ellipsoids shown at the 25% probability level).

Selected bond lengths (Å) and angles (°): Co(1)-N(1) 1.923(2), Co(1)-N(4) 1.929(2), Co(1)-Co(2) 2.1345(7), Co(2)-N(5) 1.913(2), Co(2)-N(2) 1.915(2), N(1)-C(1) 1.359(3), N(2)-C(1) 1.352(3), N(1)-Co(1)-N(4) 176.55(8), N(1)-Co(1)-Co(2) 91.33(6), N(4)-Co(1)-Co(2) 92.01(6), N(5)-Co(2)-N(2) 175.49(9), N(2)-C(1)-N(1) 113.7(2), N(2)-C(1)-N(3) 123.7(2), N(1)-C(1)-N(3) 122.5(2),

The solution magnetic moment (Evan's method) of complexes [$Co^{I}(\kappa^2$-N,N'-Priso)(η^6-C_7H_8)] (**93**) and [$Co^{I}(\kappa^2$-N,N'-Priso)(η^6-C_7H_8)] (**94**) were determined. The values measured for **93** (3.17 μ_B) and **94** (3.09 μ_B) in benzene-d_6 are relatively high

compared to that found in complex **36** (2.7 μ_B). The variable temperature solid state magnetic experiment (SQUID), which was carried out for complex **94**, supports those results (see **Figure 16**). The μ_{eff} values remain essentially constant at ~3.4 μ_B between 300 and 65 K, which is higher compared to the solution magnetic moment found for **93** (3.17 μ_B) and **94** (3.09 μ_B). The χ_M^{-1} vs T plot obeyed close to Curie behaviour, $\chi_M = C/(T - \theta)$, with the Weiss constant θ being -0.08 K and the Curie constant, 0.13 cm^3 mol^{-1} K, indicative of paramagnetic behaviour arising from thermal population of an isolated $S = 1$ state with two unpaired electrons. The rapid decrease below 50 K is indicative of second order spin-orbit coupling in this complex. Therefore, complexes **92** – **94** should be seen as cobalt(I) d^8 high spin complexes with two unpaired electrons (S = 1) per cobalt(I) centre with some second order spin-orbit coupling. Little useful information could be obtained from the NMR spectra of the paramagnetic complexes, **92** – **94**.

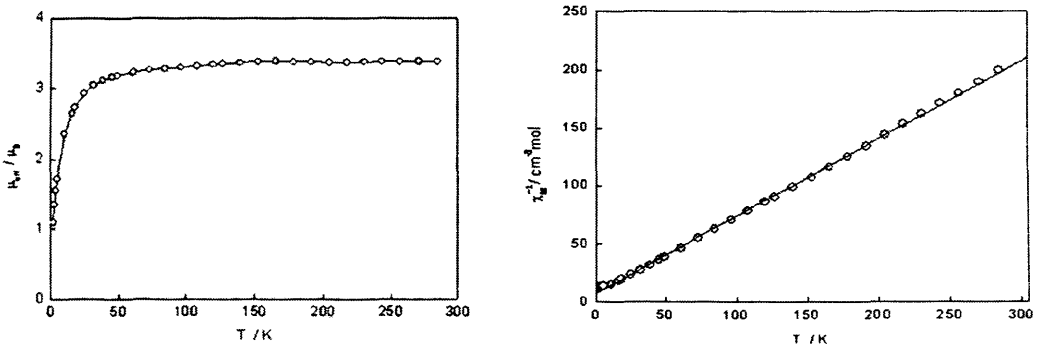

Figure 16 μ_{eff} v. T and χ^{-1}_m v. T plot of [$Co^I(\kappa^2$-N,N'-Priso)(η^6-C_7H_8)] (**94**)

The solution magnetic moment (Evan's method) of complexes [$Co^I(\kappa^2$-N,N'-Piso)]$_2$ (**95**) and [$Co^I(\kappa^2$-N,N'-Giso)]$_2$ (**96**) were determined. The observed magnetic moments found for [$Co^I(\kappa^2$-N,N'-Piso)]$_2$ (**95**), (5.35 μ_B in cyclohexane-d_{12} per dimer) and [$Co^I(\kappa^2$-N,N'-Giso)]$_2$ (**96**), (5.10 μ_B in benzene-d_6 per dimer) are consistent with four unpaired electrons with little interaction between the cobalt centres. The

variable temperature solid state magnetic experiment (SQUID), which was carried out for complex **95**, supports those results. The effective magnetic moment, μ_{eff} of complex **95**, as a function of temperature, is shown in **Figure 17** as is the corresponding χ_m^{-1} vs. temperature plot. The μ_{eff} values remain essentially constant at 5.25 μ_B at 300 K, decreasing a little down to 5.15 μ_B at 50 K, then rapidly to reach 4.15 μ_B at 2 K. The rapid decrease below 50 K is indicative of either zero field splitting of the spin ground state, that arises from second order spin-orbit coupling effects, or weak dimer-dimer antiferromagnetic coupling effects, although the lack of any such pathways from the packing diagram would suggest that the latter is not likely. Therefore, the complexes **95** and **96** should be seen as high spin cobalt d^8 centres with four unpaired electrons per dimer (S = 2).

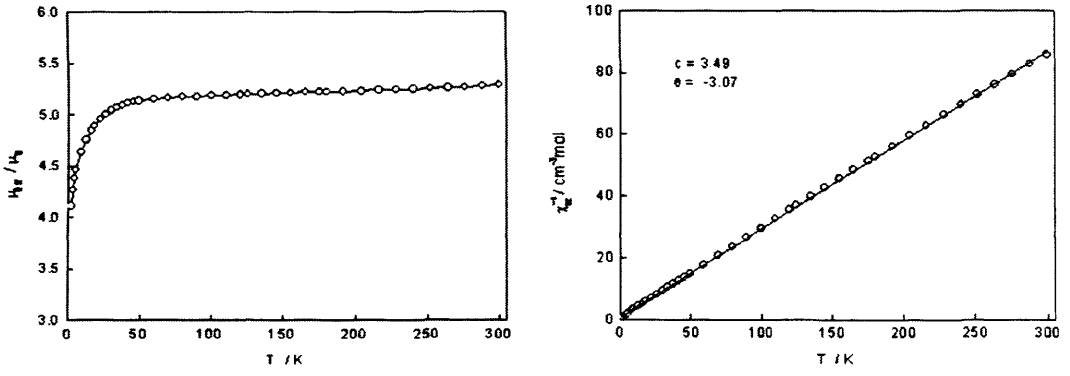

Figure 17 μ_{eff} v. T and χ^{-1}_m v. T plots of [Co(κ²-N,N'-Piso)₂] (**95**)

The very short Co-Co bond distance of complex **95** (2.1345 Å) however, let us originally assume a Co-Co interaction. The Raman spectrum of complex **95** gave credence to this as a band was observed at 277 cm^{-1} (*cf.* $Co_2(CO)_8$ = 229 cm^{-1}, $Co_4(CO)_{12}$ = 228 cm^{-1}).[116, 117] It is worth mentioning that the Co-Co distances observed in complexes **95** (2.1404 Å) and **96** (2.135 Å) are to date the shortest found in the literature. Little useful information could be obtained from the NMR spectra of the paramagnetic complexes, **95** – **96**.

As discussed in 2.1.1.2, $[Co^{I}\{(ArNCMe)_2CH\}(\eta^6\text{-}C_7H_8)]$ (**36**) was reacted with 1-adamanthyl-azide, giving the monomeric complex $[Co^{III}\{(ArNCMe)_2CH\}(NAd)]$ (**39**). (**Scheme 47**).[54]

Different products were found by reacting TMS-azide with $[Fe^{II}(^{Bu}nacnac)(H)]_2$ (**97**). That is, the reaction of two equivalents of TMS-azide with **97** in diethylether gave the paramagnetic dimeric complex $[Fe^{II}(^{Bu}nacnac)(\mu\text{-}N\text{-}N'\text{-}N_3)]_2$ (**98**), in which two $[Fe^{II}(^{Bu}nacnac)]$ fragments are bridged by two μ-N-N'-N_3 ligands ($\mu_{eff} = 4.1\ \mu_B$) (**Scheme 47**). [118]

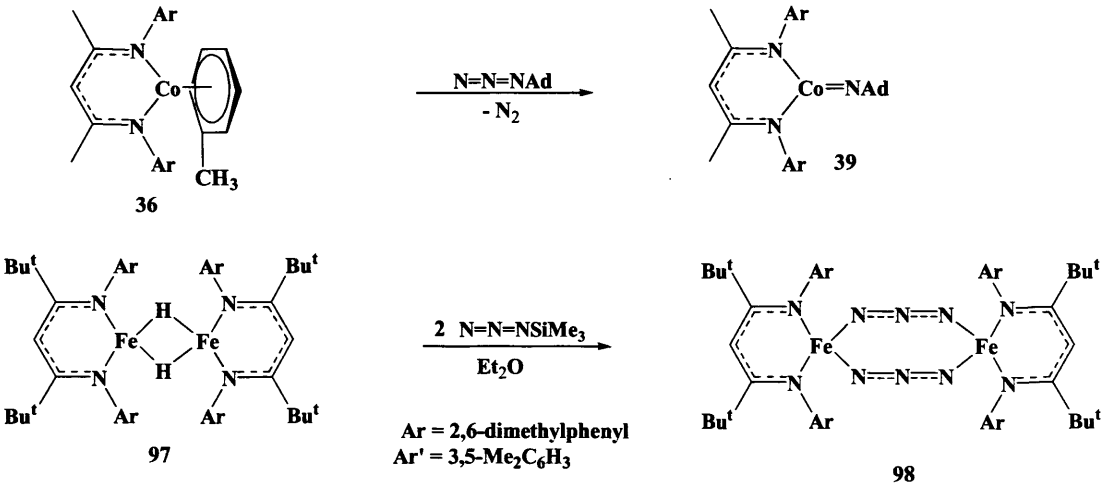

Scheme 47 Preparation of the azide complexes **39** and **98**

In contrast, the reaction of complexes $[Co^{I}(\kappa^2\text{-}N,N'\text{-}Priso)(\eta^6\text{-}C_7H_8)]$ (**93**) and $[Co^{I}(\kappa^2\text{-}N,N'\text{-}Giso)(\eta^6\text{-}C_7H_8)]$ (**94**) with TMS-azide and 1-adamantyl-azide for purposes of comparison were carried out. The reaction of two equivalents of TMS-azide with **93** in hexane gives the μ-N-N_3 dimeric complex $[Co^{II}(\kappa^2\text{-}N,N'\text{-}Piso)(\mu\text{-}N\text{-}N_3)]_2$ (**99**), bridged by two azide ligands, by loss of the TMS groups (**Scheme 48**).

The reaction of one equivalent of 1-adamantyl-azide with **94** in hexane gives the monomeric complex $[Co^{III}(\kappa^2\text{-}N,N'\text{-}Piso)(NAd)]$ (**100**) in which N-adamantyl fragment coordinates the cobalt centre after liberation of dinitrogen (**Scheme 48**).

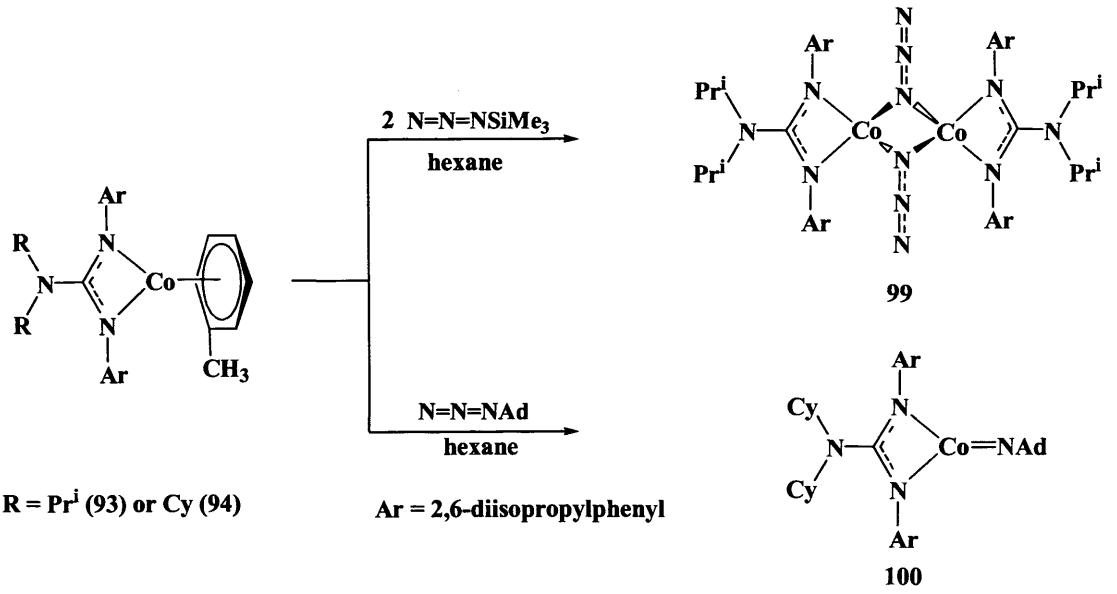

Scheme 48 Reaction of **93** or **94** with TMS- and 1-adamantyl-Azide

No β-diketiminato analogues of the μ-N-N_3 bridged dimeric complex $[Co^{II}(\kappa^2\text{-N,N'-Piso})(\mu\text{-N-N}_3)]_2$ (**99**) can be found in the literature to date. The closest similarity can be seen with the dimeric complex $[Fe^{II}(^{Bu}nacnac)(\mu\text{-N-N'-N}_3)]_2$ (**98**), showing a μ-N-N'-N_3 (end-to-end) coordination mode. In both cases the dimerization has taken place by the reaction of the toluene capped complexes, **36** or **93**, with two equivalents of TMS-azide, *via* loss of TMS groups. Of note is bis(pentafluorophenyl)boron azide[119] with an analogous μ-N-N_3 bridge, which was prepared in 2000.

A β-diketiminato complex similar to **100** is $[Co^{III}\{(ArNCMe)_2CH\}(NAd)]$ (**39**). In both complexes (**39** and **100**), the metal centres are coordinated to an N-adamantyl fragment after liberation of dinitrogen. Due to steric reasons, dimerization has not taken place in both complexes.

The molecular structure of complex $[Co^{II}(\kappa^2\text{-N,N'-Piso})(\mu\text{-N-N}_3)]_2$ (**99**) was determined by X-ray crystallography and is shown in **Figure 18**. Its cobalt centres have tetrahedral geometries. The Co-N bond distances in **99** (1.993, 1.994 Å) are

similar to those found in bis(pentafluorophenyl)boron azide (1.241, 1.113 Å). As complex **99** is very temperature sensitive above -30 °C in solution, no other data have been recorded for it.

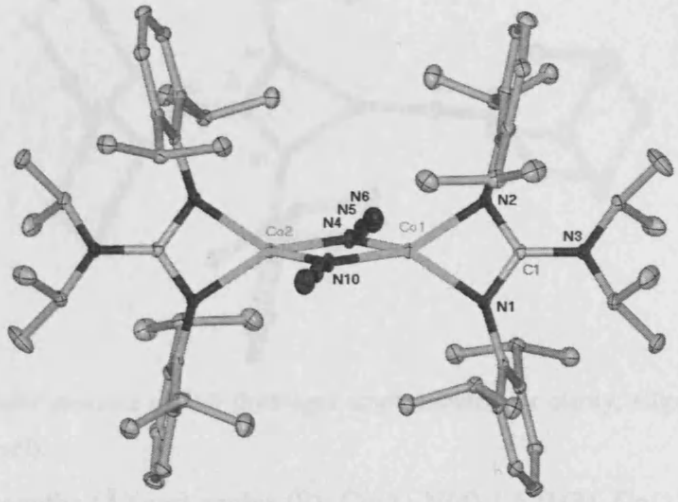

Figure 18 Molecular structure of **99** (hydrogen atoms omitted for clarity; ellipsoids shown at the 25% probability level).

Selected bond lengths (Å) and angles (°): Co(1)-N(2) 1.991(3), Co(1)-N(1) 1.994(3), Co(1)-N(10) 2.010(3), N(4)-Co(2) 2.007(3), N(4)-N(5) 1.217(4), N(5)-N(6) 1.153(4), N(2)-Co(1)-N(1) 67.25(11), N(2)-Co(1)-N(10) 139.05(12), N(1)-Co(1)-N(10) 125.20(11), N(2)-Co(1)-N(4) 121.36(11), (1)-Co(1)-N(4) 133.62(11), N(10)-Co(1)-N(4) 80.27(12).

The molecular structure of complex [$Co^{II}(\kappa^2$-N,N'-Piso)(NAd)] (**100**) was determined by X-ray crystallography and is shown in **Figure 19**. Complex **100** is analogous to [Co^{III}{$(ArNCMe)_2CH$}(NAd)] (**39**). The cobalt centres in **100** and **39** are distorted trigonal planar. The Co-N bond length in **100** (1.621 Å) is slightly shorter compared to that in complex **39** (1.624 Å) and the Co-N-C angle (172.1°) is closer to 180° than in **39** (161.5°). As complex **100** is very temperature unstable, above -30 °C in

solution, the only characterising data for this coumpound is its molecular structure determind by X-ray crystallography.

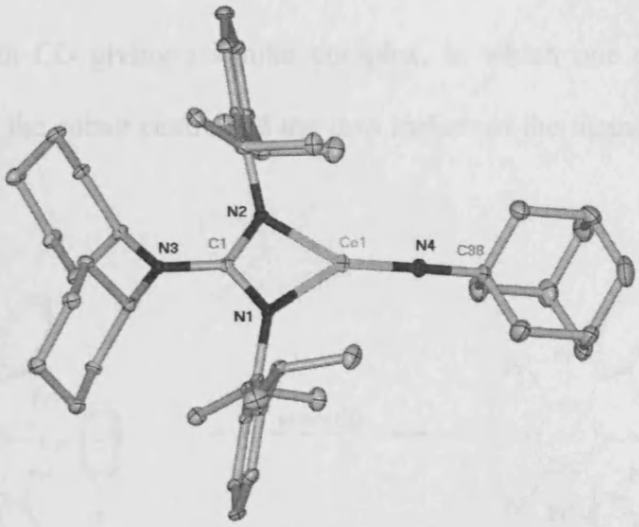

Figure 19 Molecular structure of **100** (hydrogen atoms omitted for clarity; ellipsoids shown at the 25% probability level).

Selected bond lengths (Å) and angles (°): Co(1)-N(4) 1.621(3), Co(1)-N(1) 1.942(3), Co(1)-N(2) 1.947(3), N(4)-C(38) 1.434(5), N(4)-Co(1)-N(1) 145.33(15), N(4)-Co(1)-N(2) 144.69(16), N(1)-Co(1)-N(2) 68.52(12), C(38)-N(4)-Co(1) 172.1(3).

The reaction of an excess of CO with $[Co^{I}(\kappa^{2}\text{-N,N'-Piso})]_2$ (**96**) in toluene at -90 °C gives complex **101** (**Scheme 49**).

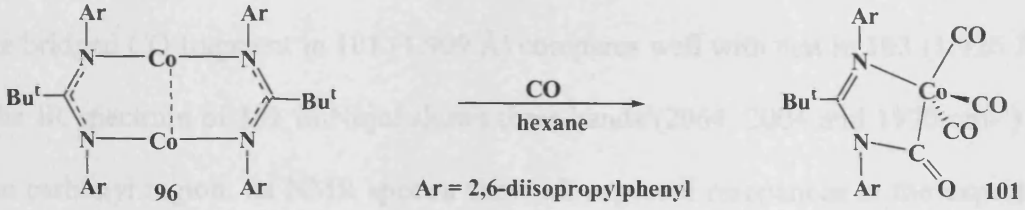

Scheme 49 Reaction of $[Co(\kappa^{2}\text{-N,N'-Piso})_2]$ (**96**) with CO

In contrast to complex **101**, no analogous β-diketiminato complex can be found in the literature. Complex **101** is a diamagnetic 18 electron species in which

three CO ligands are co-ordinated to the cobalt centre and one CO has inserted into a N-Co bond of the precursor **96**.

Recently *Power et al.* published the preparation of complex **103**,[120] by reacting **102** with CO giving a similar complex, in which one carbonyl ligand is bridged between the cobalt centre and the *ipso* carbon of the ligand system (**Scheme 50**).

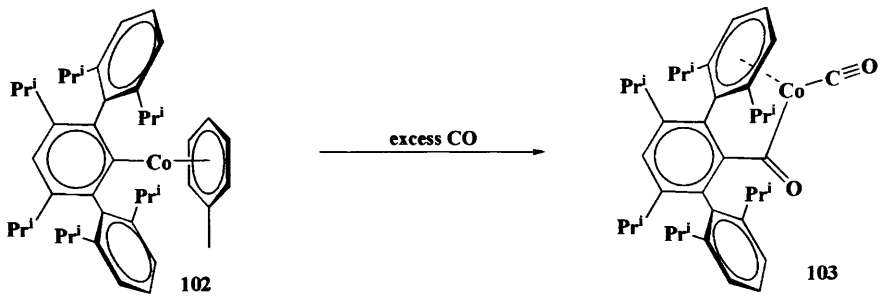

Scheme 50 Preparation of complex **103**

The molecular structure of **101** was determined by X-ray crystallography and its molecular structure is displayed in **Figure 20.** The geometry around the metal centre is square pyramidal with three CO ligands co-ordinated to the cobalt centre and one bridging between the nitrogen of the ligand and the cobalt centre. The Co-C bond lengths to the terminal CO ligands in **101** (1.773, 1.788 and 1.823 Å) are similar to that found in **103** (1.739 Å). The significantly longer Co-C bond length to the bridged CO fragment in **101** (1.909 Å) compares well with that in **103** (1.926 Å). The IR spectrum of **101** in Nujol shows three bands (2064, 2004 and 1970 cm^{-1}) in the carbonyl region. Its NMR spectra show all expected resonances in the expected regions, except the CO resonances in the $^{13}C\{^1H\}$ NMR spectrum, which are not observed.

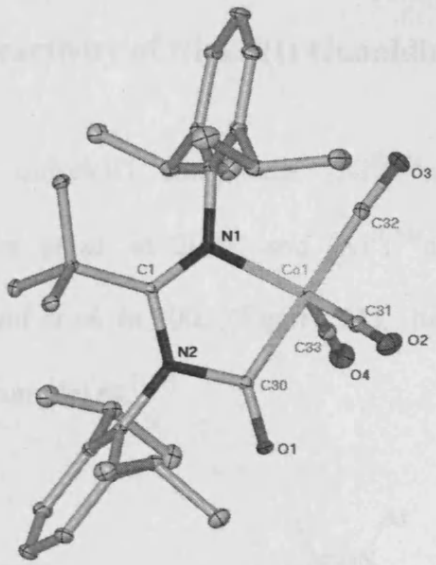

Figure 20 Molecular structure of **101** (hydrogen atoms omitted for clarity; ellipsoids shown at the 25% probability level).

Selected bond lengths (Å) and angles (°): Co(1)-C(33) 1.7733(16), Co(1)-C(31) 1.7885(16), Co(1)-C(32) 1.8233(16), Co(1)-C(30) 1.9095(14), Co(1)-N(1) 1.9790(13), O(2)-C(31) 1.1364(18), N(2)-C(30) 1.4296(18), O(3)-C(32) 1.1318(19), O(4)-C(33) 1.1411(19), C(33)-Co(1)-C(31) 121.73(7), C(33)-Co(1)-C(32) 91.88(7), C(31)-Co(1)-C(32) 97.04(7), C(33)-Co(1)-C(30) 85.16(6), C(31)-Co(1)-C(30) 87.21(6), C(32)-Co(1)-C(30) 175.67(6), C(33)-Co(1)-N(1) 121.74(6), C(31)-Co(1)-N(1) 113.94(6), C(32)-Co(1)-N(1) 97.43(6), C(30)-Co(1)-N(1) 81.52(5), O(1)-C(30)-N(2) 119.50(12), O(1)-C(30)-Co(1) 128.50(11), N(2)-C(30)-Co(1) 111.98(9), O(2)-C(31)-Co(1) 178.28(14), O(3)-C(32)-Co(1) 174.96(15), O(4)-C(33)-Co(1) 177.84(15).

2.3.3 Preparation and Reactivity of Nickel(I) Guanidinate Complexes

The β-diketiminato nickel(II) complexes $[Ni^{II}(^{Me}nacnac)(Br)_2Li(THF)_2]$ (**41**),[41] prepared by *Stephan et al.* in 2005, and $[Ni^{II}(^{Me}nacnac)(Cl)_2Li(THF)_2]$ (**104**),[121] prepared by *Holland et al.* in 2003 (**Figure 21**), have been shown to be good precursors to nickel(I) complexes.[122]

41 **Ar = 2,6-diisopropylphenyl** **104**

Figure 21 ^{Me}nacnac nickel(II) halide complexes $[Ni^{II}(^{Me}nacnac)(X)_2Li(THF)_2]$ **41** and **104**

The reduction of $[Ni^{II}(^{Me}nacnac)(Br)_2Li(THF)_2]$ (**41**) with Na/K alloy in toluene leads to the diamagnetic toluene bridged nickel(II) complex $[\{Ni^{I}(^{Me}nacnac)\}_2(\eta^3:\eta^3\text{-}C_7H_8)]$ (**42**) as discussed in 2.1.1.2 (**Scheme 51**).[41]

Complex **41** was also reacted with one equivalent of LiCp in THF at room temperature, yielding the paramagnetic monomeric Cp capped product $[Ni^{II}(^{Me}nacnac)(\eta^5\text{-}Cp)]$ (**105**). Complex **105** has been proposed to be a nickel(II) d^8 high spin system with a magnetic moment of 2.05 μ_B (**Scheme 51**).[41, 123]

Similarly the reaction of **41** with one equivalent of Li-indenyl in toluene leads to the η^3-indenyl capped complex $[Ni^{II}(^{Me}nacnac)(\eta^3\text{-}ind)]$ (**106**). In contrast to complex **105**, complex **106** is a diamagnetic nickel(II) d^8 low spin complex (**Scheme 51**).[41, 123]

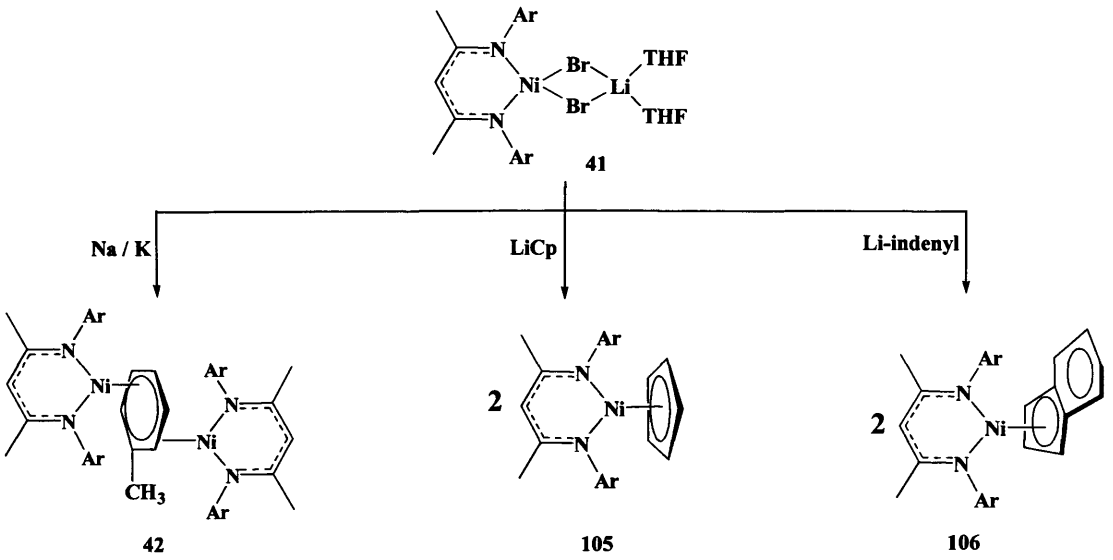

Scheme 51 Preparation of nickel(II) complexes **42**, **105** and **106**

The reaction of two equivalents of $[Ni^{II}(^{Me}nacnac)(\eta^5\text{-Cp})]$ (**105**) with $[\{Ni^{II}(^{Me}nacnac)\}_2(\eta^3{:}\eta^3\text{-}C_7H_8)]$ (**42**) in toluene led to the Cp bridged complex $[Ni(^{Me}nacnac)(\eta^2\text{-Cp})]_2$ (**107**). Complex **107** is a mixed-valence nickel(II)/nickel(I) complex with a magnetic moment of 2.74 μ_B (**Scheme 52**).[123]

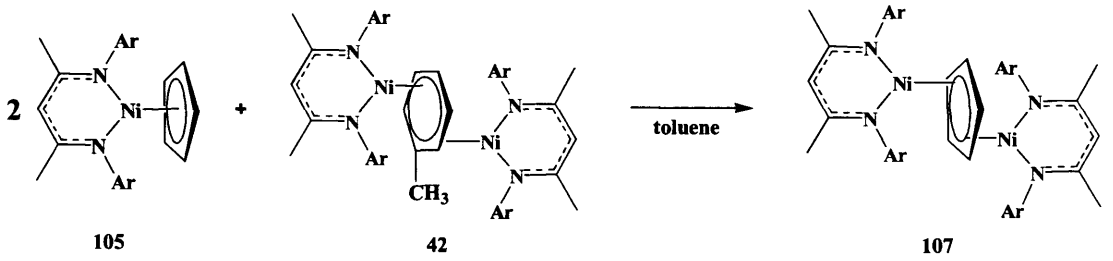

Scheme 52 Preparation of $[Ni(^{Me}nacnac)(\eta^2\text{-Cp})]_2$ (**107**)

For sake of comparison, two equivalents of $NiBr_2$ were reacted with Li[Priso] (**3K**) and Li[Giso] (**4K**) in THF at low temperature, yielding the diamagnetic nickel(II) d^8 low spin halide complexes, $[Ni^{II}(Ligand)(\mu\text{-Br})]_2$ (Ligand = Priso$^-$ (**108**) or Giso$^-$ (**109**)), after crystallisation from hexane in moderate yield (**108** = 63%, **109** = 79%) (**Scheme 53**). It is worth mentioning that an attempt was made to prepare an analogous nickel(II) Piso$^-$ complex *via* this route. However, this reaction gave only a intractable mixtures of products.

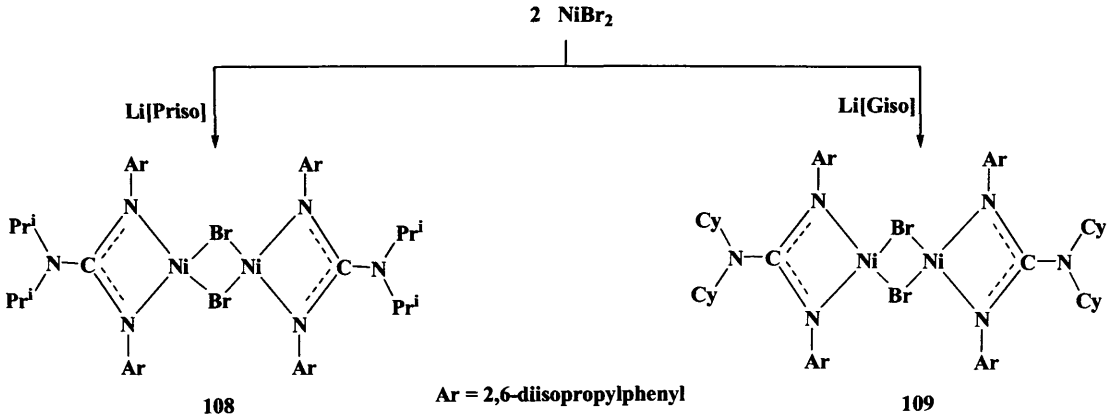

108 109

Scheme 53 Preparation of the guanidinate nickel(II) halide complexes **108** and **109**

In contrast to the dimeric bromide bridged complexes, **108** and **109**, the β-diketiminato complexes, **41** and **104**, are monomeric with two bromides bridged by a $Li(THF)_2$ fragment. However, all complexes have square planar nickel centres and show diamagnetic behaviour due to their d^8 low spin configurations.

The molecular structure of **108** was determined by X-ray crystallography and its molecular structure is displayed in **Figure 22**. The structure reveals a bromide bridged dimer, in which the nickel(II) centres are co-ordinated to two delocalised $Priso^-$ ligands, giving nickel centres with square planar geometries. The NMR spectra of the complex are consistent with its solid state structure.

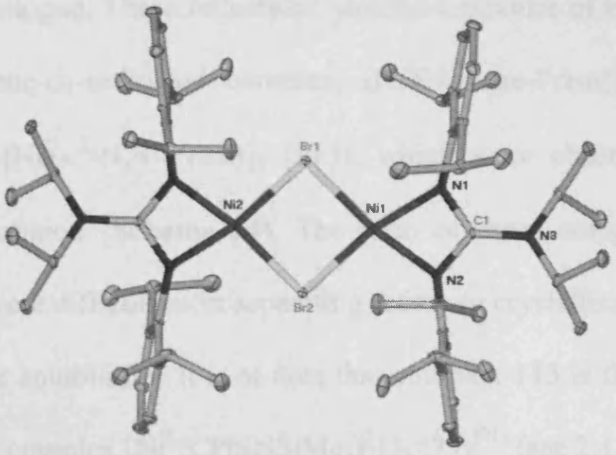

Figure 22 Molecular structure of **108** (hydrogen atoms omitted for clarity; ellipsoids shown at the 25% probability level).

Selected bond lengths (Å) and angles (°): Br(1)-Ni(2) 2.3373(13), Br(1)-Ni(1) 2.3429(10), Ni(1)-N(2) 1.883(4), Ni(1)-N(1) 1.903(4), Ni(2)-Br(1)-Ni(1) 90.75(4), N(2)-Ni(1)-N(1) 69.74(18), N(2)-Ni(1)-Br(2) 170.78(14), N(1)-Ni(1)-Br(2) 101.12(13), N(2)-Ni(1)-Br(1) 99.90(14), N(1)-Ni(1)-Br(1) 169.63(13), Br(2)-Ni(1)-Br(1) 89.25(4).

The solution state thermal stability of **108** and **109** allowed us to investigate their reduction with potassium metal in toluene, benzene or cyclohexane under a dinitrogen atmosphere. The reduction of $[Ni^{II}(\kappa^2\text{-N,N'-Priso})(\mu\text{-Br})]_2$ **108** with excess potassium in toluene or benzene at room temperature yields the diamagnetic toluene or benzene bridged complexes $[Ni^{II}(\kappa^2\text{-N,N'-Priso})_2(\eta^3{:}\eta^3\text{-solvent})]$ (solvent = C_7H_8 (**110**) or C_6H_6 (**111**)) after crystallisation from hexane in 72% and 45% yields respectively (**Scheme 54**).

As the solvent free cobalt(I) dimers $[Co^{I}(\kappa^2\text{-N,N'-Ligand})]_2$ (Ligand = Piso$^-$ (**95**), Giso$^-$ (**96**) were successfully prepared (see 2.3.2) and the thermally unstable complex $[Ni^{I}\{CPh(NSiMe_3)_2\}]_2$ (**79**) is known in the literature (see 2.1.2.2), attempts were made to reduce **108** with excess potassium in cyclohexane in order to prepare

the solvent free analogue. These reductions yielded a mixture of two main products, the dimeric N,arene-co-ordinated complex, $[Ni^{I}(N,arene\text{-}Priso)]_2$ (**112**), and the dimeric complex $[Ni^{I}(\kappa^2\text{-}N,N'\text{-}Priso)]_2$ (**113**), which were observed by ^1H NMR spectroscopy in solution (**Scheme 54**). The ratio of these complexes in solution differs and there were difficulties in separating them *via* crystallisation from hexane, due to their similar solubilities. It is of note that complex **113** is the analogue of the thermally unstable complex $[Ni^{I}\{CPh(NSiMe_3)_2\}]_2$ (**79**)[91] (see 2.1.2.2).

It is worth mentioning that attempts to reduce the complex $[Ni^{II}(\kappa^2\text{-}N,N'\text{-}Giso)(\mu\text{-}Br)]_2$ (**109**) with excess potassium in a variety of solvents (*e.g.* toluene, benzene and cyclohexane) or with magnesium in toluene or THF, under atmospheres of either argon or dinitrogen gave only intractable mixtures of products.

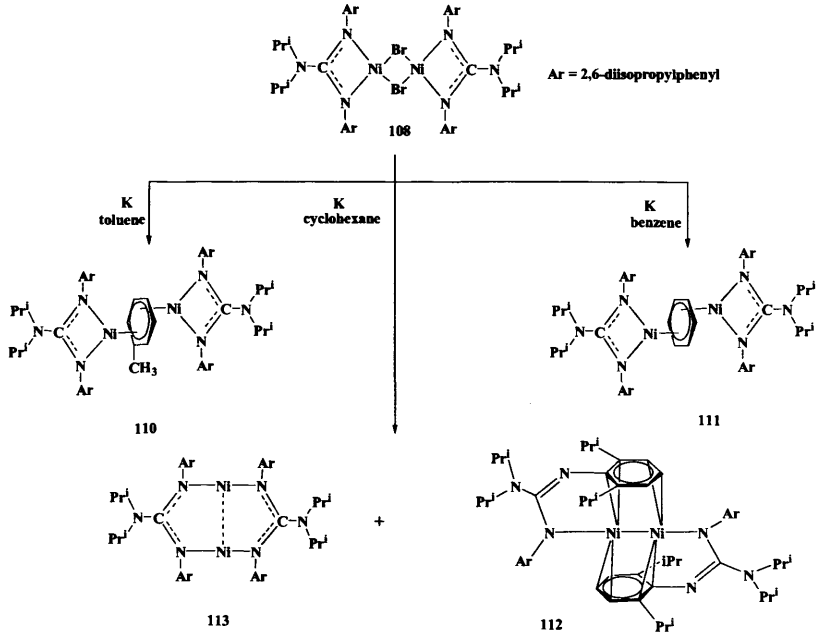

Scheme 54 Reduction of $[Ni(Priso)(\mu\text{-}Br)]_2$ (**108**)

Nickel(I) complexes are expected to be paramagnetic due to their d^9 electron configuration. However, the complexes **110** and **111** showed diamagnetic behaviour in their NMR spectra, in which all expected resonances were found. Therefore, complexes **110** and **111** should be described as containing two nickel(II) d^8 low spin

centres, bridged by a doubly reduced arene fragment in which electron transfer from nickel to toluene or benzene has taken place. This affords a compound in which the two nickel(II) centres are bridged by a dianionic toluene or benzene ligand.[41, 56]

The molecular structure of **110** and **111** was determined by X-ray crystallography and their molecular structures are displayed in **Figure 23** and **Figure 24**. The nickel centres in **110** and **111** are analogous to those in $[\{Ni^{II}(^{Me}nacnac)\}_2(\eta^3{:}\eta^3\text{-}C_7H_8)]$ **(42)**, as they are co-ordinated to a toluene or benzene molecule in an $\eta^3{:}\eta^3$ manner. The distances from the nickel centre to the centroid of the $\eta^3{:}\ \eta^3$-co-ordinated ligand of **110** (2.027 Å) and **111** (2.035 Å) are significantly shorter than those found in $[\{Ni^{II}(^{Me}nacnac)\}_2(\eta^3{:}\eta^3\text{-}C_7H_8)]$ **(42)** (2.173 Å). A reasonable explanation for this observation derives from the smaller cone angle of the Piso$^-$ ligand (*vs.* nacnac$^-$) which leads to a lesser steric interaction with the η^6-arene ligand.

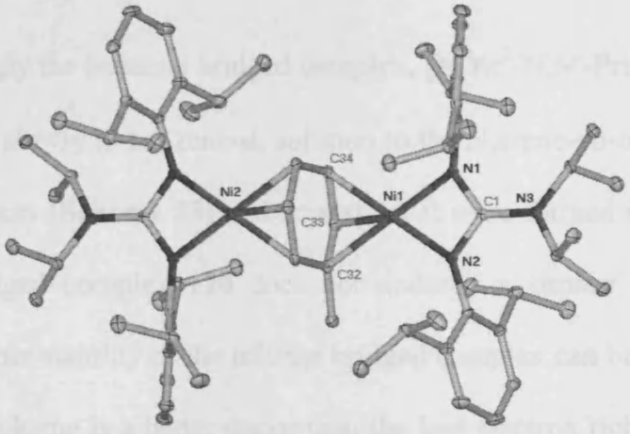

Figure 23 Molecular structure of **110** (hydrogen atoms omitted for clarity; ellipsoids shown at the 25% probability level).

Selected bond lengths (Å) and angles (°): Ni(1)-N(1) 1.9395(16), Ni(1)-N(2) 1.9591(17), Ni(1)-centroid 2.027(2), C(33)-Ni(1)-N(1) 142.55(8), C(33)-Ni(1)-N(2) 140.97(8), N(1)-Ni(1)-N(2) 68.05(7), C(33)-Ni(1)-C(34) 41.11(9), N(1)-Ni(1)-C(34) 111.68(8), N(2)-Ni(1)-C(34) 176.46(8), C(33)-Ni(1)-C(32) 40.72(9), N(1)-Ni(1)-C(32) 176.19(8), N(2)-Ni(1)-C(32) 110.22(8), C(34)-Ni(1)-C(32) 69.82(8).

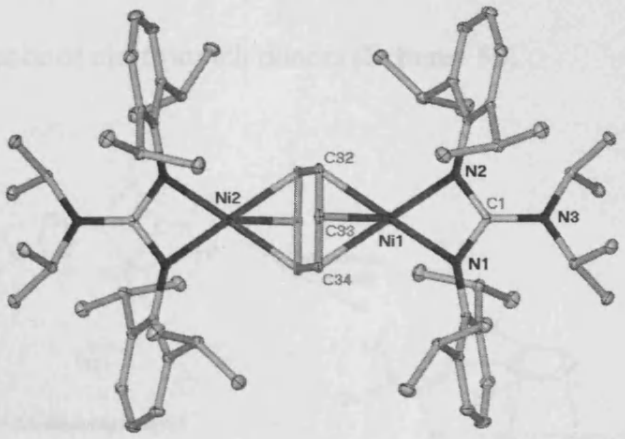

Figure 24 Molecular structure of **111** (hydrogen atoms omitted for clarity; ellipsoids shown at the 25% probability level).

Selected bond lengths (Å) and angles (°): Ni(1)-N(2) 1.9436(15), Ni(1)-N(1) 1.9488(13), Ni(1)-centroid 2.035(17), C(33)-Ni(1)-N(2) 140.72(7), C(33)-Ni(1)-N(1) 141.95(8), N(2)-Ni(1)-N(1) 68.22(6), C(33)-Ni(1)-C(34) 41.00(7), N(2)-Ni(1)-C(34) 178.27(6), N(1)-Ni(1)-C(34) 110.36(7), C(33)-Ni(1)-C(32) 40.81(8), N(2)-Ni(1)-C(32) 111.70(7), N(1)-Ni(1)-C(32) 175.19(7), C(34)-Ni(1)-C(32) 69.63(7).

Interestingly the benzene bridged complex, $[Ni^{I}(\kappa^{2}\text{-N,N'-Priso})_2(\eta^{3}:\eta^{3}\text{-}C_6H_6)]$ (**111**), rearranges slowly in benzene-d_6 solution to the N,arene-co-ordinated complex **112** after two weeks (**Scheme 55**) and crystals of it were formed in the NMR tube. The toluene bridged complex **110** does not undergo a similar rearrangement in solution. The higher stability of the toluene bridged complex can be explained by the assumption that toluene is a better donor than the less electron rich ligand, benzene. The formation to the N,arene-co-ordinated complex, **112**, probably occurs as the Ar groups (Ar = 2,6-diisopropylphenyl) are slightly more electron rich then benzene (**Scheme 55**).

After dissolving complex **112** in hexane solution and leaving the solution at room temperature for one month, crystals of the dimeric nickel(I) complex **113** were

formed. It can be assumed that complex **113** is thermodynamically the most stable species in the absence of electron rich donors (**Scheme 55**).

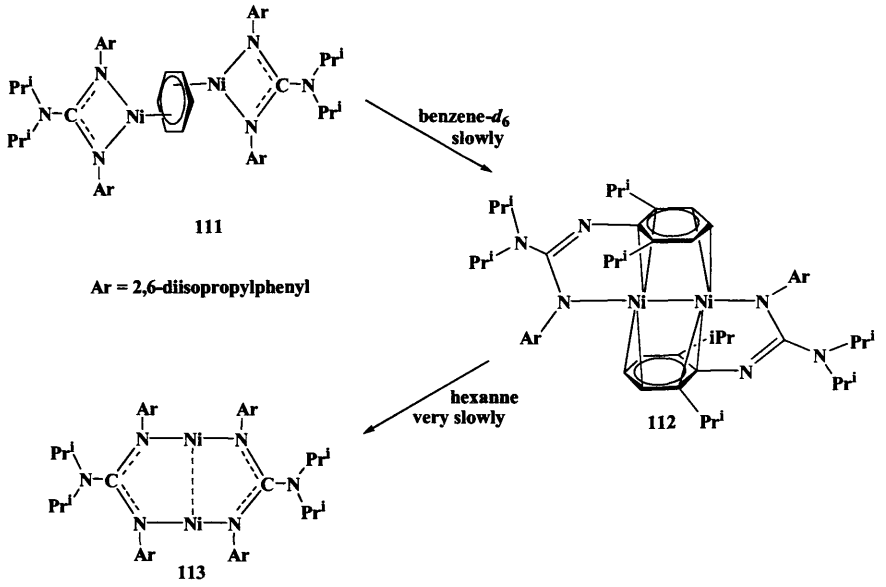

Scheme 55 Formation of the nickel dimer **113** from the benzene bridged nickel dimer **111** in the absence of electron rich donors

A similar behaviour has not been seen for β-diketiminato nickel(I) systems. This can likely be explained on steric grounds, as the Ar groups (Ar = 2,6-diisopropylphenyl) in β-diketiminato complexes enforce N,N'-chelation of the metal centre. A recent publication from *Power et al.* described the complexes **114**[124] which disply similar metal co-ordination to that found in complex **112** (**Figure 25**).

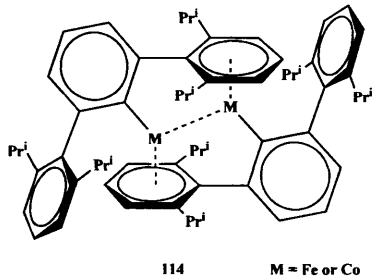

Figure 25 The terphenyl metal(I) complexes **114**

The molecular structure of $[Ni^{I}(N,arene\text{-}Piso)]_2$ (**112**) was determined by X-ray crystallography and its molecular structure is displayed in **Figure 26**. The nickel

centres are close to square planar with an N-Ni-C angle of 72.69° and Ni-Ni-C angle of 73.39°. The Ni-Ni bond length in **112** (2.6338 Å) is long and can at best be considered an interaction. The Ni-C bond lengths (ca. 2.084 Å), are similar to those in the arene capped complexes (**110**: 2.027 Å, **111**: 2.035 Å). The Ni-Ni-N angle in complex **112** is 175.76° and therefore close to linear. The NMR spectra of **112** are consistent with the solid state structure of the complex.

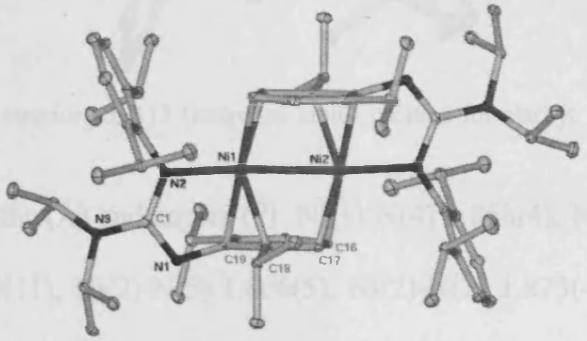

Figure 26 Molecular structure of **112** (hydrogen atoms omitted for clarity; ellipsoids shown at the 25% probability level).

Selected bond lengths (Å) and angles (°): Ni(1)-N(1) 1.984(2), Ni(1)-C(18) 2.085(3), Ni(1)-C(19) 2.159(3), Ni(1)-Ni(2) 2.6338(9), C(17)-Ni(2) 2.167(3), C(16)-Ni(2) 2.084(3), N(1)-Ni(1)-C(26) 109.65(11), N(1)-Ni(1)-C(14) 78.39(11), N(1)-Ni(1)-C(19) 104.66(11), C(14)-Ni(1)-C(19) 39.41(12), N(1)-Ni(1)-C(14) 97.78(12), N(1)-Ni(1)-Ni(2) 175.76(8), C(19)-Ni(1)-Ni(2) 73.39(9), C(14)-Ni(1)-Ni(2) 97.65(9), C(18)-Ni(1)-Ni(2) 86.43(9), C(18)-C(17)-Ni(2) 67.63(18), C(16)-C(17)-Ni(2) 111.4(2), C(17)-C(18)-Ni(2) 74.08(17), C(19)-C(18)-Ni(2) 108.0(2).

The molecular structure of $[Ni^{I}(\kappa^{2}\text{-N,N'-Priso})]_2$ (**113**) was determined by X-ray crystallography and the molecular structure is displayed in **Figure 27**. The nickel centres have T-shaped geometries with N-Ni-Ni angles of 90.14°. The Ni-N (1.858 Å) and the Ni-Ni (2.291 Å) bond lengths are similar to those found in $[Ni^{I}\{(NSiMe_3)_2CPh\}]_2$ (**79**) (Ni-N: 1.874 and 1.876 Å, Ni-Ni: 2.2938 Å).

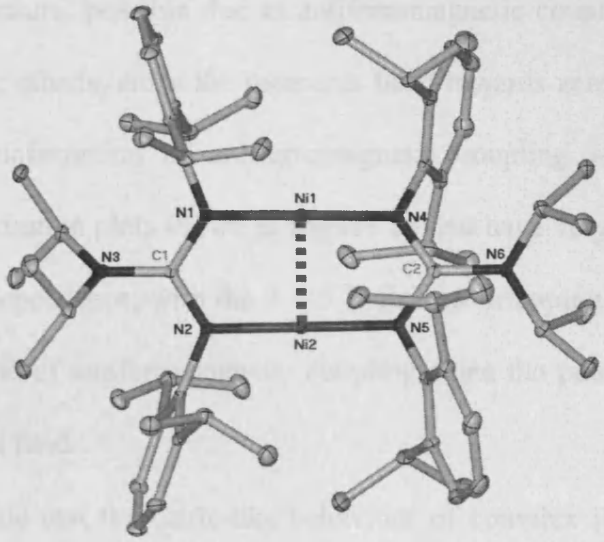

Figure 27 Molecular structure of **113** (hydrogen atoms omitted for clarity; ellipsoids shown at the 25% probability level).

Selected bond lengths (Å) and angles (°): Ni(1)-N(4) 1.858(4), Ni(1)-N(1) 1.873(4), Ni(1)-Ni(2) 2.2908(11), Ni(2)-N(5) 1.866(5), Ni(2)-N(2) 1.873(4), N(4)-Ni(1)-N(1) 179.17(18), N(4)-Ni(1)-Ni(2) 89.24(14), N(1)-Ni(1)-Ni(2) 90.14(14), N(5)-Ni(2)-N(2) 179.32(18), N(5)-Ni(2)-Ni(1) 90.37(14), N(2)-Ni(2)-Ni(1) 89.32(14).

The Raman spectrum of complex **113** points towards a Ni-Ni interaction in that complex, as a band was observed at 266 cm^{-1} (*cf.* Ni-Ni 237 cm^{-1} in $Ni_3(dpa)_4(NCS)_2$) (dpa = di(2-pyridyl)amido)).[125] The solution magnetic moment (Evan's method) of complex **113** was determined. The value measured for complex **113** (1.93 μ_B per dimer) in benzene-d_6 is quite low for a d^9 high spin complex with two unpaired electrons per dimer. The variable temperature solid state magnetic experiment (SQUID), which was carried out for complex **113**, somewhat supports those results. The magnetic moment, per dimer, remains constant at 2.3 μ_B, between 300 and 150 K, then decreases gradually to ~1 μ_B at 5 K, and more rapidly reaching 0.4 μ_B at 2 K (**Figure 28**). The temperature dependent behaviour suggests thermal population of a particular spin state above 150 K, then population of a different state

below this temperature, possible due to antiferromagnetic coupling combined with zero field splitting effects, since the moments head towards zero at 0 K (i.e. $S = 0$ ground state). Confirmation of antiferromagnetic coupling is provided by the isothermal magnetisation plots shown in **Figure 28** that have very low M values, in a linear type field dependence, with the 2 – 5 K lines overlapping above 3 T (30,000 Oe). This is typical of antiferromagnetic coupling since the pairing of spins works against the applied field.

It is notable that the Curie-like behaviour of complex $[Co^{I}(\kappa^2\text{-N,N'-Piso})]_2$ (**95**) is not shown by complex $[Ni^{I}(\kappa^2\text{-N,N'-Priso})]_2$ (**113**), despite the similar dinuclear structure of both complexes. He would anticipate that the antiferromagnetic coupling is intra-dimer rather than inter-dimer in origin.

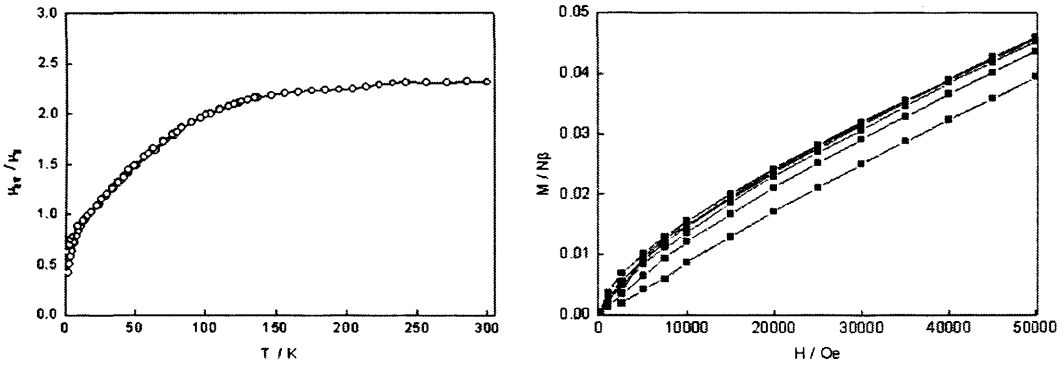

Figure 28 μ_{eff} v. T and M v. Nβ plots of $[Ni(\kappa^2\text{-N,N'-Priso})_2]$ (**113**)

The reaction of LiCp with $[Ni^{II}(\kappa^2\text{-N,N'-Ligand})(\mu\text{-Br})]_2$ (Ligand = Priso$^-$ (**108**) or Giso$^-$ (**109**)) in THF at low temperature gave the complexes $[Ni^{II}(\kappa^2\text{-N,N'-Ligand})(\eta^5\text{-Cp})]$ (Liand = Priso$^-$ (**115**) or Giso$^-$ (**116**)) in 64 and 41% yields respectively after recrystallisation from hexane (**Scheme 56**).

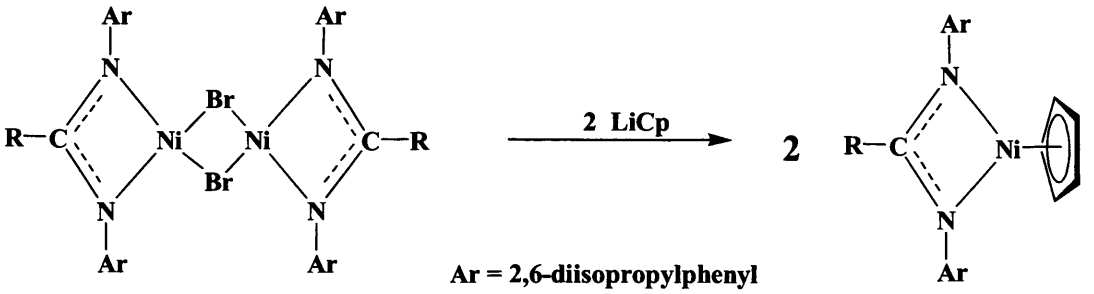

R = NPr^i_2 (108) or NCy_2 (109) R = NPr^i_2 (115) or NCy_2 (116)

Scheme 56 Preparation of [Ni(κ^2-N,N'-Ligand)(η^5-Cp)] (Liand = Priso$^-$ (115) or Giso$^-$ (116))

There are similarities between complexes **115**, **116** and [Ni^{II}(^{Me}nacnac)(η^5-Cp)] (**106**) in that the nickel centres in all are trigonal planar. However, attempts to react complexes **115** or **116** with [Ni^{II}(κ^2-N,N'-Priso)$_2$(η^3:η^3-C_7H_8)] (**110**) to form the complexes analogous to [Ni^{II}(^{Me}nacnac)(η^2-Cp)]$_2$ (**107**) only gave intractable mixtures of products.

The molecular structure of **115** was determined by X-ray crystallography and the molecular structure is displayed in **Figure 29**. It is a monomeric complex, in which the nickel centre is η^5-co-ordinated to a Cp ligand with a disturbed trigonal planar geometry. The distance from the nickel centre to the centroid of the η^5-co-ordinated Cp ligand of **115** (1.758 Å) is markedly shorter than the distance found in **106** (1.865 Å). A reasonable explanation for this observation derives from the smaller cone angle of the Priso$^-$ ligand (*vs.* nacnac$^-$) which leads to a lesser sterically interaction with the η^6-arene ligand.

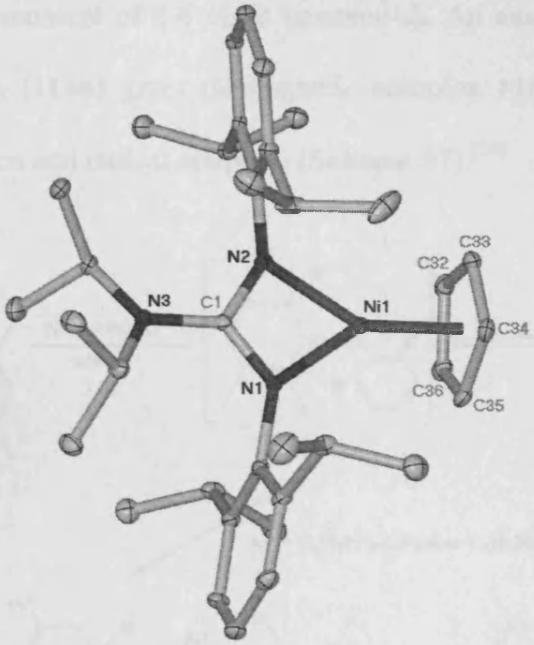

Figure 29 Molecular structure of **115** (hydrogen atoms omitted for clarity; ellipsoids shown at the 25% probability level).

Selected bond lengths (Å) and angles (°): Ni(1)-N(1) 1.904(2), Ni(1)-N(2) 1.909(2), Ni(1)-centroid 1.758(3), N(1)-Ni(1)-N(2) 69.01(10), N(1)-Ni(1)-C(33) 110.77(11), N(2)-Ni(1)-C(33) 177.46(12), N(1)-Ni(1)-C(35) 158.30(12), N(2)-Ni(1)-C(35) 116.01(12), N(1)-Ni(1)-C(34) 124.82(12), N(2)-Ni(1)-C(34) 142.80(12), N(1)-Ni(1)-C(36) 160.71(12), N(2)-Ni(1)-C(36) 114.78(12), N(1)-Ni(1)-C(32) 126.82(11), N(2)-Ni(1)-C(32) 139.17(12).

In contrast to the d^8 high spin complex **106** (2.05 μ_B), the complexes **115** and **116** have shown diamagnetic behaviour in their NMR spectra, revealing all expected resonances in their expected regions. Therefore, complexes **115** and **116** should be seen as nickel(II) d^8 low spin complexes.

Complex $[\{Ni^{II}(^{Me}nacnac)\}_2(\eta^3:\eta^3\text{-}C_7H_8)]$ (**42**) was reacted with 2,6-$Pr^i_2C_6H_3N_3$ (**116a**) in toluene giving the dimeric bridged complex **117** by liberation of dinitrogen and radical coupling (**Scheme 57**). Complex **117** is paramagnetic with a

molecular magnetic moment of 3.6 μ_B in benzene-d_6. An analogous reaction of **42** with 2,6-$Me_2C_6H_3N_3$ (**116b**) gives diamagnetic complex **118** by the liberation of dinitrogen, dihydrogen and radical coupling (**Scheme 57**).[56]

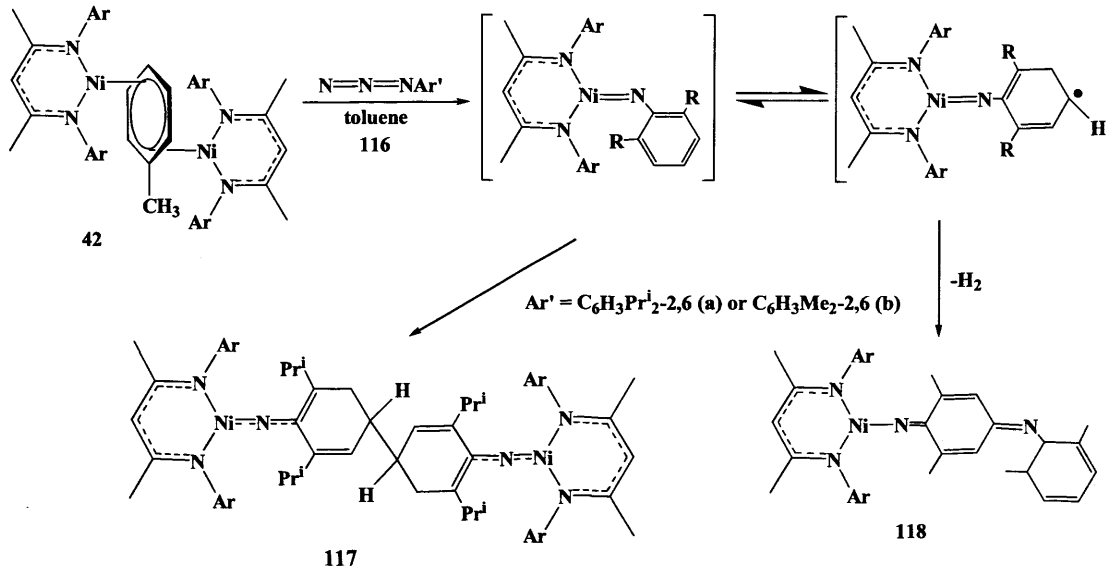

Scheme 57 Reaction of **42** with arylazides

The reduction of $[Ni^{II}(^{Me}nacnac)(\mu\text{-}Cl)]_2$ (**119**)[121] in diethyl ether with MeLi, followed by treatment with excess CO gives the nickel(I) d^9 high spin complex $[Ni^{I}(^{Me}nacnac)(CO)]$ (**120**) with a magnetic moment of ca. 1.2 μ_B (**Scheme 58**).[126]

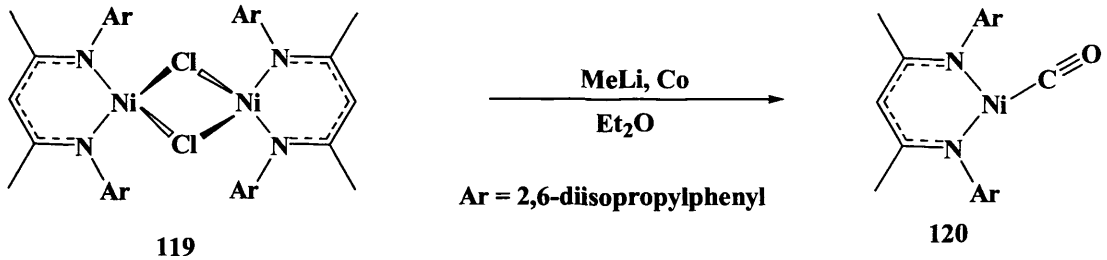

Scheme 58 Reaction of $[Ni^{II}(^{Me}nacnac)(\mu\text{-}Cl)]_2$ (**119**) with CO

For sake of comparison, the reaction of $[\{Ni^{II}(\kappa^2\text{-}N,N'\text{-}Priso)\}_2(\eta^3\text{-}C_7H_8)]$ (**111**) with two equivalents of TMS-azide in hexane at -78 °C giving the diamagnetic complex $[Ni^{II}(\kappa^2\text{-}N,N'\text{-}Priso)(\mu\text{-}N\text{-}N_3)]_2$ (**121**) after crystallisation from hexane in 53% yield (**Scheme 59**).

The reaction of $[\{Ni^{II}(\kappa^2\text{-N,N'-Priso})\}_2(\eta^3{:}\eta^3\text{-}C_7H_8)]$ **110** or $[Ni^{I}(\kappa^2\text{-N,N'-Priso})]_2$ (**113**) with excess CO in toluene gives the diamagnetic complex $[Ni(\kappa^2\text{-N,N'-Priso})(\mu\text{-CO})]_2$ (**122**) after crystallisation from hexane in 68% yield (**Scheme 59**).

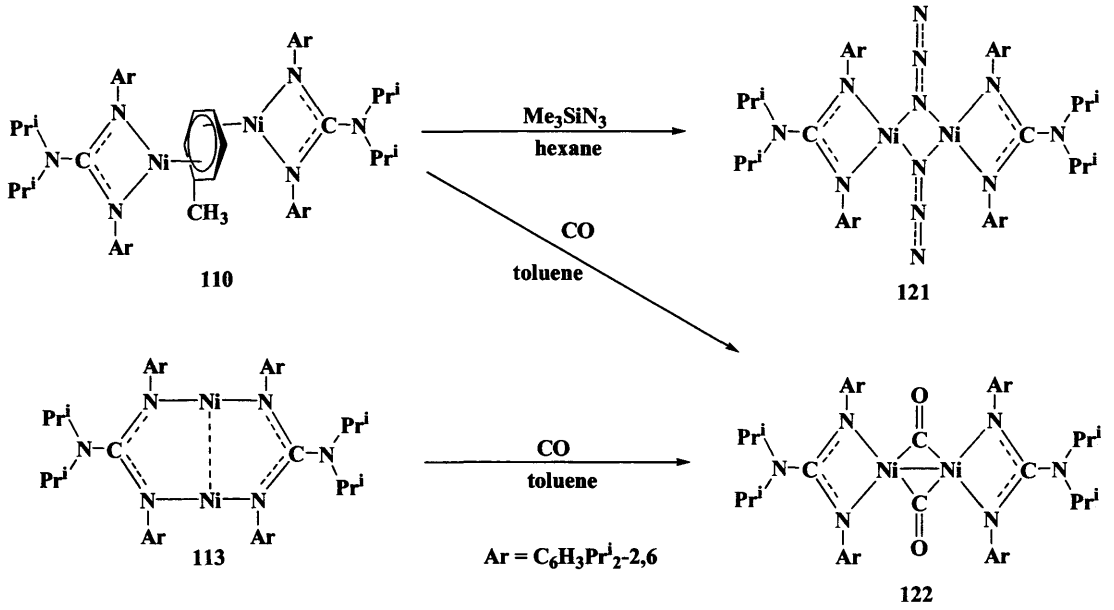

Scheme 59 Reaction of **110** with TMS-azide and **110** and **113** with CO

The IR spectrum of **121** shows a characteristic band in the azide region (2071 cm^{-1}) which is close to the band found in bis(pentafluorophenyl)boron azide (2202 cm^{-1}).[119] Complex **121** is diamagnetic due to the square planer d^8 low spin nickel(II) centres and the NMR spectra show all expected resonances.

The molecular structure of $[Ni^{II}(\kappa^2\text{-N,N'-Priso})(\mu\text{-N-}N_3)]_2$ (**121**) was determined by X-ray crystallography and the molecular structure is displayed in **Figure 30**. It is a μ-N-N_3 bridged dimer in which the two nickel centres have square planar geometries. The Ni-N bond lengths in complex **121** (1.958 and 1.926 Å) are slightly shorter than those found in the analogous cobalt(II) complex $[Co^{II}(\kappa^2\text{-N,N'-Piso})(\mu\text{-N-}N_3)]_2$ (**100**) (2.010 and 2.007 Å).

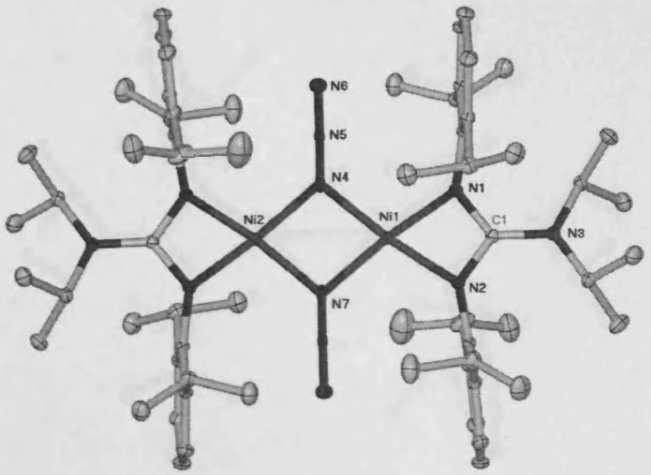

Figure 30 Molecular structure of **121** (hydrogen atoms omitted for clarity; ellipsoids shown at the 25% probability level).

Selected bond lengths (Å) and angles (°): Ni(1)-N(2) 1.886(2), Ni(1)-N(1) 1.896(2), Ni(1)-N(4) 1.958(3), Ni(1)-N(7) 1.962(3), N(4)-N(5) 1.110(4), N(5)-N(6) 1.201(4), N(4)-Ni(2) 1.962(3), N(2)-Ni(1)-N(1) 69.50(7), N(2)-Ni(1)-N(4) 174.10(7), N(1)-Ni(1)-N(4) 104.87(11), N(2)-Ni(1)-N(7) 103.64(11), N(1)-Ni(1)-N(10) 172.94(11), N(4)-Ni(1)-N(7) 82.04(13), N(5)-N(4)-Ni(1) 124.9(2), N(5)-N(4)-Ni(2) 126.8(2), Ni(1)-N(4)-Ni(2) 97.96(13).

The molecular structure of $[Ni^{II}(\kappa^2\text{-N,N'-Priso})(\mu\text{-CO})]_2$ (**122**) was determined by X-ray crystallography and the molecular structure is displayed in **Figure 31**. Complex **122** is a square planar complex with metal centres bridged by two CO molecules. The Ni-C bond distances in **122** (1.857, 1.861 Å) are significantly longer compared to those in the monomeric complex $[Ni^{I}(^{Me}nacnac)(CO)]$ (**120**) (1.770 Å). The Ni-Ni bond distance (2.437 Å) is in the normal range for Ni-Ni interaction. The IR spectrum of **122** in Nujol shows one broad band (1847 cm^{-1}) in the carbonyl region (*cf.* **120**: 2022 m^{-1}).

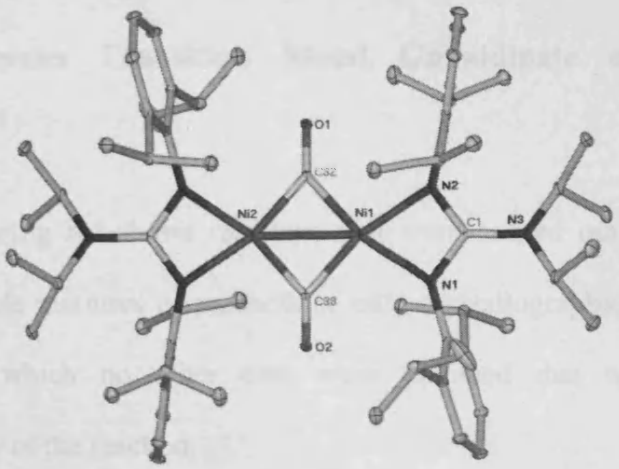

Figure 31 Molecular structure of **122** (hydrogen atoms omitted for clarity; ellipsoids shown at the 25% probability level).

Selected bond lengths (Å) and angles (°): Ni(2)-Ni(2) 2.437, Ni(1)-C(33) 1.857(2), Ni(1)-C(32) 1.8616(18), Ni(1)-N(1) 1.9477(15), Ni(1)-N(2) 1.9551(16), O(1)-C(32) 1.165(2), C(32)-Ni(2) 1.857(2), C(33)-Ni(1)-C(32) 98.11(8), C(33)-Ni(1)-N(1) 96.90(7), C(32)-Ni(1)-N(1) 164.89(7), C(33)-Ni(1)-N(2) 165.19(7), C(32)-Ni(1)-N(2) 96.63(7), N(1)-Ni(1)-N(2) 68.41(6), O(1)-C(32)-Ni(2) 139.43(15), O(1)-C(32)-Ni(1) 138.57(15), Ni(2)-C(32)-Ni(1) 81.89(8).

2.3.4 Miscellaneous Transition Metal Guanidinate and Amidinate Reactions

The following list shows reactions that ware carried out which led to no reaction, intractable mixtures of products or only crystallographically characterised compounds for which no other data were obtained due to low yields or irrereproducibility of the reaction.

Reagent	Reactant	Outcome
Preparation and reduction of iron guanidinate halides		
$FeCl_2$	K[Priso]	$[Fe(\kappa^2\text{-N,N'-Priso})(\mu\text{-Cl})]_2$ **(123)**
FeI_2	K[Giso]	$[Fe(\kappa^2\text{-N,N'-Giso})(\mu\text{-I})]_2$ **(124)**
$[Fe(\kappa^2\text{-N,N'-Priso})(\mu\text{-Cl})]_2$ **(123)**	exc. K in toluene of THF	decomposition
$[Fe(\kappa^2\text{-N,N'-Priso})(\mu\text{-Cl})]_2$ **(123)**	exc. Mg in toluene or THF	decomposition
$[Fe(\kappa^2\text{-N,N'-Giso})(\mu\text{-I})]_2$ **(124)**	exc. K in toluene of THF	decomposition
$[Fe(\kappa^2\text{-N,N'-Giso})(\mu\text{-I})]_2$ **(124)**	exc. Mg in toluene or THF	decomposition
Reactions of iron(I) amidinates		
$[Fe(N,arene\text{-}Piso)_2(\mu\text{-N})]_2$ **(86)**	$[Ga(\kappa^2\text{-N,N'-Giso})]$	no reaction
$[Fe(N,arene\text{-}Piso)_2(\mu\text{-N})]_2$ **(86)**	triphosphabenzene	no reaction
$[Fe(N,arene\text{-}Piso)_2(\mu\text{-N})]_2$ **(86)**	TMS-azide	no isolated product
$[Fe(N,arene\text{-}Piso)_2(\mu\text{-N})]_2$ **(86)**	$P{\equiv}CBu^t$	no isolated product
$[Fe(N,arene\text{-}Piso)_2(\mu\text{-N})]_2$ **(86)**	P≡CMe	decomposition
$[Fe(N,arene\text{-}Piso)_2(\mu\text{-N})]_2$ **(86)**	tetraphosphabarrelene	no reaction
$[Fe(\kappa^2\text{-N,N'-Piso})(\eta^6\text{-}C_7H_8)]$ **(87)**	H_2	no reaction
$[Fe(\kappa^2\text{-N,N'-Piso})(\eta^6\text{-}C_7H_8)]$ **(87)**	$(PhN)_2$	no isolated product
Preparation and reduction of guanidinate cobalt halides		
CoI_2	K[Priso]	$[Co(\kappa^2\text{-N,N'-Priso})(\mu\text{-I})]_2$ **(125)**
$[Co(\kappa^2\text{-N,N'-Priso})(\mu\text{-I})]_2$ **(125)**	exc. K in toluene of THF	decomposition
$[Co(\kappa^2\text{-N,N'-Priso})(\mu\text{-I})]_2$ **(125)**	exc. Mg in toluene or THF	decomposition
Reaction of cobalt(I) guanidinates		
$[Co(\kappa^2\text{-N,N'-Priso})(\eta^6\text{-}C_7H_8)]$ **(94)**	$[Ga(\kappa^2\text{-N,N'-Giso})]$	no reaction
$[Co(\kappa^2\text{-N,N'-Priso})(\eta^6\text{-}C_7H_8)]$ **(94)**	$P{\equiv}CBu^t$	$[Co(\kappa^2\text{-N,N'-Priso})(O)]_2$ **(126)**
$[Co(\kappa^2\text{-N,N'-Priso})(\eta^6\text{-}C_7H_8)]$ **(94)**	P≡CMe	decomposition
$[Co(\kappa^2\text{-N,N'-Priso})(\eta^6\text{-}C_7H_8)]$ **(94)**	H_2	no reaction
$[Co(\kappa^2\text{-N,N'-Priso})(\eta^6\text{-}C_7H_8)]$ **(94)**	$(PhN)_2$	no isolated product
Reaction of nickel(I) guanidinates		
$[Ni(\kappa^2\text{-N,N'-Priso})_2(\eta^3\text{-}C_7H_8)]$ **(111)**	P≡CMe	decomposition
$[Ni(\kappa^2\text{-N,N'-Priso})_2(\eta^3\text{-}C_7H_8)]$ **(111)**	H_2	no reaction
$[Ni(\kappa^2\text{-N,N'-Priso})_2(\eta^3\text{-}C_7H_8)]$ **(111)**	$(PhN)_2$	no isolated product
$[Ni(\kappa^2\text{-N,N'-Priso})_2(\eta^3\text{-}C_7H_8)]$ **(111)**	$P{\equiv}CBu^t$	no isolated product
$[Ni(\kappa^2\text{-N,N'-Priso})_2(\eta^3\text{-}C_7H_8)]$ **(111)**	1-adamantyl-azide	no isolated product

$[Ni(\kappa^2\text{-N,N'-Priso})]_2$ **(115)**	H_2	no reaction
$[Ni(\kappa^2\text{-N,N'-Priso})]_2$ **(115)**	P≡CMe	no reaction
Preparation and reduction of a guanidinate hafnium halide complex		
$HfCl_4$	Li[Giso]	$[Hf(\kappa^2\text{-N,N'-Piso})(Cl)_3]$ **(127)**
$[Hf(\kappa^2\text{-N,N'-Piso})(Cl)_3]$ **(127)**	exc. K in toluene of THF	decomposition
$[Hf(\kappa^2\text{-N,N'-Piso})(Cl)_3]$ **(127)**	exc. Mg in toluene of THF	decomposition
Preparation and reduction of guanidinate chromium halide complex		
$CrCl_2$	K[Piso]	$[Cr(\kappa^2\text{-N,N'-Piso})(\mu\text{-Cl})]_2$
$[Cr(\kappa^2\text{-N,N'-Piso})(\mu\text{-Cl})]_2$	exc. K in toluene of THF	decomposition
$[Cr(\kappa^2\text{-N,N'-Piso})(\mu\text{-Cl})]_2$	exc. Mg in toluene or THF	decomposition
Preparation and reduction of a guanidinate manganese halide		
$MnBr_2$	K[Piso]	$[Mn(\kappa^2\text{-N,N'-Piso})(\mu\text{-Br})]_3$ **(128)**
$[Mn(\kappa^2\text{-N,N'-Piso})(Br)]_3$ **(128)**	exc. K in toluene of THF	decomposition
$[Mn(\kappa^2\text{-N,N'-Piso})(Br)]_3$ **(128)**	exc. Mg in toluene of THF	decomposition

The molecular structure of $[Fe(Priso)(\mu\text{-Cl})]_2$ **(123)** is displayed in **Figure 33**. It is a chloride bridged dimer with iron centres co-ordinated by two delocalised $Priso^-$ ligands. The metal centres have tetrahedral geometries.

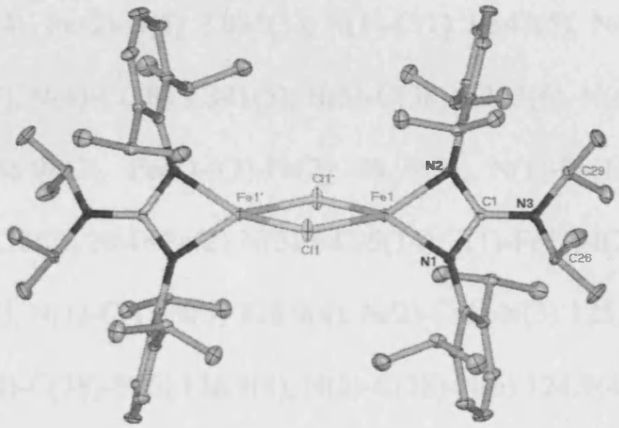

Figure 32 Molecular structure of **123** (25% thermal ellipsoids; hydrogen atoms omitted).

Selected bond lengths (Å) and angles (°): Fe(1)-N(1) 2.0169(18), Fe(1)-N(2) 2.0208(18), Fe(1)-Cl(1)' 2.3364(9), Fe(1)-Cl(1) 2.3403(9), Cl(1)-Fe(1)' 2.3364(9), N(1)-C(1) 1.352(3), C(1)-N(2) 1.350(3), C(1)-N(3) 1.373(3), N(1)-Fe(1)-N(2) 66.37(7), N(1)-Fe(1)-Cl(1)' 139.92(6), N(2)-Fe(1)-Cl(1)' 113.07(6), N(1)-Fe(1)-Cl(1) 113.43(5), N(2)-Fe(1)-Cl(1) 136.92(6), Cl(1)'-Fe(1)-Cl(1) 93.83(3), N(2)-C(1)-N(1) 109.74(18), N(2)-C(1)-N(3) 125.70(19), N(1)-C(1)-N(3) 124.55(19).

The molecular structure of complex $[Fe(Giso)(\mu\text{-}I)]_2$ (**124**) is displayed in (**Figure 31).** Complex **124** is an iodide bridged dimer with iron centres co-ordinated to two delocalised $Giso^-$ ligands. The metal centres have square planar geometries.

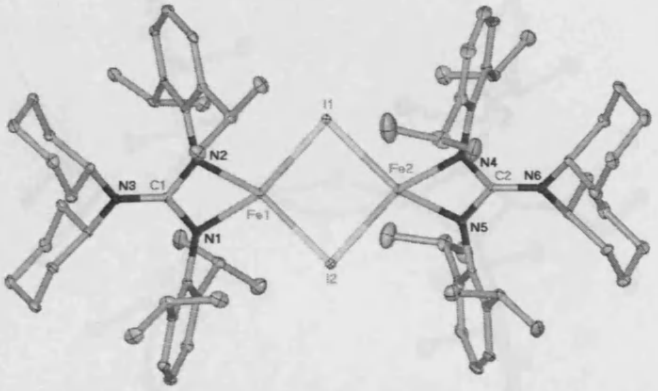

Figure 33 Molecular structure of **124** (25% thermal ellipsoids; hydrogen atoms omitted).

Selected bond lengths (Å) and angles (°): I(1)-Fe(1) 2.7055(9), I(1)-Fe(2) 2.7082(9), I(2)-Fe(1) 2.6989(9), I(2)-Fe(2) 2.7143(9), Fe(1)-N(1) 2.029(4), Fe(1)-N(2) 2.033(3), Fe(2)-N(4) 2.029(4), Fe(2)-N(5) 2.035(3), N(1)-C(1) 1.347(5), N(2)-C(1) 1.362(6), N(3)-C(1) 1.363(5), N(4)-C(38) 1.341(5), N(5)-C(38) 1.353(6), N(6)-C(38) 1.369(5), Fe(1)-I(1)-Fe(2) 86.98(2), Fe(1)-I(2)-Fe(2) 86.99(2), N(1)-Fe(1)-N(2) 64.90(14), I(2)-Fe(1)-I(1) 93.18(2), N(4)-Fe(2)-N(5) 64.95(14), I(1)-Fe(2)-I(2) 92.78(2), N(1)-C(1)-N(2) 107.2(4), N(1)-C(1)-N(3) 126.9(4), N(2)-C(1)-N(3) 125.9(4), N(4)-C(38)-N(5) 108.2(4), N(4)-C(38)-N(6) 126.9(4), N(5)-C(38)-N(6) 124.9(4).

The molecular structure of $[Co(\kappa^2\text{-N,N'-Priso})(\mu\text{-I})]_2$ (**125**) is displayed in **Figure 34**. It is an iodide bridged dimer with cobalt centres co-ordinated by two delocalised $Priso^-$ ligands. The metal centres have tetrahedral geometries.

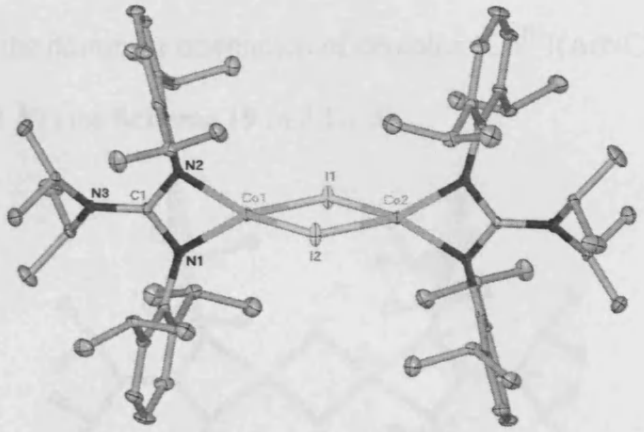

Figure 34 Molecular structure of **125** (25% thermal ellipsoids; hydrogen atoms omitted).

Selected bond lengths (Å) and angles (°): I(1)-Co(1) 2.6361(9), I(1)-Co(2) 2.6375(11), Co(1)-N(1) 1.977(3), Co(1)-N(2) 1.989(3), Co(1)-I(2) 2.6375(11), Co(1)-I(1)-Co(2) 87.56(4), N(1)-Co(1)-N(2) 67.55(12), N(1)-Co(1)-I(1) 134.43(9), N(2)-Co(1)-I(1) 118.82(9), N(1)-Co(1)-I(2) 117.06(9), N(2)-Co(1)-I(2) 131.48(9), I(1)-Co(1)-I(2) 92.44(4).

The molecular structure of $[Co(\kappa^2\text{-N,N'-Priso})(\mu\text{-O})]_2$ (**126**) was determined by X-ray crystallography and the molecular structure is displayed in **Figure 35**. Complex **126** is an oxygen bridged dimer in which the geometry around the metal centres are square planar. The Co-O bond lengths (1.7869 and 1.7872 Å) are similar to those found in the dominant orientation of complex $[Co^{III}\{(ArNCMe)_2CH\}(\mu\text{-O})]_2$ (**37**) (1.784, 1.793 Å) (see **Scheme 19** in 2.1.1.2).

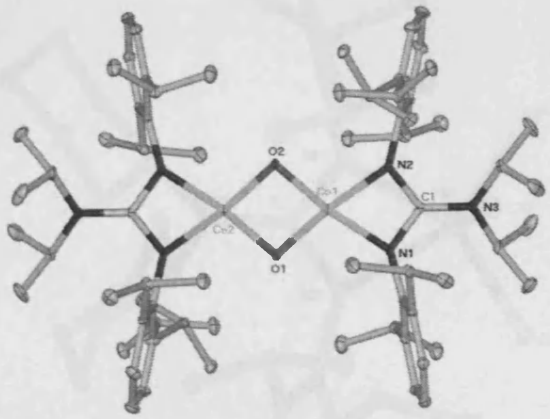

Figure 35 Molecular structure of **126** (hydrogen atoms omitted for clarity; ellipsoids shown at the 25% probability level).

Selected bond lengths (Å) and angles (°): Co(1)-O(2) 1.7869(10), Co(1)-O(1) 1.7872(12), Co(1)-N(1) 1.9210(11), Co(1)-N(2) 1.9235(13), O(1)-Co(2) 1.7869(10), O(2)-Co(1)-O(1) 83.08(5), O(2)-Co(1)-N(1) 172.39(4), O(1)-Co(1)-N(1) 104.40(5), O(2)-Co(1)-N(2) 103.58(5), O(1)-Co(1)-N(2) 173.32(4), N(1)-Co(1)-N(2) 68.94(5), Co(2)-O(1)-Co(1) 96.92(5)

The molecular structure of [Hf(Giso)$(Cl)_3$] (**127**) was determined by X-ray crystallography and the molecular structure is displayed in **Figure 36**. Complex **127** is a monomeric complex in which the hafnium centre possesses a square based pyramidal geometry.

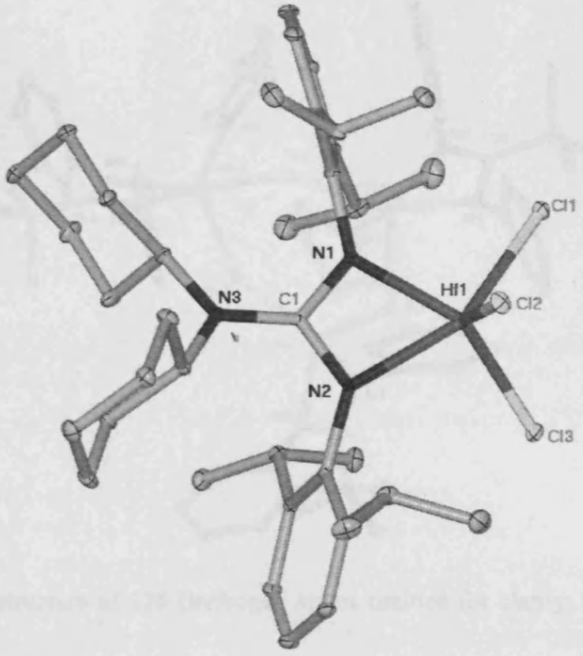

Figure 36 Molecular structure of **127** (hydrogen atoms omitted for clarity; ellipsoids shown at the 25% probability level).

Selected bond lengths (Å) and angles (°): Hf(1)-N(2) 2.130(2), Hf(1)-N(1) 2.1370(19), Hf(1)-Cl(2) 2.3312(8), Hf(1)-Cl(3) 2.3515(8), Hf(1)-Cl(1) 2.3807(12), N(2)-Hf(1)-N(1) 61.71(7), N(2)-Hf(1)-Cl(2) 101.72(6), N(1)-Hf(1)-Cl(2) 113.69(6), N(2)-Hf(1)-Cl(3) 94.32(6), N(1)-Hf(1)-Cl(3) 131.48(5), Cl(2)-Hf(1)-Cl(3) 112.16(4), N(2)-Hf(1)-Cl(1) 148.47(5), N(1)-Hf(1)-Cl(1) 88.89(6) Cl(2)-Hf(1)-Cl(1) 100.49(4), Cl(3)-Hf(1)-Cl(1) 97.73(4).

The molecular structure of $[Mn(Piso)(\mu\text{-}Br)]_3\cdot(THF)_2$ (**128**) was determined by X-ray crystallography and the molecular structure is displayed in **Figure 37**. Complex **128** displays a six membered Mn_3Br_3 ring system in which three [Mn(Piso)] fragments are bridged by three bromides.

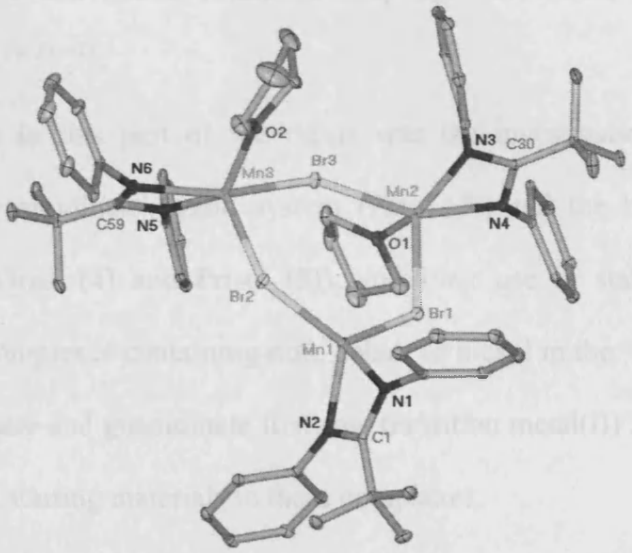

Figure 37 Molecular structure of **128** (hydrogen atoms omitted for clarity; ellipsoids shown at the 25% probability level).

Selected bond lengths (Å) and angles (°): Br(1)-Mn(1) 2.5050(9), Br(1)-Mn(2) 2.5843(8), Br(2)-Mn(1) 2.5140(8), Br(2)-Mn(3) 2.5913(8), Br(3)-Mn(2) 2.5909(9), Br(3)-Mn(3) 2.6166(9), Mn(1)-Br(1)-Mn(2) 122.11(3), Mn(1)-Br(2)-Mn(3) 123.60(3), Mn(2)-Br(3)-Mn(3) 148.78(2), Br(1)-Mn(1)-Br(2) 124.39(3), Br(1)-Mn(2)-Br(3) 99.85(3), Br(2)-Mn(3)-Br(3) 97.14(3).

2.4 Conclusion

Transition metal(I) β-diketiminato complexes are interesting complexes, the reactivity of which lends them to synthetic applications, including uses as reagents for small molecule activations, reductive couplings, and metal imide formations etc.[9, 14, 41, 46, 49, 52, 54, 58, 61]

The focus in this part of the thesis was the investigation of the mostly unexplored bulky amidinate ligand system (Piso$^-$ (**3**)) and the bulky guanidinate ligand systems (Giso$^-$ (**4**) and Priso$^-$ (**5**)), and their use in stabilising first row transition metal complexes containing iron, cobalt or nickel in the +1 oxidation state. The bulky amidinate and guanidinate first row transition metal(II) halides have been shown to be good starting materials to these complexes.

The results of this study have revealed that bulky amidinate and guanidinate ligand systems have comparable abilities to stabilise first row transition metals in the +1 oxidation state to those of the β-diketiminato ligands. A variety of highly reactive transition metal(I) complexes were prepared and attempts were made to investigate their reactivity towards different reagents and reactants. Further study of the complexes prepared in this study will be maintained in the Jones group.

2.5 Experimental

General considerations. All manipulations were carried out using standard Schlenk and glove box techniques under an atmosphere of high purity argon. hexane, THF and toluene were distilled over potassium whilst diethyl ether was distilled over Na/K then freeze/thaw degassed prior to use. ^{1}H and $^{31}P\{^{1}H\}$ NMR spectra were recorded on either a Bruker DXP400 or a Jeol Eclipse 300 spectrometer and were referenced to the residual ^{1}H resonances of the solvent used or external 85% H_3PO_4 respectively. Mass spectra were obtained from the EPSRC National Mass Spectrometry Service at Swansea University. Although molecular ion peaks displaying correct isotopic distribution patterns were observed for all new complexes, only the accurate mass data for compounds less then 1000 Da are reported. All other compounds have masses greater than 1000 Da and as such their accurate mass data are not considered meaningful. IR spectra were recorded using a Nicolet 510 FT-IR spectrometer as Nujol mulls between NaCl plates. Melting points were determined in sealed glass capillaries under dinitrogen, and are uncorrected. Solution state magnetic moments were determined using the Evans method.[127, 128] PisoH (**3H**), [77, 78] PrisoH (**4H**), [77, 78] GisoH (**5H**), [77, 78] K[Ligand] (Ligand = Piso$^-$ (**3**), Priso (**4**), Giso (**5**)) were prepared by treating **3-5H** with $K[N\{N(SiMe_3)_2\}]$ in toluene. $P{\equiv}CBu^t$[129] was synthesised by the $[Li\{N(SiMe_3)_2\}]$ catalysed elimination of hexamethyldisiloxane from $(Me_3Si)P{=}C(Bu^t)(OSiMe_3)$ and $P{\equiv}CMe$[130-132] was prepared by modified literature procedures. All other chemicals were obtained from commercial sources and used as supplied.

$[Fe^{II}(\kappa^2$-N,N'-Piso)(μ-Br)$]_2$: 83

K[Piso] (1.00 g, 2.18 mmol) in THF (20 cm^3) was added to a suspension of $FeBr_2$ (0.47 g, 2.18 mmol) in THF (20 cm^3) at –78°C. The resultant mixture was warmed to 20°C overnight. Volatiles were then removed *in vacuo* and the residue extracted with hexane (50 cm^3). Filtration, concentration and cooling to -30°C overnight yielded yellow crystals of **83**.

(0.93 g, 77 %), M.p. > 260°C; ^{1}H NMR (300 MHz, C_6D_6, 300 K): δ -21.02, -18.21, 4.25, 14.06, 19.22, 28.04; IR ν/cm^{-1} (Nujol): 1615 (m), 1251 (m), 1174 (m), 1099 (s), 757 (m); MS (EI) *m/z* (%): 554.2 [$M/2^+$, 5], 420.4 [$Piso^+$, 15]; μ_{eff} (Evans, C_6D_6, 298 K): 5.4 μ_B (per Fe centre); anal: calc. for $C_{58}H_{86}N_4Fe_2Br_2$ C 62.71 %, H 7.80 %, N 5.04 %, found: C 62.85 %, H 7.86 %, N 5.17 %.

$[Fe^{I}$(N,arene-Piso)(μ-N)$]_2$: 86

To a solution of $[Fe(\kappa^2$-N,N'-Piso)(μ-Br)$]_2$ (**83**) (0.25 g, 0.42 mmol) in toluene (40 cm^3)/THF (2 cm^3) under an atmosphere of dinitrogen at 20°C was added magnesium powder (0.10 g, 4.12 mmol). The suspension was placed in an ultrasonic bath for 1 hour then stirred for 72 h at 20°C, during which the solution changed from yellow to brown. The solution was subsequently filtered, volatiles removed *in vacuo*, and the residue extracted with hexane (10 cm^3). Concentration, filtration and cooling to -30°C overnight yielded dark brown crystals of **86**.

(0.15 g, 71 %). M.p. = 183 - 185°C; ^{1}H NMR (300 MHz, C_6D_6, 300 K): δ -1.48, 0.29, 0.92, 1.36, 1.77, 2.65, 3.29, 3.46, 5.45, 6.56, 9.62, 10.82, 19.43; IR ν/cm^{-1} (Nujol): 1519 (m), 1321 (m), 1082 (s), 835 (m), 764 (m); Raman (solid under Ar, 514 nm excitation) ν (cm^{-1}): 2005 (N-N str.); MS (EI) *m/z* (%): 475.2 [$(Piso)Fe^+$, 100], 420.3 [$Piso^+$, 10]; μ_{eff} (Evans, C_6D_6, 298 K): 2.6 μ_B (per iron dimer); μ_{eff} (SQUID): 2.5μ_B

(per iron dimer); anal: calc. for $C_{58}H_{86}N_6Fe_2$ C 71.15 %, H 8.85 %, N 8.58 %, found: C 71.63 %, H 9.06 %, N 7.92 %, parameters, R(observed) = R1 = 0.1260, wR2 = 0.1713, largest difference peak and hole: 0.538 and -0.453 e.Å^{-3}.

[Fe^{I}(κ^2-N,N'-Piso)(η^6-C_7H_8)]: 87

To a solution of [Fe(κ^2-N,N'-Piso)(μ-Br)]$_2$ (**83**) (0.25 g, 0.42 mmol) in toluene (40 cm^3)/THF (2 cm^3) under an atmosphere of argon at 20°C was added magnesium powder (0.10 g, 4.12 mmol). The suspension was placed in an ultrasonic bath for 1 h then stirred for 72 h at 20°C, during which time the colour of the solution changed from yellow to brown. The solution was subsequently filtered, volatiles removed *in vacuo*, and the residue extracted with hexane (10 cm^3). Concentration, filtration and cooling to -80°C overnight yielded red crystals of **87**.

(0.16 g, 67 %), M.p. 138 -140°C; ^{1}H NMR (300 MHz, C_6D_6, 300 K): δ -0.75, 0.28, 0.77, 1.61, 2.09, 3.52, 5.40, 6.95, 11.85, 15.95; IR ν/cm^{-1} (Nujol): 1615 (m), 1585 (m), 1310 (s), 1173 (m), 803 (m), 767 (m); MS (EI) *m/z* (%): 475.2 [(Piso)Fe$^+$, 65], 420.3 [Piso$^+$, 72]; μ_{eff} (Evans, C_6D_6, 298 K): 2.3 μ_B (per iron centre); anal: calc. for $C_{36}H_{51}N_2Fe_1$ C 76.17 %, H 9.06 %, N 4.93 %, found: C 75.56 %, H 9.60 %, N 4.47 %, parameters, R(observed) = 0.0736, wR2 = 0.1033, largest difference peak and hole: 0.453 and -0.287 e.Å^{-3}.

[Fe^{I}(κ^2-N,N'-Piso)(CO)$_3$]: 88

Compound [Fe(κ^2-N,N'-Piso)(η^6-C_7H_8)] (**87**) (50 mg, 0.088 mmol) was dissolved in toluene (10 cm^3) in a Schlenk flask and cooled to -90 °C. The Schlenk flask (*ca.* 100 cm^3 volume) was filled with CO and sealed. The colour of the solution changed from red-brown to deep green over 20 h. All volatiles were then removed from the

solution *in vacuo* and the residue extracted with hexane (10 cm^3). The extract was concentrated to *ca.* 5 cm^3 and stored at -30 °C overnight to give deep green crystals of **88**.

(30 mg, 61%), M.p. 153 - 155 °C; ^1H NMR (300 MHz, C_6D_6, 300 K): δ 0.38, 1.50, 3.21, 3.50, 7.10, 9.50; IR ν/cm^{-1} (Nujol): 2050 (s), 1965 (s), 1955 (sh.) (CO str.); MS (EI) *m/z* (%): 531.3 [M^+-CO, 14], 475.2 [(Piso)Fe^+, 100], 420.3 [$Piso^+$, 15], parameters, R(observed) = 0.0762, wR2 = 0.1733, largest difference peak and hole: 0.951 and -0.503 e.$Å^{-3}$.

N.B. **88** can also be formed in a 71% isolated yield by treating a toluene solution of $[Fe^I$(N,arene-Piso)(μ-N)$]_2$ (**86**) with CO.

$[Co^{II}(\kappa^2$-N,N'-Piso)(μ-Br)$]_2$: 89

K[Piso] (2.06 g, 4.50 mmol) in THF (40 cm^3) was added to $CoBr_2$ (1 g, 4.50 mmol) in THF (20 cm^3) at –78°C. The mixture was warmed to room temperature slowly overnight. Volatiles were removed *in vacuo* and the residue washed with hexane (15 cm^3) and extracted with toluene and filtered (100 cm^3). All volatiles were removed from the filtrate *in vacuo* yielding **89** as a green solid. (1.3 g, 52 %).

$[Co^{II}(\kappa^2$-N,N'-Priso)(μ-Br)$]_2$: 90

K[Priso] (2.25 g, 4.50 mmol) in THF (40 cm^3) was added to $CoBr_2$ (1 g, 4.5 mmol) in THF (20 cm^3) at –78°C. The mixture was warmed to room temperature slowly overnight. Volatiles were removed *in vacuo* and the residue washed with hexane (15 cm^3) and extracted with toluene and filtered (100 cm^3). All volatiles were removed from the filtrate *in vacuo* yielding **90** as a green solid.

(1.2 g, 58 %), ^1H NMR (300 MHz, C_6D_6, 300 K): δ-36.36 (s), 0.49 (s), 0.89 (s), 1.32 (s), 1.54 (s), 3.54 (s), 5.26 (s), 7.40 (m), 11.05 (s), 17.52 (s), 71.43 (s); UV-Vis

(toluene): 746 (ε = 66 $M^{-1}cm^{-1}$), 423 (ε = 422 $M^{-1}cm^{-1}$), 316 (ε = 316 $M^{-1}cm^{-1}$), 316 (ε = 1366 $M^{-1}cm^{-1}$); μ_{eff} (Evans, C_6D_6, 298 K): 5.2 μ_B (per cobalt dimer).

$[Co^{II}(\kappa^2$-N,N'-Giso)(μ-Br)$]_2$: 91

K[Giso] (1.86 g, 3.20 mmol) in THF (40 cm^3) was added to $CoBr_2$ (0.7 g, 3.20 mmol) in THF (20 cm^3) at –78°C. The mixture was warmed to room temperature slowly overnight. Volatiles were removed *in vacuo* and the residue washed with hexane (15 cm^3) and extracted with toluene and filtered (100 cm^3). All volatiles were removed from the filtrate *in vacuo* yielding **91** as a green solid. (1.0 g, 48 %).

$[Co^{I}(\kappa^2$-N,N'-Piso)(η^6-C_7H_8)]: 92

$[Co^{II}(\kappa^2$-N,N'-Piso)(μ-Br)$]_2$ (**89**) (300 mg, 0.26 mmol) in toluene (30 cm^3) was added to a potassium mirror (195 mg, 5.0 mmol) at room temperature. After stirring for 1 to 1.5 h the solution was filtered. Volatiles were then removed *in vacuo* and the residue extracted with hexane (20 cm^3). After concentration to 5 cm^3 the solution was placed at 6°C for 24 h yielding red crystals of **92**.

(250 mg, 84%),(250 mg 84%), M.p. 175 – 178 °C ^{1}H NMR (300 MHz, C_6D_6, 303 K): δ -30.16 (s), -10.13 (s), 0.25 (s), 0.79 (s), 1.25 (m), 3.33 (m), 5.40 (s), 7.05 (m); μ_{eff} (Evans, C_6D_6, 298 K): 3.17 μ_B; acc. MS/EI m/z (%): 478 [M^+, 2], 244 [Ph(Pr^i)$_2$N(Bu^t), 100]; MS (EI) calc. for $C_{36}H_{51}CoN_2$: 478.2753, found: 478.2758, parameters, R(observed) = 0.0927, wR2 = 0.1651, largest difference peak and hole: 1.660 and -0.464 e.Å^{-3}.

$[Co^{I}(\kappa^2$-N,N'-Priso)(η^6-C_7H_8)]: 93

$[Co^{II}(\kappa^2$-N,N'-Priso)(μ-Br)$]_2$ (**90**) (300 mg, 0.25 mmol) in toluene (30 cm^3) was added to a potassium mirror (195 mg, 5.0 mmol) at room temperature. After stirring

for 1 to 1.5 h the solution was filtered, volatiles were then removed *in vacuo* and the residue extracted with hexane (20 cm^3). After concentration to 5 cm^3 the solution was placed at 6°C for 24 h yielding red crystals of **93**.

(220mg, 72%), M.P. 138 °C (dec.); ^1H NMR (300 MHz, C_6D_6, 303 K): δ 27.08 (br. s), -9.65 (s), -2.02 (s), 0.90 (s), 1.26 (s), 1.92 (s), 3.46 (s), 5.14 (s), 5.38 (s), 5.51 (s), 8.18 (s), 13.48 (s), 17.86 (s); IR ν/cm^{-1} (Nujol): 1609 s, 1581 s, 1260 s, 1098 br, 1019 br, 932 s, 864 br, 799 s, 767 s; UV-Vis (toluene) : 353 (ε = 1683 $M^{-1}cm^{-1}$); μ_{eff} (Evans, C_6D_6, 298 K): 3.09 μ_B; μ_{eff} (SQUID): 3.4μ_B; MS/EI m/z (%): 462.4 [PrisoH$^+$, 10 %], 521.3 [M$^+$-toluene, 100 %]; anal: calc. for $C_{38}H_{56}CoN_3$: C 74.36 %, H 9.20 %, N 6.85 %, found: C 74.37 %, 9.51 H %, N 7.57 %, parameters, R(observed) = 0.1589, wR2 = 0.2106, largest difference peak and hole: 1.558 and -1.070 e.$Å^{-3}$.

N.B. **93** can also be formed in a 82% isolated yield by treating a toluene/THF solution of [Co(κ^2-N,N'-Priso)(Br)]$_2$ (**90**) with Mg.

[Co^I(κ^2-N,N'-Giso)(η^6-C_7H_8)]: 94

[Co^{II}(κ^2-N,N'-Giso)(μ-Br)]$_2$ (**91**) (300 mg, 0.22 mmol) in toluene (30 cm^3) was added to a potassium mirror (172 mg, 4.4 mmol) at room temperature. After stirring for 1 to 1.5 h the solution was filtered. Volatiles were then removed *in vacuo* and the residue extracted with hexane (20 cm^3). After concentration to 5 cm^3 the solution was placed at 6°C for 24 h yielding red crystals of **94**.

(210mg, 70%), M.p. 165 – 170 °C; ^1H NMR (300 MHz, C_6D_6, 303 K): δ 22.32 (br. s), 17.91 (br. s), 7.85 (br. s), 1.47 (br. s), 0.19 (br. s), -0.83 (br. s), -1.95 (br. s), -3.36 (br. s), -10.05 (br. s); IR *ν*/cm^{-1} (Nujol); 1613m, 1217m, 1157m, 1020m, 768m, 855m; MS/EI m/z (%): 603 [M$^+$-C_7H_8, 4], 543 [M$^+$-Co(C_7H_8)$^+$, 7], 92 [$C_7H_8^+$, 63];

MS (EI) calc. for $C_{37}H_{56}CoN_3$: 601.3801, found: 601.3800; anal. calc. for $C_{37}H_{56}CoN_3$: C 73.85, H 9.38, N 6.98. Found: C 73.69, H 9.38, N 6.26, parameters, R(observed) = 0.1090, wR2 = 0.2317, largest difference peak and hole: 3.428 and -0.819 e.Å^{-3}.

N.B. **94** can also be formed in a 85% isolated yield by treating a toluene/THF solution of $[Co^{II}(\kappa^2\text{-N,N'-Giso})(\mu\text{-Br})]_2$ (**91**) with Mg.

$[Co^{I}(\kappa^2\text{-N,N'-Piso})]_2$: 95

$[Co^{II}(\kappa^2\text{-N,N'-Piso})(\mu\text{-Br})]_2$ (**89**) (350 mg, 0.31 mmol) in cyclohexane (40 cm^3) was added to a potassium mirror (245 mg, 5.27 mmol) at room temperature. After stirring for 3 to 5 h the solution was filtered. Volatiles were then removed *in vacuo* and the residue extracted with hexane (20 cm^3). After concentration to 5 cm^3 the solution was placed at 6°C for 24 h yielding red crystals of **95**.

(170 mg 57%), M.p. 210-125 °C ^{1}H NMR (300 MHz, C_6D_6, 303 K): δ 26.62 (br. s), 12.54 (br. s), 8.14 (br. s), 6.36 (br. s), 4.53 (s), 4.20 (s), 2.51 (s); IR ν/cm^{-1} (Nujol): 1613m, 1315m, 1260m, 1170m, 1099m, 799m, 758m; Raman (solid under dinitrogen, 782 nm excitation) ν (cm^{-1}): 277 (Co-Co str.); μ_{eff} (Evans, C_6D_6, 298 K): 5.35 μ_B (per cobalt dimer); μ_{eff} (SQUID): 5.25μ_B (per cobalt dimer); MS/EI m/z (%): 478 [1/2M$^+$, 25], 420 [PisoH$^+$, 53], 244 [ArNHBu^{t+}, 100]; MS (EI) calc. for $C_{58}H_{86}Co_2N_4$: 957.5416, found: 957.5514; anal. calc. for $C_{58}H_{86}Co_2N_4$: C 72.78, H 9.06, N 5.85. Found: C 72.53, H 9.21, N 5.59, parameters, R(observed) = 0.0465, wR2 = 0.0957, largest difference peak and hole: 0.677 and -0.513 e.Å^{-3}.

$[Co^{I}(\kappa^2\text{-N,N'-Giso})]_2$: 96

$[Co^{II}(\kappa^2\text{-N,N'-Giso})(\mu\text{-Br})]_2$ (**91**) (500 g, 0.37 mmol) in cyclohexane (40 cm^3) was added to a potassium mirror (225 mg, 5.8 mmol) at room temperature. After stirring

for 3 to 5 h the solution was filtered. Volatiles were then removed *in vacuo* and the residue extracted with hexane (20 cm^3). After concentration to 5 cm^3 the solution was placed at 6°C for 24 h yielding red crystals of **96**.

(230 mg 52%), M.p. 210 °C; IR ν/cm^{-1} (Nujol): 1611m, 1318m, 1260m, 1160m, 1093m, 1019m, 748; μ_{eff} (Evans, C_6D_6, 298 K): 5.10 μ_B (per cobalt dimer); anal. calc. for $C_{74}H_{112}Co_2N_6$: C 73.85, H 6.98, N 9.38. Found: C 72.04, H 6.63, N 9.27, parameters, R(observed) = 0.0713, wR2 = 0.1336, largest difference peak and hole: 2.066 and -0.773 e.$Å^{-3}$.

$[Co^{II}(\kappa^2$-N,N'-Piso)(μ-N-N_3)$]_2$: 99

Me_3SiN_3 (188 mg, 0.16 mmol) was added to a solution of $[Co^{I}(\kappa^2$-N,N'-Priso)(η^3-C_7H_8)] (**93**) (100 mg, 0.16 mmol) in hexane (20 cm^3) at –78 °C. The resultant mixture was warmed to room temperature overnight. Volatiles were then removed *in vacuo* and the residue extracted with -30 °C cold hexane (10 cm^3). Filtration, concentration and storing at overnight yielded coloureles crystals of **99**.

(60 mg, 32 %).

parameters, R(observed) = 0.0790, wR2 = 0.1567, largest difference peak and hole: 1.496 and -0.758 e.$Å^{-3}$.

$[Co^{III}(\kappa^2$-N,N'-Giso)(NAd)]: 100

AdN_3 (72 mg, 0.41 mmol) was added to a solution of $[Co^{I}(\kappa^2$-N,N'-Giso)(η^3-C_7H_8)] (**94**) (280 mg, 0.41 mmol) in hexane (20 cm^3) at –78 °C. The resultant mixture was warmed to room temperature overnight. Volatiles were then removed *in vacuo* and the residue extracted with cold hexane (10 cm^3). Filtration, concentration and storing at -30 °C overnight yielded coloureles crystals of **100**.

(160 mg, 53 %).

parameters, R(observed) = 0.1156, wR2 = 0.2044, largest difference peak and hole: 1.184 and -0.417 e.Å^{-3}.

[Co^{II}{ArNC(Bu^t)N(Ar)(CO)}(CO)$_3$]: 101

[Co^I(κ^2-N,N'-Piso)]$_2$ (**95**) (70 mg, 0.07 mmol) was dissolved in toluene (10 cm^3) in a Schlenk flask and cooled to -90 °C. The Schlenk flask (*ca.* 100 cm^3 volume) was filled with CO and sealed. The colour of the solution changed from red to deep brown yellow over 20 h. All volatiles were then removed from the solution *in vacuo* and the residue extracted with hexane (10 cm^3). The extract was concentrated to *ca.* 5 cm^3 and stored at -30 °C overnight to give deep green crystals of **101**.

(30 mg 73%), M.p. 115 °C, dec. 120 °C; ^{1}H NMR (300 MHz, C_6D_6, 303 K): δ 0.79 (s, 9H, Bu^t), 1.22 (vt, $^3J_{HH}$ = 7 Hz, 12H, Pr^i), 1.36 (vt, $^3J_{HH}$ = 7 Hz, 12H, Pr^i), 3.04 (sept, $^3J_{HH}$ = 7 Hz, 2H, Pr^i-H), 3.29 (sept, $^3J_{HH}$ = 7 Hz, 2H, Pr^i-H), 7.15 – 6.8 (m, 6H, Ar-H); ^{13}C NMR (75 MHz, C_6D_6 303 K): δ 22.3 (CH(*C*H$_3$)$_2$), 23.89 (CH(*C*H$_3$)$_2$), 25.46 (CH(*C*H$_3$)$_2$), 26.35 (CH(*C*H$_3$)$_2$), 28.30 (CH(*C*H$_3$)$_2$), 30.43 (CH(*C*H$_3$)$_2$), 30.97 (C(*C*H$_3$)$_3$), 40.98 (*C*(CH$_3$)$_3$) 124.07 (*o*-C$_6$H$_3$Pr$^i_2$), 124.41 (*o*-C$_6$H$_3$Pr$^i_2$), 126.31 (*p*-C$_6$H$_3$Pr$^i_2$), 130.23 (*p*-C$_6$H$_3$Pr$^i_2$), 138.71 (*m*-C$_6$H$_3$Pr$^i_2$), 142.5 (*m*-C$_6$H$_3$Pr$^i_2$), 148.34 (*ipso*-C$_6$H$_3$Pr$^i_2$), 151.43 (*ipso*-C$_6$H$_3$Pr$^i_2$), 165.70 (CN_3); IR ν/cm^{-1} (Nujol): 2064m, 2004m, 1970m, 1661m, 1554m, 1304m, 1047m, 809m; MS/EI m/z (%): 534 [M$^+$-2CO, 2], 506 [M$^+$-3CO, 6], 478 [M$^+$-4CO, 100]; MS (EI) calc. for $C_{33}H_{41}CoN_2O_2$ (M$^+$ -2 CO): 534.2651, found: 534.2655; anal. calc. for $C_{33}H_{43}CoN_2O_4$: C 67.11, H 7.34, N 4.74. Found: C 67.12, H 7.19, N 4.80, parameters, R(observed) = 0.0420, wR2 = 0.0849, largest difference peak and hole: 0.343 and -0.365 e.Å^{-3}.

[Ni^{II}(κ^2-N,N'-Priso)(μ-Br)]$_2$: 108

Li[Priso] (1.00g, 2.14 mmol) in THF (20 cm^3) was added to a suspension of $NiBr_2$ (459 mg, 2.14 mmol) in THF (30 cm^3) at –78 °C. The resultant mixture warmed to room temperature overnight. Volatiles were then removed *in vacuo* and the residue washed with hexane (20 cm^3) and extracted with toluene (100 cm^3). Filtration, concentration and cooling to -30 °C overnight yielded green crystals of **108**.

(1.0 g 63%); M.P. 170 °C (dec.); ^{1}H NMR (300 MHz, C_6D_6, 303 K): δ 0.48 (d, $^3J_{HH}$ = 6 Hz, 12H, Pr^i), 1.28 (d, $^3J_{HH}$ = 6 Hz, 12H, Pr^i), 2.19 (d, $^3J_{HH}$ = 6 Hz, 12H, Pr^i), 3.48 (sept, $^3J_{HH}$ = 6 Hz, 2H, Pr^i-H), 4.18 (sept, $^3J_{HH}$ = 6 Hz, 2H, Pr^i-H), 6.82 (m, 6H Ar-H); ^{13}C NMR (75 MHz, C_6D_6 303 K): δ 22.98 (NCH(CH_3)$_3$), 23.20 (CH(CH_3)$_3$), 25.91 (CH(CH_3)$_3$), 28.54 (CH(CH_3)$_3$), 47.55 (NCH(CH_3)$_3$) 123.64 (o-$C_6H_3Pr^i_2$), 125.53 (*p*-$C_6H_3Pr^i_2$), 140 (*m*-$C_6H_3Pr^i_2$), 145.29 (*ipso*-$C_6H_3Pr^i_2$), 165.4 (CN_3); IR ν/cm^{-1} (Nujol): 1925m, 1858m, 1790m, 1562m, 1327m, 1051m, 933m, 799m; acc. MS/EI m/z (%): 1202.4 [M^+, 1], 601 [1/2M^+, 1], 420 [M^+-N(Pr^i)$_2$, 100]; anal. calc. for $C_{62}H_{96}Br_2N_6Ni_2$ (1202.661): C 61.92, H 8.05, N 6.99. Found: C 60.63, H 8.10, N 6.84, parameters, R(observed) = 0.0825, wR2 = 0.1616, largest difference peak and hole: 1.544 and -0.648 e.$Å^{-3}$.

[Ni^{II}(κ^2-N,N'-Giso)(μ-Br)]$_2$: 109

Li[Giso] (1.00 g, 1.83 mmol) in THF (20 cm^3) was added to a suspension of $NiBr_2$ (400 mg, 1.83 mmol) in THF (30 cm^3) at –78 °C. The resultant mixture warmed to room temperature overnight. Volatiles were then removed *in vacuo* and the residue extracted with hexane (50 cm^3). Filtration, concentration and cooling to -30 °C overnight yielded green crystals of **109**.

(1.36 g, 79 %). M.P. 255 °C (dec.); ^{1}H NMR (300 MHz, C_6D_6, 303 K): δ 0.54 (br. s 11H, C_6H_{11}), 1.14 (br. m 11 H, C_6H_{11}), 1.42 (d, $^3J_{HH}$ = 6 Hz, 12H, Pr^i), 2.24 (d, $^3J_{HH}$ = 6 Hz, 12H, Pr^i), 3.15 (sept, $^3J_{HH}$ = 6 Hz, Pr^i-H), 4.00 (sept, $^3J_{HH}$ = 6 Hz, 4H, Pr^i-H), 6.88 (m, 6H, Ar-H); ^{13}C NMR (75 MHz, C_6D_6 303 K): δ 22.96 (*C*H$_2$),) 25.75 (CH(CH$_3$)$_2$),), 26.45 (CH(CH$_3$)$_2$), 28.86 (*C*H(CH$_3$)$_2$), 32.71 (*C*H$_2$), 35.03 (*C*H$_2$), 56.70 (H*C*N), 123.59 (*o*-C$_6$H$_3$Pr$^i_2$), 125.13 (*p*-C$_6$H$_3$Pr$^i_2$), 141.04 (*m*-C$_6$H$_3$Pr$^i_2$), 144.52 (*ipso*-C$_6$H$_3$Pr$^i_2$), 168.16 (*C*N$_3$); IR ν/cm^{-1} (Nujol): 1495m, 1433m, 1226m, 1019m, 1795m; acc. MS/EI m/z (%): 1362.6 [M$^+$, 1], 681.3 [1/2M$^+$, 1], 180 N(Cy)$_2^+$, 100]; anal. calc. for $C_{74}H_{112}Br_2N_6Ni_2$ (1362.916): C65.21, H 8.28, N 6.17. Found: C 65.03, H 8.37, N 6.12.

[{Ni^{II}(κ^2-N,N'-Priso)}$_2$(η^3:η^3-C$_7$H$_8$)]: 110

[Ni^{II}(κ^2-N,N'-Priso)(μ-Br)]$_2$ (**108**) (340 mg, 0.28 mmol) in toluene (40 cm^3) was added to a potassium mirror (55 mg, 1.41 mmol) at room temperature. After stirring for 18 to 27 h the solution was filtered, volatiles were then removed *in vacuo* and the residue extracted with hexane (20 cm^3). After concentration to 5 cm^3 the solution was placed at 6°C for 24 h yielding red crystals of **110**.

(230 mg, 72%), Mp: 235 °C; ^{1}H NMR (300 MHz, C_6D_6, 303 K): δ 0.65 (d $^3J_{HH}$ = 7 Hz, 24H, Pr^i), 1.3 (d, 42H, $^3J_{HH}$ = 7 Hz, Pr^i), 1.57 (d, 24H, $^3J_{HH}$ = 7 Hz, Pr^i), 2.07 (s, Ar-CH$_3$), 3.66 (sept, $^3J_{HH}$ = 7 Hz, 4H, Pr^i-H), 3.88 (sept, $^3J_{HH}$ = 7 Hz, 8H; Pr^i-H), 6.94 (m, 12H Ar-H); ^{13}C NMR (75 MHz, C_6D_6 303 K): δ 22.84 (NCH(*C*H$_3$)$_2$), 23.68 (CH(*C*H$_3$)$_2$), 25.04 (*C*H(CH$_3$)$_2$), 27.93 (CH(*C*H$_3$)$_2$), 48.29 (NCH(*C*H$_3$)$_3$), 123.31 (*o*-C$_6$H$_5$CH$_3$), 123.44 (*p*-C$_6$H$_3$Pr$^i_2$), 143.14 (*m*-C$_6$H$_3$Pr$^i_2$), 145.17 (*ipso*-C$_6$H$_3$Pr$^i_2$), 167.39 (CN$_3$); IR ν/cm^{-1} (Nujol): 1433m, 1408m, 1327m, 1277m, 1125m, 795m, 754m, 658m; acc. MS/EI m/z (%): 1040 [M$^+$-C$_6$H$_5$CH$_3$, 100], 420 [1/2M$^+$-N(Pr^i)$_2$, 100]; MS

(EI) calc. for $C_{62}H_{96}N_6Ni_2$: 1040.6398, found 1040.6399; anal. calc. for $C_{69}H_{104}N_6Ni_2$ (1134.991): C 73.02, H 9.24, N 7.40. Found: C 71.97, H 9.21, N 7.28, parameters, R(observed) = 0.0598, wR2 = 0.1121, largest difference peak and hole: 0.449 and -0.394 e.Å^{-3}.

[{Ni^{II}(κ^2-N,N'-Priso)}$_2$(η^3:η^3-C_6H_6)]: 111

[Ni^{II}(κ^2-N,N'-Priso)(μ-Br)]$_2$ (**108**) (470 mg, 0.39 mmol) in benzene (40 cm^3) was added to a potassium mirror (200 mg, 5.11 mmol) at room temperature. After stirring for 4 to 6 h the solution was filtered, volatiles were then removed *in vacuo* and the residue extracted with hexane (20 cm^3). After concentration to 5 cm^3 the solution was placed at 6°C for 24 h yielding red crystals of **111**.

(300 mg 45%), Mp: 244 °C, Dec: 250 °C; ^{1}H NMR (300 MHz, C_6D_6, 303 K): δ 0.65 (d, $^3J_{HH}$ = 7 Hz, 24H, Pr^i), 1.33 (d$^3J_{HH}$ = 7 Hz, , 24H, Pr^i), 1.57 (d, $^3J_{HH}$ = 7 Hz, 24H, Pr^i), 3.66 (sept, $^3J_{HH}$ = 7 Hz, 4H, Pr^i-H), 3.88 (sept, $^3J_{HH}$ = 7 Hz, 8H, Pr^i-H), 6.94 (s, 12H, Ar-H); ^{13}C NMR (75 MHz, C_6D_6 303 K): δ 21.93 (NCH(CH_3)$_3$), 22.83 (CH(CH_3)$_2$), 23.67 (CH(CH_3)$_2$), 25.04 (CH(CH_3)$_2$), 27.93 (CH(CH$_3$)$_2$), 48.28 (NCH(CH_3)$_3$), 123.30 (*o*-$C_6H_3Pr^i_2$), 125.53 (*p*-$C_6H_3Pr^i_2$), 143.14 (*m*-$C_6H_3Pr^i_2$), 145.17 (*ipso*-$C_6H_3Pr^i_2$), 167.37 (CN_3); IR ν/cm^{-1} (Nujol): 1613m, 1510m, 1328m, 1278m, 1125m, 1024m, 796m, 755m; acc. MS/EI m/z (%): 1042.4 [M$^+$-C_6H_6, 100], 420.4 [1/2M$^+$-N(Pr^i)$_2$, 76%]; anal. calc. for $C_{68}H_{102}N_6Ni_2$ (1120.964): C 72.86, H 9.17, N 7.50. Found: C 71.11, H 8.78, N 6.97, parameters, R(observed) = 0.0557, wR2 = 0.0919, largest difference peak and hole: 0.416 and -0.362 e.Å^{-3}.

[Ni^I(N,arene-Priso)]$_2$: 112 and **[Ni^I(κ^2-N,N'-Priso)]$_2$: 113**

[Ni^{II}(κ^2-N,N'-Priso)(μ-Br)]$_2$ (**108**) (470 mg, 0.39 mmol) in cyclohexane (40 cm^3) was added to a potassium mirror (200 mg, 5.11 mmol) at room temperature. After stirring

for 20 to 30 h the solution was filtered, volatiles were then removed *in vacuo* and the residue extracted with hexane (20 cm^3). After concentration to 5 cm^3 the solution was placed at 6°C for 24 h yielding brown crystals of **112**.

(110 mg, 27%), Mp: 248 °C; ^{1}H NMR (300 MHz, C_6D_6, 303 K): δ 1.02 (d, $^3J_{HH}$ = 7 Hz, 24H, Pr^i), 1.22 (d, $^3J_{HH}$ = 5 Hz, 12H, Ni Pr^i), 1.34 (d, $^3J_{HH}$ = 7 Hz, 12H, Pr^i), 1.47 (d, $^3J_{HH}$ = 7 Hz, 12H, Pr^i), 1.76 (d, $^3J_{HH}$ = 5 Hz, 12H, Ni Pr^i), 3.10 (sept,, $^3J_{HH}$ = 7 Hz, 4H, Pr^i-H), 3.45 (sept,, $^3J_{HH}$ = 7 Hz, Pr^i-H), 5.18 (t, $^3J_{HH}$ = 7 Hz, 2H, Ar-H), 7.02 (s, 5H, Ar-H), 7.28 (d, 5H, $^3J_{HH}$ = 7 Hz, Ar-H); ^{13}C NMR (75 MHz, C_6D_6 303 K): δ 21.62 (NCH(CH_3)$_3$), 22.45 (CH(CH_3)$_2$), 23.85 (CH(CH_3)$_2$), 24.32 (CH(CH_3)$_2$), 25.86 (CH(CH_3)$_2$), 27.42 (CH(CH_3)$_2$), 30.58 (CH(CH_3)$_2$), 47.09 (NCH(CH_3)$_2$), 85.60 ($C_6H_3Pr^i_2$) 109.62 ($C_6H_3Pr^i_2$), 123.67 ($C_6H_3Pr^i_2$), 124.45 ($C_6H_3Pr^i_2$) 126.42 ($C_6H_3Pr^i_2$), 132.06 ($C_6H_3Pr^i_2$), 144.17 ($C_6H_3Pr^i_2$), 146.50 ($C_6H_3Pr^i_2$), 167.11 (CN_3); IR ν/cm^{-1} (Nujol): 1510m, 1427m, 1336m, 1258m, 1107m, 1031m, 801m; acc. MS/EI m/z (%): 1042 [M^+, 61], 420.4 [1/2M^+-N(Pr^i)$_2$, 100]; anal. calc. for $C_{62}H_{96}N_6Ni_2$ (1042.853): C 71.51, H 9.28, N 8.06. Found: C 60.86, H 8.28, N 5.84, parameters, R(observed) = 0.0984, wR2 = 0.1371, largest difference peak and hole: 0.767 and -0.378 e.Å^{-3}.

Leaving a hexane solution of the mixture at room temperature for 2 weeks yielding orange crystals of **[Ni^I(κ^2-N,N'-Priso)]$_2$ (113)**.

(60 mg, 15%), M.P.: 220 °C (dec.); ^{1}H NMR (300 MHz, C_6D_6, 303 K): δ -5.62 (s, 3H, Pr^i-H), -4.23 (s, 3H, Pr^i-H), -1.49 (s, 12H, Pr^i), -0.82 (s, 12H, Pr^i), 0.26 (s, 12H, Pr^i 0.70 (s, 12H, Pr^i), 1.29 (s, 12H, Pr^i), 2.99 (s, 12H, Pr^i), 7.03 (m, 6H, Ar-H), 8.51 (m, 6H, Ar-H), 12.79 (s, 3H, Pr^i-H), 17.53 (s, 3H, Pr^i-H); ^{13}C NMR (75 MHz, C_6D_6 303 K): δ -15.4 (s), -16.61 (s), -7.40 (s), 1.24 (s), 28.83 (s), 32.57 (s), 33.98 (s), 47.78 (s), 56.42 (s), 56.28 (s), 102.71 (s), 193.63 (s), 245.71 (s); IR ν/cm^{-1} (Nujol): 2365m,

1613m, 1584m, 1259m, 1105m, 1019m, 797m, 753m; Raman (solid under N_2, 782 nm excitation) ν (cm^{-1}): 266 (Ni-Ni str.); μ_{eff} (Evans, C_6D_6, 298 K): 2.1 μ_B (per nickel dimer); μ_{eff} (SQUID): 2.30μ_B (per nickel dimer); acc. MS/EI m/z (%): 1040 [M^+, 11], 520 [1/2M^+, 3], 462 [Prisoh$^+$, 100]; MS (EI) calc. for $C_{32}H_{96}N_6Ni_2$: 1040.6398, found: 1040.6400, parameters, R(observed) = 0.1155, wR2 = 0.2866, largest difference peak and hole: 3.952 and -1.230 e.Å^{-3}.

[Ni^{II}(κ^2-N,N'-Priso)(η^5-Cp)]: 115

LiCp (36 mg, 0.48 mmol) in THF (5 cm^3) was added to a solution of [Ni^{II}(κ^2-N,N'-Priso)(μ-Br)]$_2$ (**108**) (300 mg, 0.24 mmol) in THF (5 cm^3) at –78 °C. The resultant mixture warmed to room temperature overnight. Volatiles were then removed *in vacuo* and the residue extracted with hexane (30 cm^3). Filtration, concentration and cooling to -30 °C overnight yielded lilac crystals of **115**.

(190 mg, 64%), M.p. 226 °C; ^{1}H NMR (300 MHz, C_6D_6, 303 K): δ -12.22 (s 5H, Cp), 0.20 (d, $^3J_{HH}$ = 9 Hz, 12H, Pr^i), 1.46 (d, $^3J_{HH}$ = 6Hz, 12H, Pr^i), 2.60 (d, $^3J_{HH}$ = 6.0Hz, 12H, Pr^i), 3.65 (m, 2H, Pr^i-H), 5.29 (m, 4H, Pr^i-H), 5.42 (m, 2H, Ar-H), 8.09 (d$^3J_{HH}$ = 6.0Hz, , 4H, Ar-H); ^{13}C NMR (75 MHz, C_6D_6 303 K): δ 23.52 (NCH(CH_3)$_3$), 26.90 (CH(CH_3)$_2$), 31.81 (CH(CH_3)$_2$), 37.3 (CH(CH_3)$_3$), 62.55 (NCH(CH_3)$_3$), 98.20 (Cp), 118.23 (*o*-$C_6H_3Pr^i_2$), 133.58 (*p*-$C_6H_3Pr^i_2$), 160.56 (m-$C_6H_3Pr^i_2$), 168.02 (*ipso*-$C_6H_3Pr^i_2$), 184.06 (CN_3); IR ν/cm^{-1} (Nujol): 1613m, 1583m, 1416m, 1280m, 1123m, 1044m, 776m; acc. MS/EI m/z (%): 585 [M^+, 100], 100 [N(Pr^i)$_2^+$, 67]; MS (EI) calc. for: $C_{36}H_{53}N_3Ni$: 585.358, found 385.358; anal. calc. for $C_{36}H_{53}N_3Ni$ (585.358): C 73.72, H 9.11, N 7.16. Found: C 73.38, H 9.26, N 7.06 parameters, R(observed) = 0.0749, wR2 = 0.1252, largest difference peak and hole: 1.065 and -0.974 e.Å^{-3}.

[Ni^{II}(κ^2-N,N'-Giso)(η^5-Cp)]: 116

LiCp (40 mg, 0.52 mmol) in THF (5 cm^3) was added to a solution of [Ni^{II}(κ^2-N,N'-Giso)(μ-Br)]$_2$ (**109**) (350 mg, 0.26 mmol) in THF (5 cm^3) at –78 °C. The resultant mixture warmed to room temperature overnight. Volatiles were then removed *in vacuo* and the residue extracted with hexane (20 cm^3). Filtration, concentration and cooling to -30 °C overnight yielding lilac crystals of **116**.

(70 mg, 41%), M.p. 210 °C; ^{1}H NMR (300 MHz, C_6D_6, 303 K): δ-13.60 (br. s, 5H, Cp), 0.84 (m, 20H, Cy), 1.56 (d, $^3J_{HH}$ = 6 Hz, 12H, Pr^i), 2.77 (d, $^3J_{HH}$ = 6 Hz, 12H, Pr^i), 5.27 (m, 2H, Cy-H), 5.71, (m, 4H, Pr^i-H), 8.18, (d, $^3J_{HH}$ = 6 Hz, 6H, Ar-H); ^{13}C NMR (75 MHz, C_6D_6 303 K): δ 23.13 (CH_2), 25.47 (CH_2), 27.27 ($CH(CH_3)_2$), 31.82 ($CH(CH_3)_2$), 32.73 ($CH(CH_3)_2$), 34. 85 ($CH(CH_3)_2$), 37.67 ($CH(CH_3)_2$), 41.51 (CH_2), 43.70 (HCN), 71.73 (*o*-$C_6H_3Pr^i_2$), 117.59 (*p*-$C_6H_3Pr^i_2$), 134.05 (*m*-$C_6H_3Pr^i_2$), 162.54 (*ipso*-$C_6H_3Pr^i_2$); IR ν/cm^{-1} (Nujol): 2361m, 11610m, 1319m, 1280m, 1019m, 696m, 795m, 773m, 752m; acc. MS/EI m/z (%): 665 [M^+, 100], 180 [$N(Cy)_2^+$, 86]; MS (EI) calc. for $C_{42}H_{61}N_3Ni$: 665.421, found 665.4211; anal. calc. for $C_{42}H_{61}N_3Ni$ (665.421): C 75.67, H 9.22, N 6.30. Found: C 75.67, H 9.23, N 6.26.

[Ni(κ^2-N,N'-Priso)(μ-N-N_3)]$_2$: 121

Me_3SiN_3 (16.2 mg, 0.14 mmol) was added to a solution of [{Ni^{II}(κ^2-N,N'-Priso)}$_2$(η^3:η^3-C_7H_8)] (**110**) (80 mg, 0.07 mmol) in hexane (10 cm^3) at –78 °C. The resultant mixture warmed to room temperature overnight. Volatiles were then removed *in vacuo* and the residue extracted with hexane (20 cm^3). Filtration, concentration and cooling to -30 °C overnight yielding yellow crystals of **121**.

(43 mg, 53%); M.p. 195 °C; ^{1}H NMR (300 MHz, C_6D_6, 303 K): δ 0.49 (d, $^3J_{HH}$ = 6 Hz, 24H, Pr^i), 1.26 (d, $^3J_{HH}$ = 6 Hz, 24H, Pr^i), 2.36 (d, $^3J_{HH}$ = 6Hz, 24H, Pr^i), 3.47

(sept, 6 Hz, 4H, Pr^i-H), 4.09 (sept, $^3J_{HH}$ = 6 Hz, 2H, Pr^i-H), 6.81 (m, 12H Ar-H); ^{13}C NMR (75 MHz, C_6D_6 303 K): δ 22.96 ($NCH(CH_3)_3$), 23.17 ($CH(CH_3)_2$), 24.27 ($CH(CH_3)_2$), 29.00 ($CH(CH_3)_2$), 47.42 ($NCH(CH_3)3$), 123.54 (*o*-$C_6H_3Pr^i_2$), 125.62 (*p*-$C_6H_3Pr^i_2$), 137.68 (*m*-$C_6H_3Pr^i_2$), 145.11 (*ipso*-$C_6H_3Pr^i_2$), 166.73 (CN_3); IR ν/cm^{-1} (Nujol): 2077m, 1263m, 1125m, 1050m, 937m, 874m, 798m, 755m, 661m; acc. MS/EI m/z (%): 1126.5 [M^+, 10], 1068.6 [M^+-$2N_2$, 58], 420 [1/2M^+-$N(Pr^i)_2$, 100], parameters, R(observed) = 0.0712, wR2 = 0.1299, largest difference peak and hole: 0.967 and -0.448e.$Å^{-3}$.

[Ni(κ²-N,N'-Priso)(CO)]₂: 122

[{Ni^{II}(κ²-N,N'-Priso)}₂(η³:η³-C_7H_8)] (**110**) (50 mg, 0.04 mmol was dissolved in toluene (10 cm^3) in a Schlenk flask and cooled to -90 °C. The Schlenk flask (*ca.* 100 cm^3 volume) was filled with CO and sealed. The colour of the solution changed from red-brown to deep green over 20 h. All volatiles were then removed from the solution *in vacuo* and the residue extracted with hexane (10 cm^3). The extract was concentrated to *ca.* 5 cm^3 and stored at -30 °C overnight yielding deep green crystals of **122**.

(30 mg, 68%), M.P. 130 °C (dec.); ^1H NMR (300 MHz, C_6D_6, 303 K): δ 0.65 (d, $^3J_{HH}$ = 7 Hz, 12H, Pr^i), 1.23 (d, $^3J_{HH}$ = 7 Hz, 12H, Pr^i), 1.39 (d, $^3J_{HH}$ = 7 Hz, 12H, Pr^i), 3.58 (sept, $^3J_{HH}$ = 7 Hz, 6H, Pr^i-H), 3.99 (sept, $^3J_{HH}$ = 7 Hz, 4H, Pr^i-H), 7.11 (m, 12H, Ar-H); ^{13}C NMR (75 MHz, C_6D_6 303 K): δ 23.1 ($NCH(CH_3)_3$), 23.41 ($CH(CH_3)_2$), 24.64 ($CH(CH_3)_2$), 27.92 ($CH(CH_3)_2$), 49.03 ($NCH(CH_3)_2$), 123.38 (*o*-$C_6H_3Pr^i_2$), 124.96 (*p*-$C_6H_3Pr^i_2$), 140.40 (*m*-$C_6H_3Pr^i_2$), 144.81 (*ipso*-$C_6H_3Pr^i_2$), 166.81 (CN_3), 230.45 (CO); IR ν/cm^{-1} (Nujol):1847m, 1308m, 1204m, 1109m, 938m, 874m, 797m, 752m, 659m; MS/EI m/z (%): 1096 [M^+, 2], 1042 [M^+-2CO, 53], 520

[1/2M^+-CO, 100], 420 [1/2M^+-N(Pr^i)$_2$, 73]; MS (EI) calc. for $C_{64}H_{98}N_6Ni_2O_2$: 1096.6296, found: 1096.6286; anal. calc. for $C_{64}H_{98}N_6Ni_2O_2$: C 69.95, H 8.81, N 7.65. Found: C 68.41, H 8.66, N 7.32 parameters, R(observed) = 0.0484, wR2 = 0.0927, largest difference peak and hole: 0.567 and -0.515 e.Å^{-3}.

N.B. **122** can also be formed in a 76% isolated yield by treating a toluene solution of [Ni^I(κ^2-N,N'-Priso)]$_2$ (**113**) with excess CO.

2.6 References

[1] G. Wilkinson, *J. Organomet. Chem.* **1975**, *100*, 273.

[2] C. Pariya, K. H. Theopold, *Current Science* **2000**, *78*, 1345.

[3] M. E. Smith, R. A. Andersen, *J. Am. Chem. Soc.* **1996**, *118*, 11119.

[4] R. Poli, *Chem. Rev.* **1996**, *96*, 2135.

[5] W. C. Trogler, *Organometallic Radical Processes*, Elsevier, NY, Amsterdam, **1990**.

[6] J. K. Kochi, *Organometallic Mechanisms and Catalysis,*, Academic Press, New York, **1978**.

[7] R. H. Crabtree, *The Organometallic Chemistry of the Transition Metals*, John Wiley & Sons, New York, **2000**.

[8] D. Astruc, *Acc. Chem. Res.* **1991**, *24*, 36.

[9] Y.-C. Tsai, P.-Y. Wang, K.-M. Lin, S.-A. Chen, J.-M. Chen, *Chem. Commun.* **2008**, 205.

[10] F. T. Edelmann, *Adv. Organomet. Chem.* **2008**, 183.

[11] S. G. Mcgeach, *Can. J. Chem.* **1968**, 1903.

[12] J. E. Parks, R. H. Holm, *Inorg. Chem.* **1968**, 1408.

[13] C. L. Honeybourne, G. A. Webb, *Chem. Phys. Lett.* **1968**, 426.

[14] L. Bourget-Merle, M. F. Lappert, J. R. Severn, *Chem. Rev.* **2002**, *102*, 3031.

[15] P. B. Hitchcock, M. F. Lappert, Dian-Sheng, D.-S. Liu, *J. Chem. Soc., Chem. Commun.* **1994**, 1699.

[16] M. A. Fernandes, M. F. Lappert, M. Layh, B. Omondi, *Chem. Commun.* **2003**, 656.

[17] P. B. Hitchcock, M. F. Lappert, M. Layh, *Chem. Commun.* **1998**, 201.

[18] P. B. Hitchcock, M. F. Lappert, M. Layh, *J. Chem. Soc., Dalton Trans.* **2001**, 2409.

[19] Y.-L. Huang, B.-H. Huang, B.-T. Ko, C.-C. Lin, *J. Chem. Soc., Dalton Trans.* **2001**, 1359.

[20] S. Fustero, M. G. Torre, B. Pina, A. S. Fuentes, *J. Org. Chem.* **1999**, *64*, 5551.

[21] M. Stender, R. J. Wright, B. E. Eichler, J. Prust, M. M. Olmstead, H. W. Roesky, P. P. Power, *J. Chem. Soc., Dalton Trans.* **2001**, 3465.

[22] A. A. Danopoulos, G. Wilkinson, T. K. N. Sweet, M. B. Hursthouse, *J. Chem. Soc., Dalton Trans.* **1995**, 205.

[23] B.-J. Deelman, P. B. Hitchcock, M. F. Lappert, H.-K. Lee, W.-P. Leung, *J. Organomet. Chem.* **1996**, *513*, 281.

[24] A. S. Guram, R. F. Jordan, D. F. Taylor, *J. Am. Chem. Soc.* **1991**, *113*, 1833.

[25] C. Paulmier, Y. Mollier, N. Lozac'h, *Bull. Soc. Chim. Fr.* **1965**, 2463.

[26] N. Kuhn, H. Lanfermann, P. Schmitz, *Liebigs Ann. Chem.* **1987**, 727.

[27] P. Cuadrado, A. M. Gonza´lez-Nogal, *Tetrahedron Lett.* **1998**, *39*, 1446.

[28] A. Maraval, D. Arquier, A. Igau, Y. Coppel, B. Donnadieu, J.-P. Majoral, *Organometallics* **2001**, *20*, 1716.

[29] M. F. Lappert, D.-S. Liu, *J. Organomet. Chem.* **1995**, *500*, 203.

[30] P. B. Hitchcock, J. Hu, M. F. Lappert, M. Layh, D.-S. Liu, J. R. Severn, T. Shun, *An. Quim. Int. Ed.* **1996**, *92*, 186.

[31] P. L. Holland, W. B. Tolman, *J. Am. Chem. Soc.* **1999**, 7270.

[32] P. L. Holland, W. B. Tolman, *J. Am. Chem. Soc.* **2000**, 6331.

[33] P. B. Hitchcock, M. F. Lappert, D.-S. Liu, *J. Chem. Soc., Chem. Commun.* **1994**, 2637.

[34] P. B. Hitchcock, M. F. Lappert, S. Tian, *J. Chem. Soc., Dalton Trans.* **1997**, 1945.

[35] P. G. Hayes, W. E. Piers, L. W. M. Lee, L. K. Knight, M. Parvez, M. R. J. Elsegood, W. Clegg, *Organometallics* **2001**, *20*, 2533.

[36] L. W. M. Lee, W. E. Piers, M. R. J. Elsegood, W. Clegg, M. Parvez, *Organometallics* **1999**, *18*, 2947.

[37] L. K. Knight, W. E. Piers, R. McDonald, *Chem. Eur. J.* **2000**, *6*, 4322.

[38] P. B. Hitchcock, M. F. Lappert, M. Layh, D.-S. Liu, R. Sablong, T. Shun, *J. Chem. Soc., Dalton Trans.* **2000**, 2301.

[39] B. Räke, F. Zülch, Y. Ding, J. Prust, H. W. Roesky, M. Noltemeyer, H. G. Schmidt, *Z. Anorg. Allg. Chem.* **2001**, *627*, 836.

[40] W. Clegg, S. J. Coles, E. K. Cope, F. S. Mair, *Angew. Chem. Int. Ed.* **1998**, *37*, 796.

[41] G. Bai, P. Wei, D. W. Stephan, *Organometallics* **2005**, *24*, 5901.

[42] P. H. M. Budzelaar, A. B. V. Oort, A. G. Orpen, *Eur. J. Inorg. Chem.* **1998**, 1485.

[43] G. K. B. Clentsmith, V. M. E. Bates, P. B. Hitchcock, F. G. N. Cloke, *J. Am. Chem. Soc.* **1999**, *121*, 10444.

[44] C. E. Laplaza, A. L. Odom, W. M. Davis, C. C. Cummins, J. D. Protasiewicz, *J. Am. Chem. Soc.* **1995**, *117*, 4999.

[45] V. C. Gibson, C. Newton, C. Redshaw, G. A. Solan, A. J. P. White, D. J. Williams, *Eur. J. Inorg. Chem.* **2001**, 1895

[46] W. H. Monillas, G. P. A. Yap, K. H. Theopold, *Angew. Chem. Int. Ed.* **2007**, *46*, 6692.

[47] Y.-C. Tsai, P.-Y. Wang, S.-A. Chen, J.-M. Chen, *J. Am. Chem. Soc.* **2007**, *129*, 8066.

[48] J. Chai, H. Zhu, K. Most, Herbert W. Roesky, D. Vidovic, H.-G. Schmidt, M. Noltemeyer, *Eur. J. Inorg. Chem.* **2003**, *2003*, 4332.

[49] J. Chai, H. Zhu, A. C. Stuckl, H. W. Roesky, J. Magull, A. Bencini, A. Caneschi, D. Gatteschi, *J. Am. Chem. Soc.* **2005**, *127*, 9201.

[50] J. M. Smith, R. J. Lachicotte, K. A. Pittard, T. R. Cundari, G. Lukat-Rodgers, K. R. Rodgers, P. L. Holland, *J. Am. Chem. Soc.* **2001**, *123*, 9222.

[51] J. M. Smith, R. J. Lachicotte, P. L. Holland, *Organometallics* **2002**, *21*, 4808.

[52] J. M. Smith, A. R. Sadique, T. R. Cundari, K. R. Rodgers, G. Lukat-Rodgers, R. J. Lachicotte, C. J. Flaschenriem, J. Vela, P. L. Holland, *J. Am. Chem. Soc.* **2006**, *128*, 756.

[53] Y. Yu, J. M. Smith, C. J. Flaschenriem, P. L. Holland, *Inorg. Chem.* **2006**, *45*, 5742.

[54] X. Dai, P. Kapoor, T. H. Warren, *J. Am. Chem. Soc.* **2004**, *126*, 4798.

[55] S. Stella, C. Floriani, A. Chiesi-Villa, C. Guastini, *J. Chem. Soc., Dalton Trans.* **1988**, 545.

[56] G. Bai, D. W. Stephan, *Angew. Chem. Int. Ed.* **2007**, *46*, 1856.

[57] G. Bai, P. Wei, A. K. Das, D. W. Stephan, *Dalton Trans.* **2006**, 1141.

[58] X. Dai, T. H. Warren, *J. Am. Chem. Soc.* **2004**, *126*, 10085.

[59] X. Dai, T. H. Warren, *Chem. Commun.* **2001**, 1998.

[60] J. Prust, K. Most, I. Müller, A. Stasch, H. W. Roesky, I. Usón, *Eur. J. Inorg. Chem.* **2001**, *2001*, 1613.

[61] Y. Wang, B. Quillian, P. Wei, H. Wang, X. J. Yang, Y. Xie, R. B. King, P. v. R. Schleyer, H. F. Schaefer, G. H. Robinson, *J. Am. Chem. Soc.* **2005**, *127*, 11944.

[62] A. R. Sanger, *Inorg. Nucl. Chem. Letters* **1973**, *9*, 351.

[63] R. T. Roere, R. T. Oakley, R. W. Reed, *J. Organomet. Chem.* **1987**, 161.

[64] K. Vrieze, G. R. v. Koten, *Trav. Chim. Pays-Bas.* **1980**, *99*, 145.

[65] H. W. Roesky, B. Mainz, M. Noltemeyer, *Z. Naturforsch.* **1990**, *45b*, 53.

[66] F. Knösel, M. Noltemeyer, F. T. Edelmann, *Z. Naturforsch.* **1989**, *44b*, 1171.

[67] H. W. Roesky, K. V. Katti, U. Seseke, M. Witt, E. Egert, R. Herbst, G. M. Sheldrick, *Angew. Chem. Int. Ed.* **1986**, *25*, 477.

[68] H. W. Roesky, K. V. Katti, U. Seseke, H.-G. Schmidt, E. Egert, R. Herbst, G. M. Sheldrick, *J. Chem. Soc., Dalton Trans.* **1987**, 847.

[69] K. V. Katti, H. W. Roesky, M. Rietzel, *Inorg. Chem.* **1987**, *26*, 814.

[70] M. Witt, H. W. Roesky, M. Noltemeyer, G. M. Sheldrick, *Angew. Chem. Int. Ed.* **1989**, *27*, 851.

[71] H. W. Roesky, P. Olms, M. Witt, K. Keller, D. Stalke, T. Henkel, G. M. Sheldrick, *J. Chem. Soc., Chem. Commun.* **1989**, 366.

[72] H. Fußstetter, H. Nöth, *Chem. Ber.* **1979**, *112*, 3672.

[73] A. Heine, D. Fest, C. D. Habben, A. Meller, G. M. Sheldrick, *J. Chem. Soc., Chem. Commun.* **1990**, 742.

[74] D. Fest, C. D. Habben, A. Meller, G. M. Sheldrick, D. Stalke, F. Pauer, *Chem. Ber.* **1990**, *123*, 703.

[75] A. Xia, H. M. El-Kaderi, M. Jane Heeg, C. H. Winter, *J. Organomet. Chem.* **2003**, *682*, 224.

[76] C. Jones, P. C. Junk, J. A. Platts, A. Stasch, *J. Am. Chem. Soc.* **2006**, *128*, 2206.

[77] R. E. Boeré, R. T. Boeré, J. Masuda, G. Wolmershäuser, *Can. J. Chem.* **2000**, *78*, 1613.

[78] W.-X. Zhang, M. Nishiura, Z. Hou, *Chem. Commun.* **2006**, 3812.

[79] C. A. Nijhuis, E. Jellema, T. J. J. Sciarone, A. Meetsma, P. H. M. Budzelaar, B. Hessen, *Eur. J. Inorg. Chem.* **2005**, *2005*, 2089.

[80] M. L. Cole, P. C. Junk, *New J. Chem.* **2005**, *29*, 135.

[81] M. L. Cole, G. B. Deacon, P. C. Junk, K. Konstas, *Chem. Commun.* **2005**, 1581.

[82] M. L. Cole, G. B. Deacon, C. M. Forsyth, P. C. Junk, K. Konstas, J. Wang, *Chem. Eur. J.* **2007**, *13*, 8092.

[83] R. T. Boere′, V. Klassen, G. Wolmershäuser, *J. Chem. Soc., Dalton Trans.* **1998**, 4147.

[84] B. Vendemiati, G. Prini, A. Meetsma, B. Hessen, Jan H. Teuben, O. Traverso, *Eur. J. Inorg. Chem.* **2001**, 707.

[85] S. R. Foley, G. P. A. Yap, D. S. Richeson, *Inorg. Chem.* **2002**, *41*, 4149.

[86] J. R. Hagadorn, J. Arnold, *J. Organomet. Chem.* **2001**, *637-639*, 521.

[87] J. R. Hagadorn, J. Arnold, *Inorg. Chem.* **1997**, *36*, 132.

[88] B. S. Lim, A. Rahtu, J.-S. Park, R. G. Gordon, *Inorg. Chem.* **2003**, *42*, 7951.

[89] A. R. Sadique, M. J. Heeg, C. H. Winter, *Inorg. Chem.* **2001**, *40*, 6349.

[90] Z. Li, D. K. Lee, M. Coulter, L. N. J. Rodriguez, R. G. Gordon, *Dalton Trans.* **2008**, 2592.

[91] E. Nelkenbaum, M. Kapon, M. S. Eisen, *Organometallics* **2005**, *24*, 2645.

[92] J. A. R. Schmidt, J. Arnold, *J. Chem. Soc., Dalton Trans.* **2002**, 3454.

[93] G. Jin, C. Jones, P. C. Junk, A. Stasch, W. D. Woodul, *New J. Chem.* **2008**, *32*, 835.

[94] S. P. Green, C. Jones, P. C. Junk, K.-A. Lippert, A. Stasch, *Chem. Commun.* **2006**, 3978.

[95] S. P. Green, C. Jones, G. Jin, A. Stasch, *Inorg. Chem.* **2007**, *46*, 8.

[96] C. Jones, P. C. Junk, J. A. Platts, D. Rathmann, A. Stasch, *Dalton Trans.* **2005**, 2497.

[97] S. P. Green, C. Jones, A. Stasch, *Science* **2007**, *318*, 1754.

[98] Y.-C. Tsai, C.-W. Hsu, J.-S. K. Yu, G.-H. Lee, Y. Wang, T.-S. Kuo, *Angew. Chem. Int. Ed.* **2008**, *47*, 7250

[99] C. Jones, D. P. Mills, A. Stasch, *Dalton Trans.* **2008**, 4799.

[100] J. P. Coyle, W. H. Monillas, G. P. A. Yap, S. T. Barry, *Inorg. Chem.* **2008**, *47*, 683.

[101] K. Shibayama, S. W. Seidel, B. M. Novak, *Macromolecules* **1997**, *30*, 3159.

[102] Z. Li, A. Rahtu, R. G. Gordon, *J. Electrochem. Soc.* **2006**, *153*, C787.

[103] H. E. Abdou, A. A. Mohamed, J. P. Fackler-Jr., *Inorg. Chem.* **2007**, *46*, 141.

[104] H. E. Abdou, A. A. Mohamed, J. P. Fackler-Jr., *Inorg. Chem.* **2005**, *44*, 166.

[105] A. A. Mohamed, H. E. Abdou, J. P. Fackler-Jr., *Inorg. Chem.* **2006**, *45*, 11.

[106] H. E. Abdou, A. A. Mohamed, J. P. Fackler-Jr., *J. Cluster Sci.* **2007**, *18*, 630.

[107] H. E. Abdou, A. A. Mohamed, J. P. Fackler-Jr, *Inorg. Chem.* **2007**, *46*, 9692.

[108] F. A. Cotton, L. M. Daniels, C. A. Murillo, P. Schooler, *J. Chem. Soc., Dalton Trans.* **2000**, 2007.

[109] F. J. Lahoz, A. Tiripicchio, M. T. Camellini, *J. Chem. Soc., Dalton Trans.* **1985**, 1487.

[110] T. A. Betley, J. C. Peters, *J. Am. Chem. Soc.* **2004**, *126*, 6252.

[111] T. A. Betley, J. C. Peters, *J. Am. Chem. Soc.* **2003**, *125*, 10782.

[112] W. A. Chomitz, J. Arnold, *Chem. Commun.* **2007**, 4797.

[113] T. J. J. Sciarone, C. A. Nijhuis, A. Meetsma, B. Hessen, *Dalton Trans.* **2006**, 4896.

[114] N. A. Eckert, J. M. Smith, R. J. Lachicotte, P. L. Holland, *Inorg. Chem.* **2004**, *43*, 3306.

[115] S. A. Stoian, J. Vela, J. M. Smith, A. R. Sadique, P. L. Holland, E. Munck, E. L. Bominaar, *J. Am. Chem. Soc.* **2006**, *128*, 10181.

[116] J. P. Kenny, R. B. King, H. F. Schaefer, *Inorg. Chem.* **2001**, 900.

[117] C. Sourisseau, *J. Raman Spectrosc.* **1977**, *6*, 303.

[118] Y. Yu, A. R. Sadique, J. M. Smith, T. R. Dugan, R. E. Cowley, W. W. Brennessel, C. J. Flaschenriem, E. Bill, T. R. Cundari, P. L. Holland, *J. Am. Chem. Soc.* **2008**, *130*, 6624.

[119] W. Fraenk, T. M. Klapötke, B. Krumm, P. Mayer, *Chem. Commun.* **2000**, 667.

[120] H. Lei, B. D. Ellis, C. Ni, F. Grandjean, G. J. Long, P. P. Power, *Inorg. Chem.* **2008**, *in press*.

[121] N. A. Eckert, E. M. Bones, R. J. Lachicotte, P. L. Holland, *Inorg. Chem.* **2003**, *42*, 1720.

[122] J. Feldman, S. J. McLain, A. Parthasarathy, W. J. Marshall, J. C. Calabrese, S. D. Arthur, *Organometallics* **1997**, *16*, 1514.

[123] G. Bai, P. Wei, A. Das, D. W. Stephan, *Organometallics* **2006**, *25*, 5870.

[124] T. Nguyen, W. A. Merrill, C. Ni, H. Lei, J. C. Fettinger, B. D. Ellis, G. J. Long, M. Brynda, P. P. Power, *Angew. Chem. Int. Ed.* **2008**, *47*, 1.

[125] S.-H. Lai, C.-J. Hsiao, J.-W. Ling, W.-Z. n. Wang, S.-M. Peng, I.-C. Chen, *Chem. Phys. Lett.* **2008**.

[126] N. A. Eckert, A. Dinescu, T. R. Cundari, P. L. Holland, *Inorg. Chem.* **2005**, *44*, 7702.

[127] D. F. Evans, *J. Chem. Soc.* **1959**, 2003.

[128] E. M. Schubert, *J. Chem. Ed.* **1992**, *69*, 62.

[129] M. D. Francis, *PhD Thesis, University of Wales, Swansea* **1998**.

[130] J. C. Guillemin, T. Janati, J. M. Denis, *J. Org. Chem.* **2001**, *66*, 7864.

[131] G. M. Kosolapoff, *J. Am. Chem. Soc.* **1947**, *69*, 1002.

[132] D. Seyferth, R. S. Marmor, *J. Organomet. Chem.* **1973**, *59*, 237.

Appendix I

General Experimental Procedures

All manipulations were performed using standard Schlenk and glovebox techniques under an atmosphere of high purity argon or dinitrogen (BOC 99.9 %) in flame-dried glassware. All glassware was cleaned by overnight storage in an isopropyl alcohol solution of sodium hydroxide, followed by rinsing with dilute hydrochloric acid, distilled water and acetone, and was stored in an oven at 110 °C. Hexane, diethyl ether, toluene and tetrahydrofuran were pre-dried by storage over sodium wire and were refluxed under an atmosphere of high purity dinitrogen for twelve hours over either potassium or Na/K alloy prior to collection. ^{1}H and $^{13}C\{^{1}H\}$ NMR spectra were recorded on either a Bruker AMX 500 spectrometer (500.13 MHz, 125.76 MHz), Bruker DPX 400 spectrometer (400.13 MHz, 100.62 MHz), a Bruker DPX 300 spectrometer (300.13 MHz, 75.47 MHz), a Jeol Eclipse 300 spectrometer (300.52 MHz, 75.57 MHz), or a Bruker AV 200 spectrometer (200.13 MHz, 50.33 MHz) in $CDCl_3$, C_6D_6, $CDCl_2$, toluene-d_8 or THF-d_8 (freeze-thaw degassed and dried over sodium) and were referenced to the residual ^{1}H or ^{13}C resonances of the solvent used. $^{31}P\{^{1}H\}$ NMR spectra were recorded on a Jeol Eclipse 300 spectrometer operating at 121.66 MHz were referenced to 85 % H_3PO_4. EI and APCI mass spectra and accurate mass EI and APCI mass spectra were obtained from the EPSRC National Mass Spectrometric Service at Swansea University. IR spectra were recorded using a Nicolet 510 FT-IR spectrometer as Nujol mulls between NaCl plates. Melting points were determined in sealed glass capillaries under argon and are uncorrected. Microanalyses were obtained from Medac Ltd. or the Campbell Microanalytical Laboratory, University of Otago.

Appendix II

Publications in Support of this Thesis

1. Synthesis and characterization of a diphosphaalkene, a diphosphaalkyne and the first diphosphavinyl lithium complex, F. Brodkorb, M. Brym, C. Jones, C. Schulten, *J. Organomet. Chem.*, **2006**, *691*, 1025.

2. The first complexes and cyclodimerisations of methylphosphaalkyne (P≡CMe). C. Jones, C. Schulten, A. Stasch, *Dalton Trans.*, **2006**, *31*, 3733. Designated a **"hot article"**

3. Differing reactivities of P≡CMe and P≡CBut towards a triphosphabenzene and a tetraphosphabarrelene: Synthesis of new phosphaalkyne pentamers ($P_5C_5Me_nBu^t_5$-n, n = 0, 1 or 2), C. Jones, C. Schulten, A. Stasch, *Dalton Trans.*, **2007**, *19*, 1929.

4. Unusual Reactivity of Methylphosphaalkyne (P≡CMe) toward Digermenes and Distannenes: Stepwise Formations of Bridged 2,3,5,6-Tetraphospha-1,4-dimethylidenecyclohexanes, C. Jones, C. Schulten and A. Stasch, *Inorg. Chem.*, **2008**, *47*, 1273.

5. Synthesis, characterization and reactivity of a η1-methylphosphaalkyne complex, [RuH(dppe)2(η1-P≡CMe)][CF3SO3], C. Jones, C. Schulten, A. Stasch, *Eur. J. Inorg. Chem.*, **2008**, *10*, 1555.

6. Synthesis and Characterization of Amidinate–Iron(I)Complexes: Analogies with β-Diketiminate Chemistry, R. P. Rose, C. Jones, C. Schulten, S. Aldridge, A. Stasch, *Chem. Eur. J.*, **2008**, *14*, 8477.

7. Cycloaddition reactions of transition metal hydrazides with alkynes and heteroalkynes: coupling of Ti=NNPh2 with PhCCMe, PCCH, MeCN and

P≡CBu^t, J. D. Selby, A. D. Schwarz, C. Schulten, E. Clot, C. Jones, P. Mountford, *Chem. Commun.*, **2008**, 5101. Designated a **"hot article"**